Title
A Genetic Analysis of Structural and Functional Homeostatic Plasticity at the Drosophila Neuromuscular Junction

Author
Locke, Cody Justin

Publication Date
2015

Peer reviewed|Thesis/dissertation

A Genetic Analysis of Structural and Functional Homeostatic Plasticity at the *Drosophila* Neuromuscular Junction

by

Cody Justin Locke

DISSERTATION

Submitted in partial satisfaction of the requirements for the degree of

DOCTOR OF PHILOSOPHY

in

Neuroscience

in the

GRADUATE DIVISION

of the

UNIVERSITY OF CALIFORNIA, SAN FRANCISCO

Dedication

To the dreamers,

who must learn to open their eyes and embrace reality, emancipating themselves with an understanding that they are seldom in control and that humankind is far more important than their ambitions or reputations.

Acknowledgments

Science sometimes appears to be an individual endeavor, in which a coalition of lone researchers formulate their own ideas and carry out their own experiments along a journey to better understand reality. However, science is not this way. Scientists depend on each other and generations of other scientists before them to make breakthroughs. If you are a scientist, and you do not ask for advice from more experienced researchers or do not challenge your own theories for fear of proving yourself wrong, then you will soon find yourself on a dangerous path. Indeed, you will almost assuredly find yourself trailing behind your peers, losing time that cannot be recovered, and squandering opportunities for yourself and most likely others, who may not make the same mistakes as you. If you define yourself by your productivity, then you might find yourself devastated and unsure of your own future. Yet, if you are fortunate to work in a truly supportive environment, as I have, then do not quit. You have been given a rare chance to learn. Please embrace it.

As a naïve and overly ambitious graduate student, I was certain of my ideas. Yet, I was wrong. Without the contributions of anonymous peers, who attempted to replicate some of my earliest data, mostly through blinded experiments, I would have irrevocably damaged my scientific reputation and assassinated my career by publishing a series of unreproducible experiments in a high-profile academic journal. Importantly, my failures would have not only destroyed my career, but also would have damaged the careers of my adviser and my beloved colleagues. After this initial unraveling of my thesis project, I was not buried by my adviser, which may have happened to many others in this unusual situation. Graeme Davis stood by me and allowed me to correct my earlier mistakes by continuing my training and demanding more rigorous and objective experimentation. It

is this example of mentorship that I hope to emulate in my own scientific career. Grae is not “endlessly excited” about science, as has been often said about him. Instead, Grae combines a unique enthusiasm for science with a necessary degree of skepticism. Yes, Grae is a damn fine scientist and man, and anyone would benefit from training with him.

Throughout my several years as a graduate student in the Davis lab, I have seen many colleagues come and go. Each one of you has contributed to my development as a scientist and as a person in a significant way. I want to especially acknowledge some of these individuals, who have had the greatest impacts on me. To Martin Müller, Andy Frank, and Dion Dickman, you are living the dream. I remain in awe of each of you and am excited to see what else you will accomplish in your own labs. You give the rest of us hope that we are still on the right path, and you somehow have done it without losing yourselves or your hair (at least all of it!) in the process. To Ling Cheng and Lani Keller, I have enjoyed serving as your personal electrophysiologist and would have loved to do even more work with you, provided the opportunity. Please do not forget about me when you are looking for a research specialist in your own labs. To Kevin Ford, Brian Orr, and Nathan Harris, it has been a pleasure to share a bay with you. If you happen to find my pipettes anywhere, then I hope you will return them to me. Ha! To Amy Tong and Gama Ruiz, you are the heart of the Davis lab, and we would get nowhere without you. Thank you for everything that you do. To Jennifer Ortega, you have become an unlikely “ally”. When my days were darkest, your laughter and ridicule of me somehow made me feel better and optimistic about the future. As long as I have access to Rock Hall, I will try to drop by and annoy you as much as I can. Perhaps I will even bring you some chocolate zucchini bread. To the future of science, whomever you are, remember “blind is better”.

As a student in the UCSF Neuroscience Graduate Program, I have also had the opportunity to interact with many inspiring and talented people outside of the Davis lab. In particular, I would like to thank members of my thesis committee for playing a critical role in my development as a scientist. To Lily Jan, your contributions to science exceed the scores of high-profile publications and accolades that you have attained individually. Your gift of mentorship is reflected in the successes of your trainees, several of whom I consider to be dear friends. As you recommended years earlier, I should have “made a knockout” much sooner. To Mark von Zastrow, your calm and reassuring demeanor has been a relief during my thesis committee meetings. If I were a gambler, which I am not, I would bet that your extraordinary abilities as a scientist are matched by your abilities as a psychiatrist. You might expect some phone calls from me for one reason or another in the future. To Robert Edwards, my thesis committee chair (yes, Rob, you are the chair!), you always seem to have pertinent information on the tip of your tongue, and you do not miss anything. Presenting my thesis work to you has been simultaneously terrifying and immensely valuable. Thank you for pointing out the likely “quagmires” in my research. It turns out that you were correct in all cases, which came as an enormous surprise to me. Provided an opportunity, I will pay closer attention to your insightful comments from now on. Along with my thesis committee, I would like to acknowledge Roger Nicoll and Louis Reichardt, who have served as chairs of the UCSF Neuroscience Graduate Program in my tenure as a graduate student. To Roger Nicoll, if you are in the market for a postdoc, I happen to know a guy. To Louis Reichardt, your nerve to pick a first-generation college student from the reddest of states for the UCSF Neuroscience Graduate Program might not have been the best idea in retrospect. Regardless, we cannot be certain from an “n-

of-1" that Alabama students are poor fits, so it seems only fair to leave the door open for a few more. To Pat Veitch, Lucita Nacionales, and Carrie Huckaba, I thank you for your tireless efforts in keeping our program going and for ensuring that our faculty respond to the occasional email. Finally, to my classmates, I never really felt foolish until I met you. I have been consistently humbled by you and honored to study alongside you. I believe it would be a great tragedy, if any of you fail to achieve your dreams. You can surely do anything you want in life, as long as you are patient. To Josh Bagley and Jason Tien, I have missed you the most. A chance of working alongside you is enough to keep me in science. To Sama Ahmed, stay cool, stay special, and always remember to be yourself.

My dedication to science and commitment to illuminating molecular mechanisms of neurological disorders have been strengthened through my experiences in graduate school. Yet, my passion was kindled at The University of Alabama in the lab of Guy and Kim Caldwell. Affectionately known as "The Worm Shack", the Caldwell lab was an ideal place for me to begin my career. Guy and Kim allowed me, even as a freshman, to work on important questions regarding the etiology of Parkinson's disease and epilepsy. For the duration of my undergraduate studies at Alabama, the Caldwell lab was home base. In fact, I really became a scientist there. Guy and Kim created an environment, wherein I could pursue my own ideas, present at international conferences, write my papers, and mentor some of the brightest young minds around. Without Guy and Kim, it is likely that I would have failed to realize my dreams of being a scientist and ended up as a medical student or business person. As Guy once told me, I am just not "diplomatic enough" for either of those positions, and I sense that he is correct. To Guy and Kim Caldwell, I will eternally consider you my mentors and my family. You are loved and appreciated more

than I can ever express to you in words. To my former students, Professor Bwarenaba Kautu, Dr. Kyle Lee, Dr. Stacey Fox, and soon-to-be Dr. Kalen Berry at MIT, it is cruel for you to have become so much more successful than I. It was my intent to teach you only enough to match me. However, I have apparently flunked in this endeavor. Really, though, I could not be prouder of each of you. I consider having helped to guide you as the most significant accomplishments of my career. I am eager to see what you will do with your exceptional skills in the years ahead. With the current status of the academic job market, I might even be sending you my résumé. To other former colleagues in the Caldwell lab, especially Shu Hamamichi and Adam Knight, I think about you often and hope that our paths cross again soon. I am lucky to have spent my glory days with you.

Graduate school is hard. It is not only hard because of the long hours, the failed experiments, and the complexity of the material, but also it is hard because it can easily isolate one from his family and friends. Countless times in San Francisco, I have longed to go fishing with my Dad or to watch birds with my Mom on the porch in Alabama. I am truly sorry that I could not do those things with you more often. If I could have predicted how epically much of my research would have ended in disaster, then I may have been a better son to you. I have learned so much from each of you. To Dad, you have taught me to recognize the humanity in others and that no one is ever really a stranger. I have tried to use your gifts of conversation and storytelling in my daily life, albeit much to the confusion of numerous introverts, whom I have encountered in academia. To Mom, you have taught me how to distinguish between constructive criticism and when someone is just being mean. My work ethic is a direct result of having witnessed you persist through trying times, when even putting in all of the overtime hours that you could at jobs that no

one could ever like was not enough to pay the bills. Without your effort, I would not have made it this far. I still believe that my education will have been worth the struggles, if not for the currency of dollars, then at least for the currency of ideas. Nevertheless, I cannot be sure of this belief, or of others, so I appreciate your standing offer of room and board.

Fortunately, I have had the privilege of sharing my graduate school career with a central member of my family: my wife, Dr. Renee Rivas. After easily spotting Renee in a crowd of honors students, to whom I was lecturing at Alabama, we have been a team. I spent myriad hours with Renee in the Worm Shack at Alabama, where we both routinely worked to the point of exhaustion. Through this experience, I somehow managed to get Renee to fall in love with me. Renee is the only person who understands me completely and how much the ebbs and flows of graduate school have affected me. I have changed in meaningful ways at UCSF, and Renee stood by me unequivocally during the process. For your devotion to me and to your own, perhaps even more demanding, journey, I will love you and stand with you forever, my dear, Renee. Adversity can never tear us apart.

In our latter years at UCSF, Renee and I have welcomed another member of our family into this world. To Sidonie Alessandra Locke, I love and cherish you. Without you, my honey bunny, I may have given up on this journey. Perhaps when you are older, but hopefully not as old as I am at this time, you will want to read my thesis. It is my wish for you to think on my work in the context of Daddy's time and circumstances. Undoubtedly, I am proud of it and optimistic that you and others will learn from it. Please do not label it as rubbish. More than anything else, I am proud to be your father. I can see your mother in you. Sidonie, you exist to do wonderful things. 1, 2, 3… count them with me. I do you.

Abstract

The structure and function of the nervous system is continuously changing due to genetic programs and environmental interactions. Regardless, despite such a degree of plasticity, the nervous system can remain functional under normal conditions. It is widely accepted that homeostatic regulatory mechanisms, some operating at the synapse, are responsible for stabilizing neural activity in the face of perturbations. From studies of the *Drosophila* neuromuscular junction (NMJ), a model glutamatergic synapse, mechanisms of homeostatic synaptic plasticity are being unraveled. These mechanisms include, but are not limited to, enhancement of neurotransmitter release from nerve terminals and a restructuring of synaptic morphology to maintain a set point of muscle depolarization. A reduction in the postsynaptic sensitivity to the neurotransmitter, glutamate, is countered by a homeostatic increase in the amount of glutamate release at *Drosophila* NMJs. This phenomenon, termed homeostatic potentiation, can be rapidly induced by an antagonist of glutamate receptors or chronically expressed following genetic ablation of a subset of glutamate receptors. Conversely, undergrowth of fly NMJs can be offset by homeostatic increases in the number of active zones, the sites of neurotransmitter release. Likewise, overgrowth of fly NMJs can be mollified by the redistribution of neurotransmitter release machinery throughout synapses. Although several synaptic proteins have been linked to these homeostatic regulatory mechanisms, it is not currently known if these phenomena are distinct at a molecular level. Furthermore, it is unclear if homeostatic plasticity at the fly NMJ is separable from overtly similar forms of synaptic plasticity, including long-term potentiation and presynaptic homeostatic scaling, in the mammalian brain. In this thesis, I tried to address these outstanding issues via genetics, electrophysiology, and imaging.

In Chapter 2, I describe mutagenesis and characterization of the gene encoding Synaptotagmin 12 (*Syt12*) in *Drosophila*. This study indicates that *Syt12* is required for the normal growth and elaboration of the fly NMJ. Yet, counter to expectations, synaptic undergrowth in *Syt12* loss-of-function mutants was concomitant with a decreased active zone number and an enlargement of the readily-releasable pool of synaptic vesicles, as measured by two-electrode voltage-clamp recordings. These data implicate *Syt12* in the morphogenesis of synapses and in the limiting of neurotransmitter release. Additionally, these findings are consistent with a function for *Syt12* in presynaptic structural plasticity due to synaptic undergrowth. We suggest that the mechanisms of presynaptic structural plasticity are separable from those of homeostatic potentiation, which was expressed in the absence of *Syt12*, but may be related to those of presynaptic long-term potentiation.

In Chapter 3, I describe the characterization of Cdk5 and its activator, p35, in the fly. This study indicates that Cdk5 signaling is not essential for homeostatic potentiation at the fly NMJ, despite its earlier association with a similar form of homeostatic synaptic plasticity in the hippocampus. Moreover, we validated a previous report by showing that NMJ overgrowth is compensated by a decrease in active zone density in the absence of Cdk5 signaling. These results suggest that homeostatic potentiation and another form of homeostatic structural plasticity at *Drosophila* NMJs are also molecularly separable. In a series of voltage-clamp experiments, we have also gathered evidence that Cdk5 activity regulates the composition of synaptic vesicle pools, largely consistent with its role in the hippocampus. Yet, microscopical techniques revealed only weak effects, if any, of Cdk5 signaling on the distribution of synaptic vesicle markers and glutamate receptors. These findings should add to our understanding of Cdk5 in brain evolution and human disease.

Table of Contents

Chapter 2: Synaptotagmin 12 Modulates Growth and Constrains Neurotransmitter Release at the *Drosophila* Neuromuscular Junction

Chapter 3: Cdk5 Activity Does Not Control Homeostatic Potentiation at the *Drosophila* Neuromuscular Junction

List of Figures

Chapter 2

Chapter 3

List of Abbreviations

AMPA – α-amino-3-hydroxy-5-methyl-4-isoxazolepropionic acid

ARCA – autosomal-recessive cerebellar ataxia

AS – analog-sensitive

ATP – adenosine triphosphate

BMP – bone morphogenetic protein

BDNF – brain-derived neurotrophic factor

Brp – Bruchpilot

Ca^{2+} – calcium ion

CaMK – calcium/calmodulin-dependent protein kinase

cAMP – cyclic AMP

Cdk5 – cyclin-dependent kinase 5

CNQX – 6-cyano-7-nitroquinoxaline-2,3-dione

CREB – cyclic AMP response-element binding protein

CSP – cysteine string protein

Df – deficiency

Dlg – Discs large

DN – dominant-negative

DNA – deoxyribonucleic acid

eIF – eukaryotic initiation factor

EJC – excitatory junctional current

EJP – excitatory junctional potential

ENaC – epithelial sodium channel

FasII – Fasciclin II

FLP – Flippase

FMRP – fragile X mental retardation protein

FRT – Flippase recognition target

GABA – gamma-aminobutyric acid

GAP – GTPase-activating protein

Gbb – glass bottom boat

GFP – green fluorescent protein

GKAP – guanylate kinase-associated protein

GluR – glutamate receptor

K^+ – potassium ion

MAP – mitogen-activated protein

MeCP – methyl CpG binding protein

mEJP – miniature excitatory junctional potential

mEPSC – miniature excitatory postsynaptic current

mRNA – messenger ribonucleic acid

mfLTP – mossy fiber long-term potentiation

MHC – major histocompatibility complex

mIPSC – miniature inhibitory postsynaptic current

Mp – multiplexin

Na^+ – sodium ion

Narp – neuronal-activity regulated protein

NBQX – 2,3-dihydroxy-6-nitro-7-sulfamoyl-benzo[f]quinoxaline-2,3-dione

NCAM – Neural cell adhesion molecule

NMDA – N-methyl-D-aspartate

NMJ – neuromuscular junction

NSF – N-ethylmaleimide-sensitive factor

PBac – piggyBac transposon

PCR – polymerase chain reaction

PhTx – philanthotoxin

PTZ – pentylenetetrazol

RIM – Rab3-interacting molecule

RBP – RIM-binding protein

RNA – ribonucleic acid

RNA-seq – RNA sequencing

RRP – readily-releasable pool

RT – reverse transcriptase

S6K – S6 kinase

SEM – standard error of the mean

SIM – structured illumination microscopy

SNARE – soluble NSF attachment protein receptor

Srg1 – synaptotagmin-related gene 1

SUMO – small ubiquitin-like modifier

Syt – Synaptotagmin

TARP – transmembrane AMPA receptor regulatory protein

TNF-α – tumor necrosis factor-alpha

TOR – target of rapamycin

TTX – tetrodotoxin

UAS – upstream activation sequence

VAMP – vesicle-associated membrane protein

VGLUT – vesicular glutamate transporter

Chapter 1

General Introduction to Structural and Functional Homeostatic Plasticity

Summary

The nervous system is modified throughout the life of animals in response to both internal and external stimuli. Despite these perturbations to the structure and function of the nervous system, neural activity can remain balanced by expression of various forms of homeostatic plasticity (Davis, 2006; Turrigiano, 2008; Davis and Müller, 2015). There is evidence that homeostatic plasticity contributes to the etiology of neurological disease (Kamenetz *et al.*, 2003; Houweling *et al.*, 2005; Trasande and Ramirez, 2007). Thus, an understanding of the molecular and cellular mechanisms of homeostatic plasticity in the nervous system could lead to improved treatments for neurological disease. In addition, comparing and contrasting homeostatic plasticity mechanisms in diverse animal species should enhance our knowledge of brain evolution and engineering design (Davis, 2006).

Homeostatic plasticity in the nervous system, not unlike homeostatic regulation in general, is carried out in theory through the coordinated activity of sensors and effectors (Alon *et al.*, 1999; Davis, 2006). These factors respond to perturbations, or error signals, to restore network functionality to an optimal set point level via integral feedback control (Davis, 2006). At synapses, where electrochemical signals are transmitted from neurons to other neurons or muscles, homeostatic regulatory mechanisms can retarget set point values of neural activity by structural (Davis and Goodman, 1998) and functional (Davis, 2006; Turrigiano, 2008; Davis and Müller, 2015) changes. The precise mechanisms by which homeostatic plasticity is achieved depends on the nature of the perturbation, the synapse in question, and the developmental history of that synapse (Desai *et al.*, 2002; Davis, 2006). It is likely that synapses “decide” to express specific forms of homeostatic regulation to best interface with the mechanisms of learning and memory (Davis, 2006).

Homeostatic Structural Plasticity at the Fly Neuromuscular Junction

When perturbed, invertebrate (Davis *et al.*, 1996; Schuster *et al.*, 1996; Stewart *et al.*, 1996; Davis and Goodman, 1998) and vertebrate (Murthy *et al.*, 2001; Smear *et al.*, 2007; Keck *et al.*, 2013; Auer *et al.*, 2015) synapses often modulate their structural properties to achieve homeostasis. In *Drosophila*, reduced growth of the neuromuscular junction (NMJ) can be offset by a compensatory increase in the number of active zones, resulting in wild type levels of neurotransmitter release and synaptic strength (Schuster *et al.*, 1996; Stewart *et al.*, 1996; Beck *et al.*, 2012). On the contrary, enhanced growth of the fly NMJ can be offset by a compensatory decrease in the density of active zones, similarly maintaining wild type levels of neurotransmitter release and synaptic strength (Davis *et al*., 1996; Schuster *et al.*, 1996). These cell autonomous, presynaptic forms of homeostatic structural plasticity were revealed by downregulating synaptic levels of the fly ortholog of Neural Cell Adhesion Molecule (NCAM), Fasciclin II (FasII), which affects NMJ morphogenesis in a dose-dependent manner (Schuster *et al.*, 1996; Stewart *et al.*, 1996; Beck *et al.*, 2012). This shared requirement for altering the synaptic abundance of FasII, which could theoretically be sensed by a homeostatic signaling system, suggests that homeostatic structural plasticity may not be a general phenomenon at the fly NMJ.

There is now emerging evidence to support the ubiquity of homeostatic structural plasticity at fly NMJs. In a pioneering study, expression of cyclic AMP response-element binding protein (CREB) elevated neurotransmitter release at structurally expanded *FasII* mutant NMJs, but not at control NMJs (Davis *et al*., 1996). These data might point to an active, homeostatic adjustment of cyclic AMP (cAMP) signaling in response to synaptic overgrowth, instead of a mere coincidence of complex, opposing effects of altered FasII

signaling (Davis *et al.*, 1996; Schuster *et al.*, 1996; Davis and Goodman, 1998). Loss of Cdk5 signaling also leads to NMJ overgrowth and a seemingly homeostatic reduction in active zone density, resulting in wild type neurotransmitter release and synaptic strength (Kissler *et al.*, 2009). Therefore, homeostatic structural plasticity due to NMJ overgrowth does not require direct mutation of the *FasII* gene locus to be triggered. In a later report, cAMP signaling mutants were shown to have decreased numbers of boutons and active zones, which were concomitant with decreased synaptic strengths (Chen and Ganetzky, 2012). These data imply that cAMP signaling may be required for homeostatic structural plasticity due to NMJ undergrowth. In light of a common influence of cAMP signaling on both forms of homeostatic structural plasticity at *Drosophila* NMJs, it seems conceivable that homeostatic structural plasticity is a bidirectional process. Because cAMP signaling is implicated in learning and memory (Kandel, 2012), future examination of homeostatic structural plasticity in flies may also reveal how potentially antagonistic forms of synaptic plasticity coexist and how synaptic plasticity has evolved from invertebrate to vertebrate systems. Further investigation of other fly mutants with undergrown NMJs, such as BMP signaling (Aberle *et al.*, 2002; Marqués *et al.*, 2002) and ubiquitin/MAP kinase signaling mutants (Sanyal *et al.*, 2002; Collins *et al.*, 2006), or overgrown NMJs, such as *highwire* (Wan *et al.*, 2000) and *spinster* (Sweeney and Davis, 2002), will be necessary to better understand the mechanisms of homeostatic structural plasticity at the *Drosophila* NMJ. If the number of ultrastructurally defined (Stewart *et al.*, 1996) or nc82 antibody-labeled (Wagh *et al.*, 2006) active zones in any of these mutants differs from the wild type, then homeostatic structural plasticity may be deemed impaired. Else, homeostatic structural plasticity has retargeted the wild type active zone number to offset altered NMJ growth.

Homeostatic Structural Plasticity in the Vertebrate Nervous System

In vertebrates, homeostatic structural plasticity may be expressed in a number of ways. Much of the evidence for homeostatic structural plasticity in vertebrates originates from depriving the visual system of neural activity. When exposed to tetrodotoxin (TTX), which blocks neural activity by antagonizing voltage-gated sodium channels (Narahashi *et al.*, 1964), axon arbors of retinal ganglion cells in the visual system of fetal cats were increased in both size and complexity (Sretavan *et al.*, 1988). A comparable effect was also shown at TTX-treated axons in the visual system of tadpoles (Cohen-Cory, 1999). Moreover, zebrafish with a presumably null mutation in *blumenkohl*, the gene encoding the zebrafish ortholog of a vesicular glutamate transporter, were found to have reduced neurotransmitter release per vesicle (quantal size), but wild type synaptic strengths and structurally enlarged axon arbors, at retinal ganglion cell synapses (Smear *et al.*, 2007). Likewise, retinotectal axon arbors of zebrafish were enlarged following pharmacological blockade of N-methyl-D-aspartate (NMDA) receptors with MK801 (Schmidt *et al.*, 2000). These findings are consistent with the expression of homeostatic structural plasticity, as stated (Smear *et al.*, 2007), and were attributed to a compensatory retrograde signaling system that is dependent on Neurotrophin-3 (Auer *et al.*, 2015). However, these results seem to contradict other studies in the zebrafish retinotectal system, which showed that axon arbors did not change structurally when silenced with TTX treatment (Stuermer *et al.*, 1990; Gnuegge *et al.*, 2001; Hua *et al.*, 2005). Taken together, these investigations in zebrafish suggest that the expression of homeostatic structural plasticity at a specific synapse can be sensitive to the kind or degree of perturbation (Smear *et al.*, 2007; Auer *et al.*, 2015). These data also highlight a notable conflict between neural activity-based

axonal competition and homeostatic plasticity. When neural activity was suppressed in single zebrafish retinal ganglion cells by overexpression of Kir2.1, an inward rectifier K^+ channel (Fakler *et al.*, 1994; Paradis *et al.*, 2001), or dominant-negative synaptobrevin (VAMP) protein (Sørensen *et al.*, 2002), retinotectal axon arbors were reduced in both size and complexity (Hua *et al.*, 2005). These effects of neural activity suppression on single zebrafish retinotectal arbors were reversed by global activity blockade with TTX (Hua *et al.*, 2005), indicating that retinal ganglion cells may "choose" to express neural activity-based competition or homeostatic structural plasticity via mechanisms that are affected by the surrounding environment (Smear *et al.*, 2007) or stage of development.

Along with simpler vertebrate systems (Cohen-Cory, 1999; Schmidt *et al.*, 2000; Smear *et al.*, 2007; Auer *et al.*, 2015) and seemingly cats (Sretavan *et al.*, 1988), which are not genetically tractable, homeostatic structural plasticity has been observed in the rodent nervous system (Murthy *et al.*, 2001; Keck *et al.*, 2013). Hippocampal synapses in culture were found to homeostatically enlarge synaptic components, including active zones, boutons, and postsynaptic densities, as a result of neural activity deprivation by 2,3-dioxo-6-nitro-1,2,3,4-tetrahydrobenzo[f]quinoxaline-7-sonfonamide (NBQX) (Murthy *et al.*, 2001). Furthermore, cortical synapses in the visual system exhibited homeostatic restoration of neural activity, as measured by genetically encoded Ca^{2+} indicators (Tian *et al.*, 2009; Akerboom *et al.*, 2012) from behaving mice on a treadmill (Dombeck *et al.*, 2007; Keller *et al.*, 2012), in response to sensory deprivation by retinal lesions (Keck *et al.*, 2013). The apparent homeostatic plasticity in these cortical synapses was attributed to enlargement of dendritic spines in projection neurons of cortical layer 5 *in vivo* and a concomitant increase in α-amino-3-hydroxy-5-methyl-4-isoxazolepropionic acid (AMPA)

receptors, manifested by an enhanced quantal size *in vitro* (Keck *et al.*, 2013). Notably, quantal size is also controlled by a form of homeostatic functional plasticity, referred to as quantal or synaptic scaling (Turrigiano *et al.*, 1998; Davis and Goodman, 1998; Watt *et al.*, 2000; Stellwagen and Malenka, 2006). Likewise, homeostatic functional plasticity can be achieved by modulating the size of the readily-releasable pool (RRP) of synaptic vesicles (Kim and Ryan, 2010; Weyhersmüller *et al.*, 2011; Müller *et al.*, 2012), which is concomitantly enlarged by homeostatic structural plasticity in cultured hippocampal cells (Murthy *et al.*, 2001). Therefore, homeostatic structural plasticity and functional plasticity can vary common electrophysiological parameters, either through alterations to synaptic morphology or more directly to quantal components of basal synaptic transmission (del Castillo and Katz, 1954), to maintain a balance in the nervous system (Turrigiano, 1999; Davis and Goodman, 1998; Davis and Bezprozvanny, 2001; Davis, 2006; Frank, 2014).

The underlying mechanisms of homeostatic structural plasticity in the mammalian nervous system have not been characterized at the molecular level. In the future, further analysis of neural activity-deprived hippocampal (Murthy *et al.*, 2001) and cortical (Keck *et al.*, 2013) synapses may determine which, if any, principal molecular mechanisms of homeostatic structural plasticity are evolutionarily conserved from zebrafish (Auer *et al.*, 2015) or even *Drosophila* (Davis *et al.*, 1996; Schuster *et al.*, 1996; Stewart *et al.*, 1996; Davis and Goodman, 1998). Such experiments are also critical for understanding how a synapse is programmed to express a particular form of homeostatic structural plasticity, homeostatic functional plasticity, or neural-activity based competition. With a significant influence on the nervous system and plausible impact on disease etiology, homeostatic structural plasticity demands further exploration in the future (Yin and Yuan *et al.*, 2015).

Homeostatic Functional Plasticity in the Vertebrate Nervous System

In the presence of a destabilizing perturbation, the nervous system can also alter its functional properties without undergoing morphological change. This phenomenon is termed homeostatic functional plasticity and can be expressed in three general ways, as defined earlier (Davis, 2006; Davis and Müller, 2015). These three general mechanisms of homeostatic functional plasticity include modulation of ionic conductance (Turrigiano, 1999; Marder and Goaillard, 2006), synaptic scaling (Turrigiano, 2008), and presynaptic homeostasis (Davis, 2006; Davis and Müller, 2015). Each of these forms of homeostatic plasticity seem to be present in the vertebrate nervous system (Davis and Müller, 2015).

Evidence for homeostatic modulation of ionic conductance in vertebrate neurons is derived from the chronic suppression of neural activity by TTX, similar to homeostatic structural plasticity. Two-day TTX treatment enhanced the intrinsic excitability of cortical pyramidal neurons (Desai *et al*., 1999a) and inhibitory interneurons *in vitro* by increasing Na^+ currents and decreasing K^+ currents (Desai *et al.*, 1999b). These alterations in ionic conductance led to higher firing frequencies of cultured neurons, after washing out TTX, (Desai *et al.*, 1999a; Desai *et al.*, 1999b) and are thought to homeostatically restore the functionality of impaired neural circuits (Turrigiano, 1999). Unlike homeostatic structural plasticity in mammals, a molecular mechanism to explain the homeostatic modulation of ionic conductance in the vertebrate cortex has been identified. In the presence of brain-derived neurotrophic factor (BDNF), effects of TTX on intrinsic excitability were blocked, consistent with an inhibitory role of BDNF in this form of homeostatic functional plasticity (Desai *et al.*, 1999b). These investigations in rat cortex (Desai *et al.*, 1999a; Desai *et al.*, 1999b) build upon previous research with invertebrates, in which lobster stomatogastric

ganglion neurons (STG) were dissociated from their neural circuits *in vivo* and cultured (Turrigiano *et al.*, 1994; Turrigiano *et al.*, 1995). As a result of isolation in culture, these STG neurons rebalanced their ion channels, thereby switching their firing patterns from tonic to bursting (Turrigiano *et al.*, 1994; Turrigiano *et al.*, 1995). A similar phenomenon was revealed by sub-blocking voltage-gated sodium channels of dissociated cerebellar Purkinje neurons with TTX, ultimately leading to a homeostatic decrease in K^+ currents (Swensen and Bean, 2005). Ion channels were also homeostatically rebalanced due to the loss of K^+ currents in cortical pyramidal neurons of *KCND2* mutant mice (Nerbonne *et al.*, 2008), the gain of K^+ currents in STG neurons of lobsters (MacLean *et al.*, 2003), and the loss of K^+ currents in motor neurons of *shal* mutant flies (Bergquist *et al.*, 2010; Parrish *et al.*, 2014). Hence, the homeostatic modulation of ionic conductance appears to be broadly conserved across metazoan evolution. Nevertheless, additional research into the molecular mechanisms underlying this form of homeostatic functional plasticity should be carried out, as they are largely unknown (Spitzer, 2012; Parrish *et al.*, 2014).

Synaptic scaling is a bidirectional form of homeostatic functional plasticity, which modifies the cell surface abundance of various neurotransmitter receptors to counteract perturbations in neural activity (Turrigiano, 2008). In response to long-term suppression of neural activity with TTX or 6-cyano-7-nitroquinoxaline-2,3-dione (CNQX), quantal size was homeostatically increased at cortical synapses *in vitro* (Turrigiano *et al.*, 1998; Watt *et al.*, 2000). Conversely, chronic enhancement of neural activity with a $GABA_A$ receptor antagonist, bicuculline, induced a homeostatic decrease in quantal size at these cortical synapses in culture (Turrigiano *et al.*, 1998; Watt *et al.*, 2000). Similar scaling of quantal size following application of picrotoxin, a $GABA_A$ receptor antagonist, was also reported

in studies with cultured rat hippocampal (Lissin *et al.*, 1998) and spinal neurons (O'Brien *et al.*, 1998). Via microscopy (Lissin *et al.*, 1998; O'Brien *et al.*, 1998) and pharmacology (Lissin *et al.*, 1998; O'Brien *et al.*, 1998; Turrigiano *et al.*, 1998), this scaling of miniature excitatory postsynaptic currents (mEPSCs) was attributed to the surface levels of AMPA receptors on the postsynaptic plasma membrane (Turrigiano, 2008). Moreover, cortical synapses, cultured in TTX as in (Turrigiano *et al.*, 1998; Watt *et al.*, 2000), were shown to downscale the synaptic abundance of $GABA_A$ receptors and concomitantly decrease the size of miniature inhibitory postsynaptic currents (mIPSCs) (Kilman *et al.*, 2002). In a later report, TTX-induced downscaling of $GABA_A$ receptors in hippocampal synapses *in vitro* was shown to be regulated by BDNF (Swanwick *et al.*, 2006). In an earlier study, BDNF was also found to block the effects of TTX on synaptic scaling in cultured cortical pyramidal neurons and to boost quantal size in cultured interneurons (Rutherford *et al.*, 1998). Given the bidirectional requirements of BDNF on synaptic scaling (Rutherford *et al.*, 1998; Swanwick *et al.*, 2006) and a role for BDNF in modulating intrinsic excitability (Desai *et al.*, 1999b), it is plausible that these forms of homeostatic functional plasticity share evolutionary origins. However, numerous other factors, including tumor necrosis factor-alpha (TNF-α) (Stellwagen and Malenka, 2006; Kaneko *et al.*, 2008), β3 integrin (Cingolani *et al.*, 2008), Arc (Shepherd *et al.*, 2006), major histocompatibility complex 1 (MHC1) (Goddard *et al.*, 2007), retinoic acid (Aoto *et al.*, 2008; Maghsoodi *et al.*, 2008), cadherin/β-catenin signaling (Okuda *et al.*, 2007), CaMKIV (Ibata *et al.*, 2008), CaMKII (Thiagarajan *et al.*, 2002), Polo-like kinase 2, cyclin-dependent kinase 5 (Seeburg *et al.*, 2008), MeCP2 (Blackman *et al.*, 2012; Qiu *et al.*, 2012), presenilin 1/Akt signaling (Pratt *et al.*, 2011), neuronal activity-regulated protein (Narp) (Chang *et al.*, 2010), calcineurin

(Kim and Ziff, 2014), PICK1 (Anggono *et al.*, 2011), GRIP1 (Gainey *et al.*, 2015; Tan *et al.*, 2015), stargazin (a TARP) (Louros *et al.*, 2014), fragile X mental retardation protein (FMRP) (Soden and Chen, 2010), guanylate kinase-associated protein (GKAP) (Shin *et al.*, 2012), SUMOylation (Craig *et al.*, 2012), two DNA methyltransferases (Meadows *et al.*, 2015), and caspase-3 (Lo *et al.*, 2015) were all implicated in synaptic scaling. Thus, delineating the complexities of this signaling milieu requires more research into synaptic scaling and homeostatic functional plasticity in general. As homeostatic regulation of ion channels may be conserved from invertebrates to vertebrates (Turrigiano, 1999; Marder and Goaillard, 2006), so, too, may be synaptic scaling. *Drosophila* NMJs with decreased innervation exhibited homeostatic elevation of quantal size (Davis and Goodman, 1998), while *C. elegans* with decreased neurotransmitter release upregulated the expression of postsynaptic glutamate receptors (Grunwald *et al.*, 2004). Therefore, genetic analysis of synaptic scaling in simpler animal models may accelerate an understanding of this form of homeostatic functional plasticity by revealing candidate sensors or effectors to test in vertebrates and by helping to develop a parsimonious signaling model of the homeostat.

Like synaptic scaling (Turrigiano, 2008), a third subtype of homeostatic functional plasticity, referred to as presynaptic homeostasis, is widely characterized at a molecular level (Davis and Müller, 2015). As a term, presynaptic homeostasis encompasses either the potentiation (Petersen *et al.*, 1997; Frank *et al.*, 2006) or the depression (Daniels *et al.*, 2004; Gaviño *et al.*, 2015) of neurotransmitter release to rebalance synaptic function in response to a perturbation (Davis and Müller, 2015). Presynaptic homeostasis is best understood at the fly NMJ (Davis and Müller, 2015; Gaviño *et al.*, 2015), as described in detail in the following paragraphs. Yet, many studies are consistent with the existence of

presynaptic homeostasis at vertebrate synapses. Electrophysiological experiments from NMJs of patients with myasthenia gravis showed that decreased quantal size was offset by elevated neurotransmitter release (quantal content) from presynaptic nerve terminals (Cull-Candy *et al.*, 1980; Plomp *et al.*, 1995). Rodent myasthenic NMJs were also found to express this form of presynaptic homeostasis (Plomp *et al.*, 1992; Plomp *et al.*, 1995; Sandrock *et al.*, 1997), pointing to some evolutionary conservation at mammalian NMJs (Davis and Müller, 2015). From genetic analyses in mice, the homeostatic enhancement of quantal content at myasthenic NMJs was disrupted by mutations in Munc18 (Sons *et al.*, 2003), a key component of the synaptic vesicle fusion machinery (Hata *et al.*, 1993; Pevsner *et al.*, 1994), and alpha-Neurexin (Sons *et al.*, 2006), a cell adhesion molecule (Ushkaryov *et al.*, 1992) with links to neuropsychiatric disease (Südhof, 2008; Pak *et al.*, 2015). There is also considerable evidence for presynaptic homeostasis, which is not a secondary consequence of homeostatic structural plasticity (Murthy *et al.*, 2001), in the vertebrate brain (Davis and Müller, 2015). Neural activity silencing via Kir2.1 in cultured hippocampal neurons triggered a homeostatic increase in the size of the recycling pool of synaptic vesicles and a parallel increase in the frequency of mEPSCs (Burrone *et al.*, 2002). However, reminiscent of studies on neural-activity based competition (Hua *et al.*, 2005) and homeostatic structural plasticity (Smear *et al*., 2007) in zebrafish, presynaptic homeostasis in Kir2.1-expressing hippocampal neurons was elicited only after synapse formation (Burrone *et al.*, 2002). Consistent with an influence of developmental stage on presynaptic homeostasis, and maybe homeostatic functional plasticity in general (Desai *et al.*, 2002), Kir2.1-expression in hippocampal neurons before synapse formation led to a decreased number of functional synaptic inputs onto those cells (Burrone *et al.*, 2002).

Unlike presynaptic homeostasis at mammalian NMJs (Sons *et al.*, 2003; Sons *et al.*, 2006) and homeostatic structural plasticity at zebrafish retinotectal synapses (Smear *et al.*, 2007; Auer *et al.*, 2015), presynaptic homeostasis at Kir2.1-inhibited hippocampal synapses has not been associated with an underlying molecular mechanism (Burrone *et al.*, 2002; Davis and Müller, 2015). An intriguing explanation for this phenomenon stems from experiments in more physiological hippocampal circuits (Kim and Tsien, 2008; Kim and Ryan, 2010; Mitra *et al.*, 2011; Kim and Ryan, 2013). Chronic suppression of neural activity via TTX enhanced quantal size at CA3-CA1 (Schaffer collateral) synapses of rat organotypic hippocampal slice cultures, consistent with synaptic scaling (Kim and Tsien, 2008). Conversely, though, application of TTX led to enhancements in the probability of neurotransmitter release at mossy fiber synapses and recurrent CA3-CA3 synapses, as shown by augmented synaptic depression, in the same hippocampal slice cultures (Kim and Tsien, 2008). The enhancement of neurotransmitter release probability is thought to influence presynaptic homeostasis at other synapses (Frank *et al.*, 2006; Kim and Ryan, 2010; Müller and Davis, 2012; Kim and Ryan, 2013) and may indicate the expression of presynaptic homeostasis in this subset of hippocampal circuits (Kim and Tsien, 2008). A series of subsequent experiments in organotypic hippocampal slices, cultured in TTX as in (Kim and Tsien, 2008), point to an acute role for Cdk5 activity in functionally silencing some TTX-treated recurrent CA3-CA3 synapses and simultaneously boosting release of neurotransmitter from other recurrent CA3-CA3 synapses in this same network (Mitra *et al.*, 2011). This study is largely consistent with a diversity of functions for Cdk5 signaling in limiting quantal content at CA3-CA1 synapses through inhibitory effects on Ca^{2+} influx (Kim and Ryan, 2013) and the recycling pool of synaptic vesicles (Kim and Ryan, 2010).

The control of recycling pool size by Cdk5 may be homeostatically regulated, as chronic treatment of CA3-CA1 synapses *in vitro* with TTX led to decreased presynaptic levels of Cdk5 and an associated enlargement of the recycling pool of synaptic vesicles (Kim and Ryan, 2010). This effect of Cdk5 activity on the recycling pool was mediated through the phosphorylation of synapsin I, a known Cdk5 substrate (Verstegen *et al.*, 2014). Loss of Cdk5 activity may also contribute to this form of presynaptic homeostasis, referred to as presynaptic homeostatic scaling (Kim and Ryan, 2010), by elevating Ca^{2+} influx through presynaptic CaV2.2 channels (Kim and Ryan, 2013). This effect of Cdk5 signaling might underlie the TTX-induced enhancement of neurotransmitter release probability at mossy fiber synapses and recurrent CA3-CA3 synapses (Kim and Tsien, 2008), which failed to augment synaptic depression in the presence of the Cdk5 inhibitor, roscovitine (Mitra *et al.*, 2011). Despite the apparent congruence of these studies (Kim and Tsien, 2008; Kim and Ryan, 2010; Mitra *et al.*, 2011; Kim and Ryan, 2013; Verstegen *et al.*, 2014), it must be noted that contradictions exist in the current literature. In particular, Cdk5 activity has been found to promote Ca^{2+} influx and the docking of release-ready synaptic vesicles in cultured hippocampal neurons (Su *et al.*, 2012): results which are in direct opposition to other findings (Kim and Ryan, 2010; Kim and Ryan, 2013; Verstegen *et al.*, 2014). Also, roscovitine elevated basal neurotransmitter release in cultured CA3-CA1 synapses (Kim and Ryan, 2010; Kim and Ryan, 2013), but not in recurrent CA3-CA3 synapses in slices (Mitra *et al.*, 2011). Moreover, roscovitine has been seen to exhibit possibly confounding off-target effects on different Ca^{2+} channels (Yan *et al.*, 2002; Mitra *et al.*, 2011; Yazawa *et al.*, 2011) and kinases (Bach *et al.*, 2005). Thus, Cdk5 activity may differentially affect presynaptic homeostasis across neural or signaling networks in time (Mitra *et al.*, 2011).

From numerous investigations, it has become widely accepted that three forms of homeostatic functional plasticity may be expressed in the nervous system of vertebrates (Marder and Goaillard, 2006; Turrigiano, 2008; Davis and Müller, 2015). Nevertheless, it is presently unclear if the three forms of homeostatic functional plasticity are just distinct manifestations of a single homeostat, comprised of the same sensors and effectors, or if homeostatic functional plasticity has convergently evolved multiple times from separable underlying mechanisms. There are lines of evidence to buttress the former theory. Cdk5 signaling has been linked to presynaptic homeostasis (Kim and Ryan, 2010; Mitra *et al.*, 2011; Kim and Ryan, 2013; Verstegen *et al.*, 2014) and synaptic scaling (Seeburg *et al.*, 2008). Furthermore, Munc18, a canonical Cdk5 substrate (Shuang *et al.*, 1998; Fletcher *et al.*, 1999; Lilja *et al.*, 2004), was found to be essential for presynaptic homeostasis at myasthenic NMJs (Sons *et al.*, 2003). Likewise, calcineurin, which opposes Cdk5 in the control of synaptic vesicle pool composition (Kim and Ryan, 2010) and presynaptic Ca^{2+} influx (Kim and Ryan, 2013), has also been implicated in synaptic scaling (Kim and Ziff, 2014). Although such a role has not been uncovered, Cdk5 could also contribute to the homeostatic modulation of ionic conductance by directly phosphorylating numerous ion channels, such as potassium channels (Cerda and Trimmer, 2011; Vacher *et al.*, 2011) and calcium channels (Tomizawa *et al.*, 2002; Su *et al.*, 2012; Kim and Ryan, 2013), or indirectly by disrupting BDNF (Cheung *et al.*, 2007; Lai *et al.*, 2012; Zhang *et al.*, 2014). Along with previously noted roles in synaptic scaling (Rutherford *et al.*, 1998; Swanwick *et al.*, 2006) and ion channel homeostasis (Desai *et al.*, 1999b), postsynaptic release of BDNF was shown to be essential for enhanced neurotransmitter release probability due to AMPA receptor blockade with CNQX, consequently also linking BDNF to presynaptic

homeostasis (Jakawich *et al.*, 2010). β-catenin, a downstream effector of cell adhesion molecules (Peifer and Wieschaus, 1990; Noordermeer *et al.*, 1994), was similarly found to be critical for both synaptic scaling (Okuda *et al.*, 2007) and presynaptic homeostasis (Vitureira *et al.*, 2011). Cdk5 has been found to directly (Kwon *et al.*, 2000; Kesavapany *et al.*, 2001) and indirectly (Chow *et al.*, 2014) regulate the phosphorylation of β-catenin. BDNF was also found to mobilize synaptic vesicles by disrupting a β-catenin interaction with cadherin (Bamji *et al.*, 2006). These results are consistent with a common origin of mechanisms of homeostatic functional plasticity during evolution of the vertebrate brain.

Intriguingly, BDNF treatment also largely phenocopied the effects of chronic TTX treatment on retinal ganglion cell axon arbors in the tadpole visual system (Cohen-Cory, 1999). As discussed earlier, a related neurotrophic factor, Neurotrophin-3, was shown to be necessary for homeostatic structural plasticity in the zebrafish visual system (Auer *et al.*, 2015). Thus, some mechanisms of homeostatic functional plasticity and homeostatic structural plasticity also appear to share evolutionary origins. The mutual histories of the mechanisms of homeostatic plasticity in the vertebrate nervous system may also extend into invertebrates. The aforementioned unmasking of homeostatic structural plasticity by genetically ablating Cdk5 in flies (Kissler *et al.*, 2009) suggests that Cdk5 could serve as a control point in synapse morphogenesis, along with neurotransmitter release (Kim and Ryan, 2010). Impairing *C. elegans* homologs of synaptic scaling molecules (Thiagarajan *et al.*, 2002; Cingolani *et al.*, 2008; Seeburg *et al.*, 2008), CaMKII (Williams *et al.*, 2004; Locke *et al.*, 2008), Cdk5 (Locke *et al.*, 2006), and integrin (Locke *et al.*, 2009), lowered the threshold to PTZ-induced seizures through presynaptic effects. These results might also be consistent with homeostatic functional plasticity in worms (Stawicki *et al.*, 2013).

Presynaptic Homeostasis at the *Drosophila* Neuromuscular Junction

The study of homeostatic functional plasticity in vertebrate model organisms has yielded a wealth of information about brain function (Davis, 2006; Marder and Goaillard, 2006; Turrigiano, 2008; Vitureira *et al.*, 2012; Davis and Müller, 2015) and perhaps best connects these mechanisms to brain disorders (Kamenetz *et al.*, 2003; Houweling *et al.*, 2005; Trasande and Ramirez, 2007). Yet, many assessments of candidate sensors and effectors with potentially homeostatic roles in the vertebrate nervous system were direct continuations of earlier studies, which uncovered roles for these factors in other aspects of synaptic transmission. For example, the role of Cdk5 in presynaptic homeostasis was inferred from measurements of baseline presynaptic function (Kim and Ryan, 2010; Kim and Ryan, 2013), which built upon prior knowledge of presynaptic Cdk5 phosphorylation targets, not limited to N-type Ca^{2+} channels (Su *et al.*, 2012; Kim and Ryan, 2013), P/Q-type Ca^{2+} channels (Tomizawa *et al.*, 2002), amphiphysin I, dynamin I (Tomizawa *et al.*, 2003), synapsin I (Verstegen *et al.*, 2014), and Munc18 (Shuang *et al.*, 1998; Fletcher *et al.*, 1999; Lilja *et al.*, 2004). The association of BDNF to presynaptic homeostasis arose from previous reports (Jakawich *et al.*, 2010), which demonstrated that BDNF treatment can accentuate neurotransmitter release (Tyler and Pozzo-Miller, 2001; Zhang and Poo, 2002). Furthermore, a function of β-catenin in presynaptic homeostasis was inspired by a preceding study, which implicated cadherin/β-catenin in synaptic scaling (Okuda *et al.*, 2007; Vitureira *et al.*, 2011). Considering the limitations of vertebrate model systems for gene isolation (Kile and Hilton, 2005), genetic analysis in invertebrates could offer a less biased and more economical approach in elucidating basic mechanisms of homeostatic processes (Davis and Bezprozvanny, 2001; Frank *et al.*, 2013; Davis and Müller, 2015).

From the advantages afforded by fly genetics (Nüsslein-Volhard and Wieschaus, 1980; Rubin and Spradling, 1982; Yamamoto *et al*., 2014), over 400 candidate mutants have been assessed for defects in a subtype of presynaptic homeostasis and published in an ongoing genetic analysis (Dickman and Davis, 2009; Müller *et al.*, 2011; Davis and Müller, 2015). This genetic analysis has taken advantage of large-scale efforts to disrupt *Drosophila* genes via transposon mutagenesis (Rubin and Spradling, 1982; Spradling *et al.*, 1995; Bellen *et al.*, 2004; Parks *et al.*, 2004; Thibault *et al.*, 2004) and the pioneering characterization of functional properties at *Drosophila* NMJs (Jan and Jan, 1976). These studies of homeostatic functional plasticity in *Drosophila* third instar larvae have focused on an acute form of presynaptic homeostasis, by which reduced postsynaptic sensitivity to glutamate is offset by elevated release of glutamate from presynaptic nerve terminals (Frank *et al.*, 2006; Davis and Müller, 2015). Here, this phenomenon is called short-term homeostatic potentiation, referred to in prior studies as “synaptic homeostasis” (Frank *et al.*, 2006; Goold and Davis, 2007; Dickman and Davis, 2009), to distinguish it from long-term homeostatic potentiation (Petersen *et al.*, 1997; Davis *et al.*, 1998; DiAntonio *et al.*, 1999) and homeostatic depression (Daniels *et al.*, 1994; Gaviño *et al.*, 2015). Long-term homeostatic potentiation was revealed from electrophysiological recordings at fly NMJs, which carry an amorphic allele of *GluRIIA*, the gene encoding an essential subunit of a subset of postsynaptic glutamate receptors (Petersen *et al.*, 1997). Like the acute form of homeostatic potentiation (Frank *et al.*, 2006; Davis and Müller, 2015), this long-term form of homeostatic potentiation in amorphic *GluRIIA*^{SP16} mutants augments glutamate release to maintain a set point level of synaptic transmission (Petersen *et al.*, 1997). A direct mutation of the *GluRIIA* gene locus is not required for the expression of long-term

homeostatic potentiation, as perturbing the function of GluRIIA through protein kinase A activity (Davis *et al.*, 1998), p21-activated kinase impairment (Albin and Davis, 2004), or NF-kappaB signaling disruption (Heckscher *et al.*, 2007) also led to enhanced glutamate release. Given the requirement of placing GluRIIA-altering mutations in different genetic backgrounds, long-term homeostatic potentiation is fundamentally recalcitrant to genetic screens (Frank *et al.*, 2006; Davis and Müller, 2015). The discovery that acute treatment of semi-intact fly larval preparations with a glutamate receptor antagonist, philanthotoxin (PhTx), induces short-term homeostatic potentiation in as little as ten minutes (Frank *et al.*, 2006) has largely overcome a requirement for genetic screens with *GluRIIA* mutants and speeded the isolation of homeostatic signaling molecules (Davis and Müller, 2015).

Of the greater than 400 *Drosophila* mutants examined for short-term homeostatic potentiation deficits so far, thirteen hits showing normal basal synaptic transmission and NMJ morphogenesis were isolated (Dickman and Davis, 2009; Müller *et al.*, 2011; Davis and Müller, 2015). Through a series of investigations, most of these candidate hits have been independently verified and include dysbindin (Dickman and Davis, 2009), a protein with links to schizophrenia (Straub *et al.*, 2002; Talbot *et al.*, 2004), a trio of K^+ channels (Bergquist *et al.*, 2010), another ion channel and Ca^{2+}-binding protein with no previously known roles (Dickman and Davis, 2009), Rab3-GTPase-activating protein (GAP) (Müller *et al.*, 2011), a factor with effects on microcephaly and intellectual disability (Aligianis *et al.*, 2005; Aligianis *et al.*, 2006), a pair of Degenerin/Epithelial Sodium (ENaC) channels, pickpocket11 and pickpocket16 (Younger *et al.*, 2013), Rab3-interacting molecule (RIM) (Müller *et al.*, 2012), and multiplexin (*Mp*) (Wang *et al.*, 2014), a fly ortholog of Collagen XV/XVIII (Meyer and Moussian, 2009) with implications in epilepsy (Suzuki *et al.*, 2002).

Building on earlier investigations (Wang *et al.*, 1997; Starcevic *et al.*, 2004; Talbot *et al.*, 2006; Liu *et al.*, 2011), this ongoing genetic screen (Dickman and Davis, 2009; Müller *et al.*, 2011) also led to the discovery of functions for RIM-binding protein (RBP) (Müller *et al.*, 2015) and snapin (Dickman *et al.*, 2012) in homeostatic potentiation through a more candidate-based approach (Davis and Müller, 2015). Further experiments with some of these mutants also uncovered deficits in long-term homeostatic potentiation, as induced by *GluRIIA*^{SP16} (Petersen *et al.*, 1997; Dickman and Davis, 2009; Bergquist *et al.*, 2010; Müller *et al.*, 2011; Younger *et al.*, 2013; Wang *et al.*, 2014). Hence, a failure to express short-term homeostatic potentiation might universally predict an impairment in long-term homeostatic potentiation. These data further point to an evolutionary conservation of the underlying phenomenology of homeostatic potentiation in flies (Davis and Müller, 2015).

An ongoing genetic screen in *Drosophila* (Dickman and Davis, 2009; Müller *et al.*, 2011) has made it possible to rapidly assemble an inventory of homeostatic potentiation factors (Davis and Müller, 2015). Additional experiments with the validated hits from this screen have led to insights about the basic phenomenology of presynaptic homeostasis, which may extend to vertebrates (Davis, 2013; Davis and Müller, 2015). This innovative genetic analysis of presynaptic homeostasis was conceived from the demonstration that loss-of-function mutations in *cacophony*, the gene encoding the *Drosophila* ortholog of a presynaptic CaV2.1 calcium channel (Smith *et al.*, 1996; Kawasaki *et al.*, 2000), blocked short-term and long-term homeostatic potentiation (Frank *et al*., 2006). Because CaV2.1 localization is confined to active zones (Kawasaki *et al.*, 2004), these findings confirmed that homeostatic potentiation at *Drosophila* NMJs is driven by a previously hypothesized (Petersen *et al.*, 1997) trans-synaptic signaling system (Frank *et al.*, 2006; Davis, 2006).

This genetic analysis of *cacophony* also showed that homeostatic potentiation can fail to restore a set point level of synaptic transmission when the amplitude of baseline evoked responses is comparable to wild type (Frank *et al.*, 2006). Therefore, the mechanisms of homeostatic potentiation and basal neurotransmitter release can be distinguished at the molecular level (Frank *et al.*, 2006). In a follow-up report, the expression of homeostatic potentiation was correlated with an enhancement of presynaptic Ca^{2+} influx, which failed to occur in loss-of-function *cacophony* mutants (Müller and Davis, 2012). Accordingly, a homeostatic modulation of Ca^{2+} influx through a presynaptic CaV2.1 channel appears to be critical for homeostatic potentiation in *Drosophila* (Müller and Davis, 2012; Davis and Müller, 2015). A similar phenomenon was shown to compensate for the effects of neural activity blockade with TTX in dissociated hippocampal cultures (Zhao *et al.*, 2011). Cdk5 may also influence a TTX-induced homeostatic accentuation of neurotransmitter release (Kim and Ryan, 2010) through effects on CaV2.2 (Su *et al.*, 2012; Kim and Ryan, 2013). This mechanism of presynaptic homeostasis could be conserved from flies to mammals.

More recent advancements from work in *Drosophila* further implicate presynaptic Ca^{2+} influx modulation in the mechanisms of presynaptic homeostasis. In a continuation of the PhTx-based genetic screen (Frank *et al.*, 2006; Dickman and Davis, 2009; Müller *et al.*, 2011), two cotranscribed ENaC channels, pickpocket 11 and pickpocket 16, were shown to be acutely necessary in the presynaptic motor neuron for short-term and long-term homeostatic potentiation (Younger *et al.*, 2013). Through the same technique used in (Müller and Davis, 2012), investigators found that acute pharmacological inhibition of these ENaC channels with benzamil (Liu *et al.*, 2003) blocked the homeostatic elevation of presynaptic Ca^{2+} influx coinciding with genetic loss of GluRIIA (Younger *et al.*, 2013).

These results were buttressed by a genetic analysis, which showed that loss-of-function mutations in or RNA interference (Fire *et al.*, 1998; Liu *et al.*, 2013) against either ENaC channel similarly blocked homeostatic potentiation (Younger *et al.*, 2013). The proposed model from this research suggests that pickpocket 11 and pickpocket 16 are subunits of an ion channel, which is inserted into the presynaptic plasma membrane to depolarize it and increase Na^+ influx (Younger *et al.*, 2013). A resulting change in presynaptic resting membrane potential, consistent with work at the calyx of Held (Awatramani *et al.*, 2005), could directly or indirectly generate a homeostatic increase in Ca^{2+} influx presynaptically (Younger *et al.*, 2013) and a joint increase in neurotransmitter release probability (Frank *et al.*, 2006). This attractive model requires further testing, however, as there is no direct evidence for presynaptic ENaC channel trafficking at the NMJ (Davis and Müller, 2015). Mutations that ablate the C-terminus of multiplexin, which has a proteolytically cleavable endostatin (O'Reilly *et al.*, 1997) domain, were also found to interfere with expression of homeostatic potentiation at the fly NMJ through effects on CaV2.1 and presynaptic Ca^{2+} influx (Wang *et al.*, 2014). These results indicate that endostatin serves as a retrograde signal for homeostatic potentiation (Wang *et al.*, 2014) and may regulate ENaC channel or CaV2.1 function presynaptically (Davis and Müller, 2015). This endostatin-dependent homeostatic signaling system may also be analogous to the BDNF-dependent signaling system in rat hippocampal cultures (Jakawich *et al.*, 2010). Notably, multiplexin also has a thrombospondin domain (Wang *et al.*, 2014). Astrocyte-secreted thrombospondins are known to enhance synapse number in cultured retinal ganglion cells (Christopherson *et al.*, 2005). In theory, thrombospondins may influence homeostatic structural plasticity in these highly plastic neurons (Sretavan *et al.*, 1988; Cohen-Cory, 1999; Hua *et al.*, 2005;

Koch *et al.*, 2011; Auer *et al.*, 2015), in addition to presynaptic homeostasis at fly NMJs. Following this line of evidence might foster an understanding of evolutionarily conserved relationships, if any, between homeostatic functional and structural plasticity in neurons.

Although an accentuation of presynaptic Ca^{2+} influx is necessary for homeostatic potentiation at the *Drosophila* NMJ (Müller and Davis, 2012; Younger *et al.*, 2013; Wang *et al.*, 2014), it is apparently not sufficient. RIM proteins are presynaptic scaffolds (Wang *et al.*, 1997; Schoch *et al.*, 2002), which regulate presynaptic Ca^{2+} influx via biochemical interactions with voltage-gated calcium channels in mammals (Kaeser *et al.*, 2011; Han *et al.*, 2011) and flies (Graf *et al.*, 2012; Müller *et al.*, 2012). RIM proteins also determine the number of docked vesicles and, by extension, the size of the RRP (Rosenmund and Stevens, 1996; Imig *et al.*, 2014), at active zones of mammalian (Han *et al.*, 2011; Su *et al.*, 2012), fly (Müller *et al.*, 2012), and *C. elegans* (Weimer *et al.*, 2006; Gracheva *et al.*, 2008; Stigloher *et al.*, 2011) presynaptic nerve terminals. As part of the ongoing genetic screen for presynaptic homeostasis molecules in *Drosophila* (Dickman and Davis, 2009; Müller *et al.*, 2011), ablation of the gene encoding RIM was shown to perturb short-term homeostatic potentiation without impairing the homeostatic enhancement of presynaptic Ca^{2+} influx (Müller *et al.*, 2012). An earlier study correlated an increase in the size of the RRP with the expression of short-term and long-term homeostatic potentiation at the fly NMJ (Weyhersmüller *et al.*, 2011). Subsequently, a PhTx-dependent enlargement of the RRP was found to be blocked in the absence of RIM, indicating that RRP modulation is also necessary for this subtype of presynaptic homeostasis (Müller *et al.*, 2012). Hence, homeostatic potentiation may require a greater number of release-ready vesicles than is docked at baseline to benefit from elevating presynaptic Ca^{2+} influx (Müller *et al.*, 2012).

Based chiefly on the current results from genetic screening (Dickman and Davis, 2009; Müller *et al.*, 2011; Müller *et al.*, 2012), an emerging model points to the existence of distinct signaling processes, which act in parallel to carry out homeostatic potentiation at the *Drosophila* NMJ (Davis and Müller, 2015). Although RIM is needed for a wild type amount of synaptic vesicle docking (Han *et al.*, 2011; Su *et al.*, 2012; Müller *et al.*, 2012) and presynaptic Ca^{2+} influx (Kaeser *et al.*, 2011; Han *et al.*, 2011; Müller *et al.*, 2012), it is selectively required for the modulation of the RRP during homeostatic potentiation, at least in the short-term (Müller *et al.*, 2012). To date, the molecular mechanism by which RIM modulates RRP size during homeostatic potentiation is unknown (Davis and Müller, 2015). A mutation that deletes the conserved zinc finger domain, which is known to bind Munc13 in mammals (Schoch *et al.*, 2002; Südhof, 2012), implies that Munc13 could be involved in homeostatic potentiation (Müller *et al.*, 2012). A plausible mechanism, which could be tested through genetic rescue experiments in *Drosophila* rim^{103} loss-of-function mutants (Müller *et al.*, 2012), might depend on reversing Munc13 homodimerization with RIM (Deng *et al.*, 2011). This model would be supported by the genetic rescue of rim^{103} homeostatic potentiation defects through the expression of constitutively active Munc13 monomers, which may promote neurotransmitter release in the absence of RIM activity.

The association of Rab3-GAP with homeostatic potentiation (Müller *et al.*, 2011) provides an alternative model for RIM function in homeostatic potentiation (Müller *et al.*, 2012). Rab3 is a synaptic vesicle protein and small GTPase (Fischer von Mollard *et al.*, 1990). Rab3-GAP is known to stimulate the GTPase activity of Rab3 and its associated localization to the synaptic vesicle membrane (Sakane *et al.*, 2006). Fly loss-of-function experiments indicate that Rab3-GAP is critical for short-term and long-term homeostatic

potentiation, whereas Rab3 is dispensable for these phenomena (Müller *et al.*, 2011). In follow-up experiments, it was determined that constitutively active Rab3, which does not hydrolyze GTP (Clabecq *et al.*, 2000) and may have phenocopied the loss-of-function of Rab3-GAP, did not disrupt homeostatic potentiation (Müller *et al.*, 2011). Furthermore, a double mutant lacking Rab3 and Rab3-GAP exhibited normal expression of homeostatic potentiation, consistent with Rab3 acting downstream of Rab3-GAP in this phenomenon (Müller *et al.*, 2011). These unexpected results implicate a presently unknown repressor protein in the phenomenology of homeostatic potentiation (Müller *et al.*, 2011; Davis and Müller, 2015). In this model, a hypothetical repressor protein is recruited to active zones by Rab3-GTP, perhaps independent of GTPase activity, and is displaced by Rab3-GAP to allow for homeostatic potentiation (Müller *et al.*, 2011). This model must be reconciled with other reports, which showed that the loss of Rab3 is associated with a redistribution of active zone proteins and an accentuated neurotransmitter release probability (Graf *et al.*, 2009; Peled and Isacoff, 2011). However, Rab3-GAP loss did not affect morphology of the fly NMJ, suggesting that the influence of Rab3 on active zone redistribution is not dependent on Rab3-GAP (Müller *et al.*, 2011). Likewise, RIM ablation also did not affect NMJ morphology, even when examined at a higher resolution via structured illumination microscopy (Müller *et al.*, 2012). As RIM and Rab3-GAP were later shown to genetically interact during short-term homeostatic potentiation (Müller *et al.*, 2012), it is conceivable that RIM and Rab3-GAP act together to modulate the RRP size after disrupting GluRIIA. This hypothesis could be addressed by testing the RRP size after PhTx exposure, as in (Weyhersmüller *et al.*, 2011; Müller *et al.*, 2012), at Rab3-GAP-deficient NMJs. Ablating Rab3 in rim^{103} mutants (Müller *et al.*, 2012) to determine if homeostatic potentiation can

be expressed, as in (Müller *et al.*, 2011), could further test this hypothesis. It might also be important to verify that active zone size is concomitantly enlarged with the RRP size during homeostatic potentiation, as was indicated by structured illumination microscopy (Weyhersmüller *et al.*, 2011), and to determine the effects of a hypothetical Rab3-GAP/ RIM signaling axis on these covert structural alterations to the NMJ. This analysis could also further elucidate evolutionary links between the homeostatic modulation of synaptic form and physiology (Davis and Goodman, 1998; Murthy *et al.*, 2001; Keck *et al.*, 2013).

Despite a significant involvement of presynaptic homeostasis molecules, such as CaV2.1 (Frank *et al.*, 2006), multiplexin (Wang *et al.*, 2014), Rab3, Rab3-GAP (Müller *et al.*, 2011), and RIM (Müller *et al.*, 2012), in basal synaptic transmission, there is growing evidence for a distinction between baseline function and homeostatic potentiation at the molecular level. In a genetic analysis of cysteine string protein (CSP) and syntaxin, both canonically required for normal amounts of neurotransmitter release through roles in the presynaptic SNARE complex (Fernández-Chacón *et al.*, 2004; Sharma *et al.*, 2011), the expression of homeostatic potentiation in response to PhTx treatment occurred normally (Goold and Davis, 2007). PhTx similarly triggered short-term homeostatic potentiation in the absence of liprin-alpha, miro, endophilin, synaptojanin, and other regulators of basal neurotransmitter release in the search for presynaptic homeostasis molecules (Dickman and Davis, 2009; Müller *et al.*, 2011). Regardless, a molecular distinction between basal synaptic transmission and homeostatic potentiation is clearest in the study of multiplexin (Wang *et al.*, 2014). In $dmp^{\Delta C}$ mutants, which lack the endostatin-containing C-terminus of multiplexin (Meyer and Moussian, 2009) and had defects in homeostatic potentiation, quantal content was comparable to wild type controls over a range of extracellular Ca^{2+}

concentrations (Wang *et al.*, 2014). RNA interference against snapin also disrupted the expression of homeostatic potentiation without interfering with the Ca^{2+} cooperativity or sensitivity of neurotransmitter release (Dickman *et al.*, 2012). Though, contrary to these findings, genetic disruptions of Rab3-GAP and the snapin-interacting protein, dysbindin, coincided with significantly reduced quantal contents in low extracellular Ca^{2+} (0.2 mM – 0.3 mM Ca^{2+}), wild type quantal contents in higher extracellular Ca^{2+} (0.4 mM – 0.5 mM Ca^{2+}), and homeostatic potentiation impairments in higher extracellular Ca^{2+} (0.4 mM – 0.5 mM Ca^{2+}) (Dickman and Davis, 2009; Müller *et al.*, 2011). Homeostatic potentiation was blocked by the loss of Rab3-GAP or dysbindin when the recording conditions led to normal quantal contents (Dickman and Davis, 2009; Müller *et al.*, 2011), consistent with a molecular distinction of basal synaptic transmission from homeostatic potentiation, as suggested earlier (Frank *et al.*, 2006; Goold and Davis, 2007). Yet, the effects of Rab3-GAP and dysbindin on the Ca^{2+}-dependence of neurotransmitter release and short-term synaptic plasticity (Dickman and Davis, 2009; Müller *et al.*, 2011) preclude the definitive separation of these abnormalities from homeostatic potentiation deficits in these reports. As previously stated (Müller *et al.*, 2011), similarities between Rab3-GAP and dysbindin function at the fly NMJ do, however, imply a shared role for these proteins in the control of neurotransmitter release. Such an interaction may also implicate a common signaling network in clinically distinct neurological diseases at present (Straub *et al.*, 2002; Talbot *et al.*, 2004; Aligianis *et al.*, 2005; Aligianis *et al.*, 2006; Müller *et al.*, 2011). Investigating roles of dysbindin or the interactor, snapin (Starcevic *et al.*, 2004; Dickman *et al.*, 2012), in the homeostatic modulation of RRP size (Weyhersmüller *et al.*, 2011) could clarify the relationship among these factors and Rab3/RIM (Müller *et al.*, 2011; Müller *et al.*, 2012).

Homeostatic potentiation at the *Drosophila* NMJ might be orchestrated by parallel signaling pathways, which regulate either the number of release-ready synaptic vesicles (Weyhersmüller *et al.*, 2011; Müller *et al.*, 2012) or the amount of presynaptic Ca^{2+} influx (Frank *et al.*, 2006; Müller and Davis, 2012; Younger *et al.*, 2013; Wang *et al.*, 2014), in response to perturbed postsynaptic sensitivity to glutamate (Petersen *et al.*, 1997; Davis and Müller, 2015). However, a continued genetic analysis of a RIM interactor, RBP (Liu *et al.*, 2011), has suggested that the underlying mechanisms of homeostatic potentiation are coordinated at the molecular level (Müller *et al.*, 2015). Along with exhibiting severe impairments in basal neurotransmitter release, wherein evoked responses could not be detected under usual electrophysiological recording conditions (0.4 mM – 0.5 mM Ca^{2+}) (Liu *et al.*, 2011), an amorphic mutation in the gene encoding RBP abolished short-term homeostatic potentiation over a wide range of extracellular Ca^{2+} concentrations (1 mM – 15 mM Ca^{2+}) (Müller *et al.*, 2015). Consistent with plausible effects on CaV2.1 (Frank *et al.*, 2006; Müller and Davis, 2012), ENaC channels (Younger *et al.*, 2013), or multiplexin (Wang *et al.*, 2014), the loss of RBP blocked the homeostatic modulation of presynaptic Ca^{2+} influx (Müller *et al.*, 2015). In addition, RBP loss similarly impaired the homeostatic modulation of RRP size, consistent with effects on RIM (Müller *et al.*, 2012; Müller *et al.*, 2015). Thus, RBP appears to govern both of the physiological processes of homeostatic potentiation, at least in the short-term (Müller *et al.*, 2015). Interestingly, larvae carrying heterozygous amorphic mutations in *rbp* and *rim* had normal homeostatic potentiation in PhTx, consequently implying that RBP and RIM might not directly interact in this context (Müller *et al.*, 2015). Following this strategy with other mutants, doubly heterozygous for rbp^{STOP} and a second homeostasis mutant allele, should better define signaling systems

involved in homeostatic potentiation. Moreover, removing Rab3 in *rbp* nulls to determine if homeostatic potentiation can be partially or fully restored, as observed with Rab3-GAP mutants (Müller *et al.*, 2011), may also better address a potential role of Rab3-GAP/RIM signaling (Müller *et al.*, 2012) in this phenomenon. If enlargement of active zones during homeostatic potentiation (Weyhersmüller *et al.*, 2011) can be reproduced, then a strong candidate for regulating this process is RBP, which has previously been associated with ultrastructural changes to the active zone at baseline (Liu *et al.*, 2011). As suggested, it is plausible that such changes account for the homeostatic elevation of RRP size during homeostatic potentiation (Weyhersmüller *et al.*, 2011). Altered active zone ultrastructure in *rbp* nulls (Liu *et al.*, 2011) or in homeostatic potentiation (Weyhersmüller *et al.*, 2011) could in theory be related to the effects of Rab3 on active zone redistribution, which are known to alter neurotransmitter release probability (Graf *et al.*, 2009; Peled and Isacoff, 2011). Taken together, these data may help to develop a parsimonious signaling model of a homeostat regulating multiple forms of homeostatic plasticity in the nervous system.

By utilizing a suite of electrophysiological, microscopical, and genetic techniques, the phenomenological basis of homeostatic potentiation at the fly NMJ is largely known (Davis and Müller, 2015; Müller *et al.*, 2015). Both short-term and long-term homeostatic potentiation are achieved by a coordinated elevation of presynaptic Ca^{2+} influx (Frank *et al.*, 2006; Müller and Davis, 2012; Younger *et al.*, 2013; Wang *et al.*, 2014) and the RRP size (Weyhersmüller *et al.*, 2011; Müller *et al.*, 2012; Müller *et al.*, 2015). These forms of presynaptic homeostasis also share specific effectors, as all mutations that impair short-term homeostatic potentiation also impair the long-term form (Dickman and Davis, 2009; Bergquist *et al.*, 2010; Müller *et al.*, 2011; Younger *et al.*, 2013; Wang *et al.*, 2014) when

tested. However, the reverse of this statement is not supported by the evidence. That is, mutations that block long-term homeostatic potentiation do not necessarily impair short-term homeostatic potentiation (Davis and Müller, 2015). Heterozygous null mutations in or RNA interference against a fly homolog of *pax3/7*, termed *gooseberry*, was shown to block *GluRIIA*^{SP16}-induced, but not PhTx-induced, homeostatic potentiation (Marie *et al.*, 2010). Likewise, a postsynaptic signaling network composed of the target of rapamycin (TOR), eIF4E, and S6 kinase (S6K) was found to be required for long-term homeostatic potentiation (Penney *et al.*, 2012). Conversely, an earlier report demonstrated wild type short-term homeostatic potentiation in the absence of S6K (Cheng *et al.*, 2011). Hence, these data further imply that short-term and long-term homeostatic potentiation may be separable at the molecular level. These differences were attributed to a requirement for enhanced protein synthesis to maintain the expression of homeostatic potentiation over an extended time period, as in *GluRIIA*^{SP16} mutants, but not in the short-term (Marie *et al.*, 2010; Cheng *et al.*, 2011; Penney *et al.*, 2012; Davis and Müller, 2015). Importantly, these results must not be interpreted to mean translational regulators, as in (Penney *et al.*, 2012), or transcription factors, as in (Marie *et al.*, 2010), only participate in the long-term form of homeostatic potentiation. Indeed, activation of the Mad transcription factor through BMP signaling (Aberle *et al.*, 2002; Marqués *et al.*, 2002) was found to gate the expression of short-term homeostatic potentiation (Goold and Davis, 2007). The role of BMP in PhTx-induced homeostatic potentiation may be related to a previously identified role for CaMKII, which acts in muscles to inhibit a presynaptic BMP receptor-dependent retrograde signaling system that elevates glutamate release (Haghighi *et al.*, 2003). The strength of this retrograde signal, probably BMP/glass bottom boat (Gbb) itself (McCabe

et al., 2003; Goold and Davis, 2007), was inversely correlated with postsynaptic CaMKII activity and was found to affect the expression of homeostatic potentiation, induced with a dominant-negative GluRIIA (Haghighi *et al.*, 2003). A theory to parsimoniously explain these seemingly disparate results is that synthesis of postsynaptic CaMKII may depend on a TOR/eIF4E/S6K signaling axis, as seen in dendrites (Bagni *et al.*, 2000; Schratt *et al.*, 2004). CaMKII activity in muscles may also influence the synthesis of a homeostatic retrograde signal by functioning upstream of the ribosome, as in the cortex (Wang *et al.*, 2013). However, because short-term homeostatic potentiation apparently requires BMP signaling (Goold and Davis, 2007), but not S6K function (Cheng *et al.*, 2011), the milieu of retrograde/trans-synaptic signals might differ in some manner between the two forms of homeostatic potentiation. Nonetheless, studies also point to a role for CaMKII activity in synaptic scaling at hippocampal synapses (Thiagarajan *et al.*, 2002) and potentially a form of homeostatic functional plasticity at nematode NMJs (Williams *et al.*, 2004; Locke *et al.*, 2008). Dendritic TOR activity also directs synthesis of a retrograde signal, BDNF, in the AMPA receptor-dependent form of hippocampal presynaptic homeostasis (Henry *et al.*, 2012). Thus, further exploring this emerging model of homeostatic potentiation in flies could shed light on evolutionarily conserved mechanisms of homeostatic functional plasticity. Precisely defining the effects of gooseberry/Wnt signaling (Marie *et al.*, 2010), TOR/eIF4E/S6K signaling (Cheng *et al.*, 2011; Penney *et al.*, 2012), BMP/Gbb signaling (McCabe *et al.*, 2003; Goold and Davis, 2007), and CaMKII (Haghighi *et al.*, 2003) with presynaptic Ca^{2+} imaging, as in (Müller and Davis, 2012; Younger *et al.*, 2013; Wang *et al.*, 2014), or estimating RRP size, as in (Weyhersmüller *et al.*, 2011; Müller *et al.*, 2012; Müller *et al.*, 2015), after acute or chronic GluRIIA perturbations could facilitate this aim.

Acute and sustained forms of homeostatic potentiation can also be separated by involvement of a presynaptic signaling pathway composed of an Eph receptor, ephexin, and the Rho-type small GTPase, Cdc42 (Frank *et al.*, 2009). At third instar larval NMJs, the focus of most studies on presynaptic homeostasis in *Drosophila* (Frank *et al.*, 2013; Wondolowski and Dickman, 2013; Davis and Müller, 2015), this Eph/ephexin-controlled signaling pathway was found to be essential for only long-term homeostatic potentiation (Frank *et al.*, 2009). A loss-of-function mutation in the *ephexin* gene could be genetically rescued by the presynaptic overexpression of *Drosophila* CaV2.1, cacophony, indicating that ephexin somehow controls the function or abundance of this voltage-gated calcium channel during long-term homeostatic potentiation (Frank *et al.*, 2009). These data may be consistent with a model in which ephexin governs CaV2.1 expression, either through transcription or translation, in a homeostatic manner. Yet, this model necessitates more experimentation, as no direct evidence for an influence of ephexin on the expression of CaV2.1 was demonstrated. Notably, Cdc42 was found to cooperate with Cdk5, a known modulator of presynaptic homeostasis (Kim and Ryan, 2010) and biochemical interactor of voltage-gated calcium channels (Su *et al.*, 2012; Kim and Ryan, 2013), in augmenting voltage-gated calcium channel expression (Duhr *et al.*, 2014). An Eph receptor has also been found to direct transcriptional programs through CREB and c-Fos (Sheffler-Collins and Dalva, 2012), both of which are known to be active at the *Drosophila* NMJ (Davis *et al.*, 1996; Sanyal *et al.*, 2002; Collins *et al.*, 2006; Massaro *et al.*, 2009). Accordingly, an Eph/ephexin-dependent transcriptional mechanism could be employed to maintain long-term expression of homeostatic potentiation in flies and mammals. In a broader context, transcriptional or perhaps translational targets modulated by this Eph/ephexin signaling

network or other diverse signaling pathways (Goold and Davis, 2007; Frank *et al.*, 2009; Marie *et al.*, 2010; Cheng *et al.*, 2011; Penney *et al.*, 2012) associated with homeostatic potentiation have not been identified. Thus, a systems biology approach via microarrays (Schena *et al.*, 1995; Wang *et al.*, 2004; Parrish *et al.*, 2014), RNA-seq (Nagalakshmi *et al.*, 2008), or ribosome profiling (Ingolia *et al.*, 2009) might be carried out in the absence of these signaling networks, with and without acute or chronic GluRIIA perturbations, to identify differentially expressed genes. As *pickpocket11* and *pickpocket16* mRNA levels were upregulated by approximately 4-fold in *GluRIIA*^{SP16} mutants (Younger *et al.*, 2013), these ENaC channel genes are strong candidates for transcriptional control through one of the aforementioned signaling pathways. After isolating differentially expressed genes, available mutations (Bellen *et al.*, 2004; Parks *et al.*, 2004; Thibault *et al.*, 2004) in these candidate genes could be tested for disruption of homeostatic potentiation. This strategy should complement the ongoing genetic screen (Dickman and Davis, 2009; Müller *et al.*, 2011) and add to a working model of presynaptic homeostasis (Davis and Müller, 2015).

While homeostatic potentiation is the subject of numerous ongoing and published (Davis and Müller, 2015; Müller *et al.*, 2015) investigations, it is thought to be just one of two subtypes of presynaptic homeostasis at the fly NMJ (Daniels *et al.*, 2004; Gaviño *et al.*, 2015). In contrast to homeostatic potentiation, the second mechanism of presynaptic homeostasis, termed homeostatic depression, reduces presynaptic glutamate release in response to increased quantal size to maintain a set point level of synaptic transmission (Daniels *et al.*, 2004; Gaviño *et al.*, 2015). This phenomenon can be induced as a result of presynaptically overexpressing the vesicular glutamate transporter (VGLUT) (Daniels *et al.*, 2004; Gaviño *et al.*, 2015), which fills synaptic vesicles with glutamate (Bellocchio

et al., 2000; Takamori *et al.*, 2000; Fremeau *et al.*, 2001) as a function of the gene dose (Fremeau *et al.*, 2004; Wojcik *et al.*, 2004; Wilson *et al.*, 2005; Daniels *et al.*, 2006). The phenomenology of homeostatic depression has been uncovered and is not the opposite of homeostatic potentiation (Gaviño *et al.*, 2015). Conversely, homeostatic depression is driven by decreasing the abundance of presynaptic CaV2.1 channels and concomitantly decreasing the amount of presynaptic Ca^{2+} influx without altering the number of release-ready synaptic vesicles in parallel (Gaviño *et al.*, 2015). Likewise, the molecular basis of homeostatic depression could be distinguished from that of homeostatic potentiation, as previously assessed loss-of-function mutations in the genes encoding RIM (Müller *et al.*, 2012; Müller *et al.*, 2015) and CaV2.1 (Frank *et al.*, 2006; Müller and Davis, 2012) failed to interfere with this phenomenon (Gaviño *et al.*, 2015). Moreover, benzamil application, which has been shown to erase the expression of homeostatic potentiation (Younger *et al.*, 2013), did not disrupt the homeostatic response to presynaptic VGLUT upregulation (Gaviño *et al.*, 2015). Investigators also demonstrated that both homeostatic depression and potentiation can be expressed at the same NMJs after treatment with PhTx, further implying that the underlying mechanisms differ between these two forms of presynaptic homeostasis (Gaviño *et al.*, 2015). To date, no mutation has been documented to block homeostatic depression. Yet, an apparent homeostatic reduction in the levels of CaV2.1 at VGLUT-overexpressing presynaptic nerve terminals likely points to a dependence on an active signaling process (Gaviño *et al.*, 2015), consistent with a classical definition of homeostatic synaptic plasticity (Davis, 2006; Davis and Müller, 2015). An acceptance of homeostatic depression as a biologically relevant process could still be strengthened by implicating it in a gene network (Davis *et al.*, 1996; Frank *et al.*, 2006; Auer *et al.*, 2015).

Carrying out a large-scale analysis to identify homeostatic depression genes, like the ongoing quest for homeostatic potentiation genes (Dickman and Davis, 2009; Müller *et al.*, 2011), may not be economical. Given a prerequisite for VGLUT overexpression to trigger homeostatic depression at the fly NMJ, transgenes encoding VGLUT (Daniels *et al.*, 2004) and a neuronal Gal4 driver (Lin and Goodman, 1994; Mahr and Aberle, 2006) would need to be crossed into scores of mutant backgrounds (Bellen *et al.*, 2004; Parks *et al.*, 2004; Thibault *et al.*, 2004), if undertaking a similar strategy as in the homeostatic potentiation screen (Dickman and Davis, 2009; Müller *et al.*, 2011). Yet, a comparatively small-scale genetic screen for homeostatic depression factors could be initiated with the X chromosome, as previously performed (Eberl and Hiliker, 1988; Perrimon *et al.*, 1989; Yamamoto *et al.*, 2014). Alternatively, a more candidate-based analysis for homeostatic depression genes could be carried out after identifying differentially expressed genes in VGLUT overexpressors, relative to wild type, through systems biology (Nagalakshmi *et al.*, 2008; Ingolia *et al.*, 2009; Parrish *et al.*, 2014). It might also be possible to stimulate VGLUT function acutely, which could open the door to large-scale genetic screening, as done with PhTx (Frank *et al.*, 2006; Dickman and Davis, 2009; Müller *et al.*, 2011). Such technology for a rapid induction of homeostatic depression is not currently available, but might be engineered pharmacologically (Thompson *et al.*, 2005; Tamura *et al.*, 2014) or optogenetically (Boyden *et al.*, 2005; Zhang *et al.*, 2006) by altering chloride (Bellocchio *et al.*, 2000; Gradinaru *et al.*, 2010; Wietek *et al.*, 2014) or proton gradients (Chow *et al.*, 2010; Ford and Davis, 2014; Preobraschenski *et al.*, 2014) across the membrane of the synaptic vesicle. Molecular mechanisms underlying homeostatic depression (Daniels *et al.*, 2004; Gaviño *et al.*, 2015), like homeostatic potentiation (Frank *et al.*, 2009; Marie *et*

al., 2010; Cheng *et al.*, 2011; Penney *et al.*, 2012), may vary between acute and chronic forms. Therefore, determining the time course of homeostatic depression at the fly NMJ may allow for a more comprehensive assessment of potential genetic links between the two subtypes of presynaptic homeostasis than was feasible before (Gaviño *et al.*, 2015). Homeostatic depression genes may also be solid candidates to test for roles in a target-specific form of homeostatic plasticity, in which quantal content is similarly reduced as a consequence of muscle hyperinnervation at the fly NMJ (Davis and Goodman, 1998). A link between these seemingly distinct phenomena at the genetic level could further point to a core homeostat, which controls both homeostatic functional and structural plasticity.

A genetic analysis of presynaptic homeostasis in *Drosophila* has unearthed much of what is known about homeostatic plasticity in the nervous system (Frank *et al.*, 2013; Davis and Müller, 2015). The power of *Drosophila* genetics (Rubin and Spradling, 1982; Spradling *et al.*, 1995; Bellen *et al.*, 2004; Parks *et al.*, 2004; Thibault *et al.*, 2004), when coupled with electrophysiological (Jan and Jan, 1976; Davis *et al.*, 1996; Weyhersmüller *et al.*, 2011; Müller *et al.*, 2012), pharmacological (Frank *et al.* 2006), and microscopical (Atwood *et al.*, 1993; Liu *et al.*, 2011; Müller and Davis, 2012) techniques, has made the rapid isolation of presynaptic homeostasis (Petersen *et al.*, 1997) molecules a possibility (Dickman and Davis, 2009; Müller *et al.*, 2011). In no more than a decade of pursuing a molecular and cellular description of homeostatic potentiation at the *Drosophila* NMJ, as many as two dozen genes are now associated with this phenomenon (Davis and Müller, 2015; Müller *et al.*, 2015). Other genes, such as *dystrophin* (van der Plas *et al.*, 2006), a RhoGAP gene and regulator of *dystrophin*, called *crossveinless-c* (Pilgram *et al.*, 2011), and *importin 13* (Giagtzoglou *et al.*, 2009), were found to impede basal neurotransmitter

release and hypothetically also participate in the underlying mechanisms of homeostatic potentiation (Davis and Müller, 2015). A subset of genes, including *cacophony* (Frank *et al.*, 2006; Müller and Davis, 2012), *multiplexin* (Wang *et al.*, 2014), *pickpocket11*, and/or *pickpocket16* (Younger *et al.*, 2013), was found to regulate the homeostatic elevation of presynaptic Ca^{2+} influx during homeostatic potentiation. The gene, *rim*, appears to affect only the homeostatic enlargement of the RRP during homeostatic potentiation (Müller *et al.*, 2012). The gene, *rbp*, was shown to orchestrate both of these compensatory cellular processes during homeostatic potentiation (Müller *et al.*, 2015), while a subset of genes, consisting of *dysbindin* (Dickman and Davis, 2009), *snapin* (Dickman *et al.*, 2012), *rab3-GAP* (Müller *et al.*, 2011), and other unnamed factors (Dickman and Davis, 2009; Müller *et al.*, 2011) have not yet been linked to a specific phenomenological role in presynaptic homeostasis. Hence, future investigations will be required to elucidate how these genes interact in a homeostatic manner. Moreover, in light of the commonalities of homeostatic potentiation in fly NMJ (Davis and Müller, 2015) and mammalian synapses (Jakawich *et al.*, 2010; Kim and Ryan, 2010; Henry *et al.*, 2012; Kim and Ryan, 2013), it is seemingly plausible that the signaling networks underlying this phenomenon have been conserved across metazoan evolution. Similarly, relationships among presynaptic homeostasis and the homeostatic modulation of ion channels (Bergquist *et al.*, 2010; Parrish *et al.*, 2014), synaptic scaling (Thiagarajan *et al.*, 2002; Haghighi *et al.*, 2003), and structural plasticity (Davis and Goodman, 1998; Murthy *et al.*, 2001; Weyhersmüller *et al.*, 2011) may imply that a single regulatory network directs all forms of homeostatic plasticity in the nervous system. The search for homeostatic plasticity factors could shed light on human disease (Davis, 2006; Wondolowski and Dickman, 2013) and may only be at its commencement.

References

Aberle H, Haghighi AP, Fetter RD, McCabe BD, Magalhães TR, Goodman CS. wishful thinking encodes a BMP type II receptor that regulates synaptic growth in Drosophila. Neuron. 2002 Feb 14;33(4):545-58.

Akerboom J, Chen TW, Wardill TJ, Tian L, Marvin JS, Mutlu S, Calderón NC, Esposti F, Borghuis BG, Sun XR, Gordus A, Orger MB, Portugues R, Engert F, Macklin JJ, Filosa A, Aggarwal A, Kerr RA, Takagi R, Kracun S, Shigetomi E, Khakh BS, Baier H, Lagnado L, Wang SS, Bargmann CI, Kimmel BE, Jayaraman V, Svoboda K, Kim DS, Schreiter ER, Looger LL. Optimization of a GCaMP calcium indicator for neural activity imaging. J Neurosci. 2012 Oct 3;32(40):13819-40.

Albin SD, Davis GW. Coordinating structural and functional synapse development: postsynaptic p21-activated kinase independently specifies glutamate receptor abundance and postsynaptic morphology. J Neurosci. 2004 Aug 4;24(31):6871-9.

Aligianis IA, Johnson CA, Gissen P, Chen D, Hampshire D, Hoffmann K, Maina EN, Morgan NV, Tee L, Morton J, Ainsworth JR, Horn D, Rosser E, Cole TR, Stolte-Dijkstra I, Fieggen K, Clayton-Smith J, Mégarbané A, Shield JP, Newbury-Ecob R, Dobyns WB, Graham JM Jr, Kjaer KW, Warburg M, Bond J, Trembath RC, Harris LW, Takai Y, Mundlos S, Tannahill D, Woods CG, Maher ER. Mutations of the catalytic subunit of RAB3GAP cause Warburg Micro syndrome. Nat Genet. 2005 Mar;37(3):221-3.

Aligianis IA, Morgan NV, Mione M, Johnson CA, Rosser E, Hennekam RC, Adams G, Trembath RC, Pilz DT, Stoodley N, Moore AT, Wilson S, Maher ER. Mutation in Rab3 GTPase-activating protein (RAB3GAP) noncatalytic subunit in a kindred with Martsolf syndrome. Am J Hum Genet. 2006 Apr;78(4):702-7.

Alon U, Surette MG, Barkai N, Leibler S. Robustness in bacterial chemotaxis. Nature. 1999 Jan 14;397(6715):168-71.

Anggono V, Clem RL, Huganir RL. PICK1 loss of function occludes homeostatic synaptic scaling. J Neurosci. 2011 Feb 9;31(6):2188-96.

Aoto J, Nam CI, Poon MM, Ting P, Chen L. Synaptic signaling by all-trans retinoic acid in homeostatic synaptic plasticity. Neuron. 2008 Oct 23;60(2):308-20.

Atwood HL, Govind CK, Wu CF. Differential ultrastructure of synaptic terminals on ventral longitudinal abdominal muscles in Drosophila larvae. J Neurobiol. 1993 Aug;24(8):1008-24.

Auer TO, Xiao T, Bercier V, Gebhardt C, Duroure K, Concordet JP, Wyart C, Suster M, Kawakami K, Wittbrodt J, Baier H, Del Bene F. Deletion of a kinesin I motor unmasks a mechanism of homeostatic branching control by neurotrophin-3. Elife. 2015 Jun 15;4.

Awatramani GB, Price GD, Trussell LO. Modulation of transmitter release by presynaptic resting potential and background calcium levels. Neuron. 2005 Oct 6;48(1):109-21.

Bach S, Knockaert M, Reinhardt J, Lozach O, Schmitt S, Baratte B, Koken M, Coburn SP, Tang L, Jiang T, Liang DC, Galons H, Dierick JF, Pinna LA, Meggio F, Totzke F, Schächtele C, Lerman AS, Carnero A, Wan Y, Gray N, Meijer L. Roscovitine targets, protein kinases and pyridoxal kinase. J Biol Chem. 2005 Sep 2;280(35):31208-19.

Bagni C, Mannucci L, Dotti CG, Amaldi F. Chemical stimulation of synaptosomes modulates alpha -Ca2+/calmodulin-dependent protein kinase II mRNA association to polysomes. J Neurosci. 2000 May 15;20(10):RC76.

Bamji SX, Rico B, Kimes N, Reichardt LF. BDNF mobilizes synaptic vesicles and enhances synapse formation by disrupting cadherin-beta-catenin interactions. J Cell Biol. 2006 Jul 17;174(2):289-99.

Beck ES, Gasque G, Imlach WL, Jiao W, Jiwon Choi B, Wu PS, Kraushar ML, McCabe BD. Regulation of Fasciclin II and synaptic terminal development by the splicing factor beag. J Neurosci. 2012 May 16;32(20):7058-73.

Bellen HJ, Levis RW, Liao G, He Y, Carlson JW, Tsang G, Evans-Holm M, Hiesinger PR, Schulze KL, Rubin GM, Hoskins RA, Spradling AC. The BDGP gene disruption project: single transposon insertions associated with 40% of Drosophila genes. Genetics. 2004 Jun;167(2):761-81.

Bellocchio EE, Reimer RJ, Fremeau RT Jr, Edwards RH. Uptake of glutamate into synaptic vesicles by an inorganic phosphate transporter. Science. 2000 Aug 11;289(5481):957-60.

Bergquist S, Dickman DK, Davis GW. A hierarchy of cell intrinsic and target-derived homeostatic signaling. Neuron. 2010 Apr 29;66(2):220-34.

Blackman MP, Djukic B, Nelson SB, Turrigiano GG. A critical and cell-autonomous role for MeCP2 in synaptic scaling up. J Neurosci. 2012 Sep 26;32(39):13529-36.

Boyden ES, Zhang F, Bamberg E, Nagel G, Deisseroth K. Millisecond-timescale, genetically targeted optical control of neural activity. Nat Neurosci. 2005 Sep;8(9):1263-8.

Burrone J, O'Byrne M, Murthy VN. Multiple forms of synaptic plasticity triggered by selective suppression of activity in individual neurons. Nature. 2002 Nov 28;420(6914):414-8.

Cerda O, Trimmer JS. Activity-dependent phosphorylation of neuronal Kv2.1 potassium channels by CDK5. J Biol Chem. 2011 Aug 19;286(33):28738-48.

Chang MC, Park JM, Pelkey KA, Grabenstatter HL, Xu D, Linden DJ, Sutula TP, McBain CJ, Worley PF. Narp regulates homeostatic scaling of excitatory synapses on parvalbumin-expressing interneurons. Nat Neurosci. 2010 Sep;13(9):1090-7.

Chen X, Ganetzky B. A neuropeptide signaling pathway regulates synaptic growth in Drosophila. J Cell Biol. 2012 Feb 20;196(4):529-43.

Cheng L, Locke C, Davis GW. S6 kinase localizes to the presynaptic active zone and functions with PDK1 to control synapse development. J Cell Biol. 2011 Sep 19;194(6):921-35.

Cheung ZH, Chin WH, Chen Y, Ng YP, Ip NY. Cdk5 is involved in BDNF-stimulated dendritic growth in hippocampal neurons. PLoS Biol. 2007 Apr;5(4):e63.

Chow BY, Han X, Dobry AS, Qian X, Chuong AS, Li M, Henninger MA, Belfort GM, Lin Y, Monahan PE, Boyden ES. High-performance genetically targetable optical neural silencing by light-driven proton pumps. Nature. 2010 Jan 7;463(7277):98-102.

Chow HM, Guo D, Zhou JC, Zhang GY, Li HF, Herrup K, Zhang J. CDK5 activator protein p25 preferentially binds and activates GSK3β. Proc Natl Acad Sci U S A. 2014 Nov 11;111(45):E4887-95.

Cingolani LA, Thalhammer A, Yu LM, Catalano M, Ramos T, Colicos MA, Goda Y. Activity-dependent regulation of synaptic AMPA receptor composition and abundance by beta3 integrins. Neuron. 2008 Jun 12;58(5):749-62.

Clabecq A, Henry JP, Darchen F. Biochemical characterization of Rab3-GTPase-activating protein reveals a mechanism similar to that of Ras-GAP. J Biol Chem. 2000 Oct 13;275(41):31786-91.

Cohen-Cory S. BDNF modulates, but does not mediate, activity-dependent branching and remodeling of optic axon arbors in vivo. J Neurosci. 1999 Nov 15;19(22):9996-10003.

Collins CA, Wairkar YP, Johnson SL, DiAntonio A. Highwire restrains synaptic growth by attenuating a MAP kinase signal. Neuron. 2006 Jul 6;51(1):57-69.

Craig TJ, Jaafari N, Petrovic MM, Jacobs SC, Rubin PP, Mellor JR, Henley JM. Homeostatic synaptic scaling is regulated by protein SUMOylation. J Biol Chem. 2012 Jun 29;287(27):22781-8.

Daniels RW, Collins CA, Chen K, Gelfand MV, Featherstone DE, DiAntonio A. A single vesicular glutamate transporter is sufficient to fill a synaptic vesicle. Neuron. 2006 Jan 5;49(1):11-6.

Daniels RW, Collins CA, Gelfand MV, Dant J, Brooks ES, Krantz DE, DiAntonio A. Increased expression of the Drosophila vesicular glutamate transporter leads to excess glutamate release and a compensatory decrease in quantal content. J Neurosci. 2004 Nov 17;24(46):10466-74.

Davis GW. Homeostatic control of neural activity: from phenomenology to molecular design. Annu Rev Neurosci. 2006;29:307-23.

Davis GW. Homeostatic signaling and the stabilization of neural function. Neuron. 2013 Oct 30;80(3):718-28.

Davis GW, Bezprozvanny I. Maintaining the stability of neural function: a homeostatic hypothesis. Annu Rev Physiol. 2001;63:847-69.

Davis GW, DiAntonio A, Petersen SA, Goodman CS. Postsynaptic PKA controls quantal size and reveals a retrograde signal that regulates presynaptic transmitter release in Drosophila. Neuron. 1998 Feb;20(2):305-15.

Davis GW, Goodman CS. Genetic analysis of synaptic development and plasticity: homeostatic regulation of synaptic efficacy. Curr Opin Neurobiol. 1998 Feb;8(1):149-56.

Davis GW, Goodman CS. Synapse-specific control of synaptic efficacy at the terminals of a single neuron. Nature. 1998 Mar 5;392(6671):82-6.

Davis GW, Müller M. Homeostatic control of presynaptic neurotransmitter release. Annu Rev Physiol. 2015;77:251-70.

Davis GW, Schuster CM, Goodman CS. Genetic dissection of structural and functional components of synaptic plasticity. III. CREB is necessary for presynaptic functional plasticity. Neuron. 1996 Oct;17(4):669-79.

del Castillo J, Katz B. Quantal components of the end-plate potential. J Physiol. 1954 Jun 28;124(3):560-73.

Deng L, Kaeser PS, Xu W, Südhof TC. RIM proteins activate vesicle priming by reversing autoinhibitory homodimerization of Munc13. Neuron. 2011 Jan 27;69(2):317-31.

Desai NS, Cudmore RH, Nelson SB, Turrigiano GG. Critical periods for experience-dependent synaptic scaling in visual cortex. Nat Neurosci. 2002 Aug;5(8):783-9.

Desai NS, Rutherford LC, Turrigiano GG. Plasticity in the intrinsic excitability of cortical pyramidal neurons. Nat Neurosci. 1999 Jun;2(6):515-20.

Desai NS, Rutherford LC, Turrigiano GG. BDNF regulates the intrinsic excitability of cortical neurons. Learn Mem. 1999 May-Jun;6(3):284-91.

DiAntonio A, Petersen SA, Heckmann M, Goodman CS. Glutamate receptor expression regulates quantal size and quantal content at the Drosophila neuromuscular junction. J Neurosci. 1999 Apr 15;19(8):3023-32.

Dickman DK, Davis GW. The schizophrenia susceptibility gene dysbindin controls synaptic homeostasis. Science. 2009 Nov 20;326(5956):1127-30.

Dickman DK, Tong A, Davis GW. Snapin is critical for presynaptic homeostatic plasticity. J Neurosci. 2012 Jun 20;32(25):8716-24.

Dombeck DA, Khabbaz AN, Collman F, Adelman TL, Tank DW. Imaging large-scale neural activity with cellular resolution in awake, mobile mice. Neuron. 2007 Oct 4;56(1):43-57.

Duhr F, Déléris P, Raynaud F, Séveno M, Morisset-Lopez S, Mannoury la Cour C, Millan MJ, Bockaert J, Marin P, Chaumont-Dubel S. Cdk5 induces constitutive activation of 5-HT6 receptors to promote neurite growth. Nat Chem Biol. 2014 Jul;10(7):590-7.

Eberl DF, Hilliker AJ. Characterization of X-linked recessive lethal mutations affecting embryonic morphogenesis in Drosophila melanogaster. Genetics. 1988 Jan;118(1):109-20.

Fakler B, Brändle U, Glowatzki E, Zenner HP, Ruppersberg JP. Kir2.1 inward rectifier K+ channels are regulated independently by protein kinases and ATP hydrolysis. Neuron. 1994 Dec;13(6):1413-20.

Fernández-Chacón R, Wölfel M, Nishimune H, Tabares L, Schmitz F, Castellano-Muñoz M, Rosenmund C, Montesinos ML, Sanes JR, Schneggenburger R, Südhof TC. The synaptic vesicle protein CSP alpha prevents presynaptic degeneration. Neuron. 2004 Apr 22;42(2):237-51.

Fire A, Xu S, Montgomery MK, Kostas SA, Driver SE, Mello CC. Potent and specific genetic interference by double-stranded RNA in Caenorhabditis elegans. Nature. 1998 Feb 19;391(6669):806-11.

Fischer von Mollard G, Mignery GA, Baumert M, Perin MS, Hanson TJ, Burger PM, Jahn R, Südhof TC. rab3 is a small GTP-binding protein exclusively localized to synaptic vesicles. Proc Natl Acad Sci U S A. 1990 Mar;87(5):1988-92.

Fletcher AI, Shuang R, Giovannucci DR, Zhang L, Bittner MA, Stuenkel EL. Regulation of exocytosis by cyclin-dependent kinase 5 via phosphorylation of Munc18. J Biol Chem. 1999 Feb 12;274(7):4027-35.

Ford KJ, Davis GW. Archaerhodopsin voltage imaging: synaptic calcium and BK channels stabilize action potential repolarization at the Drosophila neuromuscular junction. J Neurosci. 2014 Oct 29;34(44):14517-25.

Frank CA. Homeostatic plasticity at the Drosophila neuromuscular junction. Neuropharmacology. 2014 Mar;78:63-74.

Frank CA, Kennedy MJ, Goold CP, Marek KW, Davis GW. Mechanisms underlying the rapid induction and sustained expression of synaptic homeostasis. Neuron. 2006 Nov 22;52(4):663-77.

Frank CA, Pielage J, Davis GW. A presynaptic homeostatic signaling system composed of the Eph receptor, ephexin, Cdc42, and CaV2.1 calcium channels. Neuron. 2009 Feb 26;61(4):556-69.

Frank CA, Wang X, Collins CA, Rodal AA, Yuan Q, Verstreken P, Dickman DK. New approaches for studying synaptic development, function, and plasticity using Drosophila as a model system. J Neurosci. 2013 Nov 6;33(45):17560-8.

Fremeau RT Jr, Kam K, Qureshi T, Johnson J, Copenhagen DR, Storm-Mathisen J, Chaudhry FA, Nicoll RA, Edwards RH. Vesicular glutamate transporters 1 and 2 target to functionally distinct synaptic release sites. Science. 2004 Jun 18;304(5678):1815-9.

Fremeau RT Jr, Troyer MD, Pahner I, Nygaard GO, Tran CH, Reimer RJ, Bellocchio EE, Fortin D, Storm-Mathisen J, Edwards RH. The expression of vesicular glutamate transporters defines two classes of excitatory synapse. Neuron. 2001 Aug 2;31(2):247-60.

Gainey MA, Tatavarty V, Nahmani M, Lin H, Turrigiano GG. Activity-dependent synaptic GRIP1 accumulation drives synaptic scaling up in response to action potential blockade. Proc Natl Acad Sci U S A. 2015 Jul 7;112(27):E3590-9.

Gaviño MA, Ford KJ, Archila S, Davis GW. Homeostatic synaptic depression is achieved through a regulated decrease in presynaptic calcium channel abundance. Elife. 2015 Apr 17;4.

Giagtzoglou N, Lin YQ, Haueter C, Bellen HJ. Importin 13 regulates neurotransmitter release at the Drosophila neuromuscular junction. J Neurosci. 2009 Apr 29;29(17):5628-39.

Gnuegge L, Schmid S, Neuhauss SC. Analysis of the activity-deprived zebrafish mutant macho reveals an essential requirement of neuronal activity for the development of a fine-grained visuotopic map. J Neurosci. 2001 May 15;21(10):3542-8.

Goddard CA, Butts DA, Shatz CJ. Regulation of CNS synapses by neuronal MHC class I. Proc Natl Acad Sci U S A. 2007 Apr 17;104(16):6828-33.

Goold CP, Davis GW. The BMP ligand Gbb gates the expression of synaptic homeostasis independent of synaptic growth control. Neuron. 2007 Oct 4;56(1):109-23.

Gracheva EO, Hadwiger G, Nonet ML, Richmond JE. Direct interactions between C. elegans RAB-3 and Rim provide a mechanism to target vesicles to the presynaptic density. Neurosci Lett. 2008 Oct 24;444(2):137-42.

Gradinaru V, Zhang F, Ramakrishnan C, Mattis J, Prakash R, Diester I, Goshen I, Thompson KR, Deisseroth K. Molecular and cellular approaches for diversifying and extending optogenetics. Cell. 2010 Apr 2;141(1):154-65.

Graf ER, Daniels RW, Burgess RW, Schwarz TL, DiAntonio A. Rab3 dynamically controls protein composition at active zones. Neuron. 2009 Dec 10;64(5):663-77.

Graf ER, Valakh V, Wright CM, Wu C, Liu Z, Zhang YQ, DiAntonio A. RIM promotes calcium channel accumulation at active zones of the Drosophila neuromuscular junction. J Neurosci. 2012 Nov 21;32(47):16586-96.

Grunwald ME, Mellem JE, Strutz N, Maricq AV, Kaplan JM. Clathrin-mediated endocytosis is required for compensatory regulation of GLR-1 glutamate receptors after activity blockade. Proc Natl Acad Sci U S A. 2004 Mar 2;101(9):3190-5.

Haghighi AP, McCabe BD, Fetter RD, Palmer JE, Hom S, Goodman CS. Retrograde control of synaptic transmission by postsynaptic CaMKII at the Drosophila neuromuscular junction. Neuron. 2003 Jul 17;39(2):255-67.

Han Y, Kaeser PS, Südhof TC, Schneggenburger R. RIM determines Ca^{2+} channel density and vesicle docking at the presynaptic active zone. Neuron. 2011 Jan 27;69(2):304-16.

Hata Y, Slaughter CA, Südhof TC. Synaptic vesicle fusion complex contains unc-18 homologue bound to syntaxin. Nature. 1993 Nov 25;366(6453):347-51.

Heckscher ES, Fetter RD, Marek KW, Albin SD, Davis GW. NF-kappaB, IkappaB, and IRAK control glutamate receptor density at the Drosophila NMJ. Neuron. 2007 Sep 20;55(6):859-73.

Henry FE, McCartney AJ, Neely R, Perez AS, Carruthers CJ, Stuenkel EL, Inoki K, Sutton MA. Retrograde changes in presynaptic function driven by dendritic mTORC1. J Neurosci. 2012 Nov 28;32(48):17128-42.

Houweling AR, Bazhenov M, Timofeev I, Steriade M, Sejnowski TJ. Homeostatic synaptic plasticity can explain post-traumatic epileptogenesis in chronically isolated neocortex. Cereb Cortex. 2005 Jun;15(6):834-45.

Hua JY, Smear MC, Baier H, Smith SJ. Regulation of axon growth in vivo by activity-based competition. Nature. 2005 Apr 21;434(7036):1022-6.

Ibata K, Sun Q, Turrigiano GG. Rapid synaptic scaling induced by changes in postsynaptic firing. Neuron. 2008 Mar 27;57(6):819-26.

Imig C, Min SW, Krinner S, Arancillo M, Rosenmund C, Südhof TC, Rhee J, Brose N, Cooper BH. The morphological and molecular nature of synaptic vesicle priming at presynaptic active zones. Neuron. 2014 Oct 22;84(2):416-31.

Ingolia NT, Ghaemmaghami S, Newman JR, Weissman JS. Genome-wide analysis in vivo of translation with nucleotide resolution using ribosome profiling. Science. 2009 Apr 10;324(5924):218-23.

Jakawich SK, Nasser HB, Strong MJ, McCartney AJ, Perez AS, Rakesh N, Carruthers CJ, Sutton MA. Local presynaptic activity gates homeostatic changes in presynaptic function driven by dendritic BDNF synthesis. Neuron. 2010 Dec 22;68(6):1143-58.

Jan LY, Jan YN. Properties of the larval neuromuscular junction in Drosophila melanogaster. J Physiol. 1976 Oct;262(1):189-214.

Kaeser PS, Deng L, Wang Y, Dulubova I, Liu X, Rizo J, Südhof TC. RIM proteins tether Ca2+ channels to presynaptic active zones via a direct PDZ-domain interaction. Cell. 2011 Jan 21;144(2):282-95.

Kamenetz F, Tomita T, Hsieh H, Seabrook G, Borchelt D, Iwatsubo T, Sisodia S, Malinow R. APP processing and synaptic function. Neuron. 2003 Mar 27;37(6):925-37.

Kandel ER. The molecular biology of memory: cAMP, PKA, CRE, CREB-1, CREB-2, and CPEB. Mol Brain. 2012 May 14;5:14.

Kaneko M, Stellwagen D, Malenka RC, Stryker MP. Tumor necrosis factor-alpha mediates one component of competitive, experience-dependent plasticity in developing visual cortex. Neuron. 2008 Jun 12;58(5):673-80.

Kawasaki F, Felling R, Ordway RW. A temperature-sensitive paralytic mutant defines a primary synaptic calcium channel in Drosophila. J Neurosci. 2000 Jul 1;20(13):4885-9.

Kawasaki F, Zou B, Xu X, Ordway RW. Active zone localization of presynaptic calcium channels encoded by the cacophony locus of Drosophila. J Neurosci. 2004 Jan 7;24(1):282-5.

Keck T, Keller GB, Jacobsen RI, Eysel UT, Bonhoeffer T, Hübener M. Synaptic scaling and homeostatic plasticity in the mouse visual cortex in vivo. Neuron. 2013 Oct 16;80(2):327-34.

Keller GB, Bonhoeffer T, Hübener M. Sensorimotor mismatch signals in primary visual cortex of the behaving mouse. Neuron. 2012 Jun 7;74(5):809-15.

Kesavapany S, Lau KF, McLoughlin DM, Brownlees J, Ackerley S, Leigh PN, Shaw CE, Miller CC. p35/cdk5 binds and phosphorylates beta-catenin and regulates beta-catenin/presenilin-1 interaction. Eur J Neurosci. 2001 Jan;13(2):241-7.

Kile BT, Hilton DJ. The art and design of genetic screens: mouse. Nat Rev Genet. 2005 Jul;6(7):557-67.

Kilman V, van Rossum MC, Turrigiano GG. Activity deprivation reduces miniature IPSC amplitude by decreasing the number of postsynaptic GABA(A) receptors clustered at neocortical synapses. J Neurosci. 2002 Feb 15;22(4):1328-37.

Kim J, Tsien RW. Synapse-specific adaptations to inactivity in hippocampal circuits achieve homeostatic gain control while dampening network reverberation. Neuron. 2008 Jun 26;58(6):925-37.

Kim S, Ziff EB. Calcineurin mediates synaptic scaling via synaptic trafficking of Ca2+-permeable AMPA receptors. PLoS Biol. 2014 Jul 1;12(7):e1001900.

Kim SH, Ryan TA. Balance of calcineurin Aα and CDK5 activities sets release probability at nerve terminals. J Neurosci. 2013 May 22;33(21):8937-50.

Kim SH, Ryan TA. CDK5 serves as a major control point in neurotransmitter release. Neuron. 2010 Sep 9;67(5):797-809.

Kissler AE, Pettersson N, Frölich A, Sigrist SJ, Suter B. Drosophila cdk5 is needed for locomotive behavior and NMJ elaboration, but seems dispensable for synaptic transmission. Dev Neurobiol. 2009 May;69(6):365-77.

Koch SM, Dela Cruz CG, Hnasko TS, Edwards RH, Huberman AD, Ullian EM. Pathway-specific genetic attenuation of glutamate release alters select features of competition-based visual circuit refinement. Neuron. 2011 Jul 28;71(2):235-42.

Kwon YT, Gupta A, Zhou Y, Nikolic M, Tsai LH. Regulation of N-cadherin-mediated adhesion by the p35-Cdk5 kinase. Curr Biol. 2000 Apr 6;10(7):363-72.

Lai KO, Wong AS, Cheung MC, Xu P, Liang Z, Lok KC, Xie H, Palko ME, Yung WH, Tessarollo L, Cheung ZH, Ip NY. TrkB phosphorylation by Cdk5 is required for activity-dependent structural plasticity and spatial memory. Nat Neurosci. 2012 Nov;15(11):1506-15.

Lilja L, Johansson JU, Gromada J, Mandic SA, Fried G, Berggren PO, Bark C. Cyclin-dependent kinase 5 associated with p39 promotes Munc18-1 phosphorylation and Ca(2+)-dependent exocytosis. J Biol Chem. 2004 Jul 9;279(28):29534-41.

Lin DM, Goodman CS. Ectopic and increased expression of Fasciclin II alters motoneuron growth cone guidance. Neuron. 1994 Sep;13(3):507-23.

Lissin DV, Carroll RC, Nicoll RA, Malenka RC, von Zastrow M. Rapid, activation-induced redistribution of ionotropic glutamate receptors in cultured hippocampal neurons. J Neurosci. 1999 Feb 15;19(4):1263-72.

Liu L, Johnson WA, Welsh MJ. Drosophila DEG/ENaC pickpocket genes are expressed in the tracheal system, where they may be involved in liquid clearance. Proc Natl Acad Sci U S A. 2003 Feb 18;100(4):2128-33.

Liu L, Leonard AS, Motto DG, Feller MA, Price MP, Johnson WA, Welsh MJ. Contribution of Drosophila DEG/ENaC genes to salt taste. Neuron. 2003 Jul 3;39(1):133-46.

Liu KS, Siebert M, Mertel S, Knoche E, Wegener S, Wichmann C, Matkovic T, Muhammad K, Depner H, Mettke C, Bückers J, Hell SW, Müller M, Davis GW, Schmitz D, Sigrist SJ. RIM-binding protein, a central part of the active zone, is essential for neurotransmitter release. Science. 2011 Dec 16;334(6062):1565-9.

Lo SC, Wang Y, Weber M, Larson JL, Scearce-Levie K, Sheng M. Caspase-3 deficiency results in disrupted synaptic homeostasis and impaired attention control. J Neurosci. 2015 Feb 4;35(5):2118-32.

Locke C, Berry K, Kautu B, Lee K, Caldwell K, Caldwell G. Paradigms for pharmacological characterization of C. elegans synaptic transmission mutants. J Vis Exp. 2008 Aug 18;(18). pii: 837.

Locke CJ, Kautu BB, Berry KP, Lee SK, Caldwell KA, Caldwell GA. Pharmacogenetic analysis reveals a post-developmental role for Rac GTPases in Caenorhabditis elegans GABAergic neurotransmission. Genetics. 2009 Dec;183(4):1357-72.

Locke CJ, Williams SN, Schwarz EM, Caldwell GA, Caldwell KA. Genetic interactions among cortical malformation genes that influence susceptibility to convulsions in C. elegans. Brain Res. 2006 Nov 20;1120(1):23-34.

Louros SR, Hooks BM, Litvina L, Carvalho AL, Chen C. A role for stargazin in experience-dependent plasticity. Cell Rep. 2014 Jun 12;7(5):1614-25.

MacLean JN, Zhang Y, Johnson BR, Harris-Warrick RM. Activity-independent homeostasis in rhythmically active neurons. Neuron. 2003 Jan 9;37(1):109-20.

Maghsoodi B, Poon MM, Nam CI, Aoto J, Ting P, Chen L. Retinoic acid regulates RARalpha-mediated control of translation in dendritic RNA granules during homeostatic synaptic plasticity. Proc Natl Acad Sci U S A. 2008 Oct 14;105(41):16015-20.

Mahoney RE, Rawson JM, Eaton BA. An age-dependent change in the set point of synaptic homeostasis. J Neurosci. 2014 Feb 5;34(6):2111-9.

Mahr A, Aberle H. The expression pattern of the Drosophila vesicular glutamate transporter: a mWarker protein for motoneurons and glutamatergic centers in the brain. Gene Expr Patterns. 2006 Mar;6(3):299-309.

Marder E, Goaillard JM. Variability, compensation and homeostasis in neuron and network function. Nat Rev Neurosci. 2006 Jul;7(7):563-74.

Marie B, Pym E, Bergquist S, Davis GW. Synaptic homeostasis is consolidated by the cell fate gene gooseberry, a Drosophila pax3/7 homolog. J Neurosci. 2010 Jun 16;30(24):8071-82.

Marqués G, Bao H, Haerry TE, Shimell MJ, Duchek P, Zhang B, O'Connor MB. The Drosophila BMP type II receptor Wishful Thinking regulates neuromuscular synapse morphology and function. Neuron. 2002 Feb 14;33(4):529-43.

Massaro CM, Pielage J, Davis GW. Molecular mechanisms that enhance synapse stability despite persistent disruption of the spectrin/ankyrin/microtubule cytoskeleton. J Cell Biol. 2009 Oct 5;187(1):101-17.

McCabe BD, Marqués G, Haghighi AP, Fetter RD, Crotty ML, Haerry TE, Goodman CS, O'Connor MB. The BMP homolog Gbb provides a retrograde signal that regulates synaptic growth at the Drosophila neuromuscular junction. Neuron. 2003 Jul 17;39(2):241-54.

Meadows JP, Guzman-Karlsson MC, Phillips S, Holleman C, Posey JL, Day JJ, Hablitz JJ, Sweatt JD. DNA methylation regulates neuronal glutamatergic synaptic scaling. Sci Signal. 2015 Jun 23;8(382):ra61.

Meyer F, Moussian B. Drosophila multiplexin (Dmp) modulates motor axon pathfinding accuracy. Dev Growth Differ. 2009 Jun;51(5):483-98.

Mitra A, Mitra SS, Tsien RW. Heterogeneous reallocation of presynaptic efficacy in recurrent excitatory circuits adapting to inactivity. Nat Neurosci. 2011 Dec 18;15(2):250-7.

Müller M, Davis GW. Transsynaptic control of presynaptic Ca^{2+} influx achieves homeostatic potentiation of neurotransmitter release. Curr Biol. 2012 Jun 19;22(12):1102-8.

Müller M, Genç Ö, Davis GW. RIM-binding protein links synaptic homeostasis to the stabilization and replenishment of high release probability vesicles. Neuron. 2015 Mar 4;85(5):1056-69.

Müller M, Liu KS, Sigrist SJ, Davis GW. RIM controls homeostatic plasticity through modulation of the readily-releasable vesicle pool. J Neurosci. 2012 Nov 21;32(47):16574-85.

Müller M, Pym EC, Tong A, Davis GW. Rab3-GAP controls the progression of synaptic homeostasis at a late stage of vesicle release. Neuron. 2011 Feb 24;69(4):749-62.

Murthy VN, Schikorski T, Stevens CF, Zhu Y. Inactivity produces increases in neurotransmitter release and synapse size. Neuron. 2001 Nov 20;32(4):673-82.

Nagalakshmi U, Wang Z, Waern K, Shou C, Raha D, Gerstein M, Snyder M. The transcriptional landscape of the yeast genome defined by RNA sequencing. Science. 2008 Jun 6;320(5881):1344-9.

Narahashi T, Moore JW, Scott WR. Tetrodotoxin blockage of sodium conductance increase in lobster giant axons. J Gen Physiol. 1964 May;47:965-74.

Nerbonne JM, Gerber BR, Norris A, Burkhalter A. Electrical remodelling maintains firing properties in cortical pyramidal neurons lacking KCND2-encoded A-type K+ currents. J Physiol. 2008 Mar 15;586(6):1565-79.

Noordermeer J, Klingensmith J, Perrimon N, Nusse R. dishevelled and armadillo act in the wingless signalling pathway in Drosophila. Nature. 1994 Jan 6;367(6458):80-3.

Nüsslein-Volhard C, Wieschaus E. Mutations affecting segment number and polarity in Drosophila. Nature. 1980 Oct 30;287(5785):795-801.

O'Brien RJ, Kamboj S, Ehlers MD, Rosen KR, Fischbach GD, Huganir RL. Activity-dependent modulation of synaptic AMPA receptor accumulation. Neuron. 1998 Nov;21(5):1067-78.

Okuda T, Yu LM, Cingolani LA, Kemler R, Goda Y. beta-Catenin regulates excitatory postsynaptic strength at hippocampal synapses. Proc Natl Acad Sci U S A. 2007 Aug 14;104(33):13479-84.

O'Reilly MS, Boehm T, Shing Y, Fukai N, Vasios G, Lane WS, Flynn E, Birkhead JR, Olsen BR, Folkman J. Endostatin: an endogenous inhibitor of angiogenesis and tumor growth. Cell. 1997 Jan 24;88(2):277-85.

Pak C, Danko T, Zhang Y, Aoto J, Anderson G, Maxeiner S, Yi F, Wernig M, Südhof TC. Human Neuropsychiatric Disease Modeling using Conditional Deletion Reveals Synaptic Transmission Defects Caused By Heterozygous Mutations in NRXN1. Cell Stem Cell. 2015 Aug 12. pii: S1934-5909(15)00316-1.

Paradis S, Sweeney ST, Davis GW. Homeostatic control of presynaptic release is triggered by postsynaptic membrane depolarization. Neuron. 2001 Jun;30(3):737-49.

Parks AL, Cook KR, Belvin M, Dompe NA, Fawcett R, Huppert K, Tan LR, Winter CG, Bogart KP, Deal JE, Deal-Herr ME, Grant D, Marcinko M, Miyazaki WY, Robertson S, Shaw KJ, Tabios M, Vysotskaia V, Zhao L, Andrade RS, Edgar KA, Howie E, Killpack K, Milash B, Norton A, Thao D, Whittaker K, Winner MA, Friedman L, Margolis J, Singer MA, Kopczynski C, Curtis D, Kaufman TC, Plowman GD, Duyk G, Francis-Lang HL. Systematic generation of high-resolution deletion coverage of the Drosophila melanogaster genome. Nat Genet. 2004 Mar;36(3):288-92.

Parrish JZ, Kim CC, Tang L, Bergquist S, Wang T, Derisi JL, Jan LY, Jan YN, Davis GW. Krüppel mediates the selective rebalancing of ion channel expression. Neuron. 2014 May 7;82(3):537-44.

Peifer M, Wieschaus E. The segment polarity gene armadillo encodes a functionally modular protein that is the Drosophila homolog of human plakoglobin. Cell. 1990 Dec 21;63(6):1167-76.

Peled ES, Isacoff EY. Optical quantal analysis of synaptic transmission in wild-type and rab3-mutant Drosophila motor axons. Nat Neurosci. 2011 Apr;14(4):519-26.

Penney J, Tsurudome K, Liao EH, Elazzouzi F, Livingstone M, Gonzalez M, Sonenberg N, Haghighi AP. TOR is required for the retrograde regulation of synaptic homeostasis at the Drosophila neuromuscular junction. Neuron. 2012 Apr 12;74(1):166-78.

Perrimon N, Engstrom L, Mahowald AP. Zygotic lethals with specific maternal effect phenotypes in Drosophila melanogaster. I. Loci on the X chromosome. Genetics. 1989 Feb;121(2):333-52.

Petersen SA, Fetter RD, Noordermeer JN, Goodman CS, DiAntonio A. Genetic analysis of glutamate receptors in Drosophila reveals a retrograde signal regulating presynaptic transmitter release. Neuron. 1997 Dec;19(6):1237-48.

Pevsner J, Hsu SC, Scheller RH. n-Sec1: a neural-specific syntaxin-binding protein. Proc Natl Acad Sci U S A. 1994 Feb 15;91(4):1445-9.

Pilgram GS, Potikanond S, van der Plas MC, Fradkin LG, Noordermeer JN. The RhoGAP crossveinless-c interacts with Dystrophin and is required for synaptic homeostasis at the Drosophila neuromuscular junction. J Neurosci. 2011 Jan 12;31(2):492-500.

Plomp JJ, Van Kempen GT, De Baets MB, Graus YM, Kuks JB, Molenaar PC. Acetylcholine release in myasthenia gravis: regulation at single end-plate level. Ann Neurol. 1995 May;37(5):627-36.

Plomp JJ, van Kempen GT, Molenaar PC. Adaptation of quantal content to decreased postsynaptic sensitivity at single endplates in alpha-bungarotoxin-treated rats. J Physiol. 1992 Dec;458:487-99.

Pratt KG, Zimmerman EC, Cook DG, Sullivan JM. Presenilin 1 regulates homeostatic synaptic scaling through Akt signaling. Nat Neurosci. 2011 Aug 14;14(9):1112-4.

Preobraschenski J, Zander JF, Suzuki T, Ahnert-Hilger G, Jahn R. Vesicular glutamate transporters use flexible anion and cation binding sites for efficient accumulation of neurotransmitter. Neuron. 2014 Dec 17;84(6):1287-301.

Qiu Z, Sylwestrak EL, Lieberman DN, Zhang Y, Liu XY, Ghosh A. The Rett syndrome protein MeCP2 regulates synaptic scaling. J Neurosci. 2012 Jan 18;32(3):989-94.

Rosenmund C, Stevens CF. Definition of the readily releasable pool of vesicles at hippocampal synapses.

Rubin GM, Spradling AC. Genetic transformation of Drosophila with transposable element vectors. Science. 1982 Oct 22;218(4570):348-53.

Rutherford LC, Nelson SB, Turrigiano GG. BDNF has opposite effects on the quantal amplitude of pyramidal neuron and interneuron excitatory synapses. Neuron. 1998 Sep;21(3):521-30.

Sakane A, Manabe S, Ishizaki H, Tanaka-Okamoto M, Kiyokage E, Toida K, Yoshida T, Miyoshi J, Kamiya H, Takai Y, Sasaki T. Rab3 GTPase-activating protein regulates synaptic transmission and plasticity through the inactivation of Rab3. Proc Natl Acad Sci U S A. 2006 Jun 27;103(26):10029-34.

Sandrock AW Jr, Dryer SE, Rosen KM, Gozani SN, Kramer R, Theill LE, Fischbach GD. Maintenance of acetylcholine receptor number by neuregulins at the neuromuscular junction in vivo. Science. 1997 Apr 25;276(5312):599-603.

Sanyal S, Sandstrom DJ, Hoeffer CA, Ramaswami M. AP-1 functions upstream of CREB to control synaptic plasticity in Drosophila. Nature. 2002 Apr 25;416(6883):870-4.

Schena M, Shalon D, Davis RW, Brown PO. Quantitative monitoring of gene expression patterns with a complementary DNA microarray. Science. 1995 Oct 20;270(5235):467-70.

Schmidt JT, Buzzard M, Borress R, Dhillon S. MK801 increases retinotectal arbor size in developing zebrafish without affecting kinetics of branch elimination and addition. J Neurobiol. 2000 Feb 15;42(3):303-14.

Schoch S, Castillo PE, Jo T, Mukherjee K, Geppert M, Wang Y, Schmitz F, Malenka RC, Südhof TC. RIM1alpha forms a protein scaffold for regulating neurotransmitter release at the active zone. Nature. 2002 Jan 17;415(6869):321-6. Neuron. 1996 Jun;16(6):1197-207.

Schratt GM, Nigh EA, Chen WG, Hu L, Greenberg ME. BDNF regulates the translation of a select group of mRNAs by a mammalian target of rapamycin-phosphatidylinositol 3-kinase-dependent pathway during neuronal development. J Neurosci. 2004 Aug 18;24(33):7366-77.

Schuster CM, Davis GW, Fetter RD, Goodman CS. Genetic dissection of structural and functional components of synaptic plasticity. II. Fasciclin II controls presynaptic structural plasticity. Neuron. 1996 Oct;17(4):655-67.

Seeburg DP, Feliu-Mojer M, Gaiottino J, Pak DT, Sheng M. Critical role of CDK5 and Polo-like kinase 2 in homeostatic synaptic plasticity during elevated activity. Neuron. 2008 May 22;58(4):571-83.

Sharma M, Burré J, Südhof TC. CSPα promotes SNARE-complex assembly by chaperoning SNAP-25 during synaptic activity. Nat Cell Biol. 2011 Jan;13(1):30-9.

Sheffler-Collins SI, Dalva MB. EphBs: an integral link between synaptic function and synaptopathies. Trends Neurosci. 2012 May;35(5):293-304.

Shepherd JD, Rumbaugh G, Wu J, Chowdhury S, Plath N, Kuhl D, Huganir RL, Worley PF. Arc/Arg3.1 mediates homeostatic synaptic scaling of AMPA receptors. Neuron. 2006 Nov 9;52(3):475-84.

Shuang R, Zhang L, Fletcher A, Groblewski GE, Pevsner J, Stuenkel EL. Regulation of Munc-18/syntaxin 1A interaction by cyclin-dependent kinase 5 in nerve endings. J Biol Chem. 1998 Feb 27;273(9):4957-66.

Shin SM, Zhang N, Hansen J, Gerges NZ, Pak DT, Sheng M, Lee SH. GKAP orchestrates activity-dependent postsynaptic protein remodeling and homeostatic scaling. Nat Neurosci. 2012 Dec;15(12):1655-66.

Smear MC, Tao HW, Staub W, Orger MB, Gosse NJ, Liu Y, Takahashi K, Poo MM, Baier H. Vesicular glutamate transport at a central synapse limits the acuity of visual perception in zebrafish. Neuron. 2007 Jan 4;53(1):65-77.

Smith LA, Wang X, Peixoto AA, Neumann EK, Hall LM, Hall JC. A Drosophila calcium channel alpha1 subunit gene maps to a genetic locus associated with behavioral and visual defects. J Neurosci. 1996 Dec 15;16(24):7868-79.

Soden ME, Chen L. Fragile X protein FMRP is required for homeostatic plasticity and regulation of synaptic strength by retinoic acid. J Neurosci. 2010 Dec 15;30(50):16910-21.

Sons MS, Busche N, Strenzke N, Moser T, Ernsberger U, Mooren FC, Zhang W, Ahmad M, Steffens H, Schomburg ED, Plomp JJ, Missler M. alpha-Neurexins are required for efficient transmitter release and synaptic homeostasis at the mouse neuromuscular junction. Neuroscience. 2006;138(2):433-46.

Sons MS, Verhage M, Plomp JJ. Role of Munc18-1 in synaptic plasticity at the myasthenic neuromuscular junction. Ann N Y Acad Sci. 2003 Sep;998:404-6.

Sørensen JB, Matti U, Wei SH, Nehring RB, Voets T, Ashery U, Binz T, Neher E, Rettig J. The SNARE protein SNAP-25 is linked to fast calcium triggering of exocytosis. Proc Natl Acad Sci U S A. 2002 Feb 5;99(3):1627-32.

Spitzer NC. Activity-dependent neurotransmitter respecification. Nat Rev Neurosci. 2012 Jan 18;13(2):94-106.

Spradling AC, Stern DM, Kiss I, Roote J, Laverty T, Rubin GM. Gene disruptions using P transposable elements: an integral component of the Drosophila genome project. Proc Natl Acad Sci U S A. 1995 Nov 21;92(24):10824-30.

Sretavan DW, Shatz CJ, Stryker MP. Modification of retinal ganglion cell axon morphology by prenatal infusion of tetrodotoxin. Nature. 1988 Dec 1;336(6198):468-71.

Starcevic M, Dell'Angelica EC. Identification of snapin and three novel proteins (BLOS1, BLOS2, and BLOS3/reduced pigmentation) as subunits of biogenesis of lysosome-related organelles complex-1 (BLOC-1). J Biol Chem. 2004 Jul 2;279(27):28393-401.

Stawicki TM, Takayanagi-Kiya S, Zhou K, Jin Y. Neuropeptides function in a homeostatic manner to modulate excitation-inhibition imbalance in C. elegans. PLoS Genet. 2013 May;9(5):e1003472.

Stellwagen D, Malenka RC. Synaptic scaling mediated by glial TNF-alpha. Nature. 2006 Apr 20;440(7087):1054-9.

Stewart BA, Schuster CM, Goodman CS, Atwood HL. Homeostasis of synaptic transmission in Drosophila with genetically altered nerve terminal morphology. J Neurosci. 1996 Jun 15;16(12):3877-86.

Stigloher C, Zhan H, Zhen M, Richmond J, Bessereau JL. The presynaptic dense projection of the Caenorhabditis elegans cholinergic neuromuscular junction localizes synaptic vesicles at the active zone through SYD-2/liprin and UNC-10/RIM-dependent interactions. J Neurosci. 2011 Mar 23;31(12):4388-96.

Straub RE, Jiang Y, MacLean CJ, Ma Y, Webb BT, Myakishev MV, Harris-Kerr C, Wormley B, Sadek H, Kadambi B, Cesare AJ, Gibberman A, Wang X, O'Neill FA, Walsh D, Kendler KS. Genetic variation in the 6p22.3 gene DTNBP1, the human ortholog of the mouse dysbindin gene, is associated with schizophrenia. Am J Hum Genet. 2002 Aug;71(2):337-48.

Stuermer CA, Rohrer B, Münz H. Development of the retinotectal projection in zebrafish embryos under TTX-induced neural-impulse blockade. J Neurosci. 1990 Nov;10(11):3615-26.

Su SC, Seo J, Pan JQ, Samuels BA, Rudenko A, Ericsson M, Neve RL, Yue DT, Tsai LH. Regulation of N-type voltage-gated calcium channels and presynaptic function by cyclin-dependent kinase 5. Neuron. 2012 Aug 23;75(4):675-87.

Südhof TC. Neuroligins and neurexins link synaptic function to cognitive disease. Nature. 2008 Oct 16;455(7215):903-11.

Südhof TC. The presynaptic active zone. Neuron. 2012 Jul 12;75(1):11-25.

Suzuki OT, Sertié AL, Der Kaloustian VM, Kok F, Carpenter M, Murray J, Czeizel AE, Kliemann SE, Rosemberg S, Monteiro M, Olsen BR, Passos-Bueno MR. Molecular analysis of collagen XVIII reveals novel mutations, presence of a third isoform, and possible genetic heterogeneity in Knobloch syndrome. Am J Hum Genet. 2002 Dec;71(6):1320-9.

Swanwick CC, Murthy NR, Kapur J. Activity-dependent scaling of GABAergic synapse strength is regulated by brain-derived neurotrophic factor. Mol Cell Neurosci. 2006 Mar;31(3):481-92.

Sweeney ST, Davis GW. Unrestricted synaptic growth in spinster-a late endosomal protein implicated in TGF-beta-mediated synaptic growth regulation. Neuron. 2002 Oct 24;36(3):403-16.

Swensen AM, Bean BP. Robustness of burst firing in dissociated purkinje neurons with acute or long-term reductions in sodium conductance. J Neurosci. 2005 Apr 6;25(14):3509-20.

Takamori S, Rhee JS, Rosenmund C, Jahn R. Identification of a vesicular glutamate transporter that defines a glutamatergic phenotype in neurons. Nature. 2000 Sep 14;407(6801):189-94.

Talbot K, Cho DS, Ong WY, Benson MA, Han LY, Kazi HA, Kamins J, Hahn CG, Blake DJ, Arnold SE. Dysbindin-1 is a synaptic and microtubular protein that binds brain snapin. Hum Mol Genet. 2006 Oct 15;15(20):3041-54.

Talbot K, Eidem WL, Tinsley CL, Benson MA, Thompson EW, Smith RJ, Hahn CG, Siegel SJ, Trojanowski JQ, Gur RE, Blake DJ, Arnold SE. Dysbindin-1 is reduced in intrinsic, glutamatergic terminals of the hippocampal formation in schizophrenia. J Clin Invest. 2004 May;113(9):1353-63.

Tamura Y, Ogita K, Ueda T. A new VGLUT-specific potent inhibitor: pharmacophore of Brilliant Yellow. Neurochem Res. 2014 Jan;39(1):117-28.

Tan HL, Queenan BN, Huganir RL. GRIP1 is required for homeostatic regulation of AMPAR trafficking. Proc Natl Acad Sci U S A. 2015 Aug 11;112(32):10026-31.

Thiagarajan TC, Piedras-Renteria ES, Tsien RW. alpha- and betaCaMKII. Inverse regulation by neuronal activity and opposing effects on synaptic strength. Neuron. 2002 Dec 19;36(6):1103-14.

Thibault ST, Singer MA, Miyazaki WY, Milash B, Dompe NA, Singh CM, Buchholz R, Demsky M, Fawcett R, Francis-Lang HL, Ryner L, Cheung LM, Chong A, Erickson C, Fisher WW, Greer K, Hartouni SR, Howie E, Jakkula L, Joo D, Killpack K, Laufer A, Mazzotta J, Smith RD, Stevens LM, Stuber C, Tan LR, Ventura R, Woo A, Zakrajsek I, Zhao L, Chen F, Swimmer C, Kopczynski C, Duyk G, Winberg ML, Margolis J. A complementary transposon tool kit for Drosophila melanogaster using P and piggyBac. Nat Genet. 2004 Mar;36(3):283-7.

Thompson CM, Davis E, Carrigan CN, Cox HD, Bridges RJ, Gerdes JM. Inhibitor of the glutamate vesicular transporter (VGLUT). Curr Med Chem. 2005;12(18):2041-56.

Tian L, Hires SA, Mao T, Huber D, Chiappe ME, Chalasani SH, Petreanu L, Akerboom J, McKinney SA, Schreiter ER, Bargmann CI, Jayaraman V, Svoboda K, Looger LL. Imaging neural activity in worms, flies and mice with improved GCaMP calcium indicators. Nat Methods. 2009 Dec;6(12):875-81.

Tomizawa K, Ohta J, Matsushita M, Moriwaki A, Li ST, Takei K, Matsui H. Cdk5/p35 regulates neurotransmitter release through phosphorylation and downregulation of P/Q-type voltage-dependent calcium channel activity. J Neurosci. 2002 Apr 1;22(7):2590-7.

Tomizawa K, Sunada S, Lu YF, Oda Y, Kinuta M, Ohshima T, Saito T, Wei FY, Matsushita M, Li ST, Tsutsui K, Hisanaga S, Mikoshiba K, Takei K, Matsui H. Cophosphorylation of amphiphysin I and dynamin I by Cdk5 regulates clathrin-mediated endocytosis of synaptic vesicles. J Cell Biol. 2003 Nov 24;163(4):813-24.

Trasande CA, Ramirez JM. Activity deprivation leads to seizures in hippocampal slice cultures: is epilepsy the consequence of homeostatic plasticity? J Clin Neurophysiol. 2007 Apr;24(2):154-64.

Turrigiano GG. Homeostatic plasticity in neuronal networks: the more things change, the more they stay the same. Trends Neurosci. 1999 May;22(5):221-7.

Turrigiano GG. The self-tuning neuron: synaptic scaling of excitatory synapses. Cell. 2008 Oct 31;135(3):422-35.

Turrigiano G, Abbott LF, Marder E. Activity-dependent changes in the intrinsic properties of cultured neurons. Science. 1994 May 13;264(5161):974-7.

Turrigiano G, LeMasson G, Marder E. Selective regulation of current densities underlies spontaneous changes in the activity of cultured neurons. J Neurosci. 1995 May;15(5 Pt 1):3640-52.

Turrigiano GG, Leslie KR, Desai NS, Rutherford LC, Nelson SB. Activity-dependent scaling of quantal amplitude in neocortical neurons. Nature. 1998 Feb 26;391(6670):892-6.

Tyler WJ, Pozzo-Miller LD. BDNF enhances quantal neurotransmitter release and increases the number of docked vesicles at the active zones of hippocampal excitatory synapses. J Neurosci. 2001 Jun 15;21(12):4249-58.

Ushkaryov YA, Petrenko AG, Geppert M, Südhof TC. Neurexins: synaptic cell surface proteins related to the alpha-latrotoxin receptor and laminin. Science. 1992 Jul 3;257(5066):50-6.

Vacher H, Yang JW, Cerda O, Autillo-Touati A, Dargent B, Trimmer JS. Cdk-mediated phosphorylation of the Kvβ2 auxiliary subunit regulates Kv1 channel axonal targeting. J Cell Biol. 2011 Mar 7;192(5):813-24.

van der Plas MC, Pilgram GS, Plomp JJ, de Jong A, Fradkin LG, Noordermeer JN. Dystrophin is required for appropriate retrograde control of neurotransmitter release at the Drosophila neuromuscular junction. J Neurosci. 2006 Jan 4;26(1):333-44.

Verstegen AM, Tagliatti E, Lignani G, Marte A, Stolero T, Atias M, Corradi A, Valtorta F, Gitler D, Onofri F, Fassio A, Benfenati F. Phosphorylation of synapsin I by cyclin-dependent kinase-5 sets the ratio between the resting and recycling pools of synaptic vesicles at hippocampal synapses. J Neurosci. 2014 May 21;34(21):7266-80.

Vitureira N, Letellier M, Goda Y. Homeostatic synaptic plasticity: from single synapses to neural circuits. Curr Opin Neurobiol. 2012 Jun;22(3):516-21.

Vitureira N, Letellier M, White IJ, Goda Y. Differential control of presynaptic efficacy by postsynaptic N-cadherin and β-catenin. Nat Neurosci. 2011 Dec 4;15(1):81-9.

Wagh DA, Rasse TM, Asan E, Hofbauer A, Schwenkert I, Dürrbeck H, Buchner S, Dabauvalle MC, Schmidt M, Qin G, Wichmann C, Kittel R, Sigrist SJ, Buchner E. Bruchpilot, a protein with homology to ELKS/CAST, is required for structural integrity and function of synaptic active zones in Drosophila. Neuron. 2006 Mar 16;49(6):833-44.

Wan HI, DiAntonio A, Fetter RD, Bergstrom K, Strauss R, Goodman CS. Highwire regulates synaptic growth in Drosophila. Neuron. 2000 May;26(2):313-29.

Wang CC, Held RG, Hall BJ. SynGAP regulates protein synthesis and homeostatic synaptic plasticity in developing cortical networks. PLoS One. 2013 Dec 31;8(12):e83941.

Wang P, Saraswati S, Guan Z, Watkins CJ, Wurtman RJ, Littleton JT. A Drosophila temperature-sensitive seizure mutant in phosphoglycerate kinase disrupts ATP generation and alters synaptic function. J Neurosci. 2004 May 12;24(19):4518-29.

Wang T, Hauswirth AG, Tong A, Dickman DK, Davis GW. Endostatin is a trans-synaptic signal for homeostatic synaptic plasticity. Neuron. 2014 Aug 6;83(3):616-29.

Wang Y, Okamoto M, Schmitz F, Hofmann K, Südhof TC. Rim is a putative Rab3 effector in regulating synaptic-vesicle fusion. Nature. 1997 Aug 7;388(6642):593-8.

Watt AJ, van Rossum MC, MacLeod KM, Nelson SB, Turrigiano GG. Activity coregulates quantal AMPA and NMDA currents at neocortical synapses. Neuron. 2000 Jun;26(3):659-70.

Weimer RM, Gracheva EO, Meyrignac O, Miller KG, Richmond JE, Bessereau JL. UNC-13 and UNC-10/rim localize synaptic vesicles to specific membrane domains. J Neurosci. 2006 Aug 2;26(31):8040-7.

Weyhersmüller A, Hallermann S, Wagner N, Eilers J. Rapid active zone remodeling during synaptic plasticity. J Neurosci. 2011 Apr 20;31(16):6041-52.

Wietek J, Wiegert JS, Adeishvili N, Schneider F, Watanabe H, Tsunoda SP, Vogt A, Elstner M, Oertner TG, Hegemann P. Conversion of channelrhodopsin into a light-gated chloride channel. Science. 2014 Apr 25;344(6182):409-12.

Williams SN, Locke CJ, Braden AL, Caldwell KA, Caldwell GA. Epileptic-like convulsions associated with LIS-1 in the cytoskeletal control of neurotransmitter signaling in Caenorhabditis elegans. Hum Mol Genet. 2004 Sep 15;13(18):2043-59.

Wilson NR, Kang J, Hueske EV, Leung T, Varoqui H, Murnick JG, Erickson JD, Liu G. Presynaptic regulation of quantal size by the vesicular glutamate transporter VGLUT1. J Neurosci. 2005 Jun 29;25(26):6221-34.

Wojcik SM, Rhee JS, Herzog E, Sigler A, Jahn R, Takamori S, Brose N, Rosenmund C. An essential role for vesicular glutamate transporter 1 (VGLUT1) in postnatal development and control of quantal size. Proc Natl Acad Sci U S A. 2004 May 4;101(18):7158-63.

Wondolowski J, Dickman D. Emerging links between homeostatic synaptic plasticity and neurological disease. Front Cell Neurosci. 2013 Nov 21;7:223.

Yamamoto S, Jaiswal M, Charng WL, Gambin T, Karaca E, Mirzaa G, Wiszniewski W, Sandoval H, Haelterman NA, Xiong B, Zhang K, Bayat V, David G, Li T, Chen K, Gala U, Harel T, Pehlivan D, Penney S, Vissers LE, de Ligt J, Jhangiani SN, Xie Y, Tsang SH, Parman Y, Sivaci M, Battaloglu E, Muzny D, Wan YW, Liu Z, Lin-Moore AT, Clark RD, Curry CJ, Link N, Schulze KL, Boerwinkle E, Dobyns WB, Allikmets R, Gibbs RA, Chen R, Lupski JR, Wangler MF, Bellen HJ. A drosophila genetic resource of mutants to study mechanisms underlying human genetic diseases. Cell. 2014 Sep 25;159(1):200-14.

Yan Z, Chi P, Bibb JA, Ryan TA, Greengard P. Roscovitine: a novel regulator of P/Q-type calcium channels and transmitter release in central neurons. J Physiol. 2002 May 1;540(Pt 3):761-70.

Yazawa M, Hsueh B, Jia X, Pasca AM, Bernstein JA, Hallmayer J, Dolmetsch RE. Using induced pluripotent stem cells to investigate cardiac phenotypes in Timothy syndrome. Nature. 2011 Mar 10;471(7337):230-4.

Yin J, Yuan Q. Structural homeostasis in the nervous system: a balancing act for wiring plasticity and stability. Front Cell Neurosci. 2015 Jan 20;8:439.

Younger MA, Müller M, Tong A, Pym EC, Davis GW. A presynaptic ENaC channel drives homeostatic plasticity. Neuron. 2013 Sep 18;79(6):1183-96.

Zhao C, Dreosti E, Lagnado L. Homeostatic synaptic plasticity through changes in presynaptic calcium influx. J Neurosci. 2011 May 18;31(20):7492-6.

Zhang F, Wang LP, Boyden ES, Deisseroth K. Channelrhodopsin-2 and optical control of excitable cells. Nat Methods. 2006 Oct;3(10):785-92.

Zhang HH, Zhang XQ, Xue QS, Yan-Luo, Huang JL, Zhang S, Shao HJ, Lu H, Wang WY, Yu BW. The BDNF/TrkB signaling pathway is involved in heat hyperalgesia mediated by Cdk5 in rats. PLoS One. 2014 Jan 21;9(1):e85536.

Zhang XH, Poo MM. Localized synaptic potentiation by BDNF requires local protein synthesis in the developing axon. Neuron. 2002 Nov 14;36(4):675-88.

Chapter 2

Synaptotagmin 12 Modulates Growth and Constrains Neurotransmitter Release at the *Drosophila* Neuromuscular Junction

Summary

Synaptotagmin 12 (Syt12) is a neuronally-expressed and calcium-independent member of the synaptotagmin family of membrane proteins. Syt12 expression increases during brain development in vertebrate and invertebrate species, indicating a plausible role in the growth and maturation of the nervous system. However, the effects of Syt12 loss on the structure of the nervous system have not been evaluated. A loss-of-function study in mice revealed a contributory function for Syt12 in a presynaptic form of synaptic plasticity in the hippocampus. Yet, the effects of Syt12 loss in mammals are likely to be tempered by functional redundancy among synaptotagmin isoforms. By generating and characterizing loss-of-function alleles of *Syt12* in *Drosophila*, we provide evidence for a *Syt12*-dependent component of neuromuscular junction morphogenesis. In addition, we found that the readily-releasable pool of synaptic vesicles is enlarged in the absence of *Syt12*. We also determined that Syt12 functions in the presynaptic motor neuron, where it precisely colocalizes with Synaptotagmin 1, a marker of synaptic vesicles and physical interactor of Syt12 in mammalian neurons. Our results suggest that *Syt12* is also critical for the expression of homeostatic presynaptic structural plasticity, which offsets synaptic undergrowth by increasing the number of active zones. Conversely, we show that *Syt12* is dispensable for short-term and long-term forms of homeostatic potentiation, wherein a postsynaptic decrease in glutamate sensitivity is countered by a presynaptic increase in glutamate release. These results distinguish homeostatic potentiation from hippocampal mossy fiber long-term potentiation and presynaptic structural plasticity. Moreover, these results further implicate calcium-independent synaptotagmins in the etiology of nervous system disorders and in an evolutionary conservation of synaptic structure and function.

Introduction

Synaptotagmins (Syts) are evolutionarily conserved membrane proteins that are localized to various intracellular organelles, including synaptic vesicles (Adolfsen *et al.*, 2004; Hui *et al.*, 2005; Dean *et al.*, 2012). The most characterized Syt, Synaptotagmin 1 (Syt1), is localized to presynaptic terminals (Matthew *et al.*,1981), where it functions as the calcium sensor for fast synchronous neurotransmitter release (Littleton *et al.*, 1993; Geppert *et al.*, 1994; Yoshihara and Littleton, 2002). Syt1 has also been demonstrated to regulate synaptic vesicle endocytosis (Jorgensen *et al.*, 1995; Poskanzer *et al.*, 2003; Nicholson-Tomishima and Ryan, 2004) and docking (de Wit *et al.*, 2009). Of seventeen vertebrate Syts (Adolfsen *et al.*, 2004; Bhalla *et al.*, 2008), eight Syts catalyzed SNARE-dependent membrane fusion in the presence of Ca^{2+} *in vitro*, consistent with these Syts functioning as calcium sensors (Hui *et al.*, 2005). The *Drosophila melanogaster* genome encodes seven Syt isoforms, including a minimum of three calcium sensors (Adolfsen *et* al., 2004). In addition to Syt1, flies express a second presynaptic calcium sensor, Syt7 (Adolfsen *et al.*, 2004; Sugita *et al.*, 2001; Bacaj *et al.*, 2013; Liu *et al.*, 2014), as well as a postsynaptic calcium sensor, Syt4, which stimulates the release of growth-promoting retrograde signals at the neuromuscular junction (NMJ) (Yoshihara *et al.*, 2005; Barber *et al.*, 2009). *Drosophila* and rat Syt4 isoforms were shown to have opposite effects on SNARE-dependent membrane fusion in an *in vitro* study (Wang and Chapman, 2010). Regardless, this pioneering work on fly Syt4 led to the discovery of similar postsynaptic (Mendez *et al.*, 2011) and presynaptic functions of Syt4 in mammals (Dean *et al.*, 2009) and underscores the utility of *Drosophila* in elucidating roles of central synaptic proteins.

Although Ca^{2+}-binding is required for the functionality of a subset of Syt isoforms, two evolutionarily conserved *Drosophila* Syt isoforms, Syt12 and Syt14, are predicted to not bind Ca^{2+} (Adolfsen *et al*., 2004). Like their putative vertebrate orthologs, these Syts lack a sufficient number of consensus Ca^{2+}-binding aspartate and glutamate residues to coordinate Ca^{2+}, presumably rendering these isoforms "calcium-independent" (Adolfsen *et al.*, 2004; Bhalla *et al.*, 2008). Consistent with these predictions, Syt12 failed to bind phospholipids or SNAREs in a Ca^{2+}-dependent manner, unlike Syt1 and other "calcium-dependent" Syts, in multiple studies (Hui *et al.*, 2005; Maximov *et al.*, 2007; Bhalla *et al.*, 2008). Conversely, Syt12 did bind phospholipids and SNAREs (Bhalla *et al.*, 2008), as well as Syt1 (Maximov *et al.*, 2007), in a Ca^{2+}-independent manner. As Syt1 was shown to have Ca^{2+}-independent effects on synaptic vesicle docking (Reist *et al.*, 1998; de Wit *et al*., 2009), fusion (Mahal *et al.*, 2002), endocytosis (Poskanzer *et al*., 2006; Loewen *et al.*, 2006), and positioning near Ca^{2+} channels (Young and Neher, 2009), and calcium-independent Syts are evolutionarily conserved from *Drosophila* to humans (Adolfsen *et al.*, 2004), it is plausible that calcium-independent Syts have adaptive roles in the brain.

Indeed, there is emerging evidence that calcium-independent Syts contribute to normal brain function. For example, a missense mutation in Syt14 has been implicated in a human neurodegenerative disorder, termed autosomal-recessive cerebellar ataxia (ARCA) with psychomotor retardation (Doi *et al*., 2011). Syt14 has also been associated with cerebral atrophy, seizures, and developmental delay in humans (Quintero-Rivera *et al.*, 2007). Syt12 was shown to be essential for the full expression of presynaptic mossy fiber long-term potentiation in the mouse hippocampus (Kaeser-Woo *et al.*, 2013), thus pointing to a likely influence of this calcium-independent Syt on learning and memory

(Kandel, 2012). Thyroid hormone has also been found to promote Syt12 expression in neonatal rodent brains, implying that Syt12, like Syt14 (Quintero-Rivera *et al.*, 2007; Doi *et al.*, 2011), may shape some aspects of brain development (Potter *et al.*, 2001; Itoh *et al.*, 2001). Accordingly, neuronal Syt12 expression is increased during development in a diversity of model organisms, including rats (Thompson, 1996; Potter *et al.*, 2001), mice (Itoh *et al.*, 2001; Maximov *et al.*, 2007), and flies (Adolfsen *et al.*, 2004; modENCODE Consortium *et al.*, 2010; Robinson *et al.*, 2013). Provided these key discoveries, and the recognized significance of calcium-dependent Syts in human physiology and medicine (Malenka, 2013; Südhof, 2013), calcium-independent Syts are assuredly understudied.

In the tradition of harnessing the power of *Drosophila* genetics to discover roles for Syts (DiAntonio *et al.*, 1993; Littleton *et al.*, 1993; Poskanzer *et al.*, 2003; Yoshihara and Littleton, 2002) and other genes with human disease implications (Nüsslein-Volhard and Wieschaus, 1980; Yamamoto *et al*., 2014), we sought to characterize the *Syt12* null phenotype at the fly NMJ. Via distinct transposon mutagenesis techniques (Bellen *et al.*, 2004; Parks *et al.*, 2004), we have generated two loss-of-function alleles of the calcium-independent Syt gene, *Syt12*. Using microscopy, electrophysiology, and pharmacology, we have uncovered a contributory role for *Syt12* in the growth and elaboration of NMJs, as well as an apparently inhibitory role in limiting the size of the readily-releasable pool (RRP) of synaptic vesicles. Our data imply that the mechanisms underlying homeostatic potentiation, a rapid and precise form of adaptive plasticity that maintains normal levels of muscle depolarization (Petersen *et al.*, 1997; Frank *et al.*, 2006; Dickman *et al.*, 2007; Davis and Müller, 2015), are genetically separable from those of presynaptic structural plasticity at the fly NMJ (Stewart *et al.*, 1996; Davis and Goodman, 1998) and of mossy

fiber long-term potentiation in the mouse hippocampus (Kaeser-Woo *et al.*, 2013). This examination of *Syt12* likely overcomes complications arising from functional redundancy in mammals (Kaeser-Woo *et al.*, 2013) and may enhance our understanding of calcium-independent Syts, homeostatic plasticity, and the limits of synaptic growth and function.

Results

Generation of *Syt12* loss-of-function alleles

Syt12 encodes a calcium-independent synaptotagmin, Synaptotagmin-12, which has been evolutionarily conserved from *Drosophila* to humans (Adolfsen *et al.*, 2004). Despite the presence of this gene in diverse species, relatively little is known about the molecular and cellular functions of *Syt12* or other calcium-independent synaptotagmins (Adolfsen *et al.*, 2004; Kaeser-Woo *et al.*, 2013). From generation and characterization of a *Syt12* knock-out mouse, Syt12 was found to play a contributory role in hippocampal mossy fiber long-term potentiation (mfLTP) (Kaeser-Woo *et al.*, 2013). This result is the first demonstration of an endogenous function for *Syt12*. However, the effect of *Syt12* loss in mice was mild, as the magnitude of mfLTP was reduced by merely half, and no significant changes in baseline synaptic transmission, short-term plasticity, long-term depression of inhibition, viability, or fertility were observed (Kaeser-Woo *et al.*, 2013).

As a caveat to these experiments, genes encoding other calcium-independent synaptotagmins may act redundantly with *Syt12* in mice (Kaeser-Woo *et al.*, 2013). To circumvent possible functional redundancies among synaptotagmin isoforms, we sought to characterize the null phenotype of *Syt12* in *Drosophila*. Unlike the mouse, which has genes encoding seventeen synaptotagmin isoforms (Adolfsen *et al.*, 2004; Bhalla *et al.*, 2008), *Drosophila* carries genes for only seven synaptotagmin isoforms (Adolfsen *et al.*, 2004). Moreover, *Drosophila* lacks genes encoding Syt13 and Syt16, which are likely candidates for functional redundancy with Syt12 in mice (Kaeser-Woo *et al.*, 2013). *Drosophila* Syt12 shows substantial homology to human Syt12, as the C2A and C2B

domains are 59% and 74% similar by amino acid sequence, respectively (Fig. 1B). Thus, deletion of *Syt12* in flies has the potential to uniquely uncover evolutionarily conserved roles for Syt12 and possibly other calcium-independent synaptotagmins.

To investigate the consequences of *Syt12* deletion in *Drosophila*, we carried out transposon mutagenesis of the *Syt12* gene locus using two distinct approaches. The *Syt12* gene locus is found on the X chromosome (X: 13,359,248..13,368,179) and comprises five exons in the coding region (dos Santos *et al.*, 2015) (Fig. 1A). In *P{EPgy2}EY11113* mutants, an "EY" *P* element (EY11113) (Bellen *et al.*, 2004) was inserted 4.9 kilobases upstream of the *Syt12* start codon (Fig. 1A). In *PBac{WH}f07791* and *PBac{WH}f06896* mutants, *piggyBac* transposons (Thibault *et al.*, 2004) were inserted 13.5 kilobases upstream (f07791) and 4.0 kilobases downstream (f06896) of the *Syt12* start codon, respectively (Fig. 1A). According to standard procedures (Bellen *et al.*, 2004; Thibault *et al.*, 2004), this collection of transposons was used to generate two loss-of-function alleles: $Syt12^{del}$ and a *bona fide* null allele, $Syt12^{null}$ (Fig. 1A).

Imprecise excision of the EY element, EY11113, with Δ2-3 transposase (Bellen *et al.*, 2004) resulted in deletion of 2.3 kilobases, including the first 1.5 kilobases of the *Syt12* gene locus (Fig. 1A, C). The resultant deletion, termed $Syt12^{del}$, was verified by PCR amplification and DNA sequencing with primers to genomic regions starting 200 base pairs upstream and ending 2.5 kilobases downstream of the EY11113 insertion site (Fig. 1C, E; Methods). Heat shock-driven FLP-FRT recombination between *piggyBac* transposons (Parks *et al.*, 2004), f07791 and f06896, resulted in deletion of 17.6 kilobases, including the entire 2.7-kilobase *Syt12* coding region (Fig.1A, C). The resultant deletion, termed $Syt12^{null}$, was verified by PCR amplification with three pairs of

primers to genomic regions starting 500 base pairs upstream of the f07791 insertion site and ending 400 to 700 base pairs downstream of the f06896 insertion site (Fig. 1D; Methods), as recommended for “final confirmation” (Parks *et al.*, 2004). PCR with each primer pair amplified bands of roughly 8 kilobases (Fig. 1D), instead of 18-kilobase bands expected from w^{1118} flies, consistent with *Syt12* deletion. One of these 8-kilobase products was sequenced at each end to define deletion breakpoints, which are located precisely at annotated (dos Santos *et al.*, 2015; Thibault *et al.*, 2004) f07791 and f06896 *piggyBac* insertion sites (Fig. 1A, H). For additional verification of the $Syt12^{null}$ deletion, PCR amplification with genomic primers used to confirm $Syt12^{del}$ produced no bands from $Syt12^{null}$ genomic DNA, but yielded strong bands from wild type, *PBac{WH}f07791*, and *PBac{WH}f06896* genomic DNA (Fig. 1C; Methods). Furthermore, two-sided PCR with a genomic primer and a *piggyBac* transposon-specific primer for each end of the transposon (Methods) was also used to confirm $Syt12^{null}$, as recommended (Parks *et al.*, 2004). Products from two-sided PCRs had sequences that we demonstrated to be identical to those obtained from PCR amplification across the transposon (Fig. 1G, H).

Previous investigation in *Drosophila* suggests that *Syt12* is expressed at “very low” levels throughout embryonic development and at “low” levels in adults, in which *Syt12* mRNA was enriched in heads (Adolfsen *et al.*, 2004). These data are consistent with reports by the *Drosophila* modENCODE Project (modENCODE Consortium *et al.*, 2010), FlyAtlas (Robinson *et al.*, 2013), and the FlyLight Project (Li *et al.*, 2014), likely indicating a selective role for Syt12 in the nervous system. To validate the expression of *Syt12* in the *Drosophila* central nervous system, we employed quantitative RT-PCR with brains from wild type and $Syt12^{del}$ third instar larvae. Through this technique, we reliably

detected *Syt12* mRNA in wild type larvae with two different primer/probe sets (Fig. 1E; Methods). Conversely, we determined that *Syt12* mRNA levels were reduced to 3.66% ± 1.79% (SEM) the amount of *Syt12* mRNA found in wild type controls (Fig. 1E). As an additional control, we also tested third instar larvae heterozygous for *Df(1)Exel6245*, a deficiency uncovering the *Syt12* locus, which expressed 53.5% ± 7.06% (SEM) the wild type amount of *Syt12* mRNA (Fig. 1E). Moreover, we tested third instar larvae carrying the *piggyBac* transposon, f06896, or an adjacent *piggyBac*, f00785, and observed *Syt12* mRNA expression that was similar to wild type (90.4% ± 2.89% and 132.4% ± 2.86%, respectively). These results suggest that $Syt12^{del}$ is a strong hypomorphic or amorphic allele and that *Syt12* is a common component of the *Drosophila* neuronal transcriptome.

Syt12 influences growth of the *Drosophila* larval neuromuscular junction

Studies in mammalian systems demonstrate that neuronal *Syt12* expression increases during development (Potter *et al.*, 2001; Maximov *et al.*, 2007). Expression of *Syt12*, initially termed *synaptotagmin-related gene 1* (*Srg1*), was shown to increase in developing rodent brains in a thyroid hormone-dependent manner (Thompson, 1996; Potter *et al.*, 2001; Itoh *et al.*, 2001). *Syt12* expression was also restricted to postnatal brains and increased during development in mice (Maximov *et al.*, 2007). These data are in agreement with multiple studies in *Drosophila*, which report similar changes in *Syt12* expression during development (Adolfsen *et al.*, 2004; modENCODE Consortium *et al.*, 2010; Robinson *et al.*, 2013). Given these consistencies across diverse species, we wondered if *Syt12* might influence neuronal growth and, accordingly, examined the well-characterized *Drosophila* NMJ (Atwood *et al.*, 1993; Jan and Jan, 1976) in $Syt12^{null}$.

Muscles of *Drosophila* third instar larvae have characteristic innervation patterns, which can be assessed to identify genes contributing to neuronal growth (Johansen *et al.*, 1989; Atwood *et al.*, 1993; Schuster *et al.*, 1996). Synaptic terminals on muscles 6 and 7 of third instar larvae are called “type I” and can be subdivided into two classes: Ib, which has relatively large boutons and subsynaptic reticula, and Is, which has relatively small boutons and subsynaptic reticula (Atwood *et al.*, 1993; Schuster *et al.*, 1996). To determine if *Syt12* affects neuronal growth, we analyzed type Ib and type Is boutons at muscles 6 and 7 of $Syt12^{null}$ third instar larvae. We distinguished type Ib and type Is boutons by intensity of Discs large (Dlg) staining at subsynaptic reticula and bouton size (Bhogal *et al.*, 2011). NMJs of $Syt12^{null}$ larvae had significantly fewer type Ib boutons, compared to wild type ($p < 0.01$) (Fig. 2A-C). Conversely, the number of type Is boutons for $Syt12^{null}$ NMJs was similar to wild type ($p = 0.88$) (Fig. 2A-C). These data show a 35.4% decrease and 1.95% decrease in $Syt12^{null}$ type Ib and type Is bouton numbers, respectively. Because muscle size has been shown to correlate with the size of NMJs (Schuster *et al.*, 1996), we also normalized bouton numbers to muscle areas, which were decreased by 12.3% in $Syt12^{null}$ ($p < 0.01$). However, we found similar differences between $Syt12^{null}$ and wild type for type Ib ($p < 0.01$) and type Is ($p = 0.60$) after this correction. NMJ areas of $Syt12^{null}$ larvae showed comparable trends to bouton numbers, as type Ib NMJ areas were significantly decreased in $Syt12^{null}$ ($p < 0.01$), while type Is NMJ areas in $Syt12^{null}$ were similar to wild type ($p = 0.70$) (Fig. 2E). Our data implicate *Syt12* in the selective growth and elaboration of type Ib boutons at the *Drosophila* NMJ.

NMJ growth-related parameters, including bouton number, NMJ area, and active zone number, are often, but not always, correlated (Cheng *et al.*, 2011; Kissler *et al.*,

2009). Therefore, along with characterizing the gross morphology of muscle 6/7 NMJs, we used an antibody against Bruchpilot (Brp; nc82) to visualize and count active zones of type Ib and type Is boutons (Kittel *et al.*, 2006) in *Syt12*^{null} third instar larvae. Type Ib boutons of *Syt12*^{null} larvae had significantly fewer active zones (nc82 puncta), compared to wild type ($p < 0.01$) (Fig. 2D). Likewise, type Is boutons of *Syt12*^{null} larvae showed a strong, but insignificant, trend toward fewer active zones by manual counting ($p = 0.10$) (Fig. 2D) and a significant decrease in active zone number using graylevel watershed (http://bigwww.epfl.ch/sage/soft/watershed) ($p < 0.01$). After nc82 puncta numbers were normalized to muscle areas, *Syt12*^{null} larvae had significantly fewer active zones in type Ib boutons than wild type ($p < 0.01$), but were not significantly different from wild type for active zone numbers in type Is boutons ($p = 0.30$). When calculating active zone density (nc82 puncta number/NMJ area), we uncovered slight, but significant, decreases in type Ib and type Is boutons of *Syt12*^{null} larvae ($p < 0.01$ and < 0.01) (Fig. 2F). These findings suggest that *Syt12* affects multiple NMJ growth-related parameters at distinct synapses.

To determine if the various effects on NMJ morphology in *Syt12*^{null} larvae may be attributed to loss of *Syt12* function in motor neurons, we drove expression of *UAS-Syt12* in motor neurons of *Syt12*^{null} larvae with *ok371-Gal4* (Mahr and Aberle, 2006). NMJs of *Syt12*^{null} larvae expressing *UAS-Syt12* were similar to wild type for bouton numbers ($p = 0.95$) and active zone densities ($p = 0.29$) of type Ib boutons (Fig. 2C, F). Furthermore, NMJ areas and nc82 puncta numbers of type Ib boutons in these rescued larvae were slightly, but significantly, larger than wild type ($p < 0.01$ and $= 0.03$) (Fig. 2D, E). When compared to these rescued larvae, *Syt12*^{null} larvae had smaller bouton numbers, NMJ areas, nc82 puncta numbers, and nc82 puncta densities of type Ib boutons ($p < 0.01$)

(Fig. 2C-F). Therefore, we conclude that *Syt12* expression in motor neurons is required for the normal growth of type Ib boutons. Moreover, the increased NMJ areas and nc82 densities seen in rescued larvae indicate that type Ib bouton growth may be limited by endogenous Syt12 levels and, thus, may be stimulated by elevating presynaptic Syt12.

The loss of *Syt12* had a strong effect on several NMJ growth-related parameters in type Ib boutons at muscle 6/7 (Fig. 2). Conversely, the effects of *Syt12* loss on type Is boutons were insignificant (Fig. 2C-E) or weak (Fig. 2F), when comparing $Syt12^{null}$ and wild type NMJs. Nonetheless, we analyzed type Is boutons from wild type, $Syt12^{null}$, and rescued $Syt12^{null}$ larvae in parallel. From our analysis, we discovered that type Is bouton numbers, NMJ areas, and nc82 puncta numbers were significantly increased in rescued $Syt12^{null}$ larvae, compared to wild type ($p < 0.01$) and $Syt12^{null}$ ($p < 0.01$) (Fig. 2C-E). Likewise, active zone density in type Is boutons was significantly decreased in $Syt12^{null}$ larvae, compared to rescued $Syt12^{null}$ larvae expressing *UAS-Syt12* in motor neurons ($p < 0.01$) (Fig. 2F). These results argue for an influence of *Syt12* on type Is boutons, in addition to the aforementioned effects of *Syt12* on type Ib boutons. Thus, *Syt12* may be generally necessary for normal growth and sufficient to enhance growth at muscle 6/7. Taking into account a cyclic AMP-dependent function for *Syt12* in mfLTP (Kaeser-Woo *et al.*, 2013) and a role for cyclic AMP (cAMP) in *Drosophila* NMJ growth (Zhong *et al.*, 1992; Yoshihara *et al.*, 2005), it is tempting to speculate that our noted effects of *Syt12* on NMJ growth and elaboration are somehow associated with altered cAMP signaling.

Notably, our investigation of NMJ morphology in $Syt12^{null}$ mutants has seemingly revealed a more subtle phenotype. In earlier examinations of a hypomorphic *fasciclin II* allele, $FasII^{e76}$ muscle 6/7 NMJs had 30-50% fewer boutons than wild type (Schuster *et*

al., 1996; Stewart *et al.*, 1996). Surprisingly, electrophysiological recordings from these mutant NMJs determined that synaptic strength was not altered, compared to wild type, and that the apparently normal synaptic strength could be attributed to a compensatory increase in active zone number (Stewart *et al.*, 1996; Davis and Goodman, 1998). Yet, despite a similar reduction in bouton number, $Syt12^{null}$ muscle 6/7 NMJs did not show a compensatory increase in active zone number. This inconsistency between $FasII^{e76}$ and $Syt12^{null}$ suggests that *Syt12* may participate in the mechanisms underlying presynaptic structural plasticity. Alternatively, an effect of *Syt12* loss on synaptic transmission might offset the NMJ growth deficits observed in $Syt12^{null}$ mutants, thereby negating induction of presynaptic structural plasticity due to an indirect reestablishment of a set point value.

Effects of *Syt12* on the structure of active zones at the *Drosophila* larval NMJ

The number and density of active zones at fly NMJs are not always correlated with the morphology of individual active zones (Liu *et al.*, 2011). Therefore, a change in nc82 puncta number or density in *Syt12* loss-of-function mutants might not be coupled with a change in active zone structure. To determine whether *Syt12* also affects active zone morphology, we used structured illumination microscopy (SIM) to examine nc82 puncta in boutons at muscles 6/7 and 4 of $Syt12^{del}$ third instar larvae. With SIM, nc82-labeled Brp appears as rings, instead of the spots seen with deconvolution microscopy, at planar active zones (Weyhersmüller *et al.*, 2011; Müller *et al.*, 2012). We measured the diameters of planar Brp rings in $Syt12^{del}$ and a control for the genetic background, "*Syt12* revertant" (Fig. 3; Methods), as previously described (Müller *et al.*, 2012). Brp ring diameters were similar between $Syt12^{del}$ and control at muscles 6/7 and 4, when computed as the diameter at half-maximum (Fig. 3C, D) or as the distance between two

peaks (p = 0.48 and = 0.92) (Fig. 3E, F) of fluorescence intensity line profiles. The Brp ring diameters shown here are similar to those of wild type NMJs, examined in parallel and previously reported (Müller *et al.*, 2012). Our findings suggest that *Syt12* does not regulate active zone morphology, despite influencing active zone number and density.

Effects of *Syt12* on synaptic Fasciclin II abundance at the *Drosophila* larval NMJ

Fasciclin II (FasII) is the *Drosophila* ortholog of Neural Cell Adhesion Molecule (NCAM) and influences synaptic growth in a dose-dependent manner (Schuster *et al.*, 1996; Stewart *et al.*, 1996; Beck *et al.*, 2012). A decrease in the expression of two FasII isoforms, known as FasII-A-PEST+ and FasII-A-PEST-, was specifically found to result in NMJ undergrowth (Beck *et al.*, 2012). Since we observed similar NMJ growth deficits in $Syt12^{null}$ mutants, we asked if the synaptic abundance of these FasII isoforms may be affected by the loss of *Syt12*. Using a previously characterized antibody (Van Vactor *et al.*, 1993; Beck *et al.*, 2012), we quantified levels of these two FasII isoforms at $Syt12^{null}$ NMJs and identified a 36.5% reduction, compared to wild type (n = 22; $p < 0.01$). This decrease in FasII levels at $Syt12^{null}$ NMJs is comparable to reductions (26% and 42%) seen at the NMJs of FasII splicing factor mutants, which also showed a similar amount of NMJ undergrowth (39% and 30%) (Beck *et al.*, 2012). Therefore, our findings suggest that the NMJ undergrowth in $Syt12^{null}$ mutants can be attributed to decreased levels of synaptic FasII. Furthermore, the loss of synaptic FasII was shown to induce presynaptic structural plasticity (Stewart *et al.*, 1996; Davis and Goodman, 1998), which we did not detect at $Syt12^{null}$ NMJs. Since synaptic FasII levels are decreased in $Syt12^{null}$, our data imply that the parallel reductions in bouton number and active zone number at $Syt12^{null}$

NMJs are not due to the lack of FasII-independent compensation. Instead, this defect in presynaptic structural plasticity is likely due to a failure in a FasII-associated homeostat.

FasII expression was also found to be modified in response to elevated cAMP levels at fly NMJs (Schuster *et al.*, 1996). As Syt12 activity is influenced by cAMP levels in the hippocampus (Kaeser-Woo *et al.*, 2013), these findings raise questions about an evolutionary conservation of Syt12 activity downstream of cAMP signaling. In opposition to our findings, however, elevated cAMP concentrations were correlated with decreased synaptic FasII levels and increased synaptic growth at the *Drosophila* NMJ (Schuster *et al.*, 1996) and in *Aplysia* (Bailey *et al.*, 1992; Mayford *et al.*, 1992). Hence, a relationship among Syt12, FasII, and cAMP signaling is almost certainly complex, perhaps involving positive and negative feedback (Song *et al.*, 2007), and will require further investigation.

Effects of *Syt12* on synaptic vesicle protein levels at the *Drosophila* larval NMJ

Components of active zones, such as Brp, and synaptic vesicle proteins, such as Syt1, are recruited to nascent synapses as they mature (Zhen and Jin, 1999; Patel *et al.*, 2006; Pack-Chung *et al.*, 2007). This maturation process occurs at the *Drosophila* NMJ and defines the number and density of active zones, as well as the composition of synaptic vesicles, through partially overlapping mechanisms (Pack-Chung *et al.*, 2007). To determine if *Syt12* contributes generally to synaptic maturation or more specifically to active zone development, we estimated the levels of representative synaptic vesicle proteins in $Syt12^{null}$ presynaptic terminals, according to standard methods (Heckscher *et al.*, 2007; Dickman *et al.*, 2009). The levels of cysteine string protein (CSP) (Fig. 4A-C) and Syt1 (Fig. 4A, B, D) at muscle 6/7 NMJs did not differ between $Syt12^{null}$ and wild type third instar larvae (p = 0.32 and 0.07). Similarly, CSP levels did not differ between

Syt12^{del} and *yw* controls (n = 21; *p* = 0.77), and Syt1 levels were not different between *Syt12*^{del} and *Syt12* revertant (n = 20; *p* = 0.10). We conclude that the role of *Syt12* in synaptogenesis is not widespread and could be restricted to active zone development.

Syt12 localizes to synaptic vesicles in *Drosophila* motor neuron terminals

Syt12 expression has previously been detected in the brains of rats (Potter *et al.*, 2001; Itoh *et al.*, 2001) and mice (Maximov *et al.*, 2007; Kaeser-Woo *et al.*, 2013). As described, we (Fig. 1F) and others (Adolfsen *et al.*, 2004; modENCODE Consortium *et al.*, 2010; Robinson *et al.*, 2013; Li *et al.*, 2014) have also detected *Syt12* expression in the brains of *Drosophila*. Our genetic rescue of NMJ growth defects in *Syt12*^{null} mutants with *UAS-Syt12* expression in motor neurons (Fig. 2) implies a function for Syt12 in the nervous system, perhaps directly at synapses. To determine the localization pattern of Syt12, we used an antibody against green fluorescent protein (GFP, 3E6, Invitrogen) to visualize Venus-tagged (Nagai *et al.*, 2002) Syt12, which we drove in motor neurons of wild type larvae with *ok371-Gal4* (Mahr and Aberle, 2006). Syt12-Venus trafficked to the presynaptic nerve terminals at NMJs, where it precisely colocalized with Syt1 (Fig. 5A). We detected Syt1 with a previously described antibody (Littleton *et al.*, 1993), which has been shown to specifically recognize Syt1 in wild type *Drosophila* larvae (Yoshihara *et al.*, 2002). Nonetheless, it is formally possible that this Syt1 antisera could also detect Syt12, as some antisera cross-reacts with multiple synaptotagmin isoforms (Littleton *et al.*, 1999; Adolfsen *et al.*, 2004). To rule out cross-reactivity between Syt1 and Syt12 in this experiment, we used *BG57-Gal4* (Budnik *et al.*, 1996) to overexpress Syt12-Venus in muscles and stained with anti-Syt1 (Littleton *et al.*, 1993). We found Syt12-Venus in large puncta throughout these muscles, which do not normally express Syt1 (Littleton *et*

al., 1993), but did not observe anti-Syt1 signal at these sites (Fig. 5B). Because Syt12-Venus expression was sufficient to rescue NMJ growth defects in $Syt12^{null}$ (Fig. 2), and we find no evidence for Syt1 and Syt12 cross-reactivity (Fig. 5B), we conclude that this presynaptic localization pattern of Syt12-Venus likely reflects the site of endogenous Syt12 function (Dickman *et al.*, 2009). Consistent with these findings, Syt12 has been isolated from synaptic vesicles in rats (Takamori *et al.*, 2006) and mice, in which it was shown to biochemically interact with Syt1 (Maximov *et al.*, 2007). In light of this precise colocalization between Syt12 and Syt1, fly Syt12 may also reside on synaptic vesicles.

Syt12 is dispensable for synaptic transmission at the *Drosophila* larval NMJ

Based on our observations that *Syt12* supports NMJ growth (Fig. 2) and encodes a presynaptic protein, which colocalizes with Syt1-positive synaptic vesicles (Fig. 5), we asked if *Syt12* influences functional properties of the NMJ. From electrophysiological recordings in current-clamp mode and 0.4 mM extracellular Ca^{2+} (Methods), we saw no significant differences between $Syt12^{null}$ and wild type larval NMJs for mean amplitudes of spontaneous miniature excitatory junctional potentials (mEJPs) (p = 0.57) (Fig. 6A, E) or quantal contents (p = 0.45) (Fig. 6C), even with correction for nonlinear summation (p = 0.16) (Fig. 6F). Yet, $Syt12^{null}$ mutants exhibited a slight, but significant, increase in the mean amplitude of evoked EJPs (p = 0.04) (Fig. 6B, E) and a slight, but insignificant, trend toward a decrease in the mean frequency of mEJPs (p = 0.06) (Fig. 6D, E). This small (9.9%) increase in $Syt12^{null}$ EJP amplitudes can be explained by a slight, albeit insignificant, increase (5.1%) in mEJP amplitudes. Accordingly, EJP amplitudes (n = 12; p = 1.00) and quantal contents with (n = 12; p = 0.26) or without correction for nonlinear summation (n = 12; p = 0.18) in $Syt12^{del}$ mutants were comparable to wild type under

the same experimental conditions. Finally, the moderate (18.5%) decrease in *Syt12*^{null} mEJP frequencies can be attributed to a decrease in the number of active zones (Fig. 2D) (Cheng *et al.*, 2011), as the loss of Syt12 also resulted in no significant effects on spontaneous release or other baseline parameters in mice (Kaeser-Woo *et al.*, 2013).

Given the precise presynaptic colocalization (Fig. 5) and canonical biochemical interaction between Syt12 and Syt1 (Bhalla *et al.*, 2007; Maximov *et al.*, 2007), we also assessed the ability of Ca^{2+} to trigger neurotransmitter release at *Syt12*^{null} NMJs. Since Syt1 is commonly essential for the Ca^{2+} cooperativity of synchronous neurotransmitter release (Yoshihara *et al.*, 2002; Sun *et al.*, 2007), Syt12 could hypothetically control this phenomenon through an interaction with Syt1. Nonetheless, *Syt12*^{null} and wild type EJP amplitudes were also similar at 0.2 mM extracellular Ca^{2+} (n = 17; $p = 0.87$) and 0.3 mM extracellular Ca^{2+} (n = 19; $p = 0.20$). Likewise, *Syt12*^{null} NMJs exhibited wild type quantal contents with (n = 17; $p = 0.34$) or without correction for nonlinear summation (n = 17; $p = 0.33$) at 0.2 mM extracellular Ca^{2+} and only slightly, albeit significantly, larger quantal contents with or without correction for nonlinear summation (n = 19; $p < 0.01$) at 0.3 mM extracellular Ca^{2+} (Fig. 6F). The modest increases in uncorrected and corrected quantal contents (26.8% and 36.5%, respectively) at *Syt12*^{null} NMJs at 0.3 mM extracellular Ca^{2+} can be attributed to a marginal, but significant, decrease (13.8%) in mEJP amplitude (n = 19; $p = 0.01$). Here, we find no compelling evidence for a role of *Syt12* in determining the Ca^{2+} cooperativity of synchronous release. Thus, biochemical or genetic interactions between Syt12 and Syt1 may occur without altering Ca^{2+}-dependence of release *in vivo*.

Overall, these results, which we obtained from electrophysiological recordings in subphysiological Ca^{2+} (Stewart *et al.*,1994), were somewhat unexpected. A decrease in

the number of active zones, which we have observed in *Syt12*^{null} mutants (Fig. 2), often correlates with smaller EJP amplitudes and quantal contents (Cheng *et al.*, 2011; Keller *et al.*, 2011). This lack of any reproducible electrophysiological defect in *Syt12*^{null} NMJs, across a range of extracellular Ca^{2+} concentrations, cannot be explained by presynaptic structural plasticity or by compensatory enhancement of quantal size at hypo-innervated muscles, both of which have been discovered by manipulating FasII levels (Schuster *et al.*, 1996; Stewart *et al.*, 1996; Davis and Goodman, 1998). Instead, the normal synaptic strength in *Syt12*^{null} could result from the general "robustness" (Davis, 2006) of synaptic transmission at *Drosophila* NMJs or, perhaps more interestingly, may arise from a more specific compensatory mechanism, which is inherently linked to the elimination of *Syt12*.

Syt12 is dispensable for homeostatic potentiation at the *Drosophila* larval NMJ

Homeostatic potentiation at the *Drosophila* larval NMJ is a phenomenon in which neurotransmitter release from presynaptic terminals is enhanced to offset decreases in the sensitivity of postsynaptic muscles to glutamate (Petersen *et al.*, 1997; Frank *et al.*, 2006; Gaviño *et al.*, 2015). This phenomenon has also been observed at rodent (Plomp *et al.*, 1992; Plomp *et al.*, 1995; Sandrock *et al.*, 1997) and human myasthenic (Cull-Candy *et al.*, 1980; Plomp *et al.*, 1995) NMJs, suggesting evolutionary conservation of underlying mechanisms (Davis, 2006; Davis, 2013; Davis and Müller, 2015). As seen with homeostatic potentiation, long-term potentiation at mossy fiber synapses in the CA3 region of the hippocampus also depends upon the enhancement of presynaptic neurotransmitter release (Weisskopf and Nicoll, 1995). *Syt12* was shown to contribute to the latter process, termed mfLTP (Kaeser-Woo *et al.*, 2013), and, accordingly, may reasonably contribute to homeostatic potentiation. To determine if *Syt12* participates in

homeostatic potentiation, we performed electrophysiology, pharmacology, and genetics, as previously described (Frank *et al.*, 2006), in two loss-of-function mutants (Methods).

A short-term form of homeostatic potentiation can be induced pharmacologically at fly NMJs through bath application of a glutamate receptor antagonist, philanthotoxin-433 (PhTx) (Frank *et al.*, 2006). This acute induction of homeostatic potentiation is rapid and precisely restores normal muscle depolarization within ten minutes of exposure to PhTx (Frank *et al.*, 2006; Dickman *et al.*, 2007) by way of enhancements in presynaptic Ca^{2+} influx (Müller and Davis, 2012) and the size of the readily-releasable pool (RRP) of synaptic vesicles (Weyhersmüller *et al.*, 2011; Müller *et al.*, 2012). We asked if *Syt12* is required for this form of homeostatic potentiation by assaying $Syt12^{null}$ and $Syt12^{del}$ loss-of-function mutants. In both mutants and wild type controls, PhTx application caused an approximately 50% reduction in mEJP amplitudes ($p < 0.01$) (Fig. 7A, C, G, E), as usual (Frank *et al.*, 2006). Consistent with accurate short-term homeostatic potentiation, mean EJP amplitudes following PhTx application decreased by only 5.1% in wild type (n = 16), 10.0% in $Syt12^{null}$ (n =19), and 0.03% in $Syt12^{del}$ (n =9), compared to baseline values in the absence of PhTx (n = 22, 18, and 12, respectively) (Fig. 7A, C, G, E). Mean quantal contents after PhTx application concomitantly increased by 81.6% in wild type (n = 16), 89.9% in $Syt12^{null}$ (n =19), and 68.2% in $Syt12^{del}$ (n =9), as above (Fig. 7A). These data indicate that short-term homeostatic potentiation is not dependent on *Syt12* expression.

A long-term form of homeostatic potentiation can be induced genetically at the fly NMJ with a null mutation, $GluRIIA^{SP16}$, which eliminates a subset of glutamate receptors from postsynaptic muscles (Petersen *et al.*, 1997). This form of homeostatic potentiation shares common mechanisms with short-term, PhTx-induced homeostasis (Davis, 2013;

Frank, 2014; Davis and Müller, 2015). However, short-term and long-term homeostatic potentiation differ in their requirements for small GTPase signaling (Frank *et al.*, 2009), Wnt signaling (Marie *et al.*, 2010), S6K/TOR signaling (Cheng *et al*., 2011; Penney *et al*., 2012), and presumably other mechanisms. Hence, *Syt12* could regulate long-term homeostatic potentiation, despite having no measurable effects with PhTx. Accordingly, we generated and recorded from double mutants carrying the $GluRIIA^{SP16}$ mutation and either $Syt12^{null}$ or $Syt12^{del}$. In both double mutants and $GluRIIA^{SP16}$ controls, the loss of GluRIIA led to an approximately 65% reduction in mEJP amplitudes ($p < 0.01$) (Fig. 7B, D, F, H), as usual (Petersen *et al.*, 1997; Frank *et al.*, 2006). Consistent with long-term homeostatic potentiation, average quantal contents increased by 77.3% in $GluRIIA^{SP16}$ single mutant controls (n = 14), 128.8% in $Syt12^{null}$; $GluRIIA^{SP16}$ double mutants (n =15), and 117.5% in $Syt12^{del}$; $GluRIIA^{SP16}$ double mutants (n =9), when comparing "baseline" values in $GluRIIA^{+}$ larvae (n = 22 for wild type, 18 for $Syt12^{null}$, and 12 for $Syt12^{del}$) (Fig. 7B). These data show that *Syt12* is not required for long-term homeostatic potentiation.

Our search to identify a role for *Syt12* in homeostatic potentiation has brought us to three notable conclusions. First, our results indicate that homeostatic potentiation can proceed normally at NMJs with impaired growth, including decreases in the number and density of active zones (Fig. 2). This conclusion is buttressed by a discovery that short-term homeostatic potentiation was not disrupted by alterations in BMP signaling, despite decreased bouton numbers (Goold and Davis, 2007). Second, our findings suggest that homeostatic potentiation and presynaptic structural plasticity, which may be disrupted in $Syt12^{null}$ mutants, are carried out via different mechanisms. This conclusion is supported by complementary studies, which determined that other forms of homeostatic regulation

at the *Drosophila* NMJ are separable (Frank *et al.*, 2009; Bergquist *et al.*, 2010; Gaviño *et al.*, 2015) Third, our data indicate that the mechanisms of homeostatic potentiation at the *Drosophila* NMJ and mfLTP in the hippocampus can be distinguished by the lack of a requirement for *Syt12*. Although, these two forms of synaptic plasticity probably share some evolutionarily conserved mechanisms, as Rab3 (Castillo *et al.*, 1997; Müller *et al.*, 2011) and RIM (Castillo *et al.*, 2002; Müller *et al.*, 2012) are implicated in each process.

Effects of *Syt12* overexpression on neurotransmitter release at *Drosophila* NMJs

In addition to investigating the effects of *Syt12* loss, we asked if overexpression of *Syt12* influences electrophysiological properties of the NMJ. Since rescued $Syt12^{null}$ larvae expressing *UAS-Syt12* in motor neurons showed enhanced NMJ growth (Fig. 2), one might have expected to observe concomitantly enhanced neurotransmitter release (Cheng *et al.*, 2011; Keller *et al.*, 2011). In contrast, these transgenic larvae had a mean EJP amplitude of 29.9 ± 1.78 (SEM) mV (n = 11), which was significantly lower than wild type (n = 22; $p < 0.01$) and $Syt12^{null}$ (n = 18; $p < 0.01$) mean EJPs by 22.3% and 29.3%, respectively. This decrease in synaptic strength, although subtle, probably results from decreased quantal size, as these rescued larvae had a mean mEJP amplitude of 0.52 ± 0.03 (SEM) mV (n = 11). This mean mEJP amplitude was also significantly smaller than wild type (n = 22; $p < 0.01$) and $Syt12^{null}$ (n = 18; $p < 0.01$) mean mEJPs by 35.6% and 38.7%, respectively. Therefore, the average quantal content in $Syt12^{null}$*; ok371>UAS-Syt12* trended toward an increase over wild type (n = 22; $p = 0.11$) and $Syt12^{null}$ (n = 18; $p = 0.26$), but was not significantly different in either case. These findings indicate that the stimulation of NMJ growth by *Syt12* expression counterintuitively does not lead to increased neurotransmitter release. Instead, our results argue for a possible inhibitory

function of *Syt12* in synaptic transmission, which has not been previously demonstrated. Notably, our data are also consistent with presumably cell autonomous (Schuster *et al.*, 1996) and target-specific (Davis and Goodman, 1998) regulatory mechanisms, which seem to compensate for muscle hyperinnervation by inhibiting neurotransmitter release.

As the molecular mechanisms underlying homeostatic potentiation and baseline synaptic transmission at the fly NMJ are separable (Goold and Davis, 2007; Dickman *et al.*, 2009), we applied PhTx to $Syt12^{null}$*; ok371>UAS-Syt12* larvae to test for the normal induction of synaptic homeostasis. PhTx treatment in these rescued larvae reduced the mean mEJP amplitude to 0.26 ± 0.02 (SEM) mV (n = 10), which was a 51.0% reduction from baseline (n = 11; $p < 0.01$), as expected (Frank *et al.*, 2006). Mean EJP amplitude in these larvae after PhTx treatment was 28.2 ± 1.48 (SEM) mV (n = 10), which was a 5.7% reduction from baseline (n = 11; $p = 0.47$). Moreover, mean quantal content after PhTx treatment was strongly enhanced to 115.97 ± 9.97 (SEM) (n = 10) by 97.4% over baseline (n = 11; $p < 0.01$). We conclude that *Syt12* overexpression and, by extension from other results (Fig. 2), enlargement of NMJs do not impair homeostatic potentiation. Moreover, these data imply that the mechanisms underlying a target-specific (Davis and Goodman, 1998) or a cell autonomous (Schuster *et al.*, 1996) downregulation of quantal content at hyperinnervated muscles are distinct from those of homeostatic potentiation.

Syt12 limits the size of the readily-releasable pool of synaptic vesicles at fly NMJs

Intracellular recordings in current-clamp mode are widely used to determine the electrophysiological properties of synapses (Zhang and Stewart, 2010). Yet, differences in neurotransmitter release can be masked by variations in resting membrane potentials and nonlinear summation, especially under conditions of high release probability (Zhang

and Stewart, 2010; Müller *et al.*, 2012). Consequently, we studied baseline transmission at *Syt12*-deficient synapses more directly by performing two-electrode voltage-clamp at *Syt12*^{null} larval NMJs, as described (Müller et al., 2012). From our recordings, which we carried out at a physiological Ca^{2+} concentration (Stewart *et al.*,1994), we observed that mean initial excitatory junctional currents (EJCs) in 60-Hz stimulus trains were larger at *Syt12*^{null} NMJs, compared to wild type ($p = 0.02$) (Fig. 8B, E, F, G). Likewise, cumulative EJCs, which we calculated by the "backextrapolation method" (Schneggenburger *et al.*, 1999; Weyhersmüller *et al.*, 2011; Müller *et al.*, 2012), were also significantly enhanced at *Syt12*^{null} NMJs, compared to wild type ($p < 0.01$) (Fig. 8C, E, F). By dividing the mean cumulative EJC amplitude by the mean mEJP amplitude, acquired in current-clamp, we were able to estimate RRP sizes at each NMJ (Weyhersmüller *et al.*, 2011; Müller *et al.*, 2012). Our RRP size estimations at *Syt12*^{null} NMJs were 63.7% larger than wild type ($p = 0.02$) (Fig. 8D). This difference in RRP sizes might be exaggerated by a slightly, albeit not significantly, decreased mean mEJP amplitude in *Syt12*^{null} ($p = 0.74$) (Fig. 8A), since homeostatic potentiation occurs normally in the absence of *Syt12* (Fig. 7), and RRP size is enlarged by homeostatic potentiation (Weyhersmüller *et al.*, 2011; Müller *et al.*, 2012). Regardless, an enlargement of the RRP is consistent with the larger initial EJCs seen in *Syt12*^{null}, as first elegantly described by the quantal theory (del Castillo and Katz, 1954).

Along with measuring synaptic strength and RRP size, our recordings in voltage-clamp allowed us to more closely investigate short-term plasticity (Weyhersmüller *et al.*, 2011; Müller *et al.*, 2012; Gaviño *et al.*, 2015). Through analysis of thirty stimuli from 60-Hz trains, we found that synaptic depression over the first ten stimuli of the 60-Hz trains did not differ between wild type and *Syt12*^{null} ($p = 0.25$) (Fig. 8E-H). Conversely, *Syt12*^{null}

mutants showed significantly enhanced depression at the ends ($EJC_{final}/EJC_{initial}$) of our trains, compared to wild type (p = 0.02) (Fig. 8E-H). However, this amount of depression (21.7%) is modest, despite its significance, and is largely consistent with the absence of an effect on short-term plasticity in *Syt12* knock-out mice (Kaeser-Woo *et al.*, 2013). As an estimate of release probability (P_{train}), we calculated the fraction of the RRP released by the first action potential in our 60-Hz trains, as previously done (Schneggenburger *et al.*, 1999; Gaviño *et al.*, 2015). We determined P_{train} at $Syt12^{null}$ NMJs to be 0.32 ± 0.01 (SEM) (n = 20) and P_{train} at wild type NMJs to be 0.36 ± 0.02 (SEM) (n = 13). This small (13.3%) difference in P_{train} values was significant (p < 0.04) and points to a slightly lower release probability in $Syt12^{null}$. This decrease in release probability may explain why the $Syt12^{null}$ mean RRP size increase is more pronounced than that of the mean initial EJC.

Based on the decreased number of active zones at muscle 6/7 NMJs of $Syt12^{null}$, we would have expected a correlated decrease in the estimated RRP size (Cheng *et al.*, 2011; Keller *et al.*, 2011). Contrary to these expectations, we found that $Syt12^{null}$ motor neurons have an increased number of release-ready vesicles and, thus, corresponding increases in initial and cumulative EJC amplitudes from high-frequency stimulus trains. These voltage-clamp data are consistent with our intracellular recordings (Fig. 6), which also uncovered no substantial impairments in baseline synaptic transmission at $Syt12^{null}$ NMJs. These results are also consistent with our *Syt12* overexpression data, which may point to a previously undetected role for *Syt12* in limiting neurotransmitter release, albeit perhaps only under physiological conditions or in the absence of functional redundancy.

Discussion

Genes encoding calcium-independent synaptotagmins, such as Syt12 and Syt14, are present in vertebrates, as well as *Drosophila* and other invertebrates (Fukuda, 2003; Adolfsen *et al.*, 2004; Craxton, 2010). This degree of evolutionary conservation points to a significant role for these synaptotagmin isoforms in metazoan biology (Craxton, 2010). In support of this hypothesis, mutations in Syt14 have been linked to neurodegenerative and neurodevelopmental disorders in humans (Quintero-Rivera *et al.*, 2007; Doi *et al.*, 2011). Syt12 expression is also regulated by thyroid hormone in the developing brain (Potter *et al.*, 2001; Itoh *et al.*, 2001) and is necessary for a component of hippocampal mfLTP (Kaeser-Woo *et al.*, 2013). Despite the importance of these findings, it remains unclear how calcium-independent synaptotagmins function at a molecular level *in vivo*. Additionally, mammalian genomes encode seventeen synaptotagmin isoforms, as many as nine of which are thought to be calcium-independent (Hui *et al.*, 2005; Bhalla *et al.*, 2008) and may have redundant functions (Kaeser-Woo *et al.*, 2013). In contrast, the *C. elegans* genome does not seem to encode calcium-independent synaptotagmins at all (Nonet *et al.*, 2003; Adolfsen *et al.*, 2004), thereby occluding a genetic analysis in this simpler model organism (Brenner, 1974). Further complicating the genetic analysis of calcium-independent synaptotagmins, Syt1 was shown to perform calcium-independent functions in various aspects of neurotransmitter release, including docking (Reist *et al.*, 1998; Rickman *et al.*, 2006; de Wit *et al.*, 2009), fusion (Mahal *et al.*, 2002), endocytosis (Poskanzer *et al.*, 2006; Loewen *et al.*, 2006), and positioning (Young and Neher, 2009) of synaptic vesicles. Thus, complementary approaches are required to fully understand the mysterious roles of calcium-independent synaptotagmins in the evolution of animals.

In this study, we have generated two loss-of-function alleles of *Drosophila Syt12* via transposon mutagenesis (Bellen *et al.*, 2004; Thibault *et al.*, 2004) to determine the contributions of this calcium-independent synaptotagmin to the structural and functional properties of the fly NMJ (Atwood *et al.*, 1993; Jan and Jan, 1976). Genetic analysis of calcium-independent synaptotagmins is simplified by using *Drosophila*, which has only two of these synaptotagmin isoforms: Syt12 and Syt14 (Adolfsen *et al.*, 2004). We have chosen to examine *Syt12* based on the availability of transposon insertions, which could be utilized to specifically delete *Syt12* (Bellen *et al.*, 2004; Parks *et al.*, 2004; Thibault *et al.*, 2004). In the future, using other methods of genome engineering (Jinek *et al.*, 2012; Cong *et al.*, 2013; Gratz *et al.*, 2013) to delete *Syt14* should enhance our knowledge of calcium-independent synaptotagmins. Here, we have revealed functions for *Syt12* in the structure and function of the *Drosophila* nervous system. Our results build upon *in vitro* studies (Hui *et al.*, 2005; Bhalla *et al.*, 2008) and genetic analyses in rodents (Potter *et al.*, 2001; Itoh *et al.*, 2001; Maximov *et al.*, 2007; Kaeser-Woo *et al.*, 2013) and suggest that *Syt12* promotes synaptic growth and limits neurotransmitter release at the fly NMJ.

Syt12 was originally identified as one of the first genes to be directly regulated by thyroid hormone in the developing mammalian brain (Thompson, 1996). Hypothyroidism has deleterious effects on developing brains, often resulting in ataxia, spasticity, mental retardation, and deafness (Thompson and Potter, 2000). These thyroid hormone-related abnormalities are correlated with a reduction in the densities of axons (Eayrs, 1953) and dendrites (Ruiz-Marcos *et al.*, 1979; Gould and Butcher, 1989), as well as a decrease in *Syt12* expression (Thompson, 1996; Potter *et al.*, 2001; Itoh *et al.*, 2001). These results, as well as synaptic localization of Syt12 protein (Thompson and Potter, 2000; Maximov

et al., 2007; Kaeser-Woo *et al.*, 2013), indicate that Syt12 deficiency may have a causal role in the aberrant neurite growth of the hypothyroid brain. To date, this hypothesis has not been tested in mammals. However, we have found that NMJs of *Syt12*^{null} third instar larvae are undergrown and have significantly decreased numbers of boutons and active zones. We can attribute these NMJ growth-related deficits to the loss of neuronal *Syt12* expression, as resupplying *Syt12*^{null} presynaptic motor neurons with Gal4-driven (Mahr and Aberle, 2006) Syt12 rescued the mutant phenotype. Therefore, our findings provide the first evidence for a *Syt12*-dependent modulation of synaptic growth and further imply a contribution of *Syt12* in brain development and disease (Thompson and Potter, 2000).

Given the availability of a *Syt12* knockout mouse (Kaeser-Woo *et al.*, 2013), it is possible to characterize the *Syt12* null phenotype in mammals. An electrophysiological analysis of this *Syt12* knockout revealed a specific defect in the long-term maintenance of cAMP-dependent mfLTP in the hippocampus (Kaeser-Woo *et al.*, 2013). Although a requirement for cAMP signaling in mfLTP was established in earlier reports (Huang *et al.*, 1994; Weisskopf *et al.*, 1994), Syt12 is seemingly the first phosphorylation target of cAMP signaling to affect mfLTP (Kaeser *et al.*, 2008; Yang and Calakos, 2010; Kaeser-Woo *et al.*, 2013). Nonetheless, the molecular mechanism through which Syt12 controls mfLTP has not been illuminated. Changes in synaptic morphology were correlated with expression of cAMP-dependent forms of synaptic plasticity in *Aplysia* (Bailey and Chen, 1988) and *Drosophila* (Davis *et al.*, 1996; Schuster *et al.*, 1996; Yoshihara *et al.*, 2005). Our discovery that the loss of *Syt12* leads to synaptic undergrowth at *Drosophila* NMJs is reminiscent of another study, which reports a similar degree of synaptic undergrowth in cAMP signaling mutants (Chen and Ganetzky, 2012). Hence, our discovery hints at a

plausible mechanism, which may explain the failure of *Syt12* knockout mice to maintain cAMP-dependent hippocampal mfLTP (Kaeser-Woo *et al.*, 2013). As activity-dependent growth of synapses was hypothesized to stabilize long-term potentiation (Kandel, 2012), a form of structural plasticity may depend upon the regulation of Syt12 activity in mfLTP.

The exact mechanisms underlying mfLTP in the hippocampus are not fully known (Castillo, 2012) and may involve presynaptic (Weisskopf and Nicoll, 1995; Ben-Simon *et al.*, 2015) and postsynaptic processes (Yeckel *et al.*, 1999). Regardless, some evidence indicates that mfLTP is triggered by an increase in presynaptic Ca^{2+} influx (Zalutsky and Nicoll, 1990; Mellor and Nicoll, 2001). Homeostatic potentiation at the fly NMJ (Petersen *et al.*, 1997; Frank *et al.*, 2006) is also correlated with enhancement of presynaptic Ca^{2+} influx (Müller and Davis, 2012). Moreover, *Drosophila* homeostatic potentiation depends upon regulation of presynaptic Rab3-associated molecules (Müller *et al.*, 2011; Müller *et al.*, 2012), which are necessary for hippocampal mfLTP (Castillo *et al.*, 1997; Castillo *et al.*, 2002). Despite the similarities between homeostatic potentiation at *Drosophila* NMJs and mfLTP at hippocampal synapses, both short-term (Frank *et al.*, 2006) and long-term (Petersen *et al.*, 1997) forms of homeostatic potentiation could be fully expressed in the absence of *Syt12*. Therefore, we conclude that homeostatic potentiation and mfLTP are separable phenomena. Future studies will be required to determine if relationships exist between *Syt12* and presynaptic Ca^{2+} influx in mfLTP or other kinds of synaptic plasticity, though we can report no evidence for such a relationship in fly homeostatic potentiation.

Homeostatic synaptic plasticity at *Drosophila* NMJs has been studied extensively (Davis, 2006; Davis, 2013; Davis and Müller, 2015) and can be employed to upregulate (Petersen *et al.*, 1997; Frank *et al.*, 2006) or downregulate (Gaviño *et al.*, 2015) release

of glutamate to counteract alterations in postsynaptic glutamate receptor sensitivity. The modulation of neurotransmitter release in either case does not depend on morphological changes to NMJs (Petersen *et al.*, 1997; Frank *et al.*, 2006; Gaviño *et al.*, 2015), at least at the level of deconvolution microscopy (Weyhersmüller *et al.*, 2011). However, there is evidence that *Drosophila* express homeostatic structural plasticity to offset undergrowth (Stewart *et al.*, 1996) or overgrowth (Davis *et al.*, 1996; Schuster *et al.*, 1996; Davis and Goodman, 1998) of NMJs. An undergrowth of *Drosophila* NMJs in hypomorphic *fasciclin II* mutants was inversely correlated with the number of active zones, thereby pointing to the existence of presynaptic homeostatic structural plasticity (Stewart *et al.*, 1996; Davis and Goodman, 1998). A similar effect on NMJ-growth related parameters was also seen in splicing factor mutants with impaired *fasciclin II* expression (Beck *et al.*, 2012). Unlike these Fasciclin II signaling mutants, the $Syt12^{null}$ mutant exhibited reduced numbers of boutons and active zones, implying that presynaptic structural plasticity is not accurately expressed in the absence of *Syt12*. Importantly, cAMP signaling mutants were shown to have fewer boutons and active zones in a different study with flies (Chen and Ganetzky, 2012). In contrast to these cAMP signaling mutants, which showed parallel reductions in synaptic strength, we show that $Syt12^{null}$ synaptic strengths are comparable to wild type.

In light of evidence for presynaptic structural plasticity at fly NMJs (Stewart *et al.*, 1996; Davis and Goodman, 1998), our findings raise ideas to consider. Full expression of homeostatic potentiation at $Syt12^{null}$ NMJs, which are undergrown on average, imply that this form of synaptic plasticity is distinct from presynaptic structural plasticity at the molecular level. In addition, the apparent lack of presynaptic structural plasticity in both $Syt12^{null}$ and cAMP signaling mutants (Chen and Ganetzky, 2012) suggests that a role

for Syt12 in cAMP signaling may be more ancient than previously recognized (Maximov *et al.*, 2007; Kaeser-Woo *et al.*, 2013). Altered cAMP signaling has also been shown to interfere with a compensatory downregulation of neurotransmitter release in response to NMJ overgrowth in flies (Davis *et al.*, 1996). Consequently, when viewed in a broader context, our findings and those of others (Davis *et al.*, 1996; Chen and Ganetzky, 2012) indicate that cAMP signaling may be required for the bidirectional control of presynaptic structural plasticity at the *Drosophila* NMJ. Moreover, shedding light on mechanisms of presynaptic structural plasticity in flies could have implications for understanding mfLTP and other cAMP-dependent forms of synaptic plasticity in mammalian nervous systems. Along with these ideas, yet another consideration is pertinent to our discussion. $Syt12^{null}$ NMJs are undergrown and have fewer active zones, but show relatively normal synaptic strength. Hence, it is plausible that alterations to functional properties of $Syt12^{null}$ NMJs mask or offset a concomitant weakening of synaptic strength, which would be expected from this degree of NMJ undergrowth (Stewart *et al.*, 1996; Chen and Ganetzky, 2012).

From current-clamp recordings in subphysiological extracellular Ca^{2+} (Stewart *et al.*, 1994), we determined that synaptic strengths and quantal contents at $Syt12^{null}$ NMJs were comparable to wild type. These results are largely consistent with recordings from *Syt12* knockout mice, which also exhibited no significant perturbations to basal synaptic transmission (Kaeser-Woo *et al.*, 2013). Nonetheless, the apparently normal amount of neurotransmitter release at $Syt12^{null}$ NMJs is unexpected, as a reduction in the number of active zones should lead to a concomitant decrease in quantal content (Stewart *et al.*, 1996; Kittel *et al.*, 2006; Wagh *et al.*, 2006; Keller *et al.*, 2011). Yet, a reduction in active zone numbers at $Syt12^{null}$ NMJs might not result in impaired neurotransmitter release, if

a wild type amount of release machinery is distributed throughout fewer active zones. In support of this hypothesis, we estimated RRP sizes at *Syt12*^{null} NMJs from recordings in voltage-clamp in physiological (1.5 mM) Ca^{2+} (Stewart *et al.*, 1994) with high-frequency (60-Hz) stimulation (Weyhersmüller *et al.*, 2011; Müller *et al.*, 2012; Gaviño *et al.*, 2015) and found no reduction in release-ready vesicles, as compared to wild type. In fact, we detected a 63.7% increase in the estimated RRP size at *Syt12*^{null} NMJs, relative to wild type. This enlargement of the RRP size at *Syt12*^{null} NMJs cannot be attributed to either homeostatic potentiation (Petersen *et al.*, 1997; Frank *et al.*, 2006) or homeostatic depression (Daniels *et al.*, 2004; Gaviño *et al.*, 2015), since cumulative EJCs were also significantly increased by 39.9% on average (Müller *et al.*, 2015). Based on our data, it seems reasonable to conclude that *Syt12* limits neurotransmitter release at the fly NMJ.

By characterizing the null phenotype of *Syt12* in *Drosophila*, we have uncovered functions for a calcium-independent synaptotagmin in NMJ morphogenesis and limiting synaptic transmission under physiological conditions (Stewart *et al.*, 1994; Younger *et al.*, 2013). Our results are also consistent with a role for *Syt12* in presynaptic structural plasticity (Stewart *et al.*, 1996; Davis and Goodman, 1998) and likely indicate that this form of homeostatic regulation is distinguishable from long-term (Petersen *et al.*, 1997) and short-term (Frank *et al.*, 2006) homeostatic potentiation. Yet, since the mechanisms of mfLTP in the hippocampus (Huang *et al.*, 1994; Weisskopf *et al.*, 1994; Kaeser-Woo *et al.*, 2013) and presynaptic structural plasticity at *Drosophila* NMJs (Davis *et al.*, 1996; Chen and Ganetzky, 2012) share common regulatory proteins, perhaps including Syt12, our findings might have implications for learning and memory (Kandel, 2012). Moreover, an increased number of release-ready vesicles at Syt12-deficient *Drosophila* NMJs may

evoke an alternate explanation for a disruption of cAMP-dependent hippocampal mfLTP in *Syt12* knockout mice (Kaeser-Woo *et al.*, 2013). The loss of Syt12 could occlude, not block, mfLTP, as seen following stimulation of cAMP signaling (Huang *et al.*, 1994). This occlusion of cAMP-dependent hippocampal mfLTP may occur due to an enlargement of the baseline RRP size, which is directly correlated with the degree of presynaptic cAMP signaling (Goussakov *et al.*, 2000; Nagy *et al.*, 2004). Buttressing this hypothesis, Syt12 has been shown to interfere with Syt1 *in vitro* and could limit neurotransmitter release in this manner (Maximov *et al.*, 2007; Bhalla *et al.*, 2008). However, functional redundancy may conceal effects of Syt12 activity in mammals (Maximov *et al.*, 2007; Kaeser-Woo *et al.*, 2013). Our results imply that this prediction is accurate. Accordingly, a simultaneous disruption of multiple calcium-independent synaptotagmins in the mammalian brain may unearth evolutionarily conserved functions for Syt12. Ultimately, the effects of *Syt12* on the structure and function of the *Drosophila* NMJ underscores the probable significance of calcium-independent synaptotagmins in metazoan evolution (Craxton, 2010) and may be relevant to human health and disease (Quintero-Rivera *et al.*, 2007; Doi *et al.*, 2011).

Materials and Methods

Fly stocks and genetics

Fly stocks were maintained at 22-25° C on normal food. The *Syt12*^{null} line was generated according to heat-shock driven FLP-recombinase methodology (Parks *et al.*, 2004), using *PBac{WH}f07791* and *PBac{WH}f06896*. *Syt12*^{null} is a 17.6-kilobase deletion, which removes the *Syt12* gene locus. The *Syt12*^{del} line was generated by imprecise excision of the *P{EPgy2}EY11113* element with Δ2-3 transposase according to standard genetic procedures (Bellen *et al.*, 2004). *Syt12*^{del} is a 2.3-kilobase deletion, which removes the first 1.5 kilobases of the *Syt12* gene locus. A precise excision of *P{EPgy2}EY11113*, which we call "*Syt12* revertant", was also created to control for genetic background, and the integrity of the *Syt12* locus was confirmed by sequencing. Where indicated, *yw*, instead of *Syt12* revertant, was used as a control for *Syt12*^{del}. For transgene expression in motor neurons, we used *ok371-Gal4* on the second chromosome, as previously described (Mahr and Aberle, 2006). For transgene expression in muscles, we used *BG57-Gal4* on the third chromosome (Budnik *et al.*, 1996). For long-term homeostatic potentiation experiments, we used *GluRIIA*^{SP16} (Petersen *et al.*, 1997). Fly stocks not generated by our laboratory were obtained from the Bloomington *Drosophila* Stock Center at Indiana University (Bloomington, IN), the Exelixis Collection at the Harvard Medical School (Boston, MA), or the laboratory of Lily and Yuh-Nung Jan at the University of California, San Francisco (San Francisco, CA). Standard first (X), second, and third chromosome balancers and genetic strategies were used for crosses and for maintaining mutant lines. "Wild type" refers to *w*^{1118}.

Molecular biology

Drosophila genomic DNA was extracted from adult flies according to the Quick Fly Genomic DNA Prep provided by E. Jay Rehm of the Berkeley *Drosophila* Genome Project (http://www.fruitfly.org/about/methods/inverse.pcr.html).

A genomic region containing the 5' end of the *Syt12* gene locus was PCR-amplified from w^{1118}, $Syt12^{del}$, *PBac{WH}f07791*, *PBac{WH}f06896*, and $Syt12^{null}$ genomic DNA and sequenced using the following genome-specific primers:

Forward primer:

5' CGA GAG GAG TGA CGG AAG G 3'

Reverse primer:

5' GAT AGG AAT GGT TAG TAT CG 3'

Regions of DNA containing a 7.2-kilobase *piggyBac* transposon were PCR-amplified from $Syt12^{null}$ genomic DNA using the following three pairs of genome-specific primers:

Forward primer for pair #1:

5' CGA TTG ATT GGT ATT AAG CG 3'

Reverse primer for pairs #1 and #2:

5' GGA TAT GTA ATC GAA CTT ACC 3'

Forward primer for pairs #2 and #3:

5' CCA CTG CAA TCC ATT GAG 3'

Reverse primer for pair #3:

5’ CGT TTC ATT AGC TAA TAG TAC G 3’

A PCR product containing a 7.2-kilobase *piggyBac* transposon and flanking genomic DNA from *Syt12*^{null}, which we generated using the primers for pair #2 above, was sequenced on each end with the following *piggyBac* transposon-specific primers:

Transposon-specific primer for upstream end of *piggyBac*:

5’ ACG GAT TCG CGC TAT TTA GAA AGA GAG 3’

Transposon-specific primer for downstream end of *piggyBac*:

5’ CGA TAT ACA GAC CGA TAA AAC ACA TGC G 3’

For additional confirmation of *Syt12*^{null}, two-sided PCR from *Syt12*^{null} genomic DNA was carried out using the following two pairs of genomic and transposon-specific primers:

Genomic primer for upstream end of *piggyBac*:

5’ CGA TTG ATT GGT ATT AAG CG 3’

Transposon-specific primer for upstream end of *piggyBac*:

5’ ACG GAT TCG CGC TAT TTA GAA AGA GAG 3’

Transposon-specific primer for downstream end of *piggyBac*:

5’ CGA TAT ACA GAC CGA TAA AAC ACA TGC G 3’

Genomic primer for downstream end of *piggyBac*:

5’ CGT TTC ATT AGC TAA TAG TAC G 3’

Drosophila Syt12 cDNA was obtained from the *Drosophila* Genomics Resource Center (DGRC; Bloomington, IN) as an expressed sequence tag (RE01517). The *Syt12* open reading frame was amplified by PCR and cloned into the pENTR/D-TOPO vector (Gateway Technology, Invitrogen) using the following primers:

Forward primer for *pUASt-Syt12-venus*:

5' CAC CAT GAT GAG CTT CAC CAT TAC CTT GGC 3'

Reverse primer for *pUASt-Syt12-venus*:

5' GAC GAT GCT GTT CCG CTT GG 3'

All vectors were sequenced to confirm the absence of mutations. The *Syt12* cDNA was then cloned into proper destination vectors, obtained from the *Drosophila* Gateway Vector Collection (Carnegie Institution, Baltimore, MD). Transgenic lines were generated by BestGene Inc. (Chino Hills, CA) and mapped using standard methods.

Quantitative RT-PCR

Quantitative RT-PCR was performed as previously described (Bergquist *et al.*, 2010). Primer/probe sets were designed and made by Applied Biosystems. Dm01838550_g1 and Dm01838550_g2 probes were used for quantification of *Syt12* mRNA abundance. Dm02151827_g1 (*RpL32*) and a custom primer/probe set to quantify *futsch* mRNA were used as controls. Neural-specific *futsch* (Hummel *et al.*, 2000; Lepicard *et al.*, 2014) mRNA quantification was carried out using the following primers and probe:

Forward primer:

5' GCA TCT GCT CAA GGG ATT CC 3'

Reverse primer:

5’ CCG TTC GCC GTG ACG AG 3’

Probe for *futsch*:

5’ CAC GTC GAC TTG GAA GAG GAG CTC 3’

The CNS was removed from 25 wandering third instar larvae per sample (three samples per genotype). Total RNA was isolated from each sample using an RNeasy Mini Kit (Qiagen). A DNase digestion was performed to remove potential DNA contamination (RQ1 RNase-free DNase; Promega). RT was performed (TaqMan; Applied Biosystems) using random hexamers and 1 µg of total RNA. A no-RT control was performed for each sample. Purified cDNA was used as a template in 30-µL PCR reactions (TaqMan Universal PCR Master Mix; Applied Biosystems). Each 30-µL reaction was divided into three 10-µL triplicates. In addition, one 10-µL no-RT reaction was used for each sample. The ABI Prism 7900 was used for all RT-PCRs. Cycle threshold (C_T) was determined by automated threshold analysis using SDS2.3 software according to instructions from the manufacturer (Applied Biosystems). Comparative levels of mRNA expression between control and experimental samples were determined using the $\Delta\Delta C_T$ method (Applied Biosystems User Bulletin 2). Briefly, the $\Delta\Delta C_T$ method is as follows. ΔC_T (C_T of experimental gene - C_T of reference gene) values from experimental samples were subtracted from those of control samples to calculate the $\Delta\Delta C_T$. Using the equation $2^{-\Delta\Delta CT} * 100$, the percentage expression of each gene in experimental versus control animals was calculated. Each experimental sample was compared to each wild type

sample (Applied Biosystems User Bulletin 2). For *Syt12*^{del} mutants, *Syt12* mRNA levels were determined from three runs, each using different combinations of TaqMan probes:

Probe combination for run #1:

Dm01838550_g1 (*Syt12*)

Dm02151827_g1 (*RpL32* control)

Probe combination for run #2:

Dm01838550_g2 (*Syt12*)

Dm02151827_g1 (*RpL32* control)

Probe combination for run #3:

Dm01838550_g2 (*Syt12*)

5' CAC GTC GAC TTG GAA GAG GAG CTC 3' (*futsch* control)

Relative *Syt12* mRNA levels in *Syt12*^{del}, compared to wild type, were similarly reduced in each run (99.7%, 95.7%, and 93.6%, respectively). Consequently, these data were treated as replicates and averaged for Figure 1. For *Df(1)Exel6245/+*, *Syt12* mRNA levels were determined from one run using the probe combination from run #1 above. For *PBac{WH}f06896* and *PBac{WH}f00785*, *Syt12* mRNA levels were determined from three runs, each using the same combinations of TaqMan probes as for *Syt12*^{del} above. Relative *Syt12* mRNA levels in each of these pBac lines, compared to wild type, were similar in each run (85.2%, 95.2%, and 91.0% for *PBac{WH}f06896*, respectively; 135.8%, 126.7%, and 134.7% for *PBac{WH}f00785*, respectively). Thus, as for *Syt12*^{del} mutants, these data were treated as replicates and averaged for inclusion in the text.

Electrophysiology

Recordings were obtained from muscle 6 in abdominal segment 2 or 3 of wandering third instar larvae with an AxoPatch 200B (for current-clamp recordings) or an Axoclamp 2B (for two-electrode voltage-clamp recordings), as previously described (Müller *et al.*, 2012). Recordings were made in modified HL3 saline at specified calcium concentrations (see figures and text) with the following components (and concentrations): NaCl (70 mM), KCl (5 mM), $MgCl_2$ (10 mM), $NaHCO_3$ (10 mM), sucrose (115 mM), trehalose (5 mM), HEPES pH 7.2 (5 mM), and $CaCl_2$ (0.4 mM for current-clamp recordings and 1.5 mM for two-electrode voltage-clamp recordings). For acute homeostatic challenge, semi-intact preparations with the CNS, fat, and gut intact were perfused with philanthotoxin-433 (PhTx; Sigma-Aldrich). PhTx was prepared as a stock solution (5 mM in ddH_2O) and diluted in HL3 saline to 15 μM. Following a ten-minute incubation period, the dissections were completed, and the preparations were rinsed and assayed. Muscle input resistance (R_{in}) was monitored at the beginning and end of each recording. Recordings were excluded if R_{in} changed by more than 20%. The average single action potential-evoked EJP amplitude (stimulus duration, 3 ms) or EJC amplitude (stimulus duration, 1 ms) for each recording is based on the mean peak EJP amplitudes or EJC amplitudes in response to thirty presynaptic stimuli. Quantal content was estimated for each current-clamp recording by calculating the average EJP/average mEJP, corrected for nonlinear summation (Martin, 1955) when noted, and subsequently averaging across all NMJs for a given genotype. To determine the apparent size of the readily-releasable pool (RRP), we applied the method of cumulative EJC amplitudes (Müller *et al.*, 2012; Schneggenburger *et al.*, 1999; Weyhersmuller *et*

al., 2011). Muscles were clamped to -65 mV, and EJC amplitudes during a stimulus train (60 Hz, thirty stimuli) were calculated as the difference between peak and baseline before stimulus onset of a given EJC, as previously described (Muller *et al.*, 2012*)*. The number of release-ready vesicles was obtained by back-extrapolating a line fit to the linear phase of the cumulative EJC plot (the last 200 ms of a train) to time zero and dividing the cumulative EJC amplitude at time zero by the mean mEJP amplitude recorded in the same cell (Müller *et al.*, 2012). All data for the homeostatic challenge experiments (with PhTx or *GluRIIA*^{SP16}) were collected, analyzed, and submitted with the experimenter blind to genotype.

Immunocytochemistry

Wandering third instar larvae were dissected in 0 Ca^{2+} HL3 saline and fixed. For deconvolution microscopy, fixation was performed with Bouin's fixative (Sigma-Aldrich) for two minutes or with paraformaldehyde (USB Corporation) for fifteen minutes. For structured illumination microscopy, fixation was performed with ice-cold 100% ethanol (Gold Shield) for five minutes. Larvae were washed briefly and incubated overnight at 4° C in primary antibody, washed the next day, and incubated in fluorescently conjugated secondary antibodies for two hours at room temperature. The following primary antibodies were used at the indicated dilutions: mouse anti-Brp (nc82): 1:100 (Wagh *et al.*, 2006); rabbit anti-Dlg: 1:10,000 (Lahey *et al.*, 1994); mouse anti-FasII (1D4): 1:10 (Van Vactor *et al.*, 1993); mouse anti-CSP (DCSP-2): 1:250 (Zinsmaier *et al.*, 1994); rabbit anti-Synaptotagmin 1: 1:1000 (Littleton *et al.*, 1993); mouse anti-GFP: 1:400 (3E6, Invitrogen). Antibodies against CSP, Synaptotagmin 1, and GFP were used with paraformaldehyde fixation. Alexa-conjugated secondary antibodies and directly

conjugated goat anti-HRP (Jackson Immunoresearch Laboratories, Molecular Probes) were used at 1:400. Larval preparations were mounted in Vectashield (Vector). For deconvolution microscopy, larval preparations were imaged at room temperature using an Axiovert 200 (Zeiss) inverted microscope, a 100x Plan Apochromat objective (aperture 1.4), and a cooled CCD camera (Coolsnap HQ, Roper). Intelligent Imaging Innovations (3i) SlideBook 5 software was used to capture, deconvolve, and analyze images. NMJ areas were defined by overlapping regions of Discs large (Dlg) and horseradish peroxidase (HRP) staining. Type Ib and type Is boutons were distinguished by intensity of Dlg staining and bouton size (Bhogal *et al.*, 2011). Muscles areas were calculated by using the ruler function in SlideBook 5 on images acquired with a 40x objective. Areas for muscle 6 and muscle 7 were summed. Antibody immunofluorescence levels were quantified as previously described (Heckscher *et al.*, 2007). Synaptic levels of FasII were quantified at type 1b boutons of muscle 4 NMJs. For structured illumination microscopy, larval preparations were imaged at room temperature using an ELYRA PS.1 system with an inverted LSM-710 microscope, a 63x (1.4 NA) Plan-Apochromat objective (Carl Zeiss), and an Andor iXon 885 EMCCD camera. Lateral resolution was ~ 110 nm, and axial resolution was ~300 nm. Z-stacks of whole NMJs at muscle 4 and muscle 6/7 were acquired and analyzed using Fiji and Igor, as previously described (Müller *et al.*, 2012). For characterizations of NMJ morphology, all data were collected with the experimenter blind to genotype and analyzed partially blind to genotype. Specifically, all type Ib bouton numbers were determined blind. Type Is bouton numbers and NMJ areas, as well as type Ib NMJ areas, were determined blind to genotype for 14 of 29 $Syt12^{null}$ NMJs and 13 of 26

Syt12^{null}*; ok371>UAS-Syt12* rescue NMJs. Active zone (nc82 puncta) numbers in type Ib boutons were determined blind to genotype for 16 of 16 *w*^{1118} NMJs, 14 of 28 *Syt12*^{null} NMJs, and 13 of 26 *Syt12*^{null}*; ok371>UAS-Syt12* rescue NMJs. Active zone numbers for type Ib and type Is boutons were initially counted by manually editing empty masks with pencil tools in SlideBook 5 and were later recounted blind using graylevel watershed (http://bigwww.epfl.ch/sage/soft/watershed) in Fiji. As shown in Results, recounting of active zones with graylevel watershed did not change our interpretation of findings, despite a 10% decrease in total puncta for each genotype.

Figures

Figure 1. Characterization of the *Syt12* gene locus and generated mutations. (A) Diagram of the *Drosophila Syt12* gene locus indicating the site of transposon insertions (yellow triangles), deletions (white bars), untranslated regions (gray bars), and exons (blue bars). **(B)** Comparison of *Drosophila* and human Syt12 proteins indicating percent amino acid similarity in conserved domains. **(C)** DNA bands from PCR amplification of a genomic region, which includes the 5' end of the *Syt12* gene locus. PCR with genome-specific primers produced bands of the expected size, 2.7 kilobases, from wild type (lane 2), *PBac{WH}f07791* (lane 4), and *PBac{WH}f06896* (lane 5) flies. Conversely, PCR with these primers yielded a band of approximately 370 base pairs from $Syt12^{del}$ flies (lane 3) and no band from $Syt12^{null}$ flies (lane 6). A 1 kb plus DNA ladder (lane 1) was used to estimate band sizes. **(D)** DNA bands from PCR amplification across a 7.2-kilobase *piggyBac* transposon, generated after deletion of the *Syt12* gene locus by FLP-FRT recombination in $Syt12^{null}$, using three pairs of genome-specific primers. Primer pair #1 (lanes 3-5), #2 (lanes 6-7), and #3 (lanes 8-10) produced bands of the expected size, roughly 8 kilobases, from $Syt12^{null}$ flies. PCR with these primers should yield bands over 18 kilobases from w^{1118} flies. A 1 kb plus DNA ladder (lane 1) was used to estimate band sizes. **(E)** DNA sequences of a genomic region, which includes the 5' end of the *Syt12* gene locus, from wild type and $Syt12^{del}$ flies. The wild type sequence on the top shows the genomic region from base pairs 13,358,383 to 13,358,431 on the X chromosome. The wild type sequence in the middle panel shows the genomic region from base pairs 13,360,659 to 13,360,707 on X. The $Syt12^{del}$ sequence on the bottom was determined using the same genomic primers as in wild type and reveals

breakpoints after base pair 13,358,399 and before base pair 13,360,694 on X. Breakpoints are indicated by black arrowheads. The sequence between breakpoints in *Syt12*^{del} are derived from the *P{EPgy2}* transposon used to generate the deletion. **(F)** Quantification of *Syt12* mRNA levels in *Syt12*^{del} by quantitative RT-PCR. The third instar larval *Syt12*^{del} CNS expressed 3.66% ± 1.79% (SEM) the amount of *Syt12* mRNA found in wild type (control). Brains from third instar larvae heterozygous for *Df(1)Exel6245*, a deficiency uncovering the *Syt12* locus, expressed 53.5% ± 7.06% (SEM) the amount of *Syt12* mRNA found in wild type. **(G)** DNA sequences from two-sided PCR with a genomic primer and a *piggyBac* transposon-specific primer for each end of a *piggyBac* transposon, generated after FLP-FRT recombination between f07791 and f06896, in *Syt12*^{null}. The mutant sequence on the left shows the genomic region from base pairs 13,349,721 to the f07791 insertion site on X. The mutant sequence on the right shows DNA from the f06896 insertion site to a genomic region ending at base pairs 13,367,372 on X. Breakpoints are indicated by black arrowheads. **(H)** DNA sequences from PCR amplification with genomic primers across a *piggyBac* transposon, generated after FLP-FRT recombination between f07791 and f06896, in *Syt12*^{null}. The mutant sequence on the left shows the genomic region from base pairs 13,349,724 to the *piggyBac* insertion site on X. The mutant sequence on the right shows DNA from the *piggyBac* insertion site to a genomic region ending at base pairs 13,367,372 on X. Note the similarity with the truncated DNA sequences in **(G)**. Breakpoints are indicated by black arrowheads.

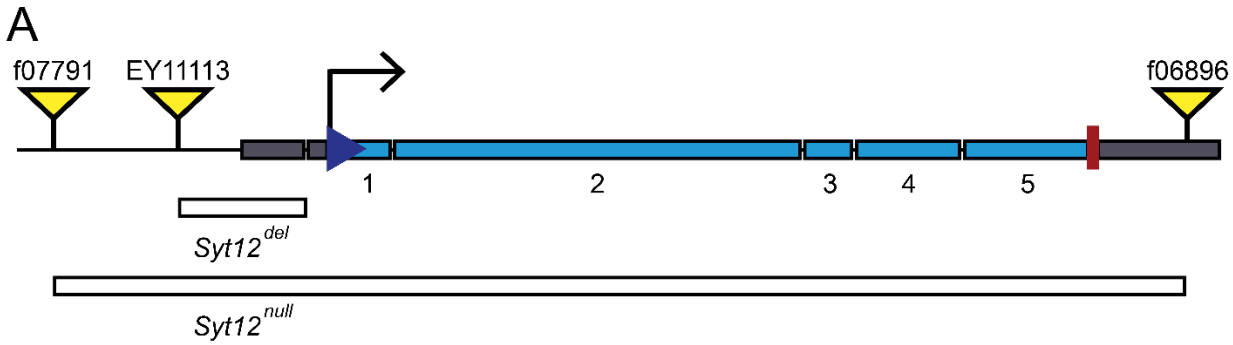
A
f07791
EY11113
f06896
1
2
3
4
5
Syt12del
Syt12null

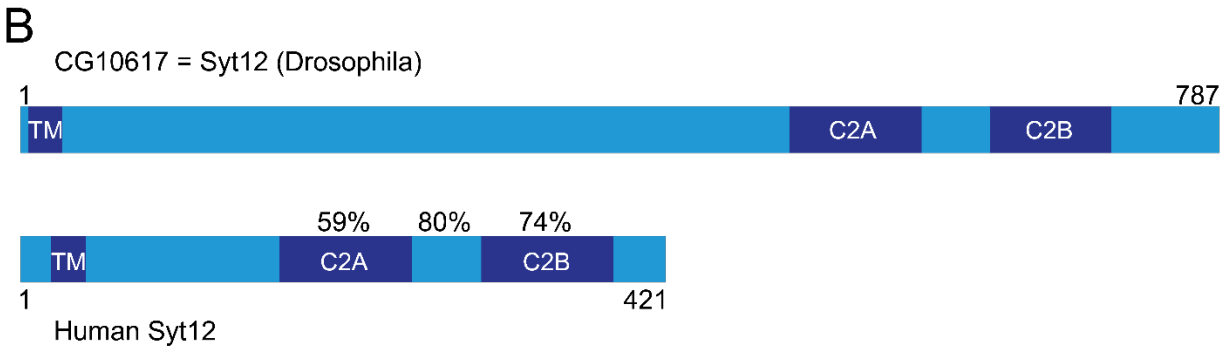
B
CG10617 = Syt12 (Drosophila)
1
787
TM
C2A
C2B
59%
80%
74%
TM
C2A
C2B
1
421
Human Syt12

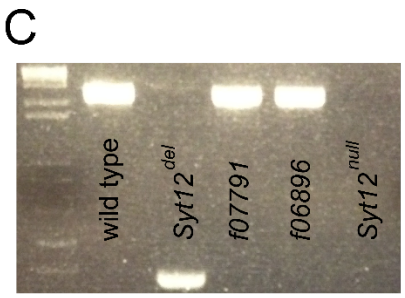
C
wild type
Syt12del
f07791
f06896
Syt12null

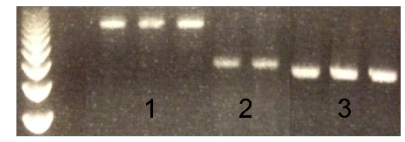
D
1
2
3

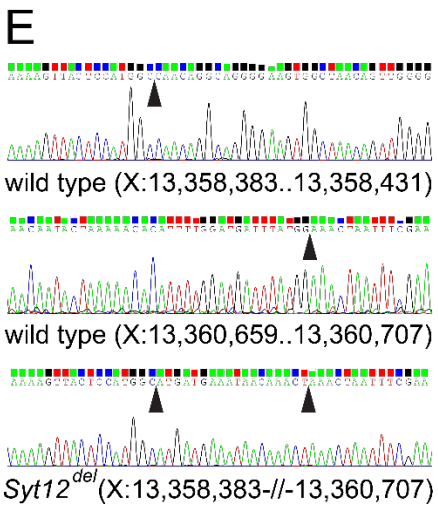
E
wild type (X:13,358,383..13,358,431)
wild type (X:13,360,659..13,360,707)
Syt12del(X:13,358,383-//-13,360,707)

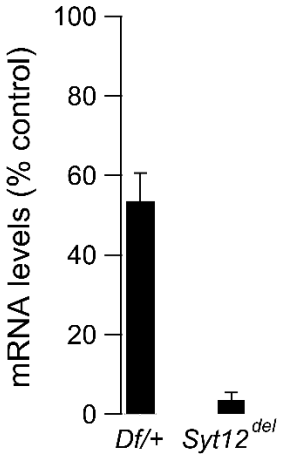
F
mRNA levels (% control)
100
80
60
40
20
0
Df/+
Syt12del

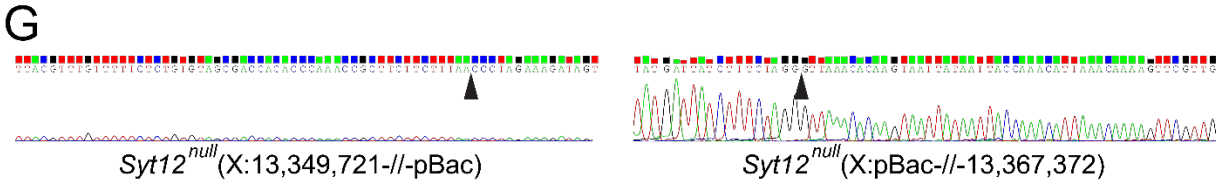
G
Syt12null(X:13,349,721-//-pBac)
Syt12null(X:pBac-//-13,367,372)

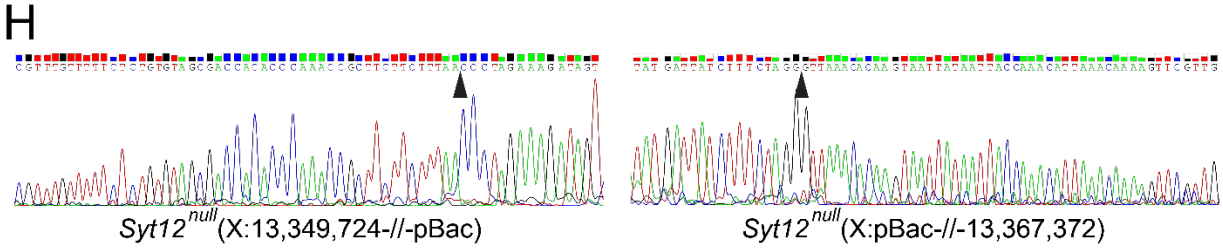
H
Syt12null(X:13,349,724-//-pBac)
Syt12null(X:pBac-//-13,367,372)

Figure 2. Effects of *Syt12* on NMJ morphology. (A-B) Wild type **(A)** and *Syt12^{null}* **(B)** NMJs costained with antibodies to Discs large (purple; DLG) and Bruchpilot (green; nc82). Scale bars = 5 μm. **(C)** Quantification of type Ib and type Is bouton numbers at muscle 6/7 comparing *w^{1118}* (n = 16 and 16), *Syt12^{null}* (n = 29 and 29) (p < 0.01 and = 0.88, Student's *t* test), and *Syt12^{null}; ok371>UAS-Syt12* (n = 26 and 26) (p = 0.95 and < 0.01, Student's *t* test). **(D)** Quantification of nc82 puncta per NMJ in type Ib and type Is boutons at muscle 6/7 comparing *w^{1118}* (n = 16 and 16), *Syt12^{null}* (n = 28 and 28) (p < 0.01 and = 0.10, Student's *t* test), and *Syt12^{null}; ok371>UAS-Syt12* n = 26 and 26) (p = 0.03 and < 0.01, Student's *t* test). **(E)** Quantification of NMJ area in type Ib and type Is boutons at muscle 6/7 comparing *w^{1118}* (n = 16 and 16), *Syt12^{null}* (n = 28 and 28) (p < 0.01 and = 0.70, Student's *t* test), and *Syt12^{null}; ok371>UAS-Syt12* (n = 26 and 26) (p = 0.29 and = 0.07, Student's *t* test). **(F)** Quantification of nc82 puncta density (nc82 puncta/NMJ area) in type Ib and type Is boutons at muscle 6/7 comparing *w^{1118}* (n = 16 and 16), *Syt12^{null}* (n = 28 and 28) (p < 0.01 and < 0.01, Student's *t* test), and *Syt12^{null}; ok371>UAS-Syt12* (n = 26 and 26) (p = 0.29 and = 0.07, Student's *t* test). All data represent mean ± SEM.

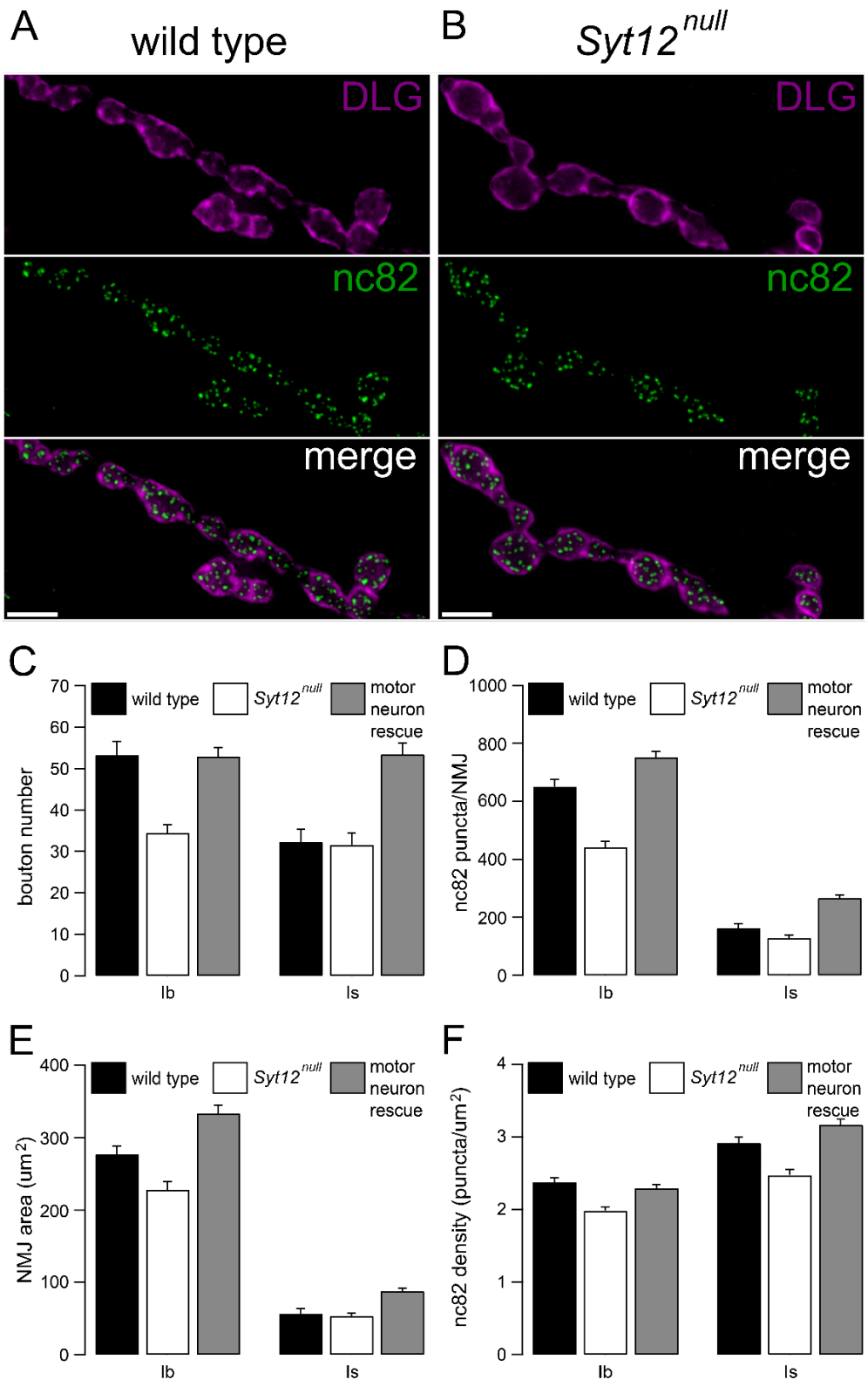
A
wild type
B
Syt12 null
DLG
nc82
merge
DLG
nc82
merge
C
bouton number
wild type
Syt12 null
motor neuron rescue
Ib
Is
D
nc82 puncta/NMJ
wild type
Syt12 null
motor neuron rescue
Ib
Is
E
NMJ area (um2)
wild type
Syt12 null
motor neuron rescue
Ib
Is
F
nc82 density (puncta/um2)
wild type
Syt12 null
motor neuron rescue
Ib
Is

Figure 3. Effects of *Syt12* on active zone morphology. (A-B) Structured illumination images of control (revertant) **(A)** and *Syt12*^{del} **(B)** NMJs (muscle 4) stained with anti-Bruchpilot (green; nc82). Scale bars = 0.5 µm. **(C)** Fluorescence intensity line profiles through all planar Brp puncta of a representative *Syt12*^{del} NMJ. Individual line profiles and the average line profile are shown in gray and black, respectively. **(D)** Cumulative frequency plot of Brp ring diameters at half maximum, the distance between two points at 50% of peak fluorescence intensity, as determined by structured illumination microscopy. **(E)** Fluorescence intensity line profiles through all planar Brp puncta of a representative *Syt12*^{del} NMJ. Individual line profiles are shown in gray and are normalized to the respective peak fluorescence. Diameter at half maximum is the distance between two points at 50% of the peak fluorescence (black crosses). Peak-to-peak diameter of a line profile was calculated as the distance between the two peaks of the intensity profile (black circles). **(F)** Average of average peak-to-peak diameters of Brp puncta at muscles 6/7 and 4 of *Syt12* revertant (n = 5 and 6) and *Syt12*^{del} mutant (n = 7 and 7; p = 0.48 and = 0.92, Student's t test) NMJs. All data represent mean ± SEM.

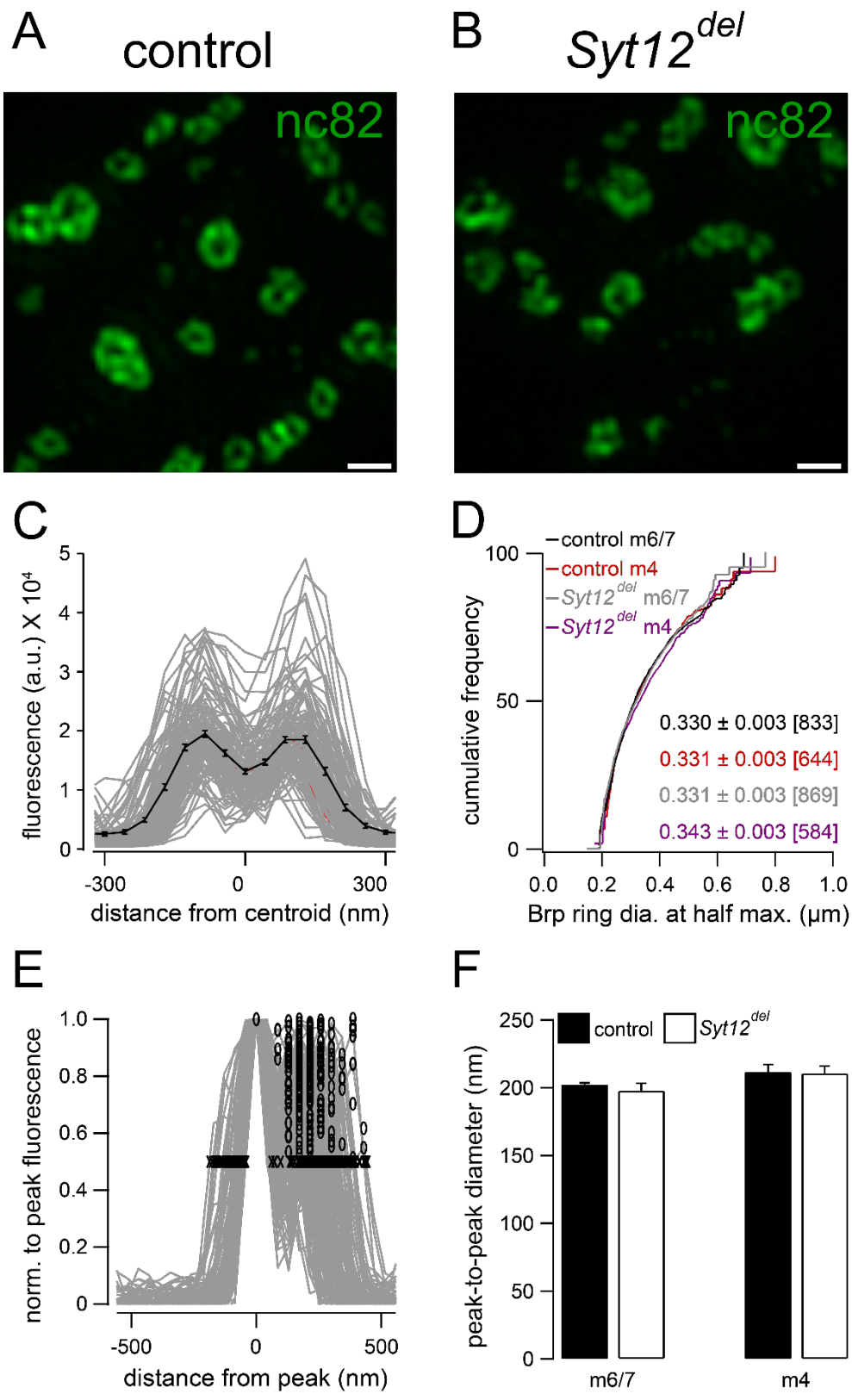
A
control
nc82
B
Syt12del
nc82
C
fluorescence (a.u.) X 10⁴
distance from centroid (nm)
D
control m6/7
control m4
Syt12del m6/7
Syt12del m4
cumulative frequency
0.330 ± 0.003 [833]
0.331 ± 0.003 [644]
0.331 ± 0.003 [869]
0.343 ± 0.003 [584]
Brp ring dia. at half max. (µm)
E
norm. to peak fluorescence
distance from peak (nm)
F
control
Syt12del
peak-to-peak diameter (nm)
m6/7
m4

Figure 4. Effects of *Syt12* on synaptic vesicle protein levels. (A-B) Syt1 (green) and CSP (purple) in presynaptic nerve terminals of w^{1118} **(A)** and $Syt12^{null}$ **(B)** at muscle 6/7. Scale bar = 5 μm. **(C)** Average synaptic fluorescence intensity of cysteine string protein (CSP) at muscle 6/7 of w^{1118} (n = 12) and $Syt12^{null}$ (n = 14; p = 0.32, Student's t test). **(D)** Average synaptic fluorescence intensity of Synaptotagmin 1 (Syt1) at muscle 6/7 of w^{1118} (n = 12) and $Sy12^{null}$ (n = 14; p = 0.07, Student's t test). All data represent mean ± SEM.

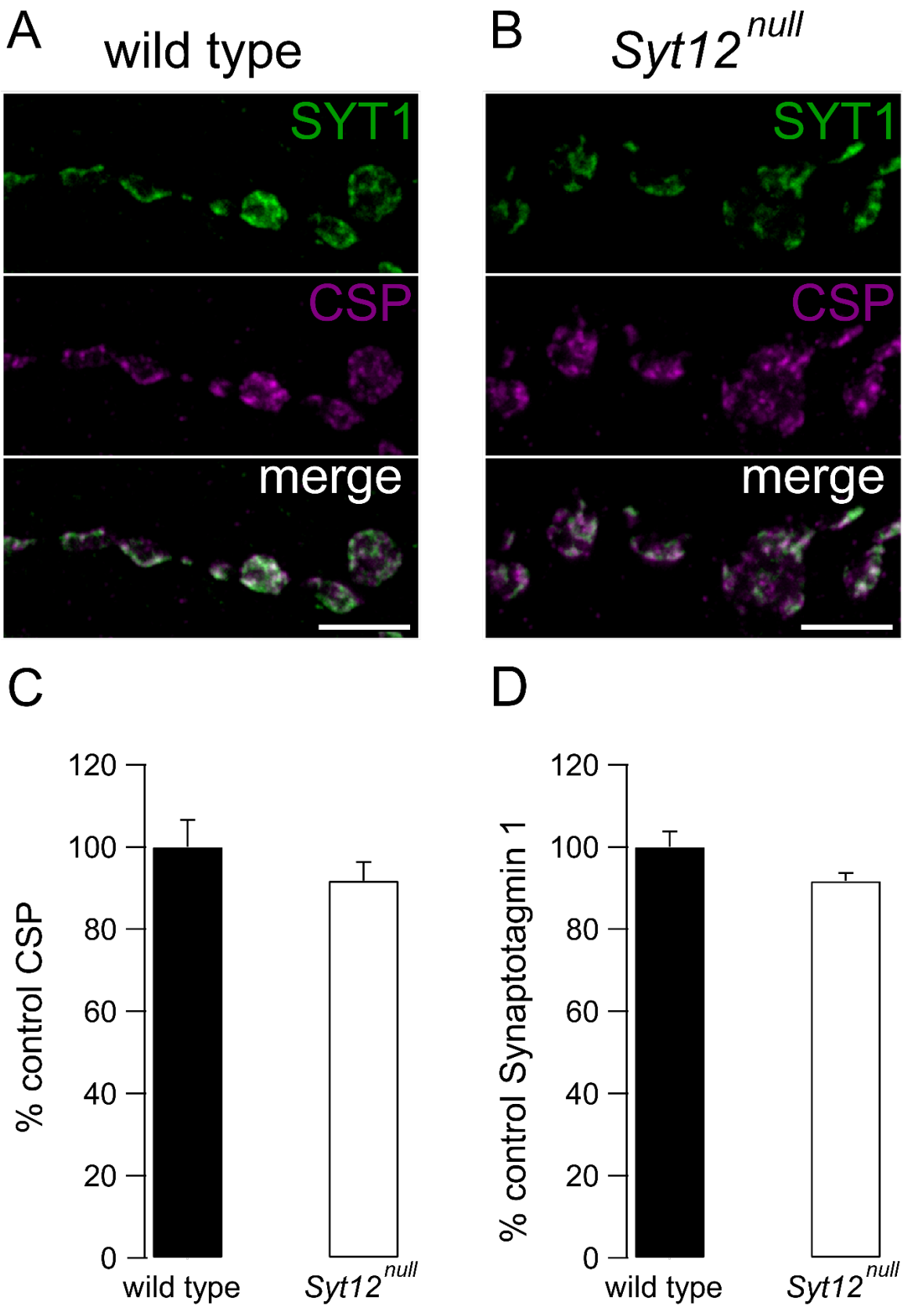
A
wild type
SYT1
CSP
merge
B
Syt12null
SYT1
CSP
merge
C
% control CSP
120
100
80
60
40
20
0
wild type
Syt12null
D
% control Synaptotagmin 1
120
100
80
60
40
20
0
wild type
Syt12null

Figure 5. Syt12 colocalizes with Syt1 in presynaptic terminals of motor neurons. **(A)** Syt12-Venus (green; SYT12) co-localizes with Syt1 (purple; SYT1) presynaptically. **(B)** Syt12-Venus (green; SYT12), overexpressed in muscles (*BG57-GAL4)*, was not detected by a polyclonal antibody to presynaptic Syt1 (purple; SYT1). Scale bars = 5 μm.

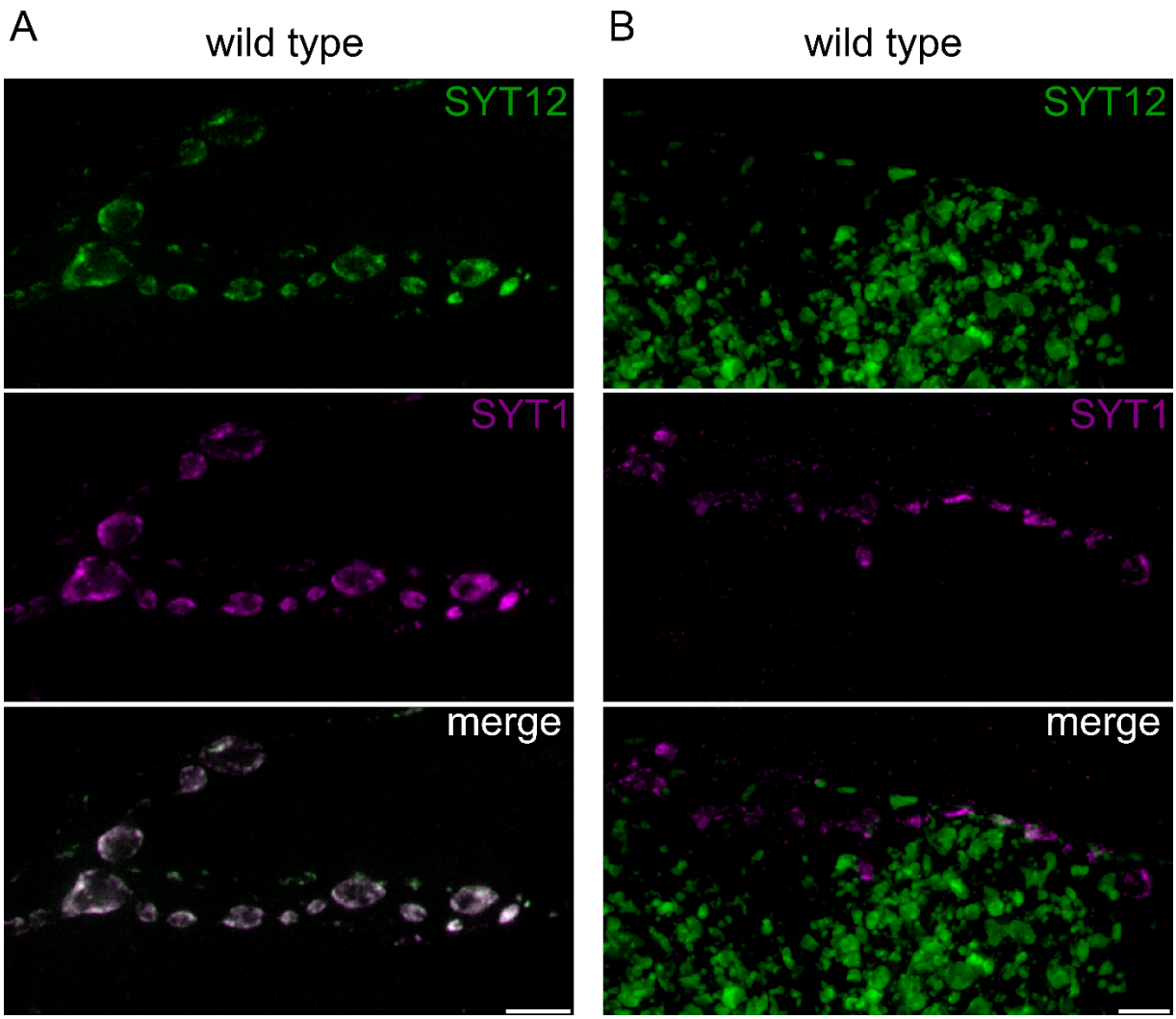
A
wild type
SYT12
SYT1
merge
B
wild type
SYT12
SYT1
merge

Figure 6. *Syt12* is dispensable for synaptic transmission. (A-D) Average mEJP amplitude **(A)**, EJP amplitude **(B)**, quantal content **(C)**, and mEJP frequency **(D)** for wild type (n = 22) and $Syt12^{null}$ (n = 18). $Syt12^{null}$ mEJP amplitudes (p = 0.57) **(A)**, quantal contents (p = 0.45) **(C)**, and mEJP frequencies (p = 0.06) **(D)** were similar to wild type. **(B)** EJP amplitudes differed slightly between wild type and $Syt12^{null}$ (p = 0.04). All data represent mean ± SEM. **(E)** Sample traces showing EJP and mEJP amplitudes for wild type and $Syt12^{null}$. Scale bars for EJPs = 5 mV, vertical, and 50 ms, horizontal. Scale bars for mEJPs = 2 mV, vertical, and 1 s, horizontal. **(F)** Quantal content in wild type and $Syt12^{null}$ (black and red, respectively) as a function of extracellular Ca^{2+} concentration. Data are corrected for nonlinear summation.

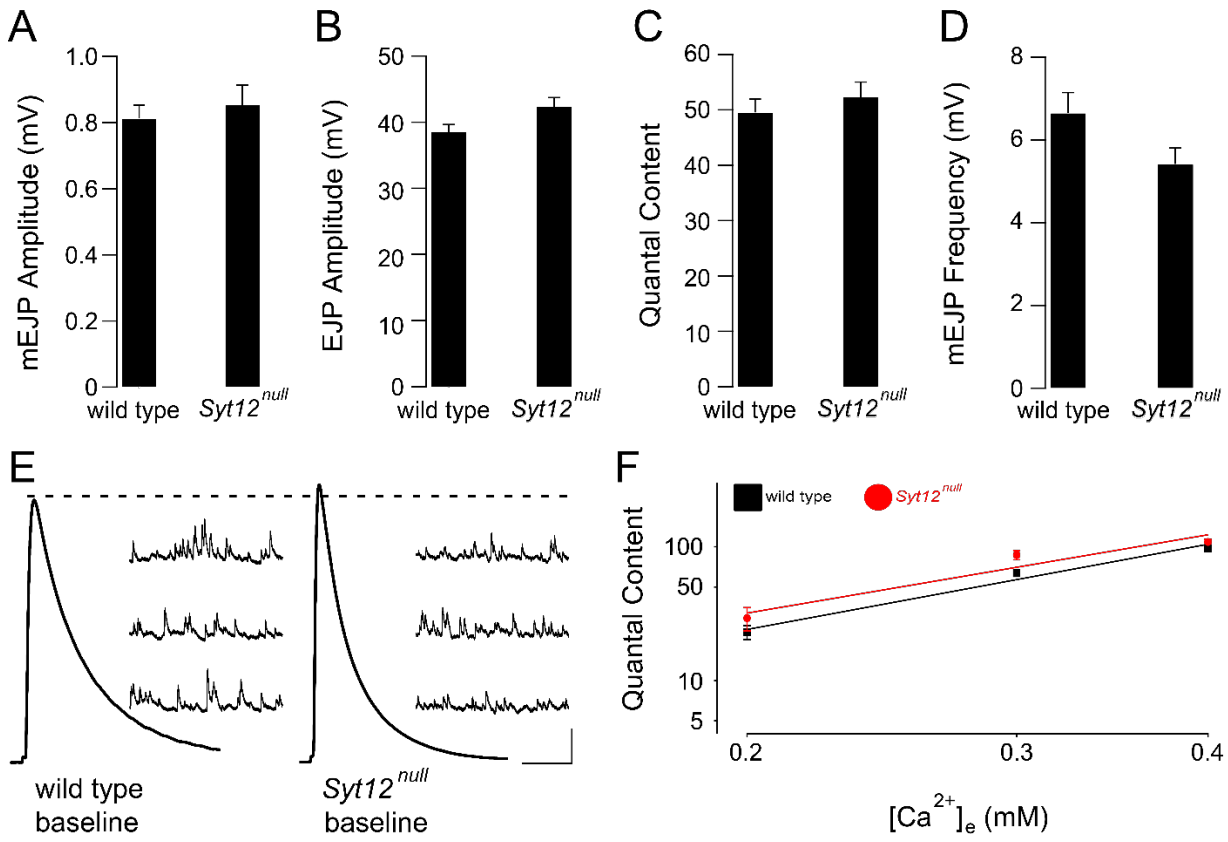
A
mEJP Amplitude (mV)
1.0
0.8
0.6
0.4
0.2
0
wild type
Syt12null
B
EJP Amplitude (mV)
50
40
30
20
10
0
wild type
Syt12null
C
Quantal Content
60
50
40
30
20
10
0
wild type
Syt12null
D
mEJP Frequency (mV)
8
6
4
2
0
wild type
Syt12null
E
wild type
baseline
Syt12null
baseline
F
wild type
Syt12null
Quantal Content
100
50
10
5
0.2
0.3
0.4
[Ca2+]e (mM)

Figure 7. *Syt12* is dispensable for short- and long-term homeostatic potentiation. **(A)** Average mEJP amplitudes (black), EJP amplitudes (gray), and quantal contents (white) normalized to each indicated genotype in the absence of PhTx. w^{1118} (- PhTx), n = 22; w^{1118} (+ PhTx), n = 16; $Syt12^{null}$ (- PhTx), n = 18; $Syt12^{null}$ (+ PhTx), n = 19; $Syt12^{del}$ (- PhTx), n = 12; $Syt12^{del}$ (+ PhTx), n = 9. PhTx treatment significantly reduced mEJP amplitudes, compared to baseline, in all genotypes ($p < 0.01$). EJP amplitudes of PhTx and control group were similar in wild type ($p = 0.33$) and $Syt12^{del}$ ($p = 0.29$), but differed slightly in $Syt12^{null}$ ($p = 0.03$). PhTx treatment induced an increase in quantal content, compared to baseline, in all genotypes ($p < 0.01$). All data represent mean ± SEM. **(B)** Average mEJP amplitudes (black), EJP amplitudes (gray), and quantal contents (white) normalized to each indicated genotype with or without a null mutation in *GluRIIA* (*GluRIIA*^{SP16}). w^{1118} (*GluRIIA*$^{+}$), n = 22; *GluRIIA*$^{-}$, n = 14; $Syt12^{null-}$ (*GluRIIA*$^{+}$), n = 18; $Syt12^{null}$; *GluRIIA*$^{-}$, n = 15; $Syt12^{del}$ (*GluRIIA*$^{+}$), n = 12; $Syt12^{del}$; *GluRIIA*$^{-}$, n = 9. Genetic ablation of *GluRIIA* significantly reduced mEJP amplitudes, compared to baseline, in both genotypes ($p < 0.01$). EJP amplitudes of *GluRIIA*$^{-}$ and control group were significantly different in all genotypes ($p < 0.01$). *GluRIIA*$^{-}$ strongly enhanced quantal content, compared to baseline, in all genotypes ($p < 0.01$). All data represent mean ± SEM. **(C)** Sample traces showing EJP and mEJP amplitudes for wild type in the presence and absence of PhTx (red and black, respectively). **(D)** Sample traces showing EJP and mEJP amplitudes for wild type (*GluRIIA*$^{+}$) and *GluRIIA*$^{-}$ (black and red, respectively). **(E)** Sample traces for $Syt12^{null}$, as in **(C)**. **(F)** Sample traces for $Syt12^{null}$, as in **(D)**. **(G)** Sample traces for $Syt12^{del}$, as in **(C)**. **(H)** Sample traces for

Syt12^{del}, as in **(D)**. Scale bars for EJPs = 5 mV, vertical, and 50 ms, horizontal. Scale bars for mEJPs = 2 mV, vertical, and 1 s, horizontal.

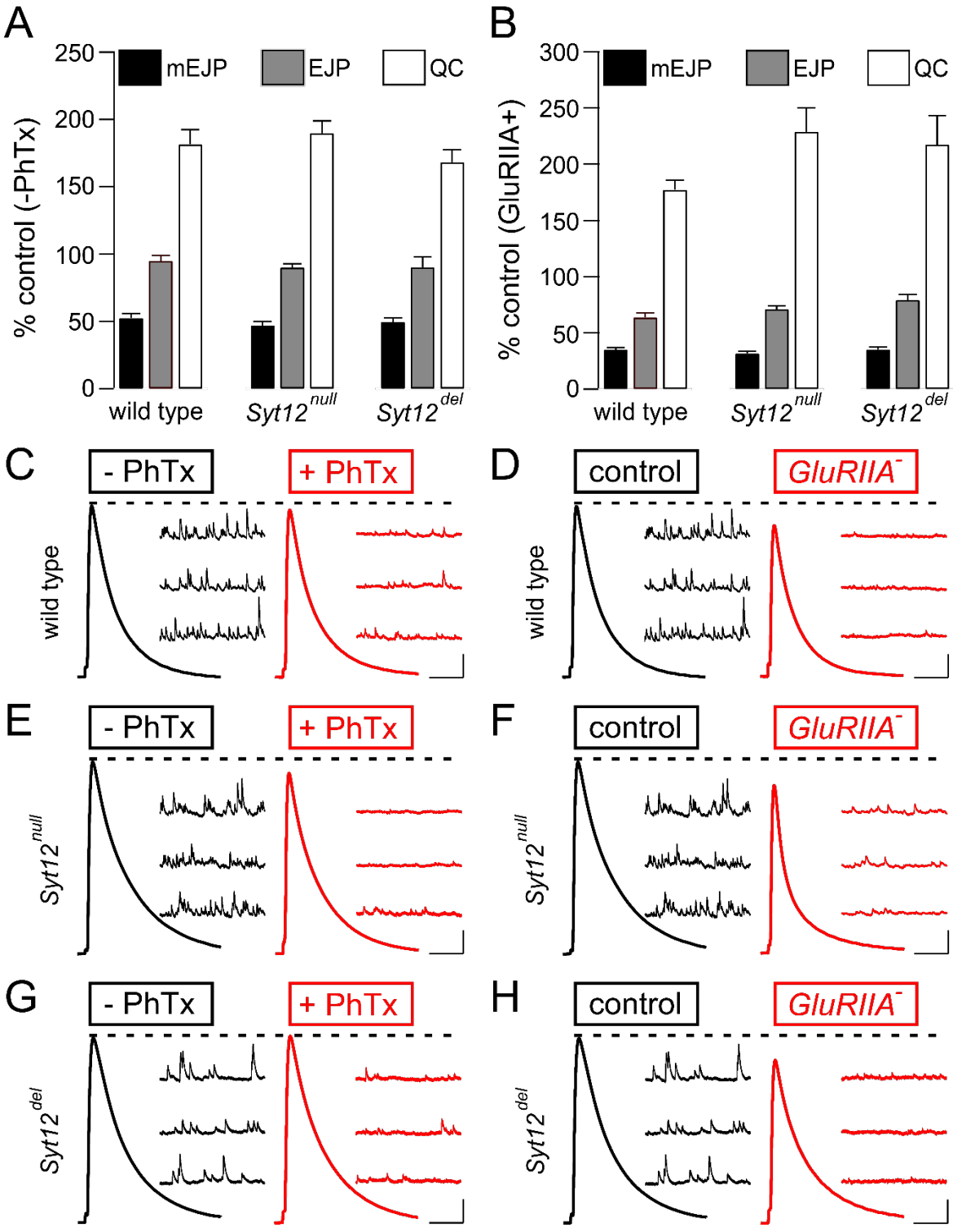
A
B
mEJP
EJP
QC
% control (-PhTx)
% control (GluRIIA+)
wild type
Syt12null
Syt12del
C
D
E
F
G
H
- PhTx
+ PhTx
control
GluRIIA-

Figure 8. *Syt12* limits RRP size in physiological calcium. (A-D) Average mEJP amplitude **(A)**, initial EJC amplitude **(B)**, cumulative (cum.) EJC amplitude **(C)**, and estimated RRP size **(D)** for wild type (n = 13) and $Syt12^{null}$ (n = 20). **(A)** $Syt12^{null}$ mEJP amplitudes (p = 0.74) were similar to wild type. $Syt12^{null}$ initial EJC amplitudes (p = 0.02) **(B)**, cumulative EJC amplitudes (p < 0.01) **(C)**, and estimated RRP sizes (p = 0.02) **(D)** were significantly increased, compared to wild type. **(E)** Sample traces showing EJC amplitudes, evoked by 60-Hz stimulation in 1.5 mM Ca^{2+}, for wild type. **(F)** Sample traces for $Syt12^{null}$, as in **(E)**. Scale bars = 100 nA, vertical, and 50 ms, horizontal. **(G)** Average amplitudes of the final (30^{th}) EJCs in 60-Hz trains did not differ between wild type and $Syt12^{null}$ (p = 0.80). **(H)** Depression over the first ten stimuli of the 60-Hz trains did not differ between wild type and $Syt12^{null}$ (p = 0.25). However, $Syt12^{null}$ mutants showed significantly enhanced depression at the ends ($EJC_{final}/EJC_{initial}$) of 60-Hz trains, compared to wild type (p = 0.02). All data represent mean ± SEM.

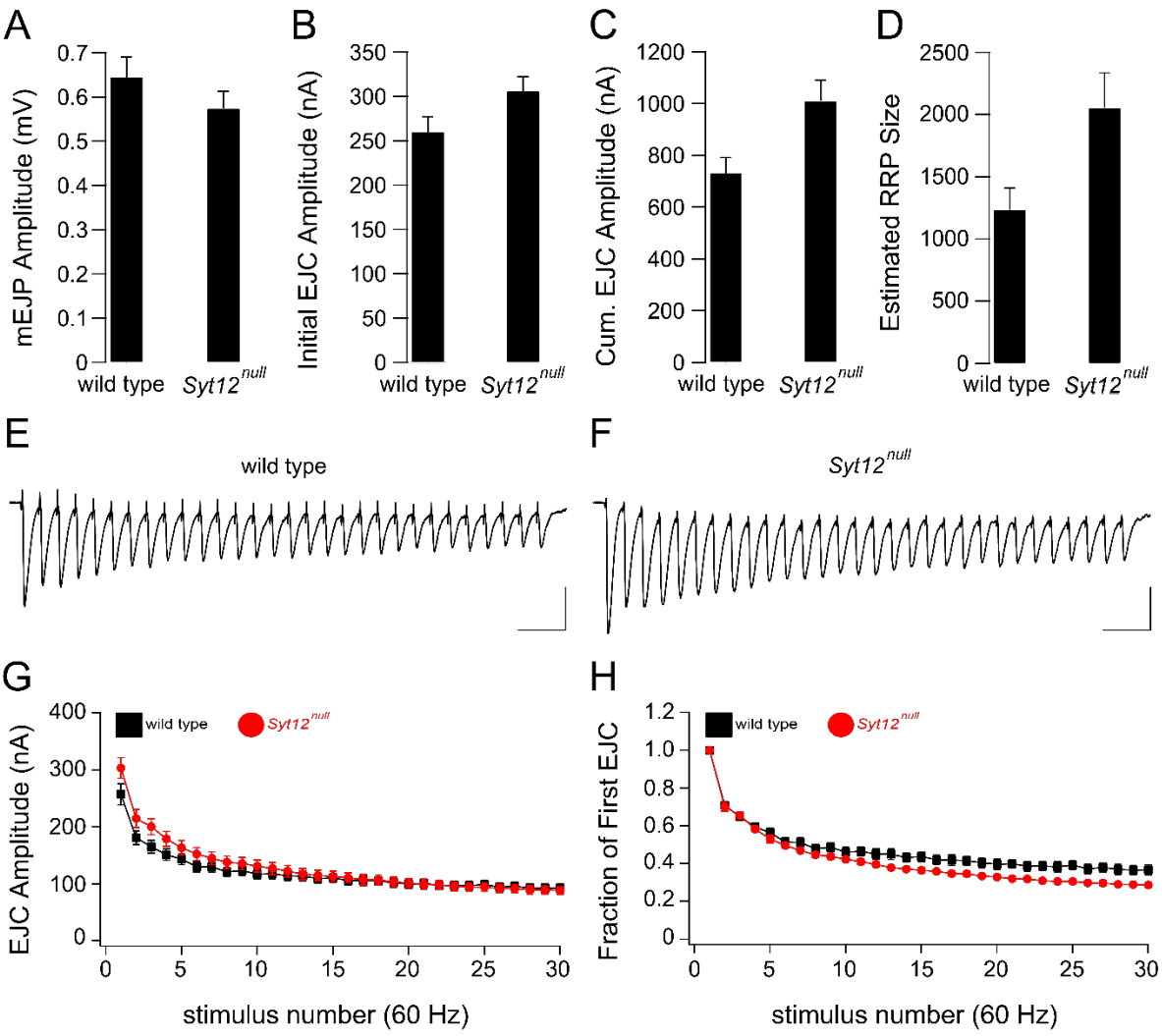
A
mEJP Amplitude (mV)
0.7
0.6
0.5
0.4
0.3
0.2
0.1
0
wild type
Syt12null
B
Initial EJC Amplitude (nA)
350
300
250
200
150
100
50
0
wild type
Syt12null
C
Cum. EJC Amplitude (nA)
1200
1000
800
600
400
200
0
wild type
Syt12null
D
Estimated RRP Size
2500
2000
1500
1000
500
0
wild type
Syt12null
E
wild type
F
Syt12null
G
EJC Amplitude (nA)
400
300
200
100
0
wild type
Syt12null
0
5
10
15
20
25
30
stimulus number (60 Hz)
H
Fraction of First EJC
1.2
1.0
0.8
0.6
0.4
0.2
0
wild type
Syt12null
0
5
10
15
20
25
30
stimulus number (60 Hz)

References

Adolfsen B, Saraswati S, Yoshihara M, Littleton JT. Synaptotagmins are trafficked to distinct subcellular domains including the postsynaptic compartment. J Cell Biol. 2004 Jul 19;166(2):249-60.

Atwood HL, Govind CK, Wu CF. Differential ultrastructure of synaptic terminals on ventral longitudinal abdominal muscles in Drosophila larvae. J Neurobiol. 1993 Aug;24(8):1008-24.

Bacaj T, Wu D, Yang X, Morishita W, Zhou P, Xu W, Malenka RC, Südhof TC. Synaptotagmin-1 and synaptotagmin-7 trigger synchronous and asynchronous phases of neurotransmitter release. Neuron. 2013 Nov 20;80(4):947-59.

Bailey CH, Chen M. Long-term memory in Aplysia modulates the total number of varicosities of single identified sensory neurons. Proc Natl Acad Sci U S A. 1988 Apr;85(7):2373-7.

Bailey CH, Chen M, Keller F, Kandel ER. Serotonin-mediated endocytosis of apCAM: an early step of learning-related synaptic growth in Aplysia. Science. 1992 May 1;256(5057):645-9.

Barber CF, Jorquera RA, Melom JE, Littleton JT. Postsynaptic regulation of synaptic plasticity by synaptotagmin 4 requires both C2 domains. J Cell Biol. 2009 Oct 19;187(2):295-310.

Beck ES, Gasque G, Imlach WL, Jiao W, Jiwon Choi B, Wu PS, Kraushar ML, McCabe BD. Regulation of Fasciclin II and synaptic terminal development by the splicing factor beag. J Neurosci. 2012 May 16;32(20):7058-73.

Bellen HJ, Levis RW, Liao G, He Y, Carlson JW, Tsang G, Evans-Holm M, Hiesinger PR, Schulze KL, Rubin GM, Hoskins RA, Spradling AC. The BDGP gene disruption project: single transposon insertions associated with 40% of Drosophila genes. Genetics. 2004 Jun;167(2):761-81.

Ben-Simon Y, Rodenas-Ruano A, Alviña K, Lam AD, Stuenkel EL, Castillo PE, Ashery U. A Combined Optogenetic-Knockdown Strategy Reveals a Major Role of Tomosyn in Mossy Fiber Synaptic Plasticity. Cell Rep. 2015 Jul 21;12(3):396-404.

Bergquist S, Dickman DK, Davis GW. A hierarchy of cell intrinsic and target-derived homeostatic signaling. Neuron. 2010 Apr 29;66(2):220-34.

Bhalla A, Chicka MC, Chapman ER. Analysis of the synaptotagmin family during reconstituted membrane fusion. Uncovering a class of inhibitory isoforms. J Biol Chem. 2008 Aug 1;283(31):21799-807.

Bhogal B, Jepson JE, Savva YA, Pepper AS, Reenan RA, Jongens TA. Modulation of dADAR-dependent RNA editing by the Drosophila fragile X mental retardation protein. Nat Neurosci. 2011 Oct 30;14(12):1517-24.

Brenner S. The genetics of Caenorhabditis elegans. Genetics. 1974 May;77(1):71-94.

Budnik V, Koh YH, Guan B, Hartmann B, Hough C, Woods D, Gorczyca M. Regulation of synapse structure and function by the Drosophila tumor suppressor gene dlg. Neuron. 1996 Oct;17(4):627-40.

Castillo PE. Presynaptic LTP and LTD of excitatory and inhibitory synapses. Cold Spring Harb Perspect Biol. 2012 Feb 1;4(2).

Castillo PE, Janz R, Südhof TC, Tzounopoulos T, Malenka RC, Nicoll RA. Rab3A is essential for mossy fibre long-term potentiation in the hippocampus. Nature. 1997 Aug 7;388(6642):590-3.

Castillo PE, Schoch S, Schmitz F, Südhof TC, Malenka RC. RIM1alpha is required for presynaptic long-term potentiation. Nature. 2002 Jan 17;415(6869):327-30.

Chen X, Ganetzky B. A neuropeptide signaling pathway regulates synaptic growth in Drosophila. J Cell Biol. 2012 Feb 20;196(4):529-43.

Cheng L, Locke C, Davis GW. S6 kinase localizes to the presynaptic active zone and functions with PDK1 to control synapse development. J Cell Biol. 2011 Sep 19;194(6):921-35.

Cong L, Ran FA, Cox D, Lin S, Barretto R, Habib N, Hsu PD, Wu X, Jiang W, Marraffini LA, Zhang F. Multiplex genome engineering using CRISPR/Cas systems. Science. 2013 Feb 15;339(6121):819-23.

Craxton M. A manual collection of Syt, Esyt, Rph3a, Rph3al, Doc2, and Dblc2 genes from 46 metazoan genomes--an open access resource for neuroscience and evolutionary biology. BMC Genomics. 2010 Jan 15;11:37.

Cull-Candy SG, Miledi R, Trautmann A, Uchitel OD. On the release of transmitter at normal, myasthenia gravis and myasthenic syndrome affected human end-plates. J Physiol. 1980 Feb;299:621-38.

Daniels RW, Collins CA, Gelfand MV, Dant J, Brooks ES, Krantz DE, DiAntonio A. Increased expression of the Drosophila vesicular glutamate transporter leads to excess glutamate release and a compensatory decrease in quantal content. J Neurosci. 2004 Nov 17;24(46):10466-74.

Davis GW. Homeostatic control of neural activity: from phenomenology to molecular design. Annu Rev Neurosci. 2006;29:307-23.

Davis GW. Homeostatic signaling and the stabilization of neural function. Neuron. 2013 Oct 30;80(3):718-28.

Davis GW, Goodman CS. Genetic analysis of synaptic development and plasticity: homeostatic regulation of synaptic efficacy. Curr Opin Neurobiol. 1998 Feb;8(1):149-56.

Davis GW, Goodman CS. Synapse-specific control of synaptic efficacy at the terminals of a single neuron. Nature. 1998 Mar 5;392(6671):82-6.

Davis GW, Müller M. Homeostatic control of presynaptic neurotransmitter release. Annu Rev Physiol. 2015;77:251-70.

Davis GW, Schuster CM, Goodman CS. Genetic dissection of structural and functional components of synaptic plasticity. III. CREB is necessary for presynaptic functional plasticity. Neuron. 1996 Oct;17(4):669-79.

Dean C, Dunning FM, Liu H, Bomba-Warczak E, Martens H, Bharat V, Ahmed S, Chapman ER. Axonal and dendritic synaptotagmin isoforms revealed by a pHluorin-syt functional screen. Mol Biol Cell. 2012 May;23(9):1715-27.

Dean C, Liu H, Dunning FM, Chang PY, Jackson MB, Chapman ER. Synaptotagmin-IV modulates synaptic function and long-term potentiation by regulating BDNF release. Nat Neurosci. 2009 Jun;12(6):767-76.

del Castillo J, Katz B. Quantal components of the end-plate potential. J Physiol. 1954 Jun 28;124(3):560-73.

de Wit H, Walter AM, Milosevic I, Gulyás-Kovács A, Riedel D, Sørensen JB, Verhage M. Synaptotagmin-1 docks secretory vesicles to syntaxin-1/SNAP-25 acceptor complexes. Cell. 2009 Sep 4;138(5):935-46.

DiAntonio A, Parfitt KD, Schwarz TL. Synaptic transmission persists in synaptotagmin mutants of Drosophila. Cell. 1993 Jul 2;73(7):1281-90.

Dickman DK, Davis GW. The schizophrenia susceptibility gene dysbindin controls synaptic homeostasis. Science. 2009 Nov 20;326(5956):1127-30.

Doi H, Yoshida K, Yasuda T, Fukuda M, Fukuda Y, Morita H, Ikeda S, Kato R, Tsurusaki Y, Miyake N, Saitsu H, Sakai H, Miyatake S, Shiina M, Nukina N, Koyano S, Tsuji S, Kuroiwa Y, Matsumoto N. Exome sequencing reveals a homozygous SYT14 mutation in adult-onset, autosomal-recessive spinocerebellar ataxia with psychomotor retardation. Am J Hum Genet. 2011 Aug 12;89(2):320-7.

dos Santos G, Schroeder AJ, Goodman JL, Strelets VB, Crosby MA, Thurmond J, Emmert DB, Gelbart WM; FlyBase Consortium. FlyBase: introduction of the Drosophila melanogaster Release 6 reference genome assembly and large-scale migration of genome annotations. Nucleic Acids Res. 2015 Jan;43(Database issue):D690-7.

Eayrs JT. Thyroid hypofunction and the development of the central nervous system. Nature. 1953 Aug 29;172(4374):403-4.

Frank CA. Homeostatic plasticity at the Drosophila neuromuscular junction. Neuropharmacology. 2014 Mar;78:63-74.

Frank CA, Kennedy MJ, Goold CP, Marek KW, Davis GW. Mechanisms underlying the rapid induction and sustained expression of synaptic homeostasis. Neuron. 2006 Nov 22;52(4):663-77.

Frank CA, Pielage J, Davis GW. A presynaptic homeostatic signaling system composed of the Eph receptor, ephexin, Cdc42, and CaV2.1 calcium channels. Neuron. 2009 Feb 26;61(4):556-69.

Fukuda M. Molecular cloning, expression, and characterization of a novel class of synaptotagmin (Syt XIV) conserved from Drosophila to humans. J Biochem. 2003 May;133(5):641-9.

Gaviño MA, Ford KJ, Archila S, Davis GW. Homeostatic synaptic depression is achieved through a regulated decrease in presynaptic calcium channel abundance. Elife. 2015 Apr 17;4.

Geppert M, Goda Y, Hammer RE, Li C, Rosahl TW, Stevens CF, Südhof TC. Synaptotagmin I: a major Ca2+ sensor for transmitter release at a central synapse. Cell. 1994 Nov 18;79(4):717-27.

Goold CP, Davis GW. The BMP ligand Gbb gates the expression of synaptic homeostasis independent of synaptic growth control. Neuron. 2007 Oct 4;56(1):109-23.

Gould E, Butcher LL. Developing cholinergic basal forebrain neurons are sensitive to thyroid hormone. J Neurosci. 1989 Sep;9(9):3347-58.

Goussakov IV, Fink K, Elger CE, Beck H. Metaplasticity of mossy fiber synaptic transmission involves altered release probability. J Neurosci. 2000 May 1;20(9):3434-41.

Gratz SJ, Cummings AM, Nguyen JN, Hamm DC, Donohue LK, Harrison MM, Wildonger J, O'Connor-Giles KM. Genome engineering of Drosophila with the CRISPR RNA-guided Cas9 nuclease. Genetics. 2013 Aug;194(4):1029-35.

Heckscher ES, Fetter RD, Marek KW, Albin SD, Davis GW. NF-kappaB, IkappaB, and IRAK control glutamate receptor density at the Drosophila NMJ. Neuron. 2007 Sep 20;55(6):859-73.

Huang YY, Li XC, Kandel ER. cAMP contributes to mossy fiber LTP by initiating both a covalently mediated early phase and macromolecular synthesis-dependent late phase. Cell. 1994 Oct 7;79(1):69-79.

Hui E, Bai J, Wang P, Sugimori M, Llinas RR, Chapman ER. Three distinct kinetic groupings of the synaptotagmin family: candidate sensors for rapid and delayed exocytosis. Proc Natl Acad Sci U S A. 2005 Apr 5;102(14):5210-4.

Hummel T, Krukkert K, Roos J, Davis G, Klämbt C. Drosophila Futsch/22C10 is a MAP1B-like protein required for dendritic and axonal development. Neuron. 2000 May;26(2):357-70.

Itoh Y, Esaki T, Kaneshige M, Suzuki H, Cook M, Sokoloff L, Cheng SY, Nunez J. Brain glucose utilization in mice with a targeted mutation in the thyroid hormone alpha or beta receptor gene. Proc Natl Acad Sci U S A. 2001 Aug 14;98(17):9913-8.

Jan LY, Jan YN. Properties of the larval neuromuscular junction in Drosophila melanogaster. J Physiol. 1976 Oct;262(1):189-214.

Jinek M, Chylinski K, Fonfara I, Hauer M, Doudna JA, Charpentier E. A programmable dual-RNA-guided DNA endonuclease in adaptive bacterial immunity. Science. 2012 Aug 17;337(6096):816-21.

Johansen J, Halpern ME, Johansen KM, Keshishian H. Stereotypic morphology of glutamatergic synapses on identified muscle cells of Drosophila larvae. J Neurosci. 1989 Feb;9(2):710-25.

Jorgensen EM, Hartwieg E, Schuske K, Nonet ML, Jin Y, Horvitz HR. Defective recycling of synaptic vesicles in synaptotagmin mutants of Caenorhabditis elegans. Nature. 1995 Nov 9;378(6553):196-9.

Kaeser PS, Kwon HB, Blundell J, Chevaleyre V, Morishita W, Malenka RC, Powell CM, Castillo PE, Südhof TC. RIM1alpha phosphorylation at serine-413 by protein kinase A is not required for presynaptic long-term plasticity or learning. Proc Natl Acad Sci U S A. 2008 Sep 23;105(38):14680-5.

Kaeser-Woo YJ, Younts TJ, Yang X, Zhou P, Wu D, Castillo PE, Südhof TC. Synaptotagmin-12 phosphorylation by cAMP-dependent protein kinase is essential for hippocampal mossy fiber LTP. J Neurosci. 2013 Jun 5;33(23):9769-80.

Kandel ER. The molecular biology of memory: cAMP, PKA, CRE, CREB-1, CREB-2, and CPEB. Mol Brain. 2012 May 14;5:14.

Keller LC, Cheng L, Locke CJ, Müller M, Fetter RD, Davis GW. Glial-derived prodegenerative signaling in the Drosophila neuromuscular system. Neuron. 2011 Dec 8;72(5):760-75.

Kissler AE, Pettersson N, Frölich A, Sigrist SJ, Suter B. Drosophila cdk5 is needed for locomotive behavior and NMJ elaboration, but seems dispensable for synaptic transmission. Dev Neurobiol. 2009 May;69(6):365-77.

Kittel RJ, Wichmann C, Rasse TM, Fouquet W, Schmidt M, Schmid A, Wagh DA, Pawlu C, Kellner RR, Willig KI, Hell SW, Buchner E, Heckmann M, Sigrist SJ. Bruchpilot promotes active zone assembly, Ca2+ channel clustering, and vesicle release. Science. 2006 May 19;312(5776):1051-4.

Lahey T, Gorczyca M, Jia XX, Budnik V. The Drosophila tumor suppressor gene dlg is required for normal synaptic bouton structure. Neuron. 1994 Oct;13(4):823-35.

Lepicard S, Franco B, de Bock F, Parmentier ML. A presynaptic role of microtubule-associated protein 1/Futsch in Drosophila: regulation of active zone number and neurotransmitter release. J Neurosci. 2014 May 14;34(20):6759-71.

Li HH, Kroll JR, Lennox SM, Ogundeyi O, Jeter J, Depasquale G, Truman JW. A GAL4 driver resource for developmental and behavioral studies on the larval CNS of Drosophila. Cell Rep. 2014 Aug 7;8(3):897-908.

Littleton JT, Bellen HJ, Perin MS. Expression of synaptotagmin in Drosophila reveals transport and localization of synaptic vesicles to the synapse. Development. 1993 Aug;118(4):1077-88.

Littleton JT, Serano TL, Rubin GM, Ganetzky B, Chapman ER. Synaptic function modulated by changes in the ratio of synaptotagmin I and IV. Nature. 1999 Aug 19;400(6746):757-60.

Littleton JT, Stern M, Schulze K, Perin M, Bellen HJ. Mutational analysis of Drosophila synaptotagmin demonstrates its essential role in Ca(2+)-activated neurotransmitter release. Cell. 1993 Sep 24;74(6):1125-34.

Liu H, Bai H, Hui E, Yang L, Evans CS, Wang Z, Kwon SE, Chapman ER. Synaptotagmin 7 functions as a Ca2+-sensor for synaptic vesicle replenishment. Elife. 2014 Feb 25;3:e01524.

Liu KS, Siebert M, Mertel S, Knoche E, Wegener S, Wichmann C, Matkovic T, Muhammad K, Depner H, Mettke C, Bückers J, Hell SW, Müller M, Davis GW, Schmitz D, Sigrist SJ. RIM-binding protein, a central part of the active zone, is essential for neurotransmitter release. Science. 2011 Dec 16;334(6062):1565-9.

Loewen CA, Royer SM, Reist NE. Drosophila synaptotagmin I null mutants show severe alterations in vesicle populations but calcium-binding motif mutants do not. J Comp Neurol. 2006 May 1;496(1):1-12.

Mahr A, Aberle H. The expression pattern of the Drosophila vesicular glutamate transporter: a marker protein for motoneurons and glutamatergic centers in the brain. Gene Expr Patterns. 2006 Mar;6(3):299-309.

Marie B, Pym E, Bergquist S, Davis GW. Synaptic homeostasis is consolidated by the cell fate gene gooseberry, a Drosophila pax3/7 homolog. J Neurosci. 2010 Jun 16;30(24):8071-82.

Martin AR. A further study of the statistical composition on the end-plate potential. J Physiol. 1955 Oct 28;130(1):114-22.

Matthew WD, Tsavaler L, Reichardt LF. Identification of a synaptic vesicle-specific membrane protein with a wide distribution in neuronal and neurosecretory tissue. J Cell Biol. 1981 Oct;91(1):257-69.

Maximov A, Shin OH, Liu X, Südhof TC. Synaptotagmin-12, a synaptic vesicle phosphoprotein that modulates spontaneous neurotransmitter release. J Cell Biol. 2007 Jan 1;176(1):113-24.

Mayford M, Barzilai A, Keller F, Schacher S, Kandel ER. Modulation of an NCAM-related adhesion molecule with long-term synaptic plasticity in Aplysia. Science. 1992 May 1;256(5057):638-44.

Mellor J, Nicoll RA. Hippocampal mossy fiber LTP is independent of postsynaptic calcium. Nat Neurosci. 2001 Feb;4(2):125-6.

Mendez JA, Bourque MJ, Fasano C, Kortleven C, Trudeau LE. Somatodendritic dopamine release requires synaptotagmin 4 and 7 and the participation of voltage-gated calcium channels. J Biol Chem. 2011 Jul 8;286(27):23928-37.

modENCODE Consortium, Roy S, Ernst J, Kharchenko PV, Kheradpour P, Negre N, Eaton ML, Landolin JM, Bristow CA, Ma L, Lin MF, Washietl S, Arshinoff BI, Ay F, Meyer PE, Robine N, Washington NL, Di Stefano L, Berezikov E, Brown CD, Candeias R, Carlson JW, Carr A, Jungreis I, Marbach D, Sealfon R, Tolstorukov MY, Will S, Alekseyenko AA, Artieri C, Booth BW, Brooks AN, Dai Q, Davis CA, Duff MO, Feng X, Gorchakov AA, Gu T, Henikoff JG, Kapranov P, Li R, MacAlpine HK, Malone J, Minoda A, Nordman J, Okamura K, Perry M, Powell SK, Riddle NC, Sakai A, Samsonova A, Sandler JE, Schwartz YB, Sher N, Spokony R, Sturgill D, van Baren M, Wan KH, Yang L, Yu C, Feingold E, Good P, Guyer M, Lowdon R, Ahmad K, Andrews J, Berger B, Brenner SE, Brent MR, Cherbas L, Elgin SC, Gingeras TR, Grossman R, Hoskins RA, Kaufman TC, Kent W, Kuroda MI, Orr-Weaver T, Perrimon N, Pirrotta V, Posakony JW, Ren B, Russell S, Cherbas P, Graveley BR, Lewis S, Micklem G, Oliver B, Park PJ, Celniker SE, Henikoff S, Karpen GH, Lai EC, MacAlpine DM, Stein LD, White KP, Kellis M. Identification of functional elements and regulatory circuits by Drosophila modENCODE. Science. 2010 Dec 24;330(6012):1787-97.

Mahal LK, Sequeira SM, Gureasko JM, Söllner TH. Calcium-independent stimulation of membrane fusion and SNAREpin formation by synaptotagmin I. J Cell Biol. 2002 Jul 22;158(2):273-82.

Malenka RC. Rapid release revealed: honoring the synapse. Cell. 2013 Sep 12;154(6):1171-4.

Müller M, Davis GW. Transsynaptic control of presynaptic Ca^{2+} influx achieves homeostatic potentiation of neurotransmitter release. Curr Biol. 2012 Jun 19;22(12):1102-8.

Müller M, Genç Ö, Davis GW. RIM-binding protein links synaptic homeostasis to the stabilization and replenishment of high release probability vesicles. Neuron. 2015 Mar 4;85(5):1056-69.

Müller M, Liu KS, Sigrist SJ, Davis GW. RIM controls homeostatic plasticity through modulation of the readily-releasable vesicle pool. J Neurosci. 2012 Nov 21;32(47):16574-85.

Müller M, Pym EC, Tong A, Davis GW. Rab3-GAP controls the progression of synaptic homeostasis at a late stage of vesicle release. Neuron. 2011 Feb 24;69(4):749-62.

Nagai T, Ibata K, Park ES, Kubota M, Mikoshiba K, Miyawaki A. A variant of yellow fluorescent protein with fast and efficient maturation for cell-biological applications. Nat Biotechnol. 2002 Jan;20(1):87-90.

Nagy G, Reim K, Matti U, Brose N, Binz T, Rettig J, Neher E, Sørensen JB. Regulation of releasable vesicle pool sizes by protein kinase A-dependent phosphorylation of SNAP-25. Neuron. 2004 Feb 5;41(3):417-29.

Nicholson-Tomishima K, Ryan TA. Kinetic efficiency of endocytosis at mammalian CNS synapses requires synaptotagmin I. Proc Natl Acad Sci U S A. 2004 Nov 23;101(47):16648-52.

Nonet ML, Grundahl K, Meyer BJ, Rand JB. Synaptic function is impaired but not eliminated in C. elegans mutants lacking synaptotagmin. Cell. 1993 Jul 2;73(7):1291-305.

Nüsslein-Volhard C, Wieschaus E. Mutations affecting segment number and polarity in Drosophila. Nature. 1980 Oct 30;287(5785):795-801.

Pack-Chung E, Kurshan PT, Dickman DK, Schwarz TL. A Drosophila kinesin required for synaptic bouton formation and synaptic vesicle transport. Nat Neurosci. 2007 Aug;10(8):980-9.

Parks AL, Cook KR, Belvin M, Dompe NA, Fawcett R, Huppert K, Tan LR, Winter CG, Bogart KP, Deal JE, Deal-Herr ME, Grant D, Marcinko M, Miyazaki WY, Robertson S, Shaw KJ, Tabios M, Vysotskaia V, Zhao L, Andrade RS, Edgar KA, Howie E, Killpack K, Milash B, Norton A, Thao D, Whittaker K, Winner MA, Friedman L, Margolis J, Singer MA, Kopczynski C, Curtis D, Kaufman TC, Plowman GD, Duyk G, Francis-Lang HL. Systematic generation of high-resolution deletion coverage of the Drosophila melanogaster genome. Nat Genet. 2004 Mar;36(3):288-92.

Patel MR, Lehrman EK, Poon VY, Crump JG, Zhen M, Bargmann CI, Shen K. Hierarchical assembly of presynaptic components in defined C. elegans synapses. Nat Neurosci. 2006 Dec;9(12):1488-98.

Penney J, Tsurudome K, Liao EH, Elazzouzi F, Livingstone M, Gonzalez M, Sonenberg N, Haghighi AP. TOR is required for the retrograde regulation of synaptic homeostasis at the Drosophila neuromuscular junction. Neuron. 2012 Apr 12;74(1):166-78.

Petersen SA, Fetter RD, Noordermeer JN, Goodman CS, DiAntonio A. Genetic analysis of glutamate receptors in Drosophila reveals a retrograde signal regulating presynaptic transmitter release. Neuron. 1997 Dec;19(6):1237-48.

Plomp JJ, Van Kempen GT, De Baets MB, Graus YM, Kuks JB, Molenaar PC. Acetylcholine release in myasthenia gravis: regulation at single end-plate level. Ann Neurol. 1995 May;37(5):627-36.

Plomp JJ, van Kempen GT, Molenaar PC. Adaptation of quantal content to decreased postsynaptic sensitivity at single endplates in alpha-bungarotoxin-treated rats. J Physiol. 1992 Dec;458:487-99.

Poskanzer KE, Fetter RD, Davis GW. Discrete residues in the c(2)b domain of synaptotagmin I independently specify endocytic rate and synaptic vesicle size. Neuron. 2006 Apr 6;50(1):49-62.

Poskanzer KE, Marek KW, Sweeney ST, Davis GW. Synaptotagmin I is necessary for compensatory synaptic vesicle endocytosis in vivo. Nature. 2003 Dec 4;426(6966):559-63.

Potter GB, Facchinetti F, Beaudoin GM 3rd, Thompson CC. Neuronal expression of synaptotagmin-related gene 1 is regulated by thyroid hormone during cerebellar development. J Neurosci. 2001 Jun 15;21(12):4373-80.

Quintero-Rivera F, Chan A, Donovan DJ, Gusella JF, Ligon AH. Disruption of a synaptotagmin (SYT14) associated with neurodevelopmental abnormalities. Am J Med Genet A. 2007 Mar 15;143A(6):558-63.

Reist NE, Buchanan J, Li J, DiAntonio A, Buxton EM, Schwarz TL. Morphologically docked synaptic vesicles are reduced in synaptotagmin mutants of Drosophila. J Neurosci. 1998 Oct 1;18(19):7662-73.

Rickman C, Jiménez JL, Graham ME, Archer DA, Soloviev M, Burgoyne RD, Davletov B. Conserved prefusion protein assembly in regulated exocytosis. Mol Biol Cell. 2006 Jan;17(1):283-94.

Robinson SW, Herzyk P, Dow JA, Leader DP. FlyAtlas: database of gene expression in the tissues of Drosophila melanogaster. Nucleic Acids Res. 2013 Jan;41(Database issue):D744-50.

Ruiz-Marcos A, Sanchez-Toscano F, Escobar del Rey F, Morreale de Escobar G. Severe hypothyroidism and the maturation of the rat cerebral cortex. Brain Res. 1979 Feb 23;162(2):315-29.

Sandrock AW Jr, Dryer SE, Rosen KM, Gozani SN, Kramer R, Theill LE, Fischbach GD. Maintenance of acetylcholine receptor number by neuregulins at the neuromuscular junction in vivo. Science. 1997 Apr 25;276(5312):599-603.

Schneggenburger R, Meyer AC, Neher E. Released fraction and total size of a pool of immediately available transmitter quanta at a calyx synapse. Neuron. 1999 Jun;23(2):399-409.

Schuster CM, Davis GW, Fetter RD, Goodman CS. Genetic dissection of structural and functional components of synaptic plasticity. II. Fasciclin II controls presynaptic structural plasticity. Neuron. 1996 Oct;17(4):655-67.

Schuster CM, Davis GW, Fetter RD, Goodman CS. Genetic dissection of structural and functional components of synaptic plasticity. I. Fasciclin II controls synaptic stabilization and growth. Neuron. 1996 Oct;17(4):641-54.

Song H, Smolen P, Av-Ron E, Baxter DA, Byrne JH. Dynamics of a minimal model of interlocked positive and negative feedback loops of transcriptional regulation by cAMP-response element binding proteins. Biophys J. 2007 May 15;92(10):3407-24.

Südhof TC. A molecular machine for neurotransmitter release: synaptotagmin and beyond. Nat Med. 2013 Oct;19(10):1227-31.

Stewart BA, Atwood HL, Renger JJ, Wang J, Wu CF. Improved stability of Drosophila larval neuromuscular preparations in haemolymph-like physiological solutions. J Comp Physiol A. 1994 Aug;175(2):179-91.

Stewart BA, Schuster CM, Goodman CS, Atwood HL. Homeostasis of synaptic transmission in Drosophila with genetically altered nerve terminal morphology. J Neurosci. 1996 Jun 15;16(12):3877-86.

Sugita S, Han W, Butz S, Liu X, Fernández-Chacón R, Lao Y, Südhof TC. Synaptotagmin VII as a plasma membrane Ca(2+) sensor in exocytosis. Neuron. 2001 May;30(2):459-73.

Sun J, Pang ZP, Qin D, Fahim AT, Adachi R, Südhof TC. A dual-Ca2+-sensor model for neurotransmitter release in a central synapse. Nature. 2007 Nov 29;450(7170):676-82.

Takamori S, Holt M, Stenius K, Lemke EA, Grønborg M, Riedel D, Urlaub H, Schenck S, Brügger B, Ringler P, Müller SA, Rammner B, Gräter F, Hub JS, De Groot BL, Mieskes G, Moriyama Y, Klingauf J, Grubmüller H, Heuser J, Wieland F, Jahn R. Molecular anatomy of a trafficking organelle. Cell. 2006 Nov 17;127(4):831-46.

Thibault ST, Singer MA, Miyazaki WY, Milash B, Dompe NA, Singh CM, Buchholz R, Demsky M, Fawcett R, Francis-Lang HL, Ryner L, Cheung LM, Chong A, Erickson C, Fisher WW, Greer K, Hartouni SR, Howie E, Jakkula L, Joo D, Killpack K, Laufer A, Mazzotta J, Smith RD, Stevens LM, Stuber C, Tan LR, Ventura R, Woo A, Zakrajsek I, Zhao L, Chen F, Swimmer C, Kopczynski C, Duyk G, Winberg ML, Margolis J. A complementary transposon tool kit for Drosophila melanogaster using P and piggyBac. Nat Genet. 2004 Mar;36(3):283-7.

Thompson CC. Thyroid hormone-responsive genes in developing cerebellum include a novel synaptotagmin and a hairless homolog. J Neurosci. 1996 Dec 15;16(24):7832-40.

Thompson CC, Potter GB. Thyroid hormone action in neural development. Cereb Cortex. 2000 Oct;10(10):939-45.

Van Vactor DV, Sink H, Fambrough D, Tsoo R, Goodman CS. Genes that control neuromuscular specificity in Drosophila. Cell. 1993 Jun 18;73(6):1137-53.

Wagh DA, Rasse TM, Asan E, Hofbauer A, Schwenkert I, Dürrbeck H, Buchner S, Dabauvalle MC, Schmidt M, Qin G, Wichmann C, Kittel R, Sigrist SJ, Buchner E. Bruchpilot, a protein with homology to ELKS/CAST, is required for structural integrity and function of synaptic active zones in Drosophila. Neuron. 2006 Mar 16;49(6):833-44.

Wang Z, Chapman ER. Rat and Drosophila synaptotagmin 4 have opposite effects during SNARE-catalyzed membrane fusion. J Biol Chem. 2010 Oct 1;285(40):30759-66.

Weisskopf MG, Castillo PE, Zalutsky RA, Nicoll RA. Mediation of hippocampal mossy fiber long-term potentiation by cyclic AMP. Science. 1994 Sep 23;265(5180):1878-82.

Weisskopf MG, Nicoll RA. Presynaptic changes during mossy fibre LTP revealed by NMDA receptor-mediated synaptic responses. Nature. 1995 Jul 20;376(6537):256-9.

Weyhersmüller A, Hallermann S, Wagner N, Eilers J. Rapid active zone remodeling during synaptic plasticity. J Neurosci. 2011 Apr 20;31(16):6041-52.

Yamamoto S, Jaiswal M, Charng WL, Gambin T, Karaca E, Mirzaa G, Wiszniewski W, Sandoval H, Haelterman NA, Xiong B, Zhang K, Bayat V, David G, Li T, Chen K, Gala U, Harel T, Pehlivan D, Penney S, Vissers LE, de Ligt J, Jhangiani SN, Xie Y, Tsang SH, Parman Y, Sivaci M, Battaloglu E, Muzny D, Wan YW, Liu Z, Lin-Moore AT, Clark RD, Curry CJ, Link N, Schulze KL, Boerwinkle E, Dobyns WB, Allikmets R, Gibbs RA, Chen R, Lupski JR, Wangler MF, Bellen HJ. A drosophila genetic resource of mutants to study mechanisms underlying human genetic diseases. Cell. 2014 Sep 25;159(1):200-14.

Yang Y, Calakos N. Acute in vivo genetic rescue demonstrates that phosphorylation of RIM1alpha serine 413 is not required for mossy fiber long-term potentiation. J Neurosci. 2010 Feb 17;30(7):2542-6.

Yeckel MF, Kapur A, Johnston D. Multiple forms of LTP in hippocampal CA3 neurons use a common postsynaptic mechanism. Nat Neurosci. 1999 Jul;2(7):625-33.

Young SM Jr, Neher E. Synaptotagmin has an essential function in synaptic vesicle positioning for synchronous release in addition to its role as a calcium sensor. Neuron. 2009 Aug 27;63(4):482-96.

Yoshihara M, Littleton JT. Synaptotagmin I functions as a calcium sensor to synchronize neurotransmitter release. Neuron. 2002 Dec 5;36(5):897-908.

Yoshihara M, Adolfsen B, Galle KT, Littleton JT. Retrograde signaling by Syt 4 induces presynaptic release and synapse-specific growth. Science. 2005 Nov 4;310(5749):858-63.

Younger MA, Müller M, Tong A, Pym EC, Davis GW. A presynaptic ENaC channel drives homeostatic plasticity. Neuron. 2013 Sep 18;79(6):1183-96.

Zalutsky RA, Nicoll RA. Comparison of two forms of long-term potentiation in single hippocampal neurons. Science. 1990 Jun 29;248(4963):1619-24.

Zhang B, Stewart B. Voltage-clamp analysis of synaptic transmission at the Drosophila larval neuromuscular junction. Cold Spring Harb Protoc. 2010 Sep 1;2010(9):pdb.prot5488.

Zhen M, Jin Y. The liprin protein SYD-2 regulates the differentiation of presynaptic termini in C. elegans. Nature. 1999 Sep 23;401(6751):371-5.

Zhong Y, Budnik V, Wu CF. Synaptic plasticity in Drosophila memory and hyperexcitable mutants: role of cAMP cascade. J Neurosci. 1992 Feb;12(2):644-51.

Zinsmaier KE, Eberle KK, Buchner E, Walter N, Benzer S. Paralysis and early death in cysteine string protein mutants of Drosophila. Science. 1994 Feb 18;263(5149):977-80.

Chapter 3

Cdk5 Activity Does Not Control Homeostatic Potentiation at the *Drosophila* Neuromuscular Junction

Summary

Cyclin-dependent kinase 5 (Cdk5) signaling controls a diversity of developmental and functional processes in the nervous system. These processes include the migration of neurons, targeting of axons, morphogenesis of synapses, recruitment of presynaptic and postsynaptic proteins, and regulation of neurotransmitter release. As Cdk5 activity is implicated in numerous aspects of synaptic structure and function, it is unclear which of these processes are directly regulated by Cdk5 signaling and which are secondarily affected by Cdk5 signaling. Here, we have simplified an investigation of Cdk5 signaling by combining electrophysiology and imaging in a genetic analysis of amorphic alleles in *Drosophila*. We demonstrate that Cdk5 signaling contributes to neurotransmitter release by evaluating synaptic transmission in a range of extracellular Ca^{2+} concentrations with low-frequency and high-frequency action potential stimulation. Moreover, we confirmed that the loss of Cdk5 signaling results in overgrowth of neuromuscular junctions and an apparently compensatory decrease in the density of active zones. Despite these effects of Cdk5 signaling ablation, we found that short-term and long-term forms of homeostatic potentiation, in which postsynaptic reductions in glutamate sensitivity are countered by presynaptic enhancements in glutamate exocytosis, were accurately expressed. These results distinguish homeostatic potentiation from a Cdk5-dependent form of homeostatic synaptic plasticity, referred to as presynaptic homeostatic scaling, in the hippocampus. Likewise, our findings suggest that a form of homeostatic structural plasticity, which is responsive to synaptic overgrowth, does not occlude homeostatic potentiation. Our data facilitate an understanding of Cdk5 signaling and homeostatic regulation in the evolution of nervous systems and may have significant implications in human health and disease.

Introduction

Homeostatic regulatory mechanisms counteract electrochemical perturbations in the nervous system by altering synaptic transmission to stabilize function (Davis, 2006; Turrigiano, 2008). The disruption of homeostatic synaptic plasticity may underlie several neurological disorders, including Alzheimer's disease (Kamenetz *et al.*, 2003), epilepsy (Houweling *et al.*, 2005), and schizophrenia (Dickman and Davis, 2009). To uncover the molecular signaling processes that control homeostatic plasticity, we have employed the *Drosophila* neuromuscular junction (NMJ). This model synapse homeostatically boosts glutamate release from presynaptic motor neurons within ten minutes after application of philanthotoxin-433 (PhTx), an antagonist of glutamate receptors (Frank *et al.*, 2006). This characteristic of fly NMJs has allowed us to conduct rapid electrophysiology-based screens to identify genes that participate in this form of homeostatic plasticity (Dickman and Davis, 2009; Müller *et al.*, 2011), which we call short-term homeostatic potentiation. Moreover, a long-term form of homeostatic potentiation at the fly NMJ can be induced by the genetic ablation of a glutamate receptor subunit, GluRIIA (Petersen *et al.*, 1997).

These short-term and long-term forms of homeostatic potentiation at *Drosophila* NMJs are achieved by increases in presynaptic Ca^{2+} influx (Müller and Davis, 2012) and the size of the readily-releasable pool (RRP) of synaptic vesicles (Weyhersmüller *et al.*, 2011; Müller *et al.*, 2012). Although impairment of RIM-binding protein (RBP) has been shown to disrupt the homeostatic modulation of Ca^{2+} influx and RRP size (Müller *et al.*, 2015), these processes may also be affected independently of each other (Müller *et al.*, 2012). Similar to the fly NMJ, hippocampal synapses respond homeostatically to long-term silencing (Murthy *et al.*, 2001; Thiagarajan *et al.*, 2005; Kim and Ryan, 2010). One hippocampal form of homeostatic plasticity, termed presynaptic homeostatic scaling, is

achieved by the conversion of resting pool synaptic vesicles into recycling pool synaptic vesicles through acute inhibition of cyclin-dependent kinase 5 (Cdk5) signaling (Kim and Ryan, 2010). Likewise, removal of Cdk5 signaling at hippocampal synapses was shown to enhance presynaptic Ca^{2+} influx, which could contribute to homeostatic scaling in this system (Kim and Ryan, 2013). Given the similarities between homeostatic scaling in the hippocampus and homeostatic potentiation at the *Drosophila* NMJ, it is conceivable that these forms of homeostatic plasticity may be linked by a common need for Cdk5 control.

By phosphorylating numerous target proteins, Cdk5 regulates axonal pathfinding (Kwon *et al.*, 1999; Connell-Crowley *et al.*, 2000), neuronal migration (Chae *et al.*,1997), and synaptic vesicle trafficking to active zones (Locke *et al.*, 2006; Ou *et al.*, 2010; Park *et al.*, 2011) during brain development. In addition to controlling the homeostatic scaling of neurotransmitter release in the hippocampus (Kim and Ryan, 2010), Cdk5 signaling has also been implicated in many other forms of synaptic plasticity, including long-term potentiation (Lai *et al.*, 2012), synaptic scaling of glutamate receptors (Seeburg *et al.*, 2008), and functional presynaptic silencing (Mitra *et al.*, 2011). Despite these important findings, the null phenotype of *Cdk5* has been elusive (Kissler *et al.*, 2009). *Cdk5* null mice die perinatally (Ohshima *et al.*, 1996), and the common Cdk5 inhibitor, roscovitine, can exhibit off-target effects (Yan *et al.*, 2002; Mitra *et al.*, 2011; Yazawa *et al.*, 2011).

Although Cdk5 signaling during development is critical for viability in mammals, it is not essential in *Drosophila* (Connell-Crowley *et al.*, 2007; Kissler *et al.*, 2009). Hence, we were able to further characterize the neural function of Cdk5 by examining flies with amorphic deletions in *cdk5* (Kissler *et al.*, 2009) and *p35*, which encodes an activator of Cdk5 (Tsai *et al.*, 1994; Connell-Crowley *et al.*, 2007). At $cdk5^{null}$ and $p35^{20C}$ NMJs, we observed robust homeostatic increases in glutamate release after acute PhTx exposure,

consistent with normal short-term homeostatic potentiation. Furthermore, we observed a similar enhancement in glutamate release at these Cdk5-deficient NMJs following the chronic reduction of glutamate sensitivity, consistent with normal long-term homeostatic potentiation. These data demonstrate that the signaling events underlying homeostatic potentiation at fly NMJs are separable from those of hippocampal homeostatic scaling.

Consistent with an earlier study, we confirmed that *cdk5*^{null} mutant NMJs have synaptic strengths that are generally indistinguishable from those of wild type controls with single action potential stimulation (Kissler *et al.*, 2009). However, by lowering the extracellular Ca^{2+} concentration in our recordings, we have revealed an effect of *cdk5* loss on the apparent Ca^{2+} cooperativity of neurotransmitter release. Also, by elevating extracellular Ca^{2+} to a physiological concentration (Stewart *et al.*, 1994) and recording in voltage-clamp, we assessed the role of Cdk5 in regulation of neurotransmitter release dynamics by stimulating at a high frequency (60-Hz). Our data indicate that Cdk5 does not significantly affect RRP size modulation at baseline or in homeostatic potentiation. On the contrary, we found that Cdk5 signaling significantly affects short-term synaptic plasticity, synaptic depression, and probability of neurotransmitter release at fly NMJs.

Unexpectedly, we saw that spontaneous miniature EJPs at *p35*^{20C} mutant NMJs are roughly half the size recorded at wild type control and *cdk5*^{null} mutant NMJs. This strong reduction in quantal size correlated with an increased quantal content, pointing to the expression of long-term homeostatic potentiation and to an intrinsic decrease in glutamate sensitivity at *p35*^{20C} mutant NMJs. We show evidence that the *p35*^{20C} mutant has impaired transport of GluRIIA-containing glutamate receptors to postsynaptic sites in *Drosophila* muscles. This result is consistent with a previously described role for *p35* in glutamate receptor trafficking (Juo *et al.*, 2007). Yet, we also show that the aberrant

levels of GluRIIA in *p35*^{20C} cannot be attributed to a p35 deficiency and are presumably linked to the genetic background. In addition, we present results from deconvolution and superresolution structured illumination microscopy, which suggest that *cdk5* and *p35* act in a common pathway to regulate the growth and elaboration of *Drosophila* larval NMJs.

With this study, we have determined that Cdk5 is not necessary for homeostatic potentiation. Furthermore, we provide evidence that Cdk5 signaling does not generally limit neurotransmitter release (Kim and Ryan, 2010; Mitra *et al.*, 2011; Kim and Ryan, 2013), as *cdk5*^{null} and *p35*^{20C} mutants show reduced release probability at the fly NMJ. These findings underscore the importance of Cdk5 signaling in the nervous system and augment our understanding of how homeostatic regulatory mechanisms have evolved.

Results

Cdk5 signaling is dispensable for short-term homeostatic potentiation at fly NMJs

When the postsynaptic sensitivity to glutamate is decreased at *Drosophila* larval NMJs, homeostatic potentiation enhances glutamate release from presynaptic terminals to reestablish a set point value of muscle depolarization (Petersen *et al.*, 1997; Frank *et al.*, 2006; Gaviño *et al.*, 2015). This homeostatic regulatory mechanism can be induced rapidly by PhTx application (Frank *et al.*, 2006) and is analogous to phenomena seen at rodent (Plomp *et al.*, 1992; Plomp *et al.*, 1995; Sandrock *et al.*, 1997) and human NMJs from patients with myasthenia gravis (Cull-Candy *et al.*, 1980; Plomp *et al.*, 1995). The processes underlying homeostatic potentiation, enhancement of presynaptic Ca^{2+} influx (Müller and Davis, 2012) and RRP size (Weyhersmüller *et al.*, 2011; Müller *et al.*, 2012), also share similarities with a form of homeostatic synaptic plasticity in the hippocampus, called presynaptic homeostatic scaling (Kim and Ryan, 2010). This hippocampal form of homeostatic plasticity requires attenuation of Cdk5 signaling (Kim and Ryan, 2010; Kim and Ryan, 2013). Conversely, Cdk5 signaling was shown to enhance the probability of neurotransmitter release in the hippocampus through effects on presynaptic Ca^{2+} influx and RIM-facilitated synaptic vesicle docking (Su *et al.*, 2012). Homeostatic potentiation in flies also depends upon the regulation of a presynaptic calcium channel, Cacophony (Frank *et al.*, 2006; Müller and Davis, 2012), and modulation of the RRP by RIM (Müller *et al.*, 2012). Based on these observations, we asked if the regulation of Cdk5 signaling is required for homeostatic potentiation in flies. Roles for Cdk5 signaling in homeostatic plasticity at fly NMJs and in the hippocampus would suggest evolutionary conservation of these phenomena, whereas the null hypothesis would suggest convergent evolution.

To determine if Cdk5 signaling is necessary for homeostatic potentiation at the fly NMJ, we first induced short-term homeostatic potentiation by applying PhTx to amorphic *cdk5*^{null} (Kissler *et al.*, 2009) and *p35*^{20C} (Connell-Crowley *et al.*, 2007) third instar larvae, as described (Frank *et al.*, 2006). To minimize genetic background effects in *p35*^{20C}, we placed this mutation over a previously described deficiency, *Df(p35)*^{C2}, which uncovers the *p35* locus (Connell-Crowley *et al.*, 2007). We then recorded in current-clamp mode using single action potential stimulation at muscle 6, segments A2 and A3 (Jan and Jan, 1976). From these recordings, we observed that PhTx application reduced spontaneous miniature excitatory junctional potential (mEJP) amplitudes in wild type controls, *cdk5*^{null}, and *p35*^{20C}*/Df* by roughly 50% (Fig. 1A, D-F), as usual (Frank *et al.*, 2006). Conversely, mean EJP amplitudes following PhTx application slightly decreased by 5.1% in wild type (n = 16), 2.2% in *cdk5*^{null} (n =18), and 15.0% in *p35*^{20C}*/Df* (n =13), compared to baseline values in the absence of PhTx (n = 22, 18, and 15, respectively) (Fig. 1B, D-F). Average quantal contents after PhTx treatment concomitantly increased by 81.6% in wild type (n = 16), 72.7% in *cdk5*^{null} (n =18), and 92.4% in *p35*^{20C}*/Df* (n =13), as above (Fig. 1C). Our results indicate that the absence of Cdk5 signaling during development does not impair the induction or expression of short-term homeostatic potentiation at the fly larval NMJ.

To rule out developmental compensation induced by the global ablation of Cdk5 signaling, we expressed a previously characterized dominant-negative Cdk5 (Connell-Crowley *et al.*, 2000) in presynaptic motor neurons using *ok371-Gal4* (Mahr and Aberle, 2006). As noted with the amorphic Cdk5 signaling mutants, *cdk5*^{null} and *p35*^{20C}, PhTx exposure in these *cdk5*^{DN} larvae decreased mean mEJP and EJP amplitudes by 49.5% and 16.4%, respectively (n = 21) (Fig. 1A, B). The slightly, but insignificantly (p = 0.06),

decreased EJP amplitude was maintained by a 74.6% increase in quantal content (Fig. 1C), consistent with normal synaptic homeostasis. From these results, we conclude that Cdk5 signaling is not required for short-term homeostatic potentiation at fly larval NMJs. Thus, short-term homeostatic potentiation at *Drosophila* NMJs and homeostatic scaling in the hippocampus (Kim and Ryan, 2010) do not share a requirement for Cdk5 control.

Notably, when determining values for baseline synaptic transmission in our PhTx experiments, we found that $cdk5^{null}$ mutants and wild type controls had indistinguishable average mEJP amplitudes ($p = 0.33$) (Fig. 1A), EJP amplitudes ($p = 0.82$) (Fig. 1B), and quantal contents ($p = 0.31$) (Fig. 1C), as shown by an earlier study (Kissler *et al.*, 2009). Here, we have extended those findings by examining baseline synaptic transmission in p35-deficient ($p35^{20C}/Df$) and $cdk5^{DN}$ larvae. As seen with $cdk5^{null}$, $p35^{20C}/Df$ and $cdk5^{DN}$ exhibited wild type mean mEJP amplitudes ($p = 0.21$ and $= 0.80$) (Fig. 1A) and quantal contents ($p = 0.79$ and $= 0.09$) (Fig. 1C). Furthermore, $p35^{20C}/Df$ had only slightly larger (11.3%) mean EJP amplitudes than wild type ($p = 0.01$), while EJP amplitudes in $cdk5^{DN}$ were not significantly different from wild type ($p = 0.13$) (Fig. 1B). These data imply that Cdk5 signaling is dispensable for baseline synaptic transmission, as suggested (Kissler *et al.*, 2009). However, our recordings here and those in the earlier study were done in subphysiological Ca^{2+} concentrations (Stewart *et al.*, 1994) with relatively low-frequency stimulation (Kissler *et al.*, 2009). Thus, Cdk5 signaling may influence baseline synaptic transmission under physiological recording conditions, as locomotion defects have been reported for both $cdk5^{null}$ (Kissler *et al.*, 2009) and $p35^{20C}$ (Connell-Crowley *et al.*, 2007).

Cdk5 signaling is dispensable for long-term homeostatic potentiation at fly NMJs

The earliest evidence for homeostatic enhancement of neurotransmitter release at *Drosophila* NMJs was uncovered by recordings from *GluRIIA*^{SP16} mutants (Petersen *et al.*, 1997). These null mutants fail to express GluRIIA-containing glutamate receptors at postsynaptic muscles and exhibit a concomitant reduction in the average quantal size (Petersen *et al.*, 1997; Frank *et al.*, 2006). However, as observed with short-term, PhTx-induced homeostatic potentiation (Frank *et al.*, 2006), this decrease in quantal size can be offset by homeostatic modulation of presynaptic Ca^{2+} influx (Müller and Davis, 2012) and RRP size (Weyhersmüller *et al.*, 2011; Müller *et al.*, 2012). Although short-term and long-term homeostatic potentiation are executed by ostensibly similar processes, these phenomena differ in their fundamental requirements for small GTPase signaling (Frank *et al.*, 2009), Wnt signaling (Marie *et al.*, 2010), S6K/TOR signaling (Cheng *et al*., 2011; Penney *et al*., 2012), and presumably other mechanisms. Moreover, the compensatory removal of Cdk5 signaling, implicated in hippocampal presynaptic homeostatic scaling, was induced by long-term exposure to tetrodotoxin (Kim and Ryan, 2010). Therefore, a more chronic perturbation, such as the genetic ablation of GluRIIA, might be needed to reveal a requirement for Cdk5 signaling in homeostatic potentiation at *Drosophila* NMJs.

To determine if Cdk5 signaling is involved in long-term homeostatic potentiation, we generated and recorded from recombinant double mutants carrying the *GluRIIA*^{SP16} mutation and cdk5^{null}. As with our PhTx recordings, our recordings here were performed in 0.4 mM extracellular Ca^{2+}, a subphysiological concentration (Stewart *et al.*, 1994), in current-clamp. In double mutants and *GluRIIA*^{SP16} controls, the loss of GluRIIA led to a roughly 65% decrease in mean mEJP amplitudes ($p < 0.01$) (Fig. 2A, D, E), as expected

(Petersen *et al.*, 1997; Frank *et al.*, 2006). Yet, mean EJP amplitudes decreased by only 36.2% in *GluRIIA*^{SP16} single mutant controls (n = 14) and by a smaller 29.0% in *cdk5*^{null}*, GluRIIA*^{SP16} mutant recombinants (n =17), as compared to "baseline" values in *GluRIIA*$^{+}$ mutants (n = 22 for wild type, 18 for *cdk5*^{null}) (Fig. 2B, D, E). As expected from accurate long-term homeostatic potentiation, the average quantal contents increased by 77.3% in *GluRIIA*^{SP16} single mutant controls (n = 14) and by 95.5% in *cdk5*^{null}*, GluRIIA*^{SP16} double mutants (n =17), as above (Fig. 2C). We conclude that Cdk5 is not needed for long-term homeostatic potentiation at fly NMJs, at least in this subphysiological Ca^{2+} concentration (Stewart *et al.*, 1994; Younger *et al*., 2013) with mere single action potential stimulation.

In accordance with these results, we discovered an unexpected phenotype in the well-studied *p35*^{20C} mutant (Connell-Crowley *et al.*, 2007; Trunova *et al.*, 2011; Trunova and Giniger, 2012). Homozygous *p35*^{20C} larvae had a mean mEJP amplitude of 0.47 ± 0.03 (SEM) mV (n = 14), which was significantly lower than wild type (n = 22; $p < 0.01$) and *cdk5*^{null} (n = 18; $p < 0.01$) mean mEJPs by 41.8% and 49.9%, respectively. Yet, the mean EJP amplitude in *p35*^{20C} mutants was 39.0 ± 1.70 (SEM) mV (n = 14), which was not significantly different from that of wild type (n = 22; $p = 0.80$) or *cdk5*^{null} (n = 18; $p = 0.70$). Accordingly, mean quantal content in *p35*^{20C} mutants was 87.6 ± 6.84 (SEM) (n = 14), which was significantly larger than that of wild type (n = 22; $p < 0.01$) and *cdk5*^{null} (n = 18; $p < 0.01$). Importantly, we cannot attribute the decreased quantal size in *p35*^{20C} to the loss of p35, as the mean mEJP amplitude in *p35*^{20C}*/Df* was not significantly different from wild type (n = 15; $p = 0.21$) (Fig. 1A). Moreover, expression of a previously studied *UAS-p35* construct (Connell-Crowley *et al.*, 2000; Trunova *et al.*, 2011) in postsynaptic muscles with *MHC-Gal4* or pan-neuronally with *elav*^{c155}*-Gal4* (Lin and Goodman, 1994)

did not rescue the quantal size deficit in *p35*^{20C} mutants, as average quantal sizes were 0.56 ± 0.04 (SEM) mV (n = 10; *p* = 0.08) and 0.44 ± 0.05 (SEM) mV (n = 12; *p* = 0.55), respectively. Regardless, these data suggest that long-term homeostatic potentiation is expressed in *p35*^{20C} and argue against a role for Cdk5 activity in synaptic homeostasis.

Cdk5 affects the apparent Ca^{2+} cooperativity of neurotransmitter release in flies

From current-clamp recordings in subphysiological (0.4 mM) Ca^{2+} (Stewart *et al.*, 1994), we failed to detect any significant effects on baseline synaptic transmission from the loss of Cdk5 (Fig. 1, 2). Nonetheless, synaptic transmission defects can sometimes be revealed by altering the extracellular Ca^{2+} concentration (Dickman and Davis, 2009; Müller *et al.*, 2011; Müller *et al.*, 2015). Consequently, we tested the Ca^{2+}-dependence of neurotransmitter release at *cdk5*^{null} NMJs. Mean EJP amplitudes in *cdk5*^{null} and wild type controls were also similar at 0.3 mM extracellular Ca^{2+} (n = 15; *p* = 0.12). Likewise, *cdk5*^{null} NMJs had a wild type average quantal content with (n = 15; *p* = 0.19) or without correction for nonlinear summation (n = 15; *p* = 0.12) at 0.3 mM extracellular Ca^{2+} (Fig. 3A). Conversely, average EJP amplitude in *cdk5*^{null} was significantly decreased, when compared to wild type controls, by 47.3% at 0.2 mM extracellular Ca^{2+} (n = 24; *p* < 0.01) (Fig. 3A, C). Moreover, *cdk5*^{null} NMJs showed decreased mean quantal contents with or without correction for nonlinear summation, when compared to wild type controls, at 0.2 mM extracellular Ca^{2+} (n = 24; *p* < 0.01) (Fig. 3A). Mean mEJP amplitudes did not differ between *cdk5*^{null} and wild type controls at 0.2 mM extracellular Ca^{2+} (n = 24; *p* = 0.12) or at 0.3 mM extracellular Ca^{2+} (n = 15; *p* = 0.80). Hence, we cannot attribute the decrease in *cdk5*^{null} quantal content to homeostatic depression (Daniels *et al.*, 2004; Gaviño *et al.*, 2015). Instead, we contend that Cdk5 loss impairs neurotransmitter release in low Ca^{2+}.

Our discovery of neurotransmitter release deficits in *cdk5*^{null} mutants is consistent with previously described effects of Cdk5 in presynaptic Ca^{2+} influx and synaptic vesicle positioning near voltage-gated Ca^{2+} channels (Su *et al.*, 2012). Perturbations in either of these processes could alter the apparent Ca^{2+} cooperativity of neurotransmitter release (Dickman and Davis, 2009; Müller *et al.*, 2011). Therefore, our data should not be taken to mean altered function of the calcium sensor for neurotransmitter release (Petersen *et al.*, 1997; Pilgram *et al.*, 2011). Although, we cannot rule out this possibility here. These data may also indicate a Ca^{2+}-dependent reduction in the probability of neurotransmitter release at *cdk5*^{null} NMJs, as has been seen in *dysbindin* (Dickman and Davis, 2009) and *Rab3-GAP* (Müller *et al.*, 2011) mutants. Reduced release probabilities in *dysbindin* and *Rab3-GAP* mutants were correlated with impaired short-term and long-term homeostatic potentiation (Dickman and Davis, 2009; Müller *et al.*, 2011). Based on our evidence that short-term (Fig. 1) and long-term (Fig. 2) homeostatic potentiation are not compromised at *cdk5*^{null} NMJs, we can conclude that defects in either form of homeostatic potentiation are distinguishable from alterations in the Ca^{2+}-dependence of neurotransmitter release.

Cdk5 localizes to presynaptic nerve terminals of motor neurons at fly larval NMJs

Cdk5 controls the activity of presynaptic voltage-gated Ca^{2+} channels (Tomizawa *et al.*, 2002; Su *et al.*, 2012; Kim and Ryan, 2013), the kinetics of vesicle endocytosis (Tomizawa *et al.*, 2003), and the composition of synaptic vesicle pools (Kim and Ryan, 2010). These effects of Cdk5 on synaptic transmission are thought to depend upon the direct phosphorylation of target proteins, including P/Q-type Ca^{2+} channels (Tomizawa *et al.*, 2002), N-type Ca^{2+} channels (Su *et al.*, 2012; Kim and Ryan, 2013), dephosphins (Tomizawa *et al.*, 2003), synapsin (Verstegen *et al.*, 2014), and Munc18 (Shuang *et al.*,

1998; Fletcher *et al.*, 1999; Lilja *et al.*, 2004), by presynaptically localized Cdk5. Cdk5 is also implicated in synaptic vesicle recruitment to active zones (Locke *et al.*, 2006; Ou *et al.*, 2010; Park *et al.*, 2011) and NMJ morphogenesis (Kissler *et al.*, 2009). Likewise, our results show a contribution of Cdk5 to the Ca^{2+}-dependence of neurotransmitter release (Fig. 3A, C). These results strongly imply a role for Cdk5 in presynaptic nerve terminals.

Although Cdk5 has been investigated in the *Drosophila* nervous system (Connell-Crowley *et al.*, 2000; Kissler *et al.*, 2009; Trunova *et al.*, 2011), little is known about the subcellular localization of fly Cdk5. However, a previously described FLAG-tagged Cdk5 (Connell-Crowley *et al.*, 2000) was shown to localize to axonal lobes of γ-neurons in the *Drosophila* mushroom bodies (Trunova *et al.*, 2011), consistent with a function for Cdk5 in presynaptic nerve terminals. To verify that Cdk5 can localize to presynaptic terminals at the *Drosophila* NMJ, we drove this FLAG-tagged Cdk5 (Connell-Crowley *et al*., 2000; Trunova *et al.*, 2011) in motor neurons of wild type larvae using *ok371-Gal4* (Mahr and Aberle, 2006) and stained with an antibody against FLAG (Sigma-Aldrich). Cdk5-FLAG trafficked to the presynaptic nerve terminals at NMJs, where it formed puncta (Fig. 3B). These Cdk5-FLAG puncta were distributed throughout presynaptic boutons and showed little overlap with a synaptic vesicle marker, Synaptotagmin 1, which we co-stained with a previously described antibody (Littleton *et al.*, 1993; Yoshihara *et al.*, 2002) (Fig. 3B). These results suggest that Cdk5 is unlikely to reside on synaptic vesicles in presynaptic terminals. Based on these observations and aforementioned effects on neurotransmitter release (Fig. 3A, C), we conclude that Cdk5 acts presynaptically at the *Drosophila* NMJ.

Cdk5 alters synaptic transmission at physiological Ca^{2+} with repetitive stimulation

Numerous studies in both vertebrate (Tomizawa *et al.*, 2002; Su *et al.*, 2012; Kim and Ryan, 2013) and invertebrate (Locke *et al.*, 2006; Ou *et al.*, 2010; Park *et al.*, 2011) model systems point to a role for Cdk5 signaling in synaptic transmission. Thus, the lack of an obvious effect on synaptic transmission in *cdk5^{null}* mutant flies (Kissler *et al.*, 2009) is unexpected. With current-clamp recordings in a lower extracellular Ca^{2+} concentration (0.2 mM) than was used in the earliest study of *cdk5^{null}* mutant flies (Kissler *et al.*, 2009), we uncovered an effect of Cdk5 on neurotransmitter release (Fig. 3A, C). Nevertheless, our current-clamp recordings with single action potential stimulation in subphysiological Ca^{2+} concentrations (Stewart *et al.*, 1994) reveal insignificant (Fig. 1, 2) or modest (Fig. 3A, C) effects of *cdk5^{null}* on synaptic transmission and are, therefore, largely consistent with this previous report (Kissler *et al.*, 2009). Despite this dearth of evidence to support a role for *Drosophila* Cdk5 in synaptic transmission, it remains plausible that recordings under physiological conditions with trains of action potentials could uncover differences.

Accordingly, we reassessed synaptic transmission at *cdk5^{null}* NMJs by employing two-electrode voltage-clamp, as described (Müller et al., 2012). This method allowed us to record in a physiological Ca^{2+} concentration (1.5 mM) without confounding influences from membrane potential variations or nonlinear summation (Zhang and Stewart, 2010; Müller *et al.*, 2012). From our recordings, we found that mean initial excitatory junctional currents (EJCs) in 60-Hz stimulus trains were not significantly different at *cdk5^{null}* NMJs, compared to wild type (p = 0.46) (Fig. 4D-G). On the contrary, cumulative EJCs, which we calculated by “backextrapolation” (Schneggenburger *et al.*, 1999; Weyhersmüller *et al.*, 2011; Müller *et al.*, 2012), were significantly increased at *cdk5^{null}* NMJs, compared to

wild type ($p < 0.01$) (Fig. 4B, D, E). By dividing the mean cumulative EJC amplitude by the mean mEJP amplitude, acquired in current-clamp, we estimated RRP sizes at each NMJ (Weyhersmüller *et al.*, 2011; Müller *et al.*, 2012). The mean estimated RRP size at *cdk5*^{null} NMJs was 35.8% larger than wild type, albeit not significantly different ($p = 0.20$) (Fig. 4C). This difference in RRP sizes may be underestimated due to a slightly, but not significantly, increased mean mEJP amplitude in *cdk5*^{null} ($p = 0.12$) (Fig. 4A). We cannot determine from these data if Cdk5 influences recycling pool or resting pool sizes in flies, as it does in the hippocampus (Kim and Ryan, 2010). Regardless, our results show that the loss of Cdk5 at fly NMJs has no significant effects on RRP size or synaptic strength.

Given the enhancement of cumulative EJC amplitudes (Fig. 4B) at *cdk5*^{null} NMJs, the lack of an effect on initial EJC amplitudes (Fig. 4A) suggested an additional change in the mechanisms underlying synaptic transmission. For *cdk5*^{null} NMJs to exhibit a wild type synaptic strength, the significant increase in cumulative EJC amplitudes and strong trend toward an increase in RRP size would presumably be countered by a decrease in the probability of neurotransmitter release (del Castillo and Katz, 1954; Weyhersmüller *et al.*, 2011). To estimate the probability of release (P_{train}), we calculated the fraction of the RRP released by the first action potential in our 60-Hz trains, as previously defined (Schneggenburger *et al.*, 1999; Gaviño *et al.*, 2015). We determined the P_{train} at *cdk5*^{null} NMJs to be 0.28 ± 0.01 (SEM) (n = 16) and the P_{train} at wild type NMJs to be 0.38 ± 0.02 (SEM) (n = 9). This 27.4% difference in P_{train} values was significant ($p < 0.01$) and points to a lower release probability in *cdk5*^{null}. These data are consistent with effects of Cdk5 on presynaptic Ca^{2+} influx and synaptic vesicle docking at voltage-gated Ca^{2+} channels

(Su *et al.*, 2012). Moreover, these data are consistent with the reduced neurotransmitter release at *cdk5*^{null} NMJs, which we detected by lowering extracellular Ca^{2+} (Fig. 3A, C).

In addition to measuring synaptic strength, RRP size, and release probability at *cdk5*^{null} NMJs, we were able to more closely examine short-term plasticity with voltage-clamp (Weyhersmüller *et al.*, 2011; Müller *et al.*, 2012; Gaviño *et al.*, 2015). Challenging *cdk5*^{null} with thirty stimuli from 60-Hz trains showed no difference in synaptic depression over the first ten stimuli between wild type and *cdk5*^{null}, despite a strong trend ($p = 0.08$) (Fig. 4D-G). In contrast, *cdk5*^{null} mutants exhibited significantly enhanced depression at the ends ($EJC_{final}/EJC_{initial}$) of these high-frequency trains, when compared to wild type ($p < 0.01$) (Fig. 4G), such that the final average EJC in *cdk5*^{null} was 32.9% smaller than wild type (Fig. 4F). These results suggest an effect of Cdk5 extending beyond the RRP.

Importantly, neurotransmitter release at the end points of our trains is not due to release from the RRP, which is associated with depression prior to a plateau at steady-state (Dobrunz and Stevens, 1997; Schneggenburger *et al.*, 1999; Müller *et al.*, 2012). Instead, the enhanced steady-state depression in *cdk5*^{null} may be attributed to abnormal depletion of the reserve pool of synaptic vesicles, which maintains steady-state synaptic transmission (Murthy and Stevens, 1998; Gitler *et al.*, 2004). Supporting this hypothesis, inhibition of Cdk5 was shown to accelerate depletion of recycling pool synaptic vesicles, which consists of the RRP and reserve pool (Kim and Ryan, 2010). Moreover, this effect of Cdk5 on the composition of synaptic vesicle pools depended upon phosphorylation of synapsin (Verstegen *et al.*, 2014), which controls reserve pool size in mammals (Rosahl *et al.*, 1995; Gitler *et al.*, 2004) and flies (Akbergenova and Bykhovskaia, 2010; Denker

et al., 2011). Thus, our data provide evidence that Cdk5 regulates synaptic vesicle pool organization throughout evolution and has a potential to influence homeostatic plasticity.

Reevaluation of a role for Cdk5 in homeostatic potentiation at physiological Ca^{2+}

Through voltage-clamp recordings in physiological Ca^{2+} (Stewart *et al.*, 1994), we could more thoroughly investigate effects of Cdk5 signaling on homeostatic potentiation (Petersen *et al.*, 1997; Weyhersmüller *et al.*, 2011; Müller *et al.*, 2012). Because $cdk5^{null}$ mutants showed abnormalities in various parameters of baseline synaptic transmission (Fig. 4), a reevaluation of these mutants in the context of homeostatic potentiation may also illuminate previously unrecognized relationships between basal and compensatory mechanisms of neurotransmitter release. As previously described (Fig. 2), we tested the effects of Cdk5 ablation on synaptic homeostasis by recording from recombinant double mutants, which carried the $GluRIIA^{SP16}$ null mutation (Petersen *et al.*, 1997) and $cdk5^{null}$ (Kissler *et al.*, 2009). In double mutants and $GluRIIA^{SP16}$ controls, loss of GluRIIA led to 53.2% (n = 12) and 48.1% (n = 8) decreases in mean mEJP amplitudes, respectively ($p < 0.01$) (Fig. 4A). Yet, the mean initial EJC amplitudes from 60-Hz trains of thirty stimuli decreased by 4.8% in $cdk5^{null}$, $GluRIIA^{SP16}$ mutant recombinants to 249.4 ± 18.1 (SEM) nA (n = 12; $p = 0.55$) and by 17.0% in $GluRIIA^{SP16}$ controls to 203.9 ± 14.5 (SEM) nA (n = 8; $p = 0.10$). As a result, mean initial quantal contents increased by 93.7% in $cdk5^{null}$, $GluRIIA^{SP16}$ mutant recombinants to 705.5 ± 70.8 (SEM) (n = 12; $p < 0.01$) and 55.5% in $GluRIIA^{SP16}$ controls to 596.2 ± 62.5 (SEM) (n = 8; $p < 0.01$). Based on our findings, we conclude that Cdk5 is dispensable for homeostatic potentiation in physiological Ca^{2+}, as it is in low Ca^{2+} (Fig. 2). Our results strongly indicate a mechanistic difference between homeostatic potentiation and presynaptic scaling in hippocampi (Kim and Ryan, 2010).

Enlargement of the RRP was shown to underlie homeostatic potentiation at the *Drosophila* NMJ (Weyhersmüller *et al.*, 2011; Müller *et al.*, 2012). In accordance with these results, we determined that mean cumulative EJC amplitude was 12.6% larger in *GluRIIA*^{SP16} mutants, compared to wild type ($p = 0.32$) (Fig. 4B), and was concomitant with a 136.1% increase in mean estimated RRP size ($p < 0.01$) (Fig. 4C). However, it is unclear if homeostatic potentiation can maintain baseline cumulative EJC amplitudes in mutants with aberrant synaptic transmission, such as *cdk5*^{null}. Indeed, mean cumulative EJC amplitude in *cdk5*^{null}*, GluRIIA*^{SP16} double mutants was decreased by merely 16.8%, compared to *cdk5*^{null} single mutants, which was not significantly different ($p = 0.12$) (Fig. 4B). In addition, mean estimated RRP size was increased by 78.2% in double mutants, as above, which was significantly different from baseline (Fig. 4C). As the *cdk5*^{null} mean cumulative EJC was 48.7% larger than wild type ($p < 0.01$) (Fig. 4B, D, E), these results argue against a ceiling effect (Müller *et al.*, 2011), wherein homeostatic potentiation may fail to return muscle depolarization to a set point value that is significantly higher than in wild type. Furthermore, as *cdk5*^{null} mutants exhibited deficits in the probability of release and steady-state synaptic transmission (Fig. 4F, G), we can more clearly distinguish the mechanisms of homeostatic potentiation and basal neurotransmitter release (Goold and Davis, 2007; Dickman *et al.*, 2009). In conclusion, we find that homeostatic potentiation does not require Cdk5 activity at physiological Ca^{2+} with single or repetitive stimulation.

p35 is not essential for long-term homeostatic potentiation at physiological Ca^{2+}

To buttress our findings that Cdk5 contributes to neurotransmitter release, but is dispensable for homeostatic potentiation, we recorded from amorphic *p35*^{20C} (Connell-Crowley *et al.*, 2007) larval NMJs in voltage-clamp (Zhang and Stewart, 2010; Müller *et*

al., 2012) at physiological Ca^{2+} (Stewart *et al.*, 1994). From recordings in current-clamp, we had previously identified a substantial (41.8%; n = 14; $p < 0.01$) reduction in quantal size at $p35^{20C}$ mutant NMJs. Unexpectedly, we were unable to attribute this quantal size decrease to p35 loss, as the average mEJP amplitude in $p35^{20C}/Df$ was not significantly different from wild type (n = 15; $p = 0.21$) (Fig. 1A), and the expression of a well-studied *UAS-p35* construct (Connell-Crowley *et al.*, 2000; Trunova *et al.*, 2011) could not rescue the mutant phenotype. Nonetheless, we recorded from $p35^{20C}$ and $cdk5^{null}$ mutant NMJs in parallel and, consequently, have found notable similarities. We determined that mean initial EJC amplitude in 60-Hz stimulus trains was slightly decreased by 20.0% in $p35^{20C}$ to 196.6 ± 11.9 (SEM) nA, compared to wild type (n = 11; $p = 0.05$). This modest drop in synaptic strength was concomitant with a 69.0% increase in average quantal content to 648.1 ± 66.7 (SEM) (n = 11; $p < 0.01$). We also observed a 52.0% decrease in average quantal size, determined in current-clamp, which was significantly smaller than wild type (n = 11; $p < 0.01$) (Fig. 5A). Consistent with accurate homeostatic potentiation, we found that mean cumulative EJC amplitude at $p35^{20C}$ NMJs was not significantly different from wild type (n = 11; $p = 0.39$) (Fig. 5B), and that the average RRP size estimate in $p35^{20C}$ was 134.3% larger than wild type (n = 11; $p < 0.01$) (Fig. 5C). These results with $p35^{20C}$ are similar to data with $GluRIIA^{SP16}$ null mutants (Petersen *et al.*, 1997), which exhibited a 48.1% decrease in mean quantal size (n = 8; $p < 0.01$) (Fig. 5A), a 17.0% decrease in mean initial EJC amplitude (n = 8; $p = 0.10$), a 55.5% increase in mean quantal content (n = 8; $p < 0.01$), a 12.6% increase in mean cumulative EJC amplitude (n = 8; $p = 0.32$) (Fig. 5B), and a 136.1% increase in mean RRP size (n = 8; $p < 0.01$) (Fig. 5C), relative to wild type. Accordingly, our findings argue for a p35-independent expression of long-

term homeostatic potentiation at *p35*^{20C} null NMJs. In addition, our data confirm the lack of a requirement for Cdk5 signaling in homeostatic potentiation at the *Drosophila* NMJ.

p35 affects synaptic transmission at physiological Ca^{2+} with repetitive stimulation

Along with testing the effects of the Cdk5 activator, p35 (Lew *et al.*, 1994; Tsai *et al.*, 1994), in synaptic homeostasis (Petersen *et al.*, 1997; Frank *et al.*, 2006), we further assessed a role of Cdk5 signaling in short-term plasticity (Fig. 4F, G) by recording from *p35*^{20C} null larvae (Connell-Crowley *et al.*, 2007) in voltage-clamp (Weyhersmüller *et al.*, 2011; Müller *et al.*, 2012; Gaviño *et al.*, 2015). By evoking neurotransmitter release with thirty stimuli from 60-Hz trains, we calculated P_{train} as an estimate of release probability of the RRP (Schneggenburger *et al.*, 1999; Gaviño *et al.*, 2015) in *p35*^{20C} mutants. From this analysis, we determined the P_{train} at *p35*^{20C} NMJs to be 0.28 ± 0.01 (SEM) (n = 11). This P_{train} value in *p35*^{20C} was indistinguishable from the previously determined P_{train} of 0.28 ± 0.01 (SEM) (n = 16), which we measured in *cdk5*^{null}. This 27.7% decreased P_{train} value was significantly different from wild type ($p < 0.01$) and indicates a lower release probability in *p35*^{20C}. Although, we calculated P_{train} in *GluRIIA*^{SP16} mutants to be 0.31 ± 0.02 (SEM) (n = 8), which was not significantly different from *p35*^{20C} ($p = 0.31$). Hence, we cannot attribute the decreased release probability at *p35*^{20C} NMJs to the loss of p35, as this phenotype may be secondary to long-term homeostatic potentiation. Regardless, this 10.9% reduction in the *p35*^{20C} P_{train} value, compared to *GluRIIA*^{SP16}, is suggestive of a role for p35 in presynaptic release probability (Gaviño *et al.*, 2015). Additionally, these data are consistent with impaired neurotransmitter release in *cdk5*^{null} at low extracellular Ca^{2+} (Fig. 3A, C) and at physiological Ca^{2+} (Stewart *et al.*, 1994), as shown by the P_{train}.

Cdk5 signaling has been associated with the maintenance of the reserve pool of synaptic vesicles in the hippocampus (Kim and Ryan, 2010; Verstegen *et al.*, 2014). In line with these findings, we noted an enhancement of steady-state depression at $cdk5^{null}$ NMJs (Fig. 4F, G), which could be explained by enhanced depletion of the reserve pool (Murthy and Stevens, 1998; Gitler *et al.*, 2004; Verstegen *et al.*, 2014). In support of this hypothesis, $p35^{20C}$ null mutants exhibited significantly enhanced depression at the ends ($EJC_{final}/EJC_{initial}$) of our high-frequency (60-Hz) trains of thirty stimuli, compared to wild type ($p < 0.01$) (Fig. 5E), such that the final mean EJC in $p35^{20C}$ was 64.7% smaller than wild type (Fig. 5D). Unlike the aforementioned P_{train} reduction in $p35^{20C}$, this increase in steady-state depression is not attributable to an indirect effect of long-term homeostatic potentiation, as $p35^{20C}$ had significantly greater depression than $GluRIIA^{SP16}$ ($p < 0.01$) (Fig. 5D, E). Yet, it should be noted that $GluRIIA^{SP16}$ mutants also exhibited significantly enhanced depression at the ends ($EJC_{final}/EJC_{initial}$) of our stimulus trains, compared to wild type ($p = 0.03$), and probably point to an overestimation of the effects of $p35^{20C}$ on steady-state depression. Furthermore, depression over the first ten stimuli of the 60-Hz trains was also significantly increased in $p35^{20C}$ nulls, compared to wild type ($p < 0.01$) and $GluRIIA^{-}$ ($p < 0.01$) (Fig. 5D, E). These data suggest that p35 may contribute to the release dynamics of the RRP, which governs synaptic depression until the steady-state is met (Dobrunz and Stevens, 1997; Schneggenburger *et al.*, 1999; Müller *et al.*, 2012). However, this effect of p35 on short-term release dynamics may result from the addition of insignificant trends toward enhanced synaptic depression, which we saw at NMJs of $cdk5^{null}$ ($p = 0.08$) (Fig. 4G) and $GluRIIA^{SP16}$ ($p = 0.37$) (Fig. 5E) larvae. In summary, our

data regarding steady-state depression in *p35*^{20C} reinforces similar results from *cdk5*^{null} and further implicates Cdk5 signaling in the evolutionary conservation of reserve pools.

Effects of Cdk5 signaling on postsynaptic glutamate receptor composition in flies

While Cdk5 has been linked to a multitude of presynaptic signaling mechanisms (Tomizawa *et al.*, 2003; Su *et al.*, 2012; Kim and Ryan, 2013; Verstegen *et al.*, 2014), it can also signal postsynaptically (Hawasli *et al.*, 2007; Seeburg *et al.*, 2008; Bianchetta *et al.*, 2011; Lai *et al.*, 2012). Of particular importance here, Cdk5 was found to regulate AMPA receptor composition (Poore *et al.*, 2010), NMDA receptor degradation (Hawasli *et al.*, 2007), NMDA receptor-induced endocytosis of AMPA receptors (Bianchetta *et al*., 2011), and homeostatic AMPA receptor downscaling (Seeburg *et al.*, 2008), pointing to diverse effects on glutamate receptors at mammalian synapses. Likewise, Cdk5 and its activator, p35 (Lew *et al.*, 1994; Tsai *et al.*, 1994), control glutamate receptor trafficking in *C. elegans* (Juo *et al.*, 2007), suggesting an evolutionary conservation of postsynaptic Cdk5 activity. With the availability of amorphic *cdk5*^{null} (Kissler *et al.*, 2009) and *p35*^{20C} (Connell-Crowley *et al.*, 2007) mutants, we were able to further investigate postsynaptic effects of Cdk5 signaling on glutamate receptors by studying the *Drosophila* larval NMJ.

To examine glutamate receptor trafficking in the absence of Cdk5 signaling, we imaged the fly NMJs at muscles 6 and 7, from which our electrophysiological recordings were carried out, as well as NMJs at muscle 4. These NMJs possess “type I” synapses, which contain dense postsynaptic specializations with two kinds of glutamate receptors: GluRIIA-containing receptors and GluRIIB-containing receptors (Petersen *et al.*, 1997; Marrus *et al.*, 2004). As described (Heckscher *et al.*, 2007), we determined the levels of GluRIIA and GluRIIB at these type I synapses of *cdk5*^{null} and *p35*^{20C} mutants by staining

with previously characterized antibodies to each subunit (Marrus *et al.*, 2004). We found that muscle 6/7 NMJs in *cdk5*^{null} had a significant (24.2%) increase in GluRIIA levels, as compared to wild type ($p < 0.01$) (Fig. 6A, B, D). Likewise, *cdk5*^{null} muscle 4 NMJs had a significant (27.0%) increase in GluRIIA levels, compared to wild type ($p < 0.01$) (Fig. 6A, B, D). These enhanced GluRIIA levels in *cdk5*^{null} were countered by decreased GluRIIB levels at muscle 6/7 (15.1%) and muscle 4 (24.1%) ($p < 0.01$) (Fig. 6A, B, E), consistent with competition between GluRIIA and GluRIIB (Marrus *et al.*, 2004). Conversely, NMJs at muscle 6/7 in *p35*^{20C} showed a vast (67.5%) decrease in GluRIIA levels, compared to wild type ($p < 0.01$) (Fig. 6A, C, D). Muscle 4 NMJs in *p35*^{20C} also showed a substantial decrease (62.3%) in GluRIIA levels, compared to wild type ($p < 0.01$) (Fig. 6A, C, D). In addition, the reduced GluRIIA levels in *p35*^{20C} were concomitant with enhanced GluRIIB levels at muscle 6/7 (144.4%) and muscle 4 (130.2%) ($p < 0.01$) (Fig. 6A, C, E), thereby also consistent with competition between GluRIIA and GluRIIB (Marrus *et al.*, 2004). We also assayed levels of GluRIIC, which is interdependent with GluRIIA and GluRIIB for its postsynaptic recruitment (Marrus *et al.*, 2004; Qin *et al.*, 2005), in *cdk5*^{null} and *p35*^{20C}. At *cdk5*^{null} muscle 6/7 and muscle 4 NMJs, GluRIIC levels were comparable to wild type ($p = 0.62$ and $= 0.88$) (Fig. 6F). However, GluRIIC levels in *p35*^{20C} were significantly, albeit modestly, decreased by 16.8% and 15.5% at muscles 6/7 and 4, respectively ($p < 0.01$) (Fig. 6F). These results point to an evolutionarily conserved influence of Cdk5 signaling on the trafficking of glutamate receptors in *Drosophila*. Yet, these data are contradictory, as the loss of Cdk5 and the loss of p35 generally produce the same phenotype (Su and Tsai, 2011; Connell-Crowley *et al.*, 2007; Juo *et al.*, 2007; Trunova *et al.*, 2011). Hence, we have interpreted our data in the context of electrophysiological and genetic methods.

Overall, our analysis of glutamate receptor levels in *cdk5*^{null} and *p35*^{20C} amorphic mutants correlates with our electrophysiological recordings from NMJs at muscle 6. The moderate increase in GluRIIA levels at *cdk5*^{null} NMJs was accompanied by a moderate decrease in GluRIIB levels (Fig. 6). This altered composition of glutamate receptors did not produce a significant change in *cdk5*^{null}, as quantal sizes increased over wild type by merely 16.3% in low (0.4 mM) Ca^{2+} ($p = 0.33$) (Fig. 1A) and 18.0% in physiological (1.5 mM) Ca^{2+} ($p = 0.12$) (Fig. 4A). Overexpressing one copy of a *UAS-GluRIIA* transgene in muscle 6 was previously shown to increase quantal size by 35% (Petersen *et al.*, 1997). Moreover, quantal size was not significantly changed in *discs large* mutants, which lose GluRIIB-containing receptors from muscle 6 (Chen and Featherstone, 2005). Therefore, it is unlikely that quantal size would differ at *cdk5*^{null} NMJs in light of these observations.

In contrast, the robust decrease in GluRIIA abundance in *p35*^{20C} (Fig. 6A, C, D) correlates with 41.8% and 52.0% decreases in quantal size at 0.4 mM extracellular Ca^{2+} (0.47 ± 0.03 mV) and at 1.5 mM extracellular Ca^{2+} (Fig. 5A), compared to wild type ($p < 0.01$). The deficits in *p35*^{20C} quantal size are phenocopied by *GluRIIA*^{SP16} null mutants, which had similar quantal size deficits at these Ca^{2+} concentrations, as above (Fig. 2A, 5A). Nonetheless, it is unlikely that the quantal size deficits or by extension the GluRIIA decline in *p35*^{20C} can be attributed to the loss of p35, as previously discussed. Again, by placing the *p35*^{20C} allele over a deficiency uncovering the *p35* locus (Connell-Crowley *et al.*, 2007), we found that loss of p35 did not affect quantal size (Fig. 1A). Also in support of this hypothesis, expression of *UAS-p35* (Connell-Crowley *et al.*, 2000; Trunova *et al.*, 2011) did not rescue the quantal size impairments in *p35*^{20C}. Consequently, we interpret the selective loss of GluRIIA in *p35*^{20C} mutants as a secondary effect of an unidentified

genetic modifier. Notably, we were able to rescue the quantal size deficits in *p35^{20C}* by postsynaptic expression of *UAS-GluRIIA* with *BG57-Gal4* (Budnik *et al.*, 1996). Average mEJP amplitude in these rescued *p35^{20C}; BG57-Gal4/UAS-GluRIIA* larvae was 0.81 ± 0.07 (SEM) mV at 0.4 mM Ca^{2+}, which was not significantly different from wild type (n = 14; *p* = 1.00). Ultimately, these data buttress our conclusion that long-term homeostatic potentiation, which is commonly induced through the selective loss of GluRIIA (Petersen *et al.*, 1997; Frank *et al*., 2006), can be expressed independently of p35/Cdk5 signaling.

Effects of Cdk5 signaling on synaptic vesicle trafficking at the *Drosophila* NMJ

Cdk5 activity has been implicated in the recruitment of synaptic vesicle proteins to nerve terminals in *C. elegans* (Locke *et al.*, 2006; Ou *et al.*, 2010; Park *et al.*, 2011) and in mammals (Easley-Neal *et al.*, 2013). We were able to further assess the role of Cdk5 activity on synaptic vesicle trafficking by imaging *cdk5^{null}* (Kissler *et al.*, 2009) and *p35^{20C}* (Connell-Crowley *et al.*, 2007) mutant fly NMJs. According to standard methods (Heckscher *et al.*, 2007; Dickman *et al.*, 2009), we estimated levels of Synaptotagmin 1 (Syt1) and cysteine string protein (CSP) at muscle 6/7 NMJs. Levels of Syt1 (Fig. 7A, C, D) and CSP (Fig. 7B-D) did not differ between *cdk5^{null}* and wild type third instar larvae (*p* = 0.09 and 0.10). Likewise, CSP levels were also similar in *p35^{20C}* and wild type controls (*p* = 0.49) (Fig. 7B), whereas Syt1 levels were significantly, but marginally, increased in *p35^{20C}* (*p* = 0.01) (Fig. 7A). Our results are consistent with a hypothesis, in which Cdk5 signaling is not required for synaptic vesicle transport in all neurons, but is necessary in subsets (Locke *et al.*, 2006; Ou *et al.*, 2010; Park *et al.*, 2011). Furthermore, these data indicate that perturbations in neurotransmitter release at *cdk5^{null}* or *p35^{20C}* NMJs (Fig. 3-5) are not secondary consequences of general synaptic vesicle trafficking abnormalities.

Effects of Cdk5 signaling on the growth and elaboration of the *Drosophila* NMJ

An earlier study on *Drosophila* describes a role for Cdk5 in the morphogenesis of NMJs (Kissler *et al.*, 2009). In this study, $cdk5^{null}$ NMJs were found to have an increased number of boutons and a decreased density of active zones, which were visualized by antibody labeling against Bruchpilot (Brp; nc82) (Kittel *et al.*, 2006; Wagh *et al.*, 2006), at muscle 4 (Kissler *et al.*, 2009). The decreased active zone density in $cdk5^{null}$ mutants was suggested to arise from a compensatory mechanism, which offset increased NMJ growth (Kissler *et al.*, 2009). Despite observing no significant changes in basal synaptic transmission at muscle 6 NMJs of $cdk5^{null}$ larvae, no quantification of the morphology of muscle 6 NMJs was reported (Kissler *et al.*, 2009). Hence, the correlation between NMJ morphology and synaptic transmission in $cdk5^{null}$ is difficult to interpret from such results alone. Also, it is unclear if p35, an evolutionarily conserved activator of Cdk5 (Lew *et al.*, 1994; Tsai *et al.*, 1994; Connell-Crowley *et al.*, 2007), controls Cdk5 during NMJ growth.

To clarify our understanding of Cdk5 activity in neurotransmitter release and NMJ morphogenesis, we imaged the NMJs at muscle 4 and muscle 6/7 of $cdk5^{null}$ (Kissler *et al.*, 2009) and $p35^{20C}$ (Connell-Crowley *et al.*, 2007) mutants. Consistent with the earlier study (Kissler *et al.*, 2009), we found that the average bouton number at $cdk5^{null}$ muscle 4 NMJs was 67.7% larger than wild type ($p < 0.01$) (Fig. 8A, B, D). We also determined that the average bouton number at $p35^{20C}$ muscle 4 NMJs was 44.9% larger, compared to wild type ($p < 0.01$) (Fig. 8A, C, D), thereby indicating dependence of Cdk5 for p35 in NMJ growth. Upon investigating muscle 6/7 NMJs, however, we observed milder effects of Cdk5 on growth. The average bouton number at muscle 6/7 NMJs was merely 26.7% larger in $cdk5^{null}$ ($p < 0.05$) (Fig. 8A, B, D) and just trended toward significance in $p35^{20C}$

(p = 0.17) (Fig. 8A, C, D), compared to wild type. These data imply that Cdk5 signaling plays a more significant role in the growth of subsets of NMJs and may not act globally.

To assess whether Cdk5-dependent changes in bouton numbers were correlated with changes in the distribution of active zones, we quantified nc82 puncta numbers and densities in Cdk5 signaling mutants. Similarly consistent with the earlier report (Kissler *et al.*, 2009), the average active zone (nc82) number and density at muscle 4 NMJs in $cdk5^{null}$ were 12.2% larger (Fig. 8E) ($p < 0.05$) and 26.7% smaller (Fig. 8F) ($p < 0.01$), respectively, relative to wild type. Likewise, average nc82 number and density at $p35^{20C}$ muscle 4 NMJs were 20.1% larger (Fig. 8E) ($p < 0.01$) and 6.5% smaller (Fig. 8F) ($p < 0.01$), respectively, compared to wild type. Loss of Cdk5 signaling had similar effects on active zone distribution at muscle 6/7 NMJs, as average nc82 number and density were 7.3% (Fig. 8E) ($p = 0.35$) and 22.6% smaller (Fig. 8F) ($p < 0.01$) in $cdk5^{null}$ mutants and 3.0% larger (Fig. 8E) ($p = 0.72$) and 10.3% smaller (Fig. 8F) ($p < 0.01$) in $p35^{20C}$ nulls, compared to wild type. Our findings are in accordance with a current model, wherein the loss of Cdk5 signaling leads to excessive NMJ elaboration and compensatory reduction of active zone density to preserve a set point active zone number (Kissler *et al.*, 2009).

Despite the significant and inverse alterations in bouton number and active zone density at Cdk5-deficient NMJs, it should be noted that Cdk5 is implicated in aspects of synaptogenesis in *C. elegans* (Locke *et al.*, 2006; Ou *et al.*, 2010; Park *et al.*, 2011) and mammalian (Samuels *et al.*, 2007; Easley-Neal *et al.*, 2013) nervous systems. Hence, it remains formally possible that the aforementioned inverse changes in NMJ morphology of $cdk5^{null}$ (Kissler *et al.*, 2009) and $p35^{20C}$ (Connell-Crowley *et al.*, 2007) mutants do not result from a compensatory mechanism, but are simply a coincidence of opposing Cdk5

activities. Yet, in an earlier study of a hypomorphic *fasciclin II* allele, *FasII*^{e86} muscle 6/7 NMJs had 50% more boutons than wild type, but had no apparent difference in synaptic strength (Schuster *et al.*, 1996). The failure of elevated bouton number to concomitantly enhance synaptic strength at *FasII*^{e86} NMJs was linked to a compensatory redistribution of active zones throughout the larger NMJs (Schuster *et al.*, 1996; Davis and Goodman, 1998). Accordingly, it is plausible that a similar or identical form of presynaptic structural plasticity is expressed in these null Cdk5 signaling mutants and in *FasII*^{e86} mutants. This hypothesis is supported by evidence that either pharmacologic (Prithviraj *et al.*, 2012) or genetic disruption of Cdk5 signaling altered the localization of FasII in *Drosophila* axons (Trunova *et al.*, 2011). Our data can also be explained by expression of a target-specific form of homeostatic plasticity, in which muscle hyperinnervation led to a compensatory decrease in neurotransmitter release per bouton at NMJs (Davis and Goodman, 1998).

By extension from these (Fig. 8) and other data (Fig. 1, 2, 4, 5), we have arrived at three notable conclusions. First, these data imply that short-term and long-term forms of homeostatic potentiation are not impaired by enhanced NMJ elaboration or reduced active zone density. Second, these data argue for the existence of distinct homeostatic regulatory mechanisms, which act to inhibit neurotransmitter release at hyperinnervated muscles (Schuster *et al.*, 1996; Davis and Goodman, 1998; Kissler *et al.*, 2009) without interfering with mechanisms underlying homeostatic potentiation at the *Drosophila* NMJ. Third, our observation that nc82 puncta numbers were comparable to wild type at Cdk5-deficient muscle 6/7 NMJs (Fig. 8) is consistent with estimated RRP sizes from voltage-clamp recordings (Fig. 4C) and suggests that the number of release-ready vesicles per active zone at fly NMJs may be maintained at a set point under physiological conditions.

Effects of Cdk5 signaling on the structure of active zones at the *Drosophila* NMJ

At the *Drosophila* NMJ, decreases in the number and density of active zones has been correlated with ultrastructural changes in the morphology of active zones (Graf *et al.*, 2009). Yet, these NMJ growth-related parameters are not always correlated with the active zone structure (Liu *et al.*, 2011). To determine whether Cdk5 signaling influences active zone structure, in addition to NMJ morphology (Fig. 8), we carried out structured illumination microscopy (SIM) to examine nc82 puncta in boutons at muscles 6/7 and 4 of $cdk5^{null}$ (Kissler *et al.*, 2009) and $p35^{20C}$ (Connell-Crowley *et al.*, 2007) mutants. With SIM, nc82-labeled Brp appears as rings, instead of the spots observed in deconvolution microscopy, at planar active zones (Weyhersmüller *et al.*, 2011; Müller *et al.*, 2012). We measured the diameters of planar Brp rings in null Cdk5 signaling third instar larvae, as previously described (Müller *et al.*, 2012). Average Brp ring diameters at $cdk5^{null}$ muscle 6/7 and 4 NMJs differed slightly from wild type, when computed as the diameter at half-maximum ($p = 0.05$ and $= 0.03$) (Fig. 9D, E, I) or as the distance between two peaks ($p = 0.06$ and $= 0.02$) (Fig. 9G, H) of fluorescence intensity line profiles. Likewise, average Brp ring diameter at $p35^{20C}$ muscle 4 NMJs was significantly increased, relative to wild type, when calculated as diameter at half-maximum (Fig. 9F, I) ($p < 0.01$) or as peak-to-peak diameter ($p < 0.01$) (Fig. 9H). Conversely, the average Brp ring diameter at $p35^{20C}$ muscle 6/7 NMJs was indistinguishable from wild type, when computed in either way ($p = 0.87$ and $= 0.51$) (Fig. 9F, H, I). These results are consistent with only modest effects, if any, of p35/Cdk5 signaling on the morphology of active zones at the *Drosophila* NMJ.

Despite statistically significant differences, mean active zone diameters of $cdk5^{null}$ mutants were only 6-7% different from wild type. Furthermore, $p35^{20C}$ null mutant active

zone diameters were only 1-8% different from wild type. Our findings suggest that Cdk5 has no more than a marginal influence on active zone morphology, despite alterations in active zone density. Supporting this hypothesis, we examined in parallel and previously reported that the mean Brp ring diameter was not altered in mutants lacking RIM (Müller *et al.*, 2012), which was found to interact with Cdk5 in synaptic vesicle docking at active zones (Su *et al.*, 2012). Moreover, enlargement of Brp rings has been directly correlated with an increased probability of neurotransmitter release (Graf *et al.*, 2009; Peled and Isacoff, 2011), which is in opposition to the reduced probability of release (P_{train}) that we demonstrated at $cdk5^{null}$ and $p35^{20C}$ NMJs (Fig. 4, 5). Therefore, we conclude that Brp is not redistributed into fewer and larger puncta (Graf *et al.*, 2009) in the absence of Cdk5.

Effects of Cdk5 on synaptic Fasciclin II abundance at the *Drosophila* larval NMJ

NMJ growth in flies is regulated by Fasciclin II (FasII), an ortholog of Neural Cell Adhesion Molecule (NCAM) (Schuster *et al.*, 1996; Stewart *et al.*, 1996). Reduction of FasII expression by 50% led to a roughly 50% increase in the number of boutons at the *Drosophila* larval NMJ (Schuster *et al.*, 1996). Because we (Fig. 8) and others (Kissler *et al.*, 2009) noted a similar degree of NMJ overgrowth in $cdk5^{null}$ mutants, we asked if synaptic levels of FasII are affected by the loss of Cdk5 signaling. By using a previously characterized antibody (Van Vactor *et al.*, 1993), we measured synaptic FasII levels at $cdk5^{null}$ NMJs and observed a 36.1% reduction, relative to wild type ($n = 21$; $p < 0.01$). Therefore, our data suggest that the NMJ overgrowth in $cdk5^{null}$ mutants is attributable to decreased abundance of synaptic FasII. Moreover, loss of synaptic FasII was shown to induce a homeostatic decrease in active zone density to counteract NMJ overgrowth (Schuster *et al.*, 1996), which may also occur in $cdk5^{null}$ (Kissler *et al.*, 2006). Based on

these findings and others, which link Cdk5 to the neuronal distribution of FasII (Trunova *et al.*, 2011; Prithviraj *et al.*, 2012), we hypothesize that a FasII-associated homeostat is activated at the *Drosophila* NMJ in the absence of Cdk5 signaling. Moreover, this FasII-associated homeostat must be distinct from the GluRIIA-dependent homeostat, which is induced by decreased sensitivity to glutamate (Petersen *et al.*, 1997; Frank *et al.*, 2006).

Effects of acute Cdk5 inhibition on neurotransmitter release at physiological Ca^{2+}

Acute inhibition of Cdk5 has been shown to stimulate neurotransmitter release by increasing the number of recycling pool synaptic vesicles (Kim and Ryan, 2010) and the presynaptic influx of Ca^{2+} following action potentials (Kim and Ryan, 2013). The removal of Cdk5 activity pharmacologically was also found to functionally unsilence synapses in response to tetrodotoxin-dependent neural activity blockade (Kim and Ryan, 2010; Mitra *et al.*, 2011). Given some effects of Cdk5 signaling on the development of NMJs (Fig. 6-9), as well as some reservations about the specificity of common Cdk5 inhibitors (Yan *et al.*, 2002; Mitra *et al.*, 2011; Yazawa *et al.*, 2011), we employed an alternative approach to investigate acute effects of Cdk5 signaling on neurotransmitter release at the fly NMJ.

A chemical-genetic approach to inhibit protein kinases (Shah *et al.*, 1997; Bishop *et al.*, 2000) has been used to elucidate numerous signaling mechanisms in the nervous system (Choi *et al.*, 2008; Yoshii *et al.*, 2008; Ultanir *et al.*, 2012; Friedel *et al.*, 2015). In this tradition, we genetically engineered *Drosophila* Cdk5 to be acutely inactivated by an ATP analog, which is not recognized by endogenous protein kinases (Shah *et al.*, 1997; Ultanir *et al.*, 2012). To create this analog-sensitive Cdk5, we mutated an evolutionarily conserved phenylalanine residue at position 80 to glycine, as described (Kraybill *et al.*, 2002; Merrick *et al.*, 2011; Horiuchi *et al.*, 2012). We expressed this transgene, which

we placed under control of an upstream activation sequence (UAS), in *cdk5*^{null} (Kissler *et al.*, 2009) neurons with *elav*^{c155}*-Gal4* (Lin and Goodman, 1994). Subsequently, we inhibited Cdk5 in these "*cdk5*^{AS}" mutants by bath applying 1-NM-PP1 (100 μM; Kevan Shokat lab), an ATP analog that is commonly utilized to inhibit analog-sensitive cyclin-dependent kinases (Ubersax *et al.*, 2003; Horiuchi *et al.*, 2012; Gravells *et al.*, 2013) (Methods). We then recorded from *cdk5*^{AS} muscle 6 NMJs in the presence of 1-NM-PP1 (100 μM) with two-electrode voltage-clamp (Müller et al., 2012). As discussed, voltage-clamp allowed us to record in physiological (1.5 mM) extracellular Ca^{2+} (Stewart *et al.*, 1994) with repetitive stimulation, while avoiding the confounds of membrane potential differences and nonlinear summation (Zhang and Stewart, 2010; Müller *et al.*, 2012).

For our analysis of the acute effects of Cdk5 signaling on functional properties of the *Drosophila* NMJ, we first considered baseline synaptic transmission. From voltage-clamp recordings in *cdk5*^{AS} transgenic larvae, we found that mean initial EJC amplitude in 60-Hz stimulus trains were not significantly different, compared to wild type ($p = 0.11$) (Fig. 10D-G). Conversely, mean cumulative EJC amplitude was significantly increased at *cdk5*^{AS} NMJs, compared to wild type ($p < 0.01$) (Fig. 10B, D, E). By dividing the mean cumulative EJC amplitude by the mean mEJP amplitude, acquired in current-clamp, we estimated RRP sizes at each NMJ (Weyhersmüller *et al.*, 2011; Müller *et al.*, 2012). The mean estimated RRP size at *cdk5*^{AS} NMJs was 56.7% larger than wild type, but was not significantly different ($p = 0.07$) (Fig. 10C). The difference in estimated RRP size may be underestimated due to a slightly, but not significantly, increased mean mEJP amplitude in *cdk5*^{null} ($p = 0.35$) (Fig. 10A). These data demonstrate that *cdk5*^{AS} is strikingly similar to *cdk5*^{null}, which also had a wild type mean mEJP amplitude (Fig. 4A), mean initial EJC

amplitude (Fig. 4D-G), and mean estimated RRP size (Fig. 4C), but had an abnormally and significantly larger mean cumulative EJC amplitude (Fig. 4B, D, E). Thus, the acute and chronic loss of Cdk5 signaling has similar effects on baseline synaptic transmission.

The chronic loss of Cdk5 signaling in amorphic *cdk5*^{null} mutants also reduced the probability of neurotransmitter release, as estimated by the P_{train} (Schneggenburger *et al.*, 1999; Gaviño *et al.*, 2015). Accordingly, we asked if the acute loss of Cdk5 signaling in *cdk5*^{AS} mutants, treated with 1-NM-PP1, similarly influenced release probability. We determined the P_{train} at *cdk5*^{AS} NMJs to be 0.28 ± 0.01 (SEM) (n = 13) and the P_{train} at wild type NMJs to be 0.38 ± 0.02 (SEM) (n = 9). This P_{train} value in *cdk5*^{AS} was identical to the previously determined P_{train} values of 0.28 ± 0.01 (SEM) (n = 16) and 0.28 ± 0.01 (SEM) (n = 11), which were obtained from *cdk5*^{null} and *p35*^{20C} NMJs, respectively. This 26.3% difference in P_{train} values was significant ($p < 0.01$) and indicates a lower release probability upon acute inhibition of Cdk5. These results suggest that the effects of Cdk5 on presynaptic Ca^{2+} influx and synaptic vesicle docking at voltage-gated Ca^{2+} channels (Su *et al.*, 2012), which may underlie the decreased release probability in *cdk5*^{AS} (Müller *et al.*, 2011), are likely independent of a developmental requirement for Cdk5 signaling.

We previously described effects of chronic Cdk5 removal on short-term plasticity (Fig. 4D-G). Hence, we asked if acute removal of Cdk5 in *cdk5*^{AS} mutants, treated with 1-NM-PP1, also altered short-term plasticity. Challenging *cdk5*^{AS} with thirty stimuli from 60-Hz trains showed no change in synaptic depression over the first ten stimuli between wild type and *cdk5*^{AS} ($p = 0.58$) (Fig. 10D-G). On the contrary, *cdk5*^{AS} mutants exhibited significantly enhanced depression at the ends ($EJC_{final}/EJC_{initial}$) of these high-frequency trains, as compared to wild type ($p = 0.02$) (Fig. 10G). The final average EJC in *cdk5*^{AS}

was 9.0% smaller than wild type, which was not a significant difference (p = 0.47) (Fig. 10F). Synaptic depression prior to the steady-state is associated with release from the RRP (Dobrunz and Stevens, 1997; Schneggenburger *et al.*, 1999; Müller *et al.*, 2012), whereas steady-state depression results from depletion of the reserve pool of synaptic vesicles (Murthy and Stevens, 1998; Gitler *et al.*, 2004). As Cdk5 was implicated in the control of reserve pool size (Kim and Ryan, 2010; Verstegen *et al.*, 2014), we attributed an enhancement of steady-state depression in *cdk5*^{null} (Fig. 4D-G) and *p35*^{20C} (Fig. 5D, E) mutants to an abnormal depletion of the reserve pool. From our recordings in *cdk5*^{AS} mutants, we can separate the effects of Cdk5 signaling on development from its effects on the composition of synaptic vesicle pools, which seem to be more acute. Our results are consistent with those of earlier studies (Kim and Ryan, 2010; Verstegen *et al.*, 2014) and add more evidence that Cdk5 is a conserved regulator of neurotransmitter release.

Effects of acute Cdk5 inhibition on homeostatic potentiation at physiological Ca^{2+}

Acute loss of Cdk5 signaling was shown to disrupt the expression of presynaptic homeostatic scaling in the hippocampus (Kim and Ryan, 2010; Verstegen *et al.*, 2014). We have provided evidence that this hippocampal form of homeostatic plasticity differs molecularly from homeostatic potentiation at the *Drosophila* NMJ via chronic removal of Cdk5 signaling with amorphic alleles: *cdk5*^{null} (Kissler *et al.*, 2009) and *p35*^{20C} (Connell-Crowley *et al.*, 2007) (Fig. 1, 2, 4, 5). Yet, it is formally possible that the chronic loss of Cdk5 signaling is offset by developmental compensation (Marek and Davis, 2000), as is seen with other kinase signaling pathways (Madhani and Fink, 1998). Consequently, we asked if acute loss of Cdk5 signaling via *cdk5*^{AS} interferes with homeostatic potentiation.

To investigate the effects of acute Cdk5 removal on homeostatic potentiation, we recorded from *cdk5*^{AS} muscle 6 NMJs in the presence of 1-NM-PP1 (100 μM) with two-electrode voltage-clamp in physiological (1.5 mM) Ca^{2+} (Stewart *et al.*, 1994) with high-frequency (60-Hz) repetitive stimulation (Müller et al., 2012). We induced homeostatic potentiation by bath applying PhTx (Frank *et al.*, 2006) ten minutes after treatment with 1-NM-PP1 (Methods). This step was taken to ensure that analog-sensitive Cdk5 would be inhibited at the earliest stages of homeostatic potentiation. Furthermore, recording in 1-NM-PP1 ensured that analog-sensitive Cdk5 would continue to be inhibited after the induction of homeostatic potentiation, thus allowing us to test a role for Cdk5 signaling in the sustained expression of homeostasis. We found that PhTx treatment reduced the mean mEJP amplitude, measured in current-clamp, by 53.2% (n = 7) in *cdk5*^{AS} and by 55.9% (n = 8) in wild type controls ($p < 0.01$) (Fig. 10A), compared to baseline values in the absence of PhTx (n = 13 and 9, respectively). Consistent with accurate short-term homeostatic potentiation, mean initial EJC amplitudes from 60-Hz trains of thirty stimuli decreased by 0.1% in *cdk5*^{AS} to 293.6 ± 24.6 (SEM) nA (n = 7; $p = 1.00$) and by 4.8% in wild type controls to 234.0 ± 18.1 (SEM) nA (n = 8; $p = 0.66$), as above. Hence, average initial quantal contents increased by 90.9% in *cdk5*^{AS} to 808.3 ± 62.8 (SEM) (n = 7; $p < 0.01$) and 105.1% in wild type to 786.5 ± 77.3 (SEM) (n = 8; $p < 0.01$), as above. Upon considering the effects of acute Cdk5 loss on homeostatic potentiation during repetitive stimulation, mean cumulative EJC amplitudes decreased by 10.5% in *cdk5*^{AS} (n = 7; $p = 0.33$) and increased by 26.4% in wild type (n = 8; $p = 0.06$), when compared to baseline (Fig. 10B). Accordingly, average estimated RRP sizes increased by 61.6% in *cdk5*^{AS} (n = 7; $p < 0.01$) and by 170.9% in wild type (n = 8; $p < 0.01$) over the baselines (Fig. 10C).

Our findings indicate that the acute loss, like the chronic loss (Fig. 1, 2, 4, 5), of Cdk5 signaling does not impair homeostatic potentiation, even under physiological (1.5 mM Ca^{2+}) conditions with repetitive stimulation. Our results also provide more evidence that acute perturbations in neurotransmitter release (Fig. 10) do not necessarily interfere with homeostatic potentiation, consistent with other discoveries (Goold and Davis, 2007; Dickman *et al.*, 2009). Perhaps most notably, the abnormal steady-state depression and enhanced depletion of the reserve pool (Kim and Ryan, 2010; Verstegen *et al.*, 2014) at *cdk5*^{AS} NMJs did not disrupt homeostatic potentiation. As homeostatic potentiation also occurred in amorphic Cdk5 signaling mutants with heightened steady-state depression (Fig. 4D-G, 5D, E), we suggest that homeostatic potentiation and control of reserve pool size, which can be considered homeostatic, differ in their requirements for Cdk5 activity.

Discussion

Signaling through the proline-directed serine/threonine kinase, Cdk5, has been associated with a multitude of functional and developmental processes in the nervous system (Su and Tsai, 2011). These Cdk5-dependent processes include, but are unlikely to be restricted to, acute presynaptic (Tomizawa *et al.*, 2002; Su *et al.*, 2012; Kim and Ryan, 2013; Verstegen *et al.*, 2014) and postsynaptic (Hawasli *et al.*, 2007; Seeburg *et al.*, 2008; Bianchetta *et al.*, 2011; Lai *et al.*, 2012) mechanisms of synaptic transmission, as well as developmental control of neuronal migration (Ohshima *et al.*, 1996; Chae *et al.*, 1997), aging (Patrick *et al.*, 1999; Lin *et al.*, 2007; Trunova and Giniger, 2012), axon guidance (Kwon *et al.*, 1999; Ledda *et al.*, 2000; Connell-Crowley *et al.*, 2000), synapse morphogenesis (Kissler *et al.*, 2009), and synaptogenesis from invertebrates (Locke *et al.*, 2006; Juo *et al.*, 2007; Ou *et al.*, 2010; Park *et al.*, 2011) to vertebrates (Samuels *et al.*, 2007; Easley-Neal *et al.*, 2013). Cdk5 has also been found to signal in non-neuronal cells, such as adipocytes (Lalioti *et al.*, 2009; Choi *et al.*, 2010; Choi *et al.*, 2011; Banks *et al.*, 2015), pancreatic beta-cells (Lilja *et al.*, 2001; Lilja *et al.*, 2004; Wei *et al.*, 2005), endothelial cells (Liebl *et al.*, 2010; Liebl *et al.*, 2015), and various kinds of cancer cells (Liang *et al.*, 2013; Pozo *et al.*, 2013; Tripathi *et al.*, 2014; Yu *et al.*, 2015). Accordingly, the continued investigation of Cdk5 signaling could have myriad implications for human health and disease and may shed light on evolutionarily conserved biological principles.

Here, we build upon prior reports (Connell-Crowley *et al.*, 2000; Connell-Crowley *et al.*, 2007; Lin *et al.*, 2007; Kissler *et al.*, 2009; Trunova *et al.*, 2011) to elucidate a role for Cdk5 signaling at the fly NMJ, for which structural and functional characteristics are well-described (Atwood *et al.*, 1993; Jan and Jan, 1976). The genetic analysis of Cdk5 signaling is simplified by the use of *Drosophila*, which encodes only one Cdk5 activator,

p35 (Connell-Crowley, *et al.*, 2000; Trunova and Giniger, 2012), unlike in mammalian models (Zheng *et al.*, 1998; Ko *et al*., 2001). Moreover, null alleles of *cdk5* (Kissler *et al.*, 2009) and *p35* (Connell-Crowley *et al.*, 2007), along with a well-studied dominant-negative Cdk5 (Connell-Crowley *et al.*, 2000), have been generated in *Drosophila*. As in mammals (Lew *et al.*, 1994; Tsai *et al.*, 1994), p35 expression is also neural-specific in *Drosophila* (Connell-Crowley *et al.*, 2000; Robinson *et al.*, 2013). By taking advantage of this existing knowledge, we have uncovered roles for Cdk5 signaling in regulating the apparent Ca^{2+} cooperativity of neurotransmitter release, probability of neurotransmitter release at physiological Ca^{2+}, and steady-state synaptic transmission at the *Drosophila* NMJ. Yet, we found no evidence to support a function for Cdk5 signaling in short-term (Frank *et al.*, 2006) or long-term (Petersen *et al.*, 1997) homeostatic potentiation, RRP size modulation (Schneggenburger *et al.*, 1999; Weyhersmüller *et al.*, 2011; Müller *et al.*, 2012), or synaptic vesicle trafficking (Locke *et al.*, 2006; Ou *et al.*, 2010; Park *et al.*, 2011). We have also replicated a study of NMJ morphology in $cdk5^{null}$ mutants (Kissler *et al.*, 2009) and examined null $p35^{20C}$ mutants (Connell-Crowley *et al.*, 2007) in parallel.

As first noted in a previous study of $cdk5^{null}$ mutants (Kissler *et al.*, 2009), genetic ablation of Cdk5 has no substantial effect on synaptic transmission at *Drosophila* NMJs in subphysiological Ca^{2+} (Stewart *et al.*, 1994) with low-frequency stimulation. However, we discovered a significant impairment of neurotransmitter release at $cdk5^{null}$ NMJs from recordings in low (0.2 mM) extracellular Ca^{2+}, which yielded a shift in the apparent Ca^{2+} cooperativity of neurotransmitter release. Likewise, we discovered that the loss of Cdk5 in both null mutants, $cdk5^{null}$ (Kissler *et al.*, 2009) and $p35^{20C}$ mutants (Connell-Crowley *et al.*, 2007), led to decreased neurotransmitter release probabilities from recordings in physiological (1.5 mM) extracellular Ca^{2+} (Stewart *et al.*, 1994) with high-frequency (60-

Hz) stimulation (Weyhersmüller *et al.*, 2011; Müller *et al.*, 2012; Gaviño *et al.*, 2015). We hypothesize that these changes in the Ca^{2+}-dependence of neurotransmitter release are due to direct effects of Cdk5 signaling on presynaptic voltage-gated Ca^{2+} channels or to indirect effects of Cdk5 signaling on the docking of synaptic vesicles near voltage-gated Ca^{2+} channels, as reported in the mouse hippocampus (Su *et al.*, 2012). Hence, despite Cdk5 being largely dispensable for synaptic transmission at the *Drosophila* NMJ (Kissler *et al.*, 2009), we suggest that Cdk5 influences neurotransmitter release under conditions of very low release probability and in physiological conditions with repetitive stimulation. We also provide evidence for presynaptic Cdk5 localization, consistent with these roles.

While more accurately simulating a physiological condition, recordings in voltage-clamp (Zhang and Stewart, 2010; Müller *et al.*, 2012) with physiological Ca^{2+} (Stewart *et al.*, 1994) and high-frequency (60-Hz) stimulation allows one to estimate sizes of distinct pools of synaptic vesicles (Weyhersmüller *et al.*, 2011; Müller *et al.*, 2012; Gaviño *et al.*, 2015). Two synaptic vesicle pools, the RRP and reserve pool, underlie neurotransmitter release at the fly NMJ (Kuromi and Kidokoro, 1998; Verstreken *et al.*, 2005). Equivalent "recycling" pools of synaptic vesicles have been defined in mammalian systems (Murthy and Stevens, 1998; Gitler *et al.*, 2004; Kim and Ryan, 2010; Verstegen *et al.*, 2014). In *Drosophila* and mammals, neurotransmitters are generally released from the RRP. Yet, high-frequency stimulation depletes the RRP and unlocks neurotransmitter release from the reserve pool. A phosphorylation target of Cdk5, synapsin (Matsubara *et al.*, 1996), is important for regulating reserve pool size in *Drosophila* (Akbergenova and Bykhovskaia, 2010; Denker *et al.*, 2011) and mammals (Rosahl *et al.*, 1995; Gitler *et al.*, 2004). A role for Cdk5 signaling in regulation of the reserve pool is implied by studies at hippocampal synapses, which demonstrate that acute inhibition of Cdk5 enhances the recycling pool

(the RRP and reserve pool) (Kim and Ryan, 2010) via loss of synapsin phosphorylation (Verstegen *et al.*, 2014). From our voltage-clamp recordings, we determined that loss of Cdk5 had no significant effect on the RRP size at the *Drosophila* NMJ. Conversely, the removal of Cdk5 or p35 led to a significant defect in steady-state synaptic transmission, consistent with abnormal depletion of the reserve pool. Provided these data, we suggest that Cdk5 plays an evolutionarily conserved role in the maintenance of the reserve pool.

It is important to note that our observed effects of Cdk5 signaling on organization of synaptic vesicle pools at the *Drosophila* NMJ may be counter to expectations, based on earlier reports in mammals. The acute inhibition of Cdk5 signaling correlated with an enhancement of the recycling pool size at hippocampal synapses (Kim and Ryan, 2010; Verstegen *et al.*, 2014). Because the recycling pool includes the reserve pool, as well as the RRP, one might have predicted an enlargement of both pools in Cdk5-deficient flies. Although we saw a trend toward a larger RRP size at $cdk5^{null}$ NMJs, our data indicate a relative decrease in the reserve pool size. We also described a similar result from acute inhibition of ATP analog-sensitive Cdk5 (Shah *et al.*, 1997; Bishop *et al.*, 2000; Kraybill *et al.*, 2002; Merrick *et al.*, 2011). Hence, recycling pool size is apparently not enhanced by the loss, chronic or acute, of Cdk5 signaling at fly NMJs. Regardless, it is tempting to speculate that the altered composition of synaptic vesicle pools at Cdk5-deficient NMJs is in some way related to the synapsin-dependent effects of Cdk5 signaling in mammals (Kim and Ryan, 2010; Verstegen *et al.*, 2014). In line with this hypothesis, a single gene encodes various synapsin isoforms in *Drosophila* (Klagges *et al.*, 1996). Furthermore, a mass spectrometric analysis of these fly synapsin isoforms identified seven unique sites of phosphorylation, two of which may be targeted by Cdk5 (Nuwal *et al.*, 2011). A future investigation of these synapsin isoforms in the context of Cdk5 signaling may clarify the

relationship between these factors and the regulation of synaptic vesicle pool dynamics.

At hippocampal synapses, Cdk5 activity does not merely constrain recycling pool size at baseline (Kim and Ryan, 2010; Verstegen *et al.*, 2014). Instead, chronic activity blockade with tetrodotoxin results in the degradation of Cdk5 (Kim and Ryan, 2010), a concomitant decrease in the phosphorylation of synapsin (Verstegen *et al.*, 2014), and a homeostatic enhancement of recycling pool size. This Cdk5-dependent form of synaptic plasticity, termed presynaptic homeostatic scaling (Kim and Ryan, 2010), is reminiscent of homeostatic potentiation in *Drosophila* (Petersen *et al.*, 1997; Frank *et al*., 2006), as both phenomena are associated with enlargement of the recycling pool (Weyhersmüller *et al.*, 2011; Müller *et al.*, 2012). Hence, we hypothesized that homeostatic potentiation in *Drosophila* would be occluded by the loss of Cdk5 signaling, as the RRP might resist further modulation in response to decreased glutamate sensitivity. Moreover, removal of Cdk5 activity was also found to enhance (Kim and Ryan, 2013) or contradictorily reduce (Su *et al.*, 2012) presynaptic Ca^{2+} influx in the hippocampus. In addition to enlargement of the RRP (Weyhersmüller *et al.*, 2011; Müller *et al.*, 2012), homeostatic potentiation at fly NMJs also depends on an enhancement of presynaptic Ca^{2+} influx (Müller and Davis, 2012). Thus, we hypothesized that homeostatic potentiation in *Drosophila* might also be occluded or impaired by an inability to modulate presynaptic Ca^{2+} influx in the absence of Cdk5 signaling. It was also plausible that Cdk5 signaling could be essential for either short-term homeostatic potentiation, induced by PhTx (Frank *et al.*, 2006; Dickman *et al.*, 2009), or long-term homeostatic potentiation, induced by genetic ablation of GluRIIA (Petersen *et al.*, 1997). However, despite its great potential to participate in homeostatic potentiation, we demonstrate that Cdk5 signaling is dispensable for both short-term and long-term forms of this phenomenon under subphysiological or physiological conditions.

The lack of a requirement for Cdk5 signaling in homeostatic potentiation points to a more considerable degree of robustness in the homeostat than previously recognized. With genetic and pharmacological disruption of Cdk5 signaling, we present evidence for Cdk5-mediated regulation of the Ca^{2+}-dependence of neurotransmitter release, synaptic depression, and glutamate receptor composition. We have also confirmed that removal of Cdk5 signaling leads to abnormal NMJ morphogenesis, as first reported in an earlier study (Kissler *et al.*, 2009). Our results are in accordance with those of previous studies, which suggest that homeostatic potentiation can occur normally in the presence of NMJ growth deficits and aberrant synaptic transmission (Goold and Davis, 2007; Dickman *et al.*, 2009). Yet, our data facilitate these earlier findings by showing that reduced release probability and weakened steady-state transmission do not necessarily interfere with the mechanisms of homeostatic potentiation. Notably, an inverse correlation between NMJ size and active zone density in null Cdk5 signaling mutants may indicate the expression of hyperinnervation-dependent cell autonomous (Schuster *et al.*, 1996) or target-specific (Davis and Goodman, 1998) regulatory mechanisms. If so, then our results would imply that homeostatic potentiation and presynaptic structural plasticity (Schuster *et al.*, 1996; Davis and Goodman, 1998) may be carried out spatiotemporally at the same synapses.

Upon comparing and contrasting the roles of Cdk5 signaling at *Drosophila* NMJs and mammalian synapses, our data raise questions about the evolutionary conservation of synaptic transmission and homeostatic plasticity. Our noted effects of Cdk5 signaling loss on the Ca^{2+}-dependence of neurotransmitter release (Tomizawa *et al.*, 2002; Su *et al.*, 2012), the reorganization of synaptic vesicle pools (Kim and Ryan, 2010; Verstegen *et al.*, 2014), and the composition of glutamate receptors (Hawasli *et al.*, 2007; Seeburg *et al.*, 2008; Bianchetta *et al.*, 2011; Lai *et al.*, 2012) are consistent with some degree of

evolutionary conservation from invertebrates to vertebrates. Reports that Cdk5 signaling also directs axon guidance in mammals (Kwon *et al.*, 1999; Ledda *et al.*, 2000) and flies (Connell-Crowley *et al.*, 2000) similarly point to evolutionary conservation in the nervous system. In contrast, Cdk5 signaling is not necessary for a homeostatic enhancement of neurotransmitter release at fly NMJs, despite being required in a similar phenomenon at hippocampal synapses (Kim and Ryan, 2010; Verstegen *et al.*, 2014). Thus, presynaptic homeostatic scaling (Kim and Ryan, 2010) and fly homeostatic potentiation (Petersen *et al.*, 1997; Frank *et al.*, 2006) are separable processes. Future studies into the molecular mechanisms underlying each phenomenon may determine if other components of these homeostats are shared, or if vertebrate and invertebrate synapses convergently evolved distinct homeostats with superficially similar characteristics. A more reductionist study of a compensatory enhancement of acetylcholine release at myasthenic mammalian NMJs (Cull-Candy *et al.*, 1980; Plomp *et al.*, 1992; Plomp *et al.*, 1995; Sandrock *et al.*, 1997) may also illuminate shared molecular mechanisms of homeostatic plasticity. Intriguingly, Munc18, which was shown to be a phosphorylation target of Cdk5 (Shuang *et al.*, 1998; Fletcher *et al.*, 1999; Lilja *et al.*, 2004), is one of the few synaptic proteins necessary for homeostatic compensation in response to myasthenia gravis (Sons *et al.*, 2003; Sons *et al.*, 2006). Perhaps utilizing an ATP analog-sensitive Cdk5 (Shah *et al.*, 1997; Bishop *et al.*, 2000; Kraybill *et al.*, 2002; Merrick *et al.*, 2011) in homeostatically regulated neurons to catalog substrates, as done with other synaptic kinases (Ultanir *et al.*, 2012; Ultanir *et al.*, 2014), would further an understanding of the evolution of homeostatic plasticity. The enigmatic nature of Cdk5 signaling in homeostatic plasticity and synaptic transmission is beginning to be revealed. Our study is one of many steps to come in this critical journey.

Materials and Methods

Fly stocks and genetics

Fly stocks were maintained at 22-25° C on normal food. For pan-neuronal transgene expression, we used *elav^{c155}-Gal4* on the first (X) chromosome, as previously described (Lin and Goodman, 1994). For transgene expression in muscles, we used *BG57-Gal4* (Budnik *et al.*, 1996) or *MHC-Gal4* (Lin and Goodman, 1994) on the third chromosome. For long-term homeostatic potentiation experiments, we used *GluRIIA^{SP16}* (Petersen *et al.*, 1997). The *cdk5^{null}* mutant and *UAS-cdk5* transgenic line were kindly provided by Beat Suter (University of Bern, Bern, Switzerland). The *p35^{20C}* mutant, *Df(p35)^{C2}* (*p35* deficiency), *UAS-cdk5^{DN}-FLAG* transgenic line, and *UAS-p35* transgenic line were kind gifts from Edward Giniger (National Institutes of Health, Bethesda, MD). The *UAS-cdk5^{AS}* transgenic line, used for acute inhibition of Cdk5 with an ATP analog (1-NM-PP1), was generated by mutating the phenylalanine residue at position 80 to glycine, as described (Kraybill *et al.*, 2002; Merrick *et al.*, 2011; Horiuchi *et al.*, 2012). All other fly stocks not created in our laboratory were obtained from the Bloomington *Drosophila* Stock Center at Indiana University (Bloomington, IN). Standard first (X), second, and third balancer chromosomes and genetic strategies were used for crosses and for maintaining mutant lines. “Wild type” refers to *w^{1118}*.

Electrophysiology

Recordings were obtained from muscle 6 in abdominal segment 2 or 3 of wandering third instar larvae with an AxoPatch 200B (for current-clamp recordings) or an Axoclamp 2B (for two-electrode voltage-clamp recordings), as previously described (Müller *et al.*,

2012). Recordings were made in modified HL3 saline at specified calcium concentrations (see figures and text) with the following components (and concentrations): NaCl (70 mM), KCl (5 mM), $MgCl_2$ (10 mM), $NaHCO_3$ (10 mM), sucrose (115 mM), trehalose (5 mM), HEPES pH 7.2 (5 mM), and $CaCl_2$ (0.4 mM for current-clamp recordings and 1.5 mM for two-electrode voltage-clamp recordings). For acute homeostatic challenge, semi-intact preparations with the CNS, fat, and gut intact were perfused with philanthotoxin-433 (PhTx; Sigma-Aldrich). PhTx was prepared as a stock solution (5 mM in ddH_2O) and diluted in HL3 saline to 15 μM. Following a ten-minute incubation period, the dissections were completed, and the preparations were rinsed and assayed. For acute inhibition of an analog-sensitive Cdk5, *elav^{c155}-Gal4; cdk5^{null}*; *UAS-cdk5^{F80G}*/+ ("*cdk5^{AS}*") semi-intact preparations, as above, were bathed in 100 μM 1-NM-PP1 (Kevan Shokat lab) in the absence or presence of PhTx, as indicated, for ten minutes. The *cdk5^{AS}* preparations were also treated with 100 μM 1-NM-PP1 prior to bath application of PhTx to ensure inhibition of the analog-sensitive Cdk5 at the earliest stages of homeostatic potentiation. As above, dissections were completed after a ten-minute incubation period in PhTx, and the preparations were rinsed and assayed in the presence of additional 100 μM 1-NM-PP1 to ensure inhibition of the analog-sensitive Cdk5 after the induction of homeostatic potentiation. Muscle input resistance (R_{in}) was monitored at the beginning and end of each recording. Recordings were excluded if R_{in} changed by more than 20%. The average single action potential-evoked EJP amplitude (stimulus duration, 3 ms) or EJC amplitude (stimulus duration, 1 ms) for each recording is based on the mean peak EJP amplitudes or EJC amplitudes in response to thirty presynaptic stimuli. Quantal content was estimated for each current-clamp recording by

calculating the average EJP/average mEJP, corrected for nonlinear summation (Martin, 1955) when noted, and subsequently averaging across all NMJs for a given genotype. To determine the apparent size of the readily-releasable pool (RRP), we applied the method of cumulative EJC amplitudes (Müller *et al.*, 2012; Schneggenburger *et al.*, 1999; Weyhersmuller *et al.*, 2011). Muscles were clamped to -65 mV, and EJC amplitudes during a stimulus train (60 Hz, thirty stimuli) were calculated as the difference between peak and baseline before stimulus onset of a given EJC, as previously described (Muller *et al.*, 2012*)*. The number of release-ready vesicles was obtained by back-extrapolating a line fit to the linear phase of the cumulative EJC plot (the last 200 ms of a train) to time zero and dividing the cumulative EJC amplitude at time zero by the mean mEJP amplitude recorded in the same cell (Müller *et al.*, 2012). All data for homeostatic challenge experiments in current-clamp (with PhTx or *GluRIIA*$^{-}$) were collected, analyzed, and submitted with the experimenter blind to genotype.

Immunocytochemistry

Wandering third instar larvae were dissected in 0 Ca^{2+} HL3 saline and fixed. For deconvolution microscopy, fixation was performed with Bouin's fixative (Sigma-Aldrich) for two minutes or with paraformaldehyde (USB Corporation) for fifteen minutes. For structured illumination microscopy, fixation was performed with ice-cold 100% ethanol (Gold Shield) for five minutes. Larvae were washed briefly and incubated overnight at 4° C in primary antibody, washed the next day, and incubated in fluorescently conjugated secondary antibodies for two hours at room temperature. The following primary antibodies were used at the indicated dilutions: mouse anti-GluRIIA (8B4D2): 1:100 (Developmental Studies Hybridoma Bank); rabbit anti-GluRIIB: 1:2,500 (Marrus *et al.*,

2004); rabbit anti-GluRIIC: 1:2,500 (Marrus *et al.*, 2004); mouse anti-Brp (nc82): 1:100 (Wagh *et al.*, 2006); rabbit anti-Dlg: 1:10,000 (Lahey *et al.*, 1994); mouse anti-CSP (DCSP-2): 1:250 (Zinsmaier *et al.*, 1994); rabbit anti-Synaptotagmin 1: 1:1000 (Littleton *et al.*, 1993); mouse anti-FLAG M2: 1:200 (Sigma-Aldrich); mouse anti-FasII (1D4): 1:10 (Van Vactor *et al.*, 1993). Antibodies against fly GluRs were used with Bouin's fixation. Antibodies against CSP, Synaptotagmin 1, and FLAG were used with paraformaldehyde fixation. Alexa-conjugated secondary antibodies and directly conjugated goat anti-HRP (Jackson Immunoresearch Laboratories, Molecular Probes) were used at 1:400. Larval preparations were mounted in Vectashield (Vector). For deconvolution microscopy, larval preparations were imaged at room temperature using an Axiovert 200 (Zeiss) inverted microscope, a 100x Plan Apochromat objective (aperture 1.4), and a cooled CCD camera (Coolsnap HQ, Roper). Intelligent Imaging Innovations (3i) SlideBook 5 software was used to capture, deconvolve, and analyze images. NMJ areas were defined by Discs large (Dlg) staining. Only type Ib boutons were considered in our analysis of NMJ-growth parameters, consistent with other studies (Kissler *et al.*, 2009; Cheng *et al.*, 2011). Type Ib and type Is boutons were distinguished by intensity of Dlg staining and bouton size (Bhogal *et al.*, 2011). Active zone numbers were counted by manually editing empty masks with pencil tools in SlideBook 5. Antibody immunofluorescence levels were quantified as previously described (Heckscher *et al.*, 2007). Synaptic levels of FasII were quantified at type 1b boutons of muscle 4 NMJs. For structured illumination microscopy, larval preparations were imaged at room temperature using an ELYRA PS.1 system with an inverted LSM-710 microscope, a 63x (1.4 NA) Plan-Apochromat objective (Carl Zeiss), and an Andor iXon 885 EMCCD

camera. Lateral resolution was ~ 110 nm, and axial resolution was ~300 nm. Z-stacks of whole NMJs at muscle 4 and muscle 6/7 were acquired and analyzed using Fiji and Igor, as previously described (Müller *et al.*, 2012).

Figures

Figure 1. Cdk5 signaling is dispensable for short-term homeostatic potentiation. **(A)** Average mEJP amplitudes for indicated genotypes in saline (black) or saline with PhTx (white). w^{1118} (- PhTx), n = 22; w^{1118} (+ PhTx), n = 16; $cdk5^{null}$ (- PhTx), n = 18; $cdk5^{null}$ (+ PhTx), n = 18; $p35^{20C}/Df(p35)^{C2}$ (- PhTx), n = 15; $p35^{20C}/Df(p35)^{C2}$ (+ PhTx), n = 13; $cdk5^{DN}$ (- PhTx), n = 10; $cdk5^{DN}$ (+ PhTx), n = 21. PhTx treatment significantly reduced mEJP amplitudes, compared to baseline, in all genotypes ($p < 0.01$). Baseline mEJP amplitudes of $cdk5^{null}$ ($p = 0.33$), $p35^{20C}/Df(p35)^{C2}$ ($p = 0.21$), and $cdk5^{DN}$ ($p = 0.80$) were similar to wild type. **(B)** Average EJP amplitude, as in **(A)**. EJP amplitudes of PhTx and control group were similar in wild type ($p = 0.33$), $cdk5^{null}$ ($p = 0.80$), and $cdk5^{DN}$ ($p = 0.06$), but differed slightly in $p35^{20C}/Df(p35)^{C2}$ ($p = 0.01$). Baseline EJP amplitudes of $cdk5^{null}$ ($p = 0.82$) and $cdk5^{DN}$ ($p = 0.13$) were similar to wild type, but differed slightly from wild type in $p35^{20C}/Df(p35)^{C2}$ ($p = 0.02$). **(C)** Average quantal content, as in **(A)**. PhTx treatment induced an increase in quantal content, compared to baseline, in all genotypes ($p < 0.01$). Baseline quantal contents of $cdk5^{null}$ ($p = 0.31$), $p35^{20C}/Df(p35)^{C2}$ ($p = 0.79$), and $cdk5^{DN}$ ($p = 0.09$) were similar to wild type. All data represent mean ± SEM. **(D)** Sample traces showing EJP and mEJP amplitudes for wild type in the presence and absence of PhTx (red and black, respectively). **(E)** Sample traces for $cdk5^{null}$, as in **(D)**. **(F)** Sample traces for $p35^{20C}/Df(p35)^{C2}$, as in **(D)**. Scale bars for EJPs = 5 mV, vertical, and 50 ms, horizontal. Scale bars for mEJPs = 2 mV, vertical, and 1 s, horizontal.

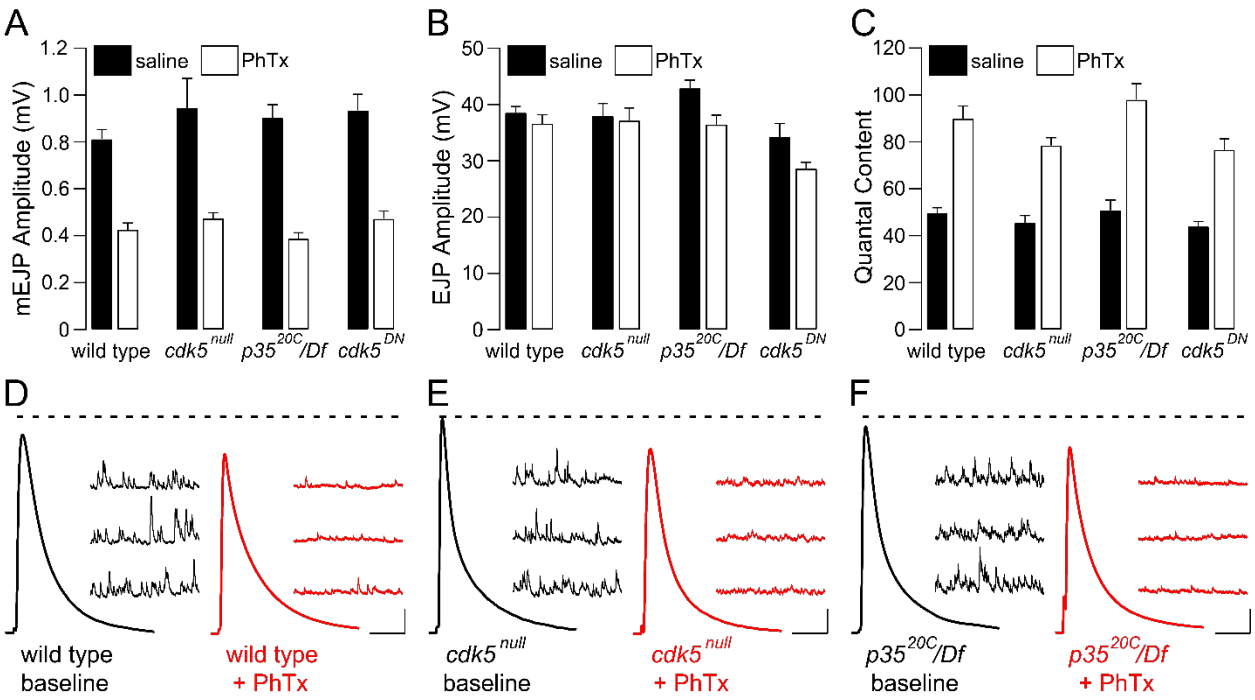
A
B
C
saline
PhTx
mEJP Amplitude (mV)
EJP Amplitude (mV)
Quantal Content
wild type
cdk5 null
p35 20C/Df
cdk5 DN
D
E
F
wild type
baseline
wild type
+ PhTx
cdk5 null
baseline
cdk5 null
+ PhTx
p35 20C/Df
baseline
p35 20C/Df
+ PhTx

Figure 2. Cdk5 signaling is dispensable for long-term homeostatic potentiation. **(A)** Average mEJP amplitudes for indicated control (black) or *GluRIIA*$^{-}$ (*GluRIIA*^{SP16}) genotypes (white). *w*^{1118} (*GluRIIA*$^{+}$), n = 22; *GluRIIA*$^{-}$, n = 14; *cdk5*^{null} (*GluRIIA*$^{+}$), n = 18; *cdk5*^{null}*, GluRIIA*$^{-}$, n = 17. Genetic ablation of *GluRIIA* significantly reduced mEJP amplitudes, compared to baseline, in both genotypes ($p < 0.01$). **(B)** Average EJP amplitude, as in **(A)**. EJP amplitudes of *GluRIIA*$^{-}$ and control group were slightly different in wild type ($p < 0.01$) and in *cdk5*^{null} ($p < 0.01$). **(C)** Average quantal content, as in **(A)**. *GluRIIA*$^{-}$ strongly enhanced quantal content, compared to baseline, in all genotypes ($p < 0.01$). All data represent mean ± SEM. **(D)** Sample traces showing EJP and mEJP amplitudes for wild type (*GluRIIA*$^{+}$) and *GluRIIA*$^{-}$ (black and red, respectively). **(E)** Sample traces for *cdk5*^{null}, as in **(D)**. Scale bars for EJPs = 5 mV, vertical, and 50 ms, horizontal. Scale bars for mEJPs = 2 mV, vertical, and 1 s, horizontal.

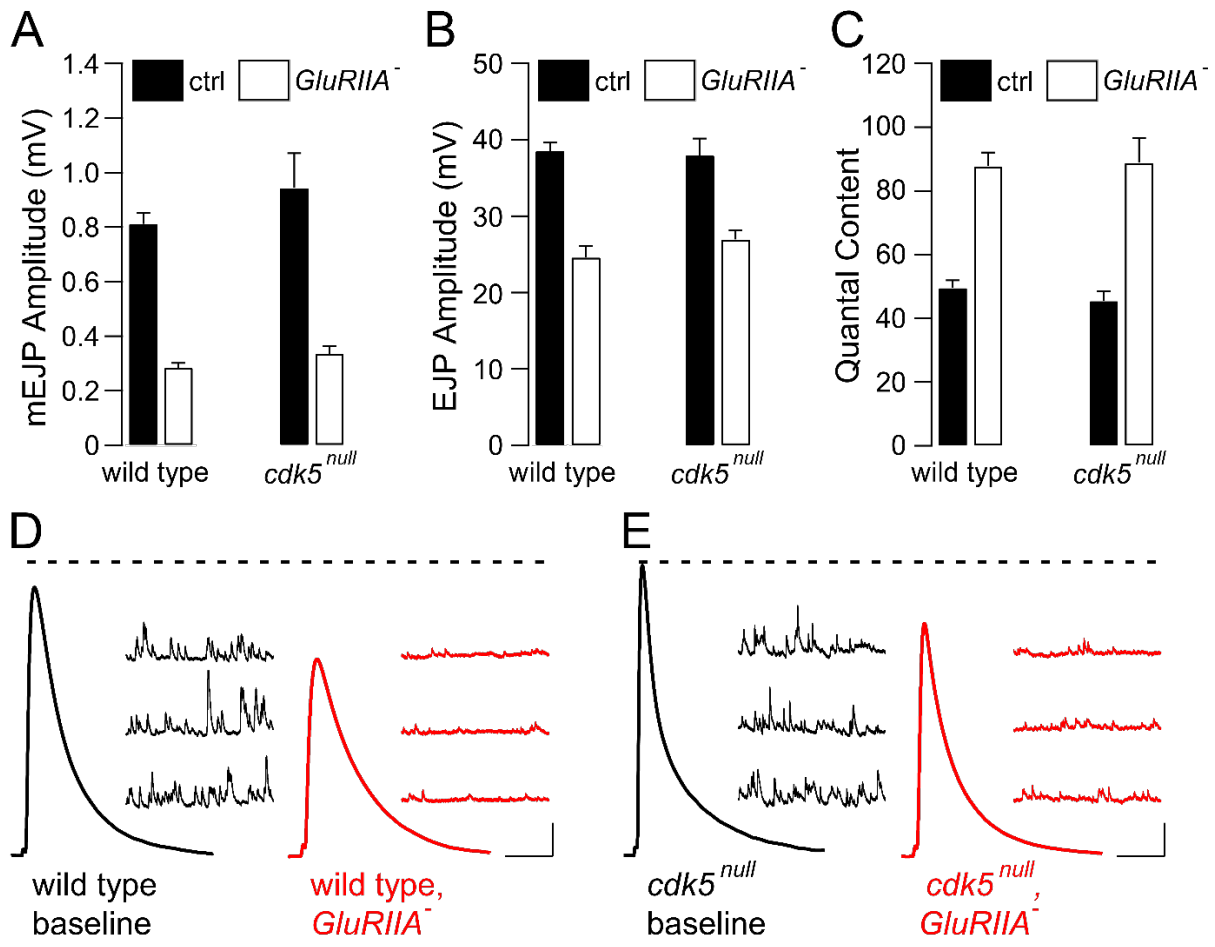
A
mEJP Amplitude (mV)
1.4
1.2
1.0
0.8
0.6
0.4
0.2
0
ctrl
GluRIIA-
wild type
cdk5null
B
EJP Amplitude (mV)
50
40
30
20
10
0
ctrl
GluRIIA-
wild type
cdk5null
C
Quantal Content
120
100
80
60
40
20
0
ctrl
GluRIIA-
wild type
cdk5null
D
wild type
baseline
wild type,
GluRIIA-
E
cdk5null
baseline
cdk5null,
GluRIIA-

Figure 3. Cdk5 affects the apparent Ca^{2+} cooperativity of neurotransmitter release and localizes to presynaptic nerve terminals. (A) Quantal content in wild type and *cdk5*^{null} (black and red, respectively) as a function of extracellular calcium concentration. Data are corrected for nonlinear summation. **(B)** FLAG-Cdk5 (CDK5; green) and Synaptotagmin 1 (SYT1; purple) in presynaptic nerve terminals of wild type animals, expressing *UAS-cdk5*^{DN}*-FLAG*, at muscle 6/7. Scale bar = 5 μm. **(C)** Sample traces showing EJP and mEJP amplitudes for wild type and *cdk5*^{null} in 0.2 mM Ca^{2+}. Scale bars for EJPs = 5 mV, vertical, and 50 ms, horizontal. Scale bars for mEJPs = 2 mV, vertical, and 1 s, horizontal.

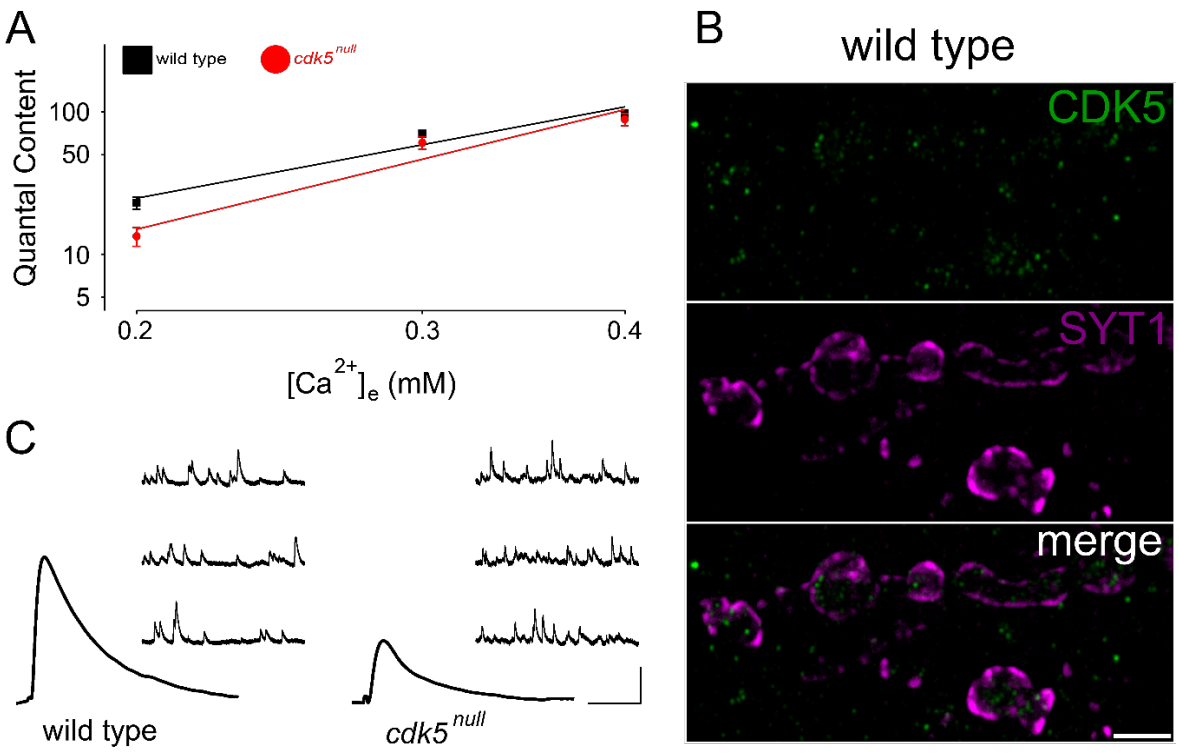
A
wild type
cdk5 null
Quantal Content
100
50
10
5
0.2
0.3
0.4
[Ca2+]e (mM)
B
wild type
CDK5
SYT1
merge
C
wild type
cdk5 null

Figure 4. Cdk5 is not required for the modulation of RRP size during homeostatic potentiation, but contributes to neurotransmitter release at physiological Ca^{2+}. (A) Average mEJP amplitudes for indicated control (black) or *GluRIIA*$^{-}$ (*GluRIIA*^{SP16}) genotypes (white). *w*^{1118} (*GluRIIA*$^{+}$), n = 9; *GluRIIA*$^{-}$, n = 8; *cdk5*^{null} (*GluRIIA*$^{+}$), n = 16; *cdk5*^{null}*, GluRIIA*$^{-}$, n = 12. Genetic ablation of *GluRIIA* significantly reduced mEJP amplitudes, compared to baseline, in both genotypes ($p < 0.01$). Baseline mEJP amplitudes of *cdk5*^{null} were similar to wild type ($p = 0.12$). **(B)** Average cumulative (cum.) EJC amplitude, as in **(A)**. Cumulative EJC amplitudes of *GluRIIA*$^{-}$ and control group were similar in wild type ($p = 0.32$) and in *cdk5*^{null} ($p = 0.12$). Baseline cumulative EJC amplitudes of *cdk5*^{null} were significantly increased, compared to wild type ($p < 0.01$). **(C)** Average estimated RRP size, as in **(A)**. *GluRIIA*$^{-}$ strongly enhanced RRP size, compared to baseline, in wild type and in *cdk5*^{null} ($p < 0.01$). Baseline RRP sizes of *cdk5*^{null} were not significantly different from wild type ($p = 0.20$). **(D)** Sample traces showing EJC amplitudes, evoked by 60-Hz stimulation in 1.5 mM Ca^{2+}, for wild type (*GluRIIA*$^{+}$) (top, black) and *GluRIIA*$^{-}$ (bottom, red). **(E)** Sample traces for *cdk5*^{null}, as in **(D)**. Scale bars = 100 nA, vertical, and 50 ms, horizontal. **(F)** Average amplitudes of the final (30th) EJCs in 60-Hz trains were significantly smaller in *cdk5*^{null}, compared to wild type ($p = 0.02$). **(G)** Depression over the first ten stimuli of the 60-Hz trains did not differ significantly between wild type and *cdk5*^{null} ($p = 0.08$). However, *cdk5*^{null} mutants showed significantly enhanced depression at the ends ($EJC_{final}/EJC_{initial}$) of 60-Hz trains, compared to wild type ($p < 0.01$). All data represent mean ± SEM.

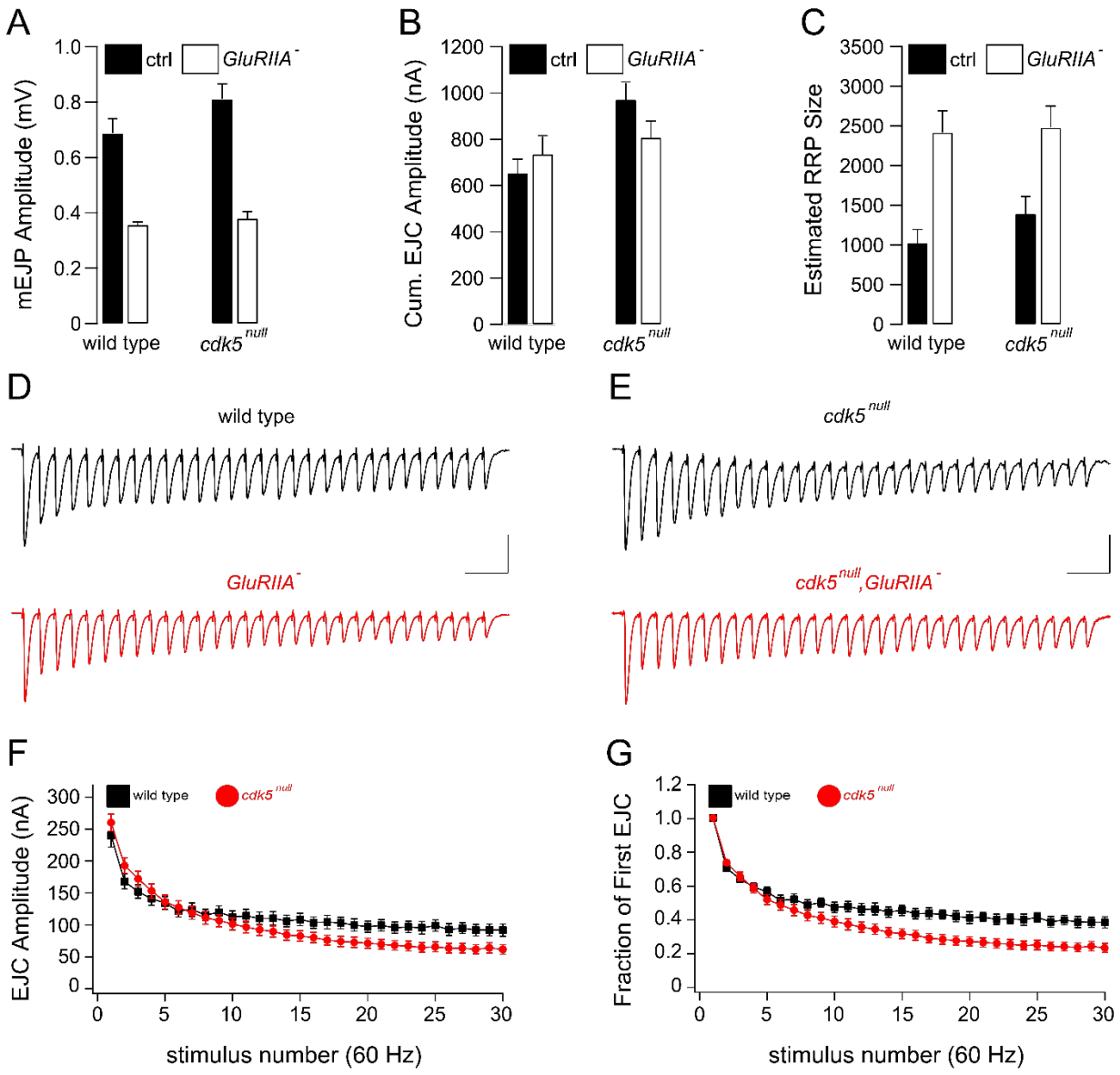
A
mEJP Amplitude (mV)
1.0
0.8
0.6
0.4
0.2
0
ctrl
GluRIIA-
wild type
cdk5null
B
Cum. EJC Amplitude (nA)
1200
1000
800
600
400
200
0
ctrl
GluRIIA-
wild type
cdk5null
C
Estimated RRP Size
3500
3000
2500
2000
1500
1000
500
0
ctrl
GluRIIA-
wild type
cdk5null
D
wild type
GluRIIA-
E
cdk5null
cdk5null,GluRIIA-
F
EJC Amplitude (nA)
300
250
200
150
100
50
0
wild type
cdk5null
0
5
10
15
20
25
30
stimulus number (60 Hz)
G
Fraction of First EJC
1.2
1.0
0.8
0.6
0.4
0.2
0
wild type
cdk5null
0
5
10
15
20
25
30
stimulus number (60 Hz)

Figure 5. p35 is not necessary for the modulation of RRP size during homeostatic potentiation, but contributes to neurotransmitter release at physiological Ca^{2+}. (A) Average mEJP amplitudes for indicated wild type, $p35^{20C}$, or $GluRIIA^{-}$ ($GluRIIA^{SP16}$) genotypes. w^{1118}, n = 9; $p35^{20C}$, n = 11; $GluRIIA^{-}$, n = 8. Genetic ablation of *p35* and *GluRIIA* significantly reduced mEJP amplitudes, compared to wild type, in both genotypes ($p < 0.01$). **(B)** Average cumulative (cum.) EJC amplitude, as in **(A)**. Cumulative EJC amplitudes of $p35^{20C}$ ($p = 0.39$) and $GluRIIA^{-}$ ($p = 0.32$) were similar to wild type. **(C)** Average estimated RRP size, as in **(A)**. Estimated RRP sizes of $p35^{20C}$ and $GluRIIA^{-}$ were significantly enhanced, compared to wild type ($p < 0.01$). **(D)** Average amplitudes of the final (30^{th}) EJCs in 60-Hz trains were significantly smaller in $p35^{20C}$, compared to wild type ($p < 0.01$) and $GluRIIA^{-}$ ($p < 0.01$). **(E)** Depression over the first ten stimuli of the 60-Hz trains was significantly enhanced in $p35^{20C}$, compared to wild type ($p < 0.01$) and $GluRIIA^{-}$ ($p < 0.01$). Similarly, $p35^{20C}$ null mutants exhibited significantly enhanced depression at the ends ($EJC_{final}/EJC_{initial}$) of 60-Hz trains, relative to wild type ($p < 0.01$) and $GluRIIA^{-}$ ($p < 0.01$). All data represent mean ± SEM.

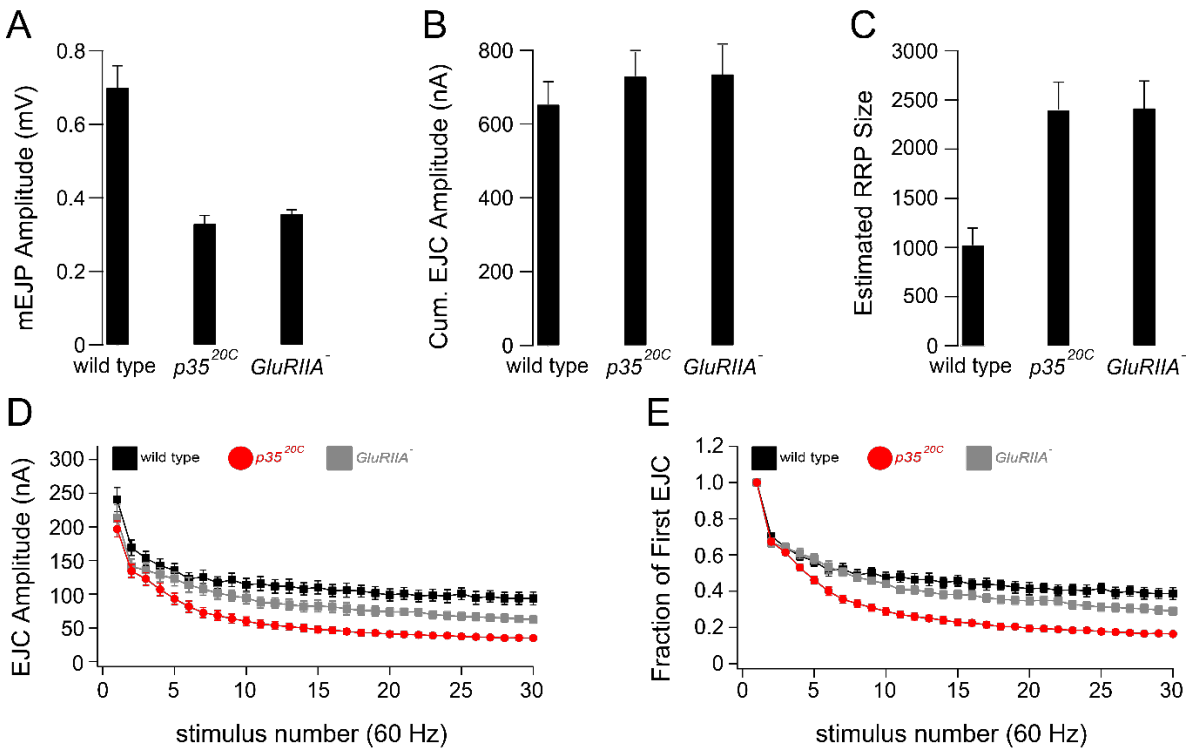
A
mEJP Amplitude (mV)
0.8
0.6
0.4
0.2
0
wild type
p35 20C
GluRIIA-
B
Cum. EJC Amplitude (nA)
800
600
400
200
0
wild type
p35 20C
GluRIIA-
C
Estimated RRP Size
3000
2500
2000
1500
1000
500
0
wild type
p35 20C
GluRIIA-
D
EJC Amplitude (nA)
300
250
200
150
100
50
0
wild type
p35 20C
GluRIIA-
0
5
10
15
20
25
30
stimulus number (60 Hz)
E
Fraction of First EJC
1.2
1.0
0.8
0.6
0.4
0.2
0
wild type
p35 20C
GluRIIA-
0
5
10
15
20
25
30
stimulus number (60 Hz)

Figure 6. Effects of Cdk5 signaling on postsynaptic glutamate receptor composition. (A-C) Wild type **(A),** *cdk5^{null}* **(B)**, and *p35^{20C}* **(C)** NMJs (muscle 4) costained with antibodies to GluRIIA (green) and GluRIIB (purple). Scale bars = 5 μm. **(D)** Quantification of GluRIIA fluorescence intensity at muscles 6/7 and 4 comparing *w^{1118}* (n = 16 and 23), *cdk5^{null}* (n = 16 and 24) ($p < 0.01$ and < 0.01, Student's *t* test), and *p35^{20C}* (n = 15 and 23) ($p < 0.01$ and < 0.01, Student's *t* test). **(E)** Quantification of GluRIIB fluorescence intensity at muscles 6/7 and 4 comparing *w^{1118}* (n = 16 and 23), *cdk5^{null}* (n = 16 and 24) ($p < 0.01$ and < 0.01, Student's *t* test), and *p35^{20C}* (n = 15 and 23) ($p < 0.01$ and < 0.01, Student's *t* test). **(F)** Quantification of GluRIIC fluorescence intensity at muscles 6/7 and 4 comparing *w^{1118}* (n = 12 and 16), *cdk5^{null}* (n = 12 and 16) ($p = 0.62$ and 0.88, Student's *t* test), and *p35^{20C}* (n = 16 and 17) ($p < 0.01$ and < 0.01, Student's *t* test). All data represent mean ± SEM.

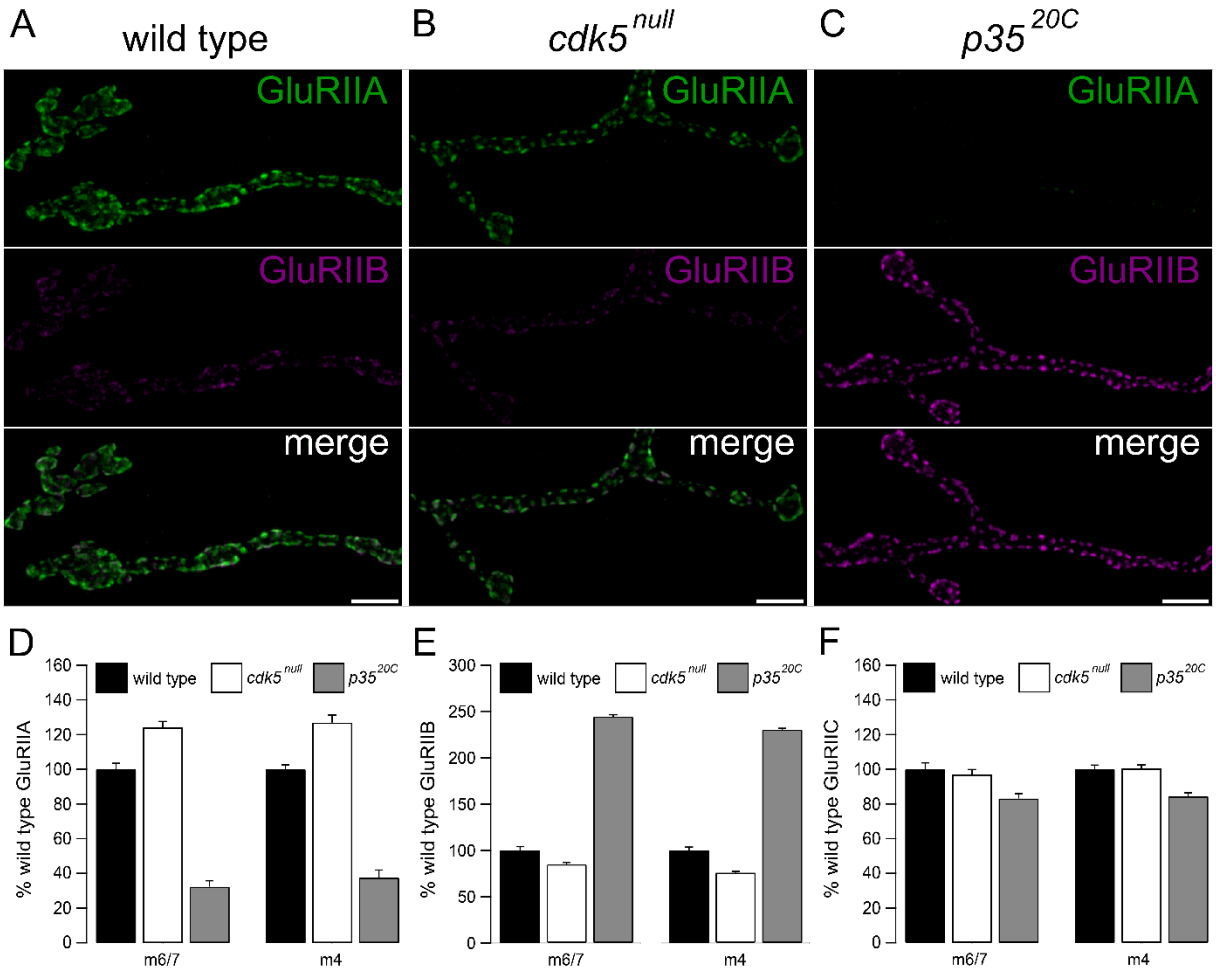
A
wild type
B
cdk5 null
C
p35 20C
GluRIIA
GluRIIB
merge
D
E
F
wild type
cdk5 null
p35 20C
% wild type GluRIIA
% wild type GluRIIB
% wild type GluRIIC
m6/7
m4

Figure 7. Effects of Cdk5 on synaptic vesicle protein levels. (A) Average synaptic fluorescence intensity of Synaptotagmin 1 (Syt1) at muscle 6/7 of w^{1118} (n = 16), $cdk5^{null}$ (n = 15; p = 0.09, Student's t test), and $p35^{20C}$ (n = 16; p = 0.01, Student's t test). **(B)** Average synaptic fluorescence intensity of cysteine string protein (CSP) at muscle 6/7 of w^{1118} (n = 16), $cdk5^{null}$ (n = 15; p = 0.10, Student's t test), and $p35^{20C}$ (n = 16; p = 0.49, Student's t test). **(C-D)** Syt1 (green) and CSP (purple) in presynaptic nerve terminals of w^{1118} **(C)** and $cdk5^{null}$ **(D)** at muscle 6/7. Scale bar = 5 μm. All data represent mean ± SEM.

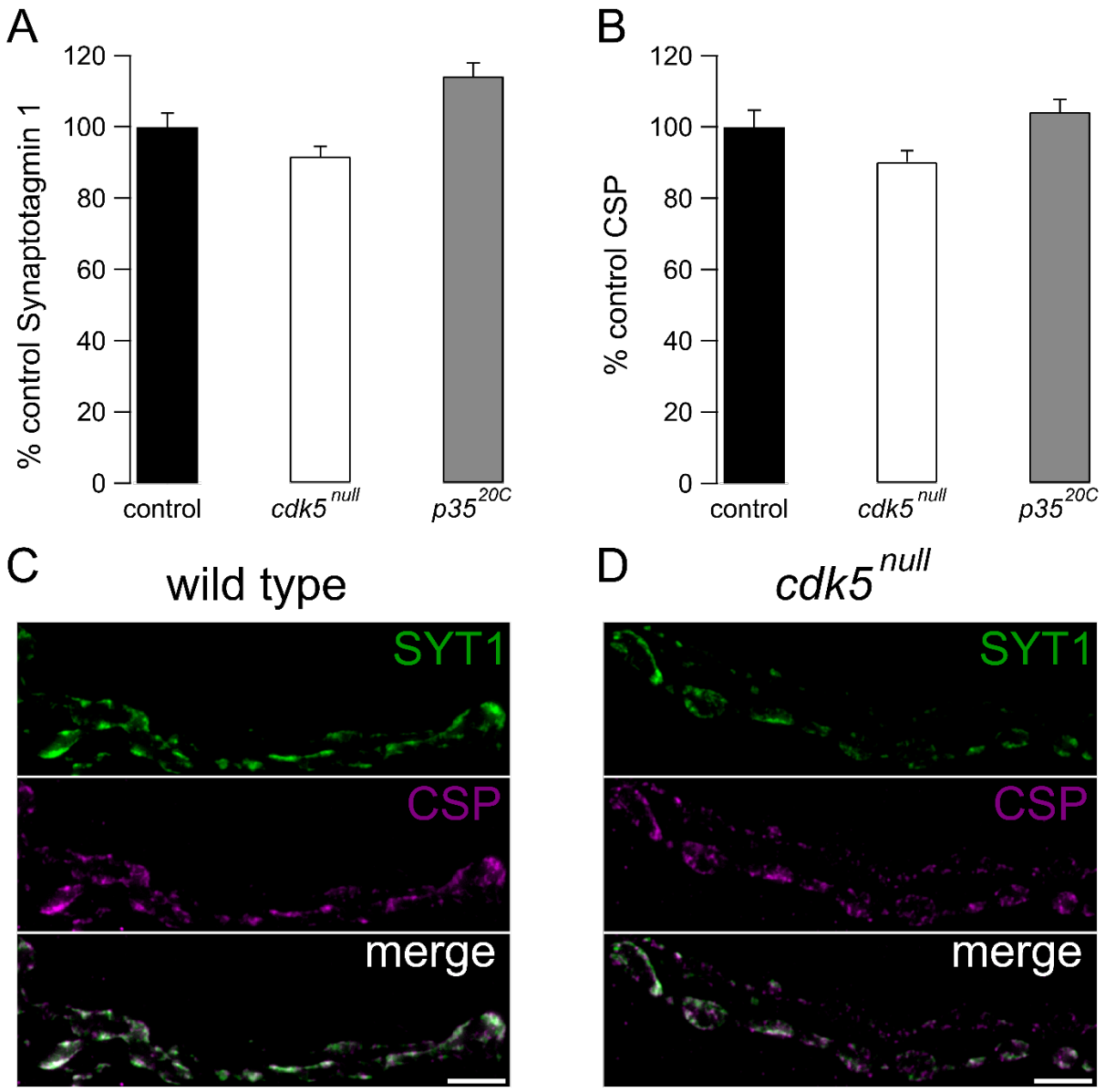
A
% control Synaptotagmin 1
120
100
80
60
40
20
0
control
cdk5 null
p35 20C
B
% control CSP
120
100
80
60
40
20
0
control
cdk5 null
p35 20C
C
wild type
SYT1
CSP
merge
D
cdk5 null
SYT1
CSP
merge

Figure 8. Effects of Cdk5 signaling on NMJ morphology. (A-C) Wild type **(A),** *cdk5^{null}* **(B)**, and *p35^{20C}* **(C)** NMJs (muscle 4) costained with antibodies to Discs large (purple; DLG) and Bruchpilot (green; nc82). Scale bars = 5 μm. **(D)** Quantification of bouton number at muscles 6/7 and 4 comparing *w^{1118}* (n = 12 and 18), *cdk5^{null}* (n = 16 and 23) ($p < 0.05$ and < 0.01, Student's *t* test), and *p35^{20C}* (n = 16 and 24) ($p = 0.17$ and < 0.01, Student's *t* test). **(E)** Quantification of nc82 puncta per NMJ at muscles 6/7 and 4 comparing *w^{1118}* (n = 12 and 18), *cdk5^{null}* (n = 16 and 23) ($p = 0.35$ and < 0.05, Student's *t* test), and *p35^{20C}* (n = 16 and 24) ($p = 0.72$ and < 0.01, Student's *t* test). **(F)** Quantification of nc82 puncta density per NMJ at muscles 6/7 and 4 comparing *w^{1118}* (n = 12 and 18), *cdk5^{null}* (n = 16 and 23) ($p < 0.01$ and < 0.01, Student's *t* test), and *p35^{20C}* (n = 16 and 24) ($p < 0.01$ and < 0.01, Student's *t* test). All data represent mean ± SEM.

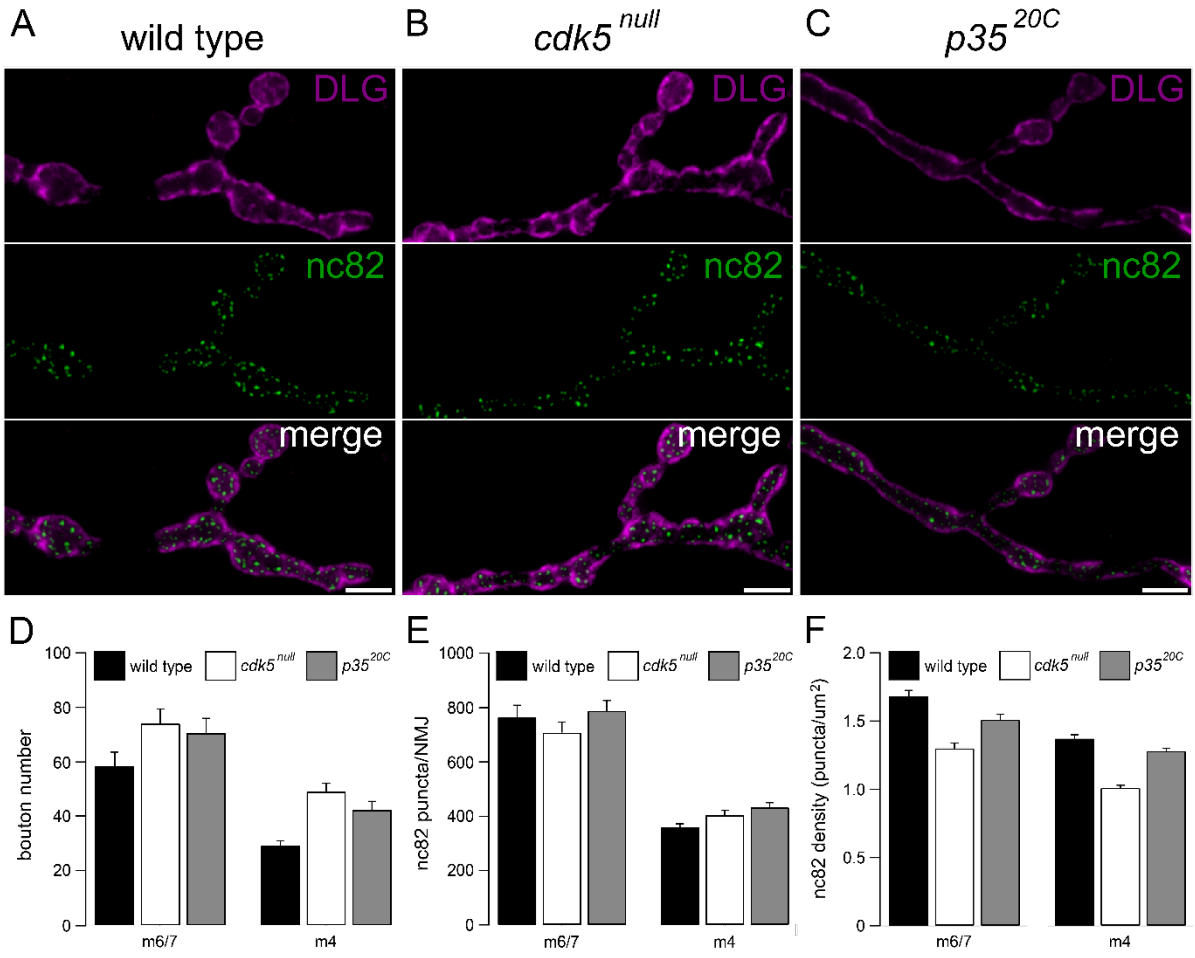
A
wild type
B
cdk5 null
C
p35 20C
DLG
nc82
merge
D
bouton number
E
nc82 puncta/NMJ
F
nc82 density (puncta/um2)
wild type
cdk5 null
p35 20C
m6/7
m4

Figure 9. Effects of Cdk5 signaling on active zone morphology. (A-C) Structured illumination images of wild type **(A),** *cdk5*^{null} **(B)**, and *p35*^{20C} **(C)** NMJs (muscle 4) stained with anti-Bruchpilot (green; nc82). Scale bars = 0.5 μm. **(D)** Fluorescence intensity line profiles through all planar Brp puncta of a representative *cdk5*^{null} NMJ. Individual line profiles and the average line profile are shown in gray and black, respectively. **(E-F)** Cumulative frequency plot of *cdk5*^{null} **(E)** and *p35*^{20C} **(F)** Brp ring diameters at half maximum, the distance between two points at 50% of peak fluorescence intensity, as determined by structured illumination microscopy. **(G)** Fluorescence intensity line profiles through all planar Brp puncta of a representative *cdk5*^{null} NMJ. Individual line profiles are shown in gray and are normalized to the respective peak fluorescence. Diameter at half maximum is the distance between two points at 50% of the peak fluorescence (black crosses). Peak-to-peak diameter of a line profile was calculated as the distance between the two peaks of the intensity profile (black circles). **(H)** Average of average peak-to-peak diameters of Brp puncta at muscles 6/7 and 4 of *w*^{1118} (n = 9 and 9), *cdk5*^{null} (n = 9 and 11; p = 0.06 and 0.02, Student's t test), and *p35*^{20C} (n = 9 and 8; p = 0.51 and < 0.01, Student's t test) NMJs. **(I)** Average of average diameters at half maximum of Brp puncta at muscles 6/7 and 4 of *w*^{1118} (n = 9 and 9), *cdk5*^{null} (n = 9 and 11; p = 0.05 and 0.03, Student's t test), and *p35*^{20C} (n = 9 and 8; p = 0.87 and < 0.01, Student's t test) NMJs. All data represent mean ± SEM.

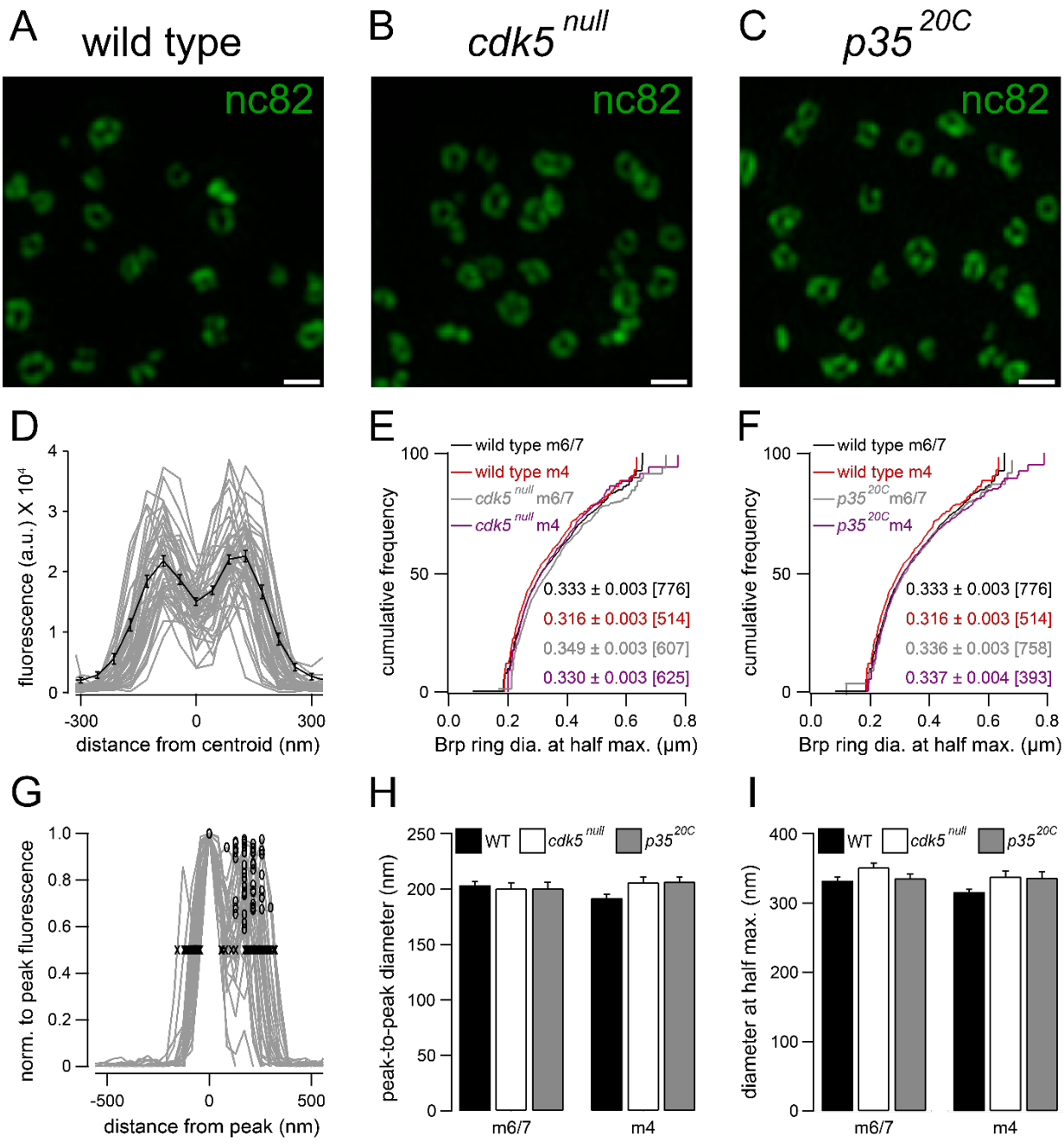
A
wild type
nc82
B
cdk5 null
nc82
C
p35 20C
nc82
D
fluorescence (a.u.) X 10⁴
distance from centroid (nm)
E
wild type m6/7
wild type m4
cdk5 null m6/7
cdk5 null m4
cumulative frequency
0.333 ± 0.003 [776]
0.316 ± 0.003 [514]
0.349 ± 0.003 [607]
0.330 ± 0.003 [625]
Brp ring dia. at half max. (µm)
F
wild type m6/7
wild type m4
p35 20C m6/7
p35 20C m4
cumulative frequency
0.333 ± 0.003 [776]
0.316 ± 0.003 [514]
0.336 ± 0.003 [758]
0.337 ± 0.004 [393]
Brp ring dia. at half max. (µm)
G
norm. to peak fluorescence
distance from peak (nm)
H
WT
cdk5 null
p35 20C
peak-to-peak diameter (nm)
m6/7
m4
I
WT
cdk5 null
p35 20C
diameter at half max. (nm)
m6/7
m4

Figure 10. Acute inhibition of Cdk5 does not affect the modulation of RRP size during homeostatic potentiation, but perturbs neurotransmitter release at physiological Ca^{2+}. (A) Average mEJP amplitudes for indicated genotypes in saline (black) or saline with PhTx (white). Here, "*cdk5*^{AS}" refers to *elav*^{c155}*-Gal4; cdk5*^{null}; *UAS-cdk5*^{F80G}/+. Wild type (- PhTx), n = 9; wild type (+ PhTx), n = 8; *cdk5*^{AS} (- PhTx), n = 13; *cdk5*^{AS} (+ PhTx), n = 7. PhTx treatment significantly reduced mEJP amplitudes, compared to baseline, in all genotypes ($p < 0.01$). Baseline mEJP amplitudes of *cdk5*^{AS} ($p = 0.35$) were similar to wild type. **(B)** Average cumulative (cum.) EJC amplitude, as in **(A)**. Cumulative EJC amplitudes of PhTx and control group were similar in wild type ($p = 0.06$) and in *cdk5*^{AS} ($p = 0.33$). Baseline cumulative EJC amplitudes of *cdk5*^{AS} were significantly increased, compared to wild type ($p < 0.01$). **(C)** Average estimated RRP size, as in **(A)**. PhTx treatment strongly enhanced RRP size, compared to baseline, in wild type and in *cdk5*^{AS} ($p < 0.01$). Baseline RRP sizes of *cdk5*^{AS} were not significantly different from wild type ($p = 0.07$). **(D)** Sample traces showing EJC amplitudes, evoked by 60-Hz stimulation in 1.5 mM Ca^{2+}, for wild type in the absence (top, black) and presence of PhTx (bottom, red). **(E)** Sample traces for *cdk5*^{AS}, as in **(D)**. Scale bars = 100 nA, vertical, and 50 ms, horizontal. **(F)** Average amplitudes of the final (30th) EJCs in 60-Hz trains did not differ significantly between wild type and *cdk5*^{AS} ($p = 0.47$). **(G)** Depression over the first ten stimuli of the 60-Hz trains did not differ significantly between wild type and *cdk5*^{AS} ($p = 0.58$). However, *cdk5*^{AS} mutants showed significantly enhanced depression at the ends ($EJC_{final}/EJC_{initial}$) of 60-Hz trains, compared to wild type ($p = 0.02$). All data represent mean ± SEM.

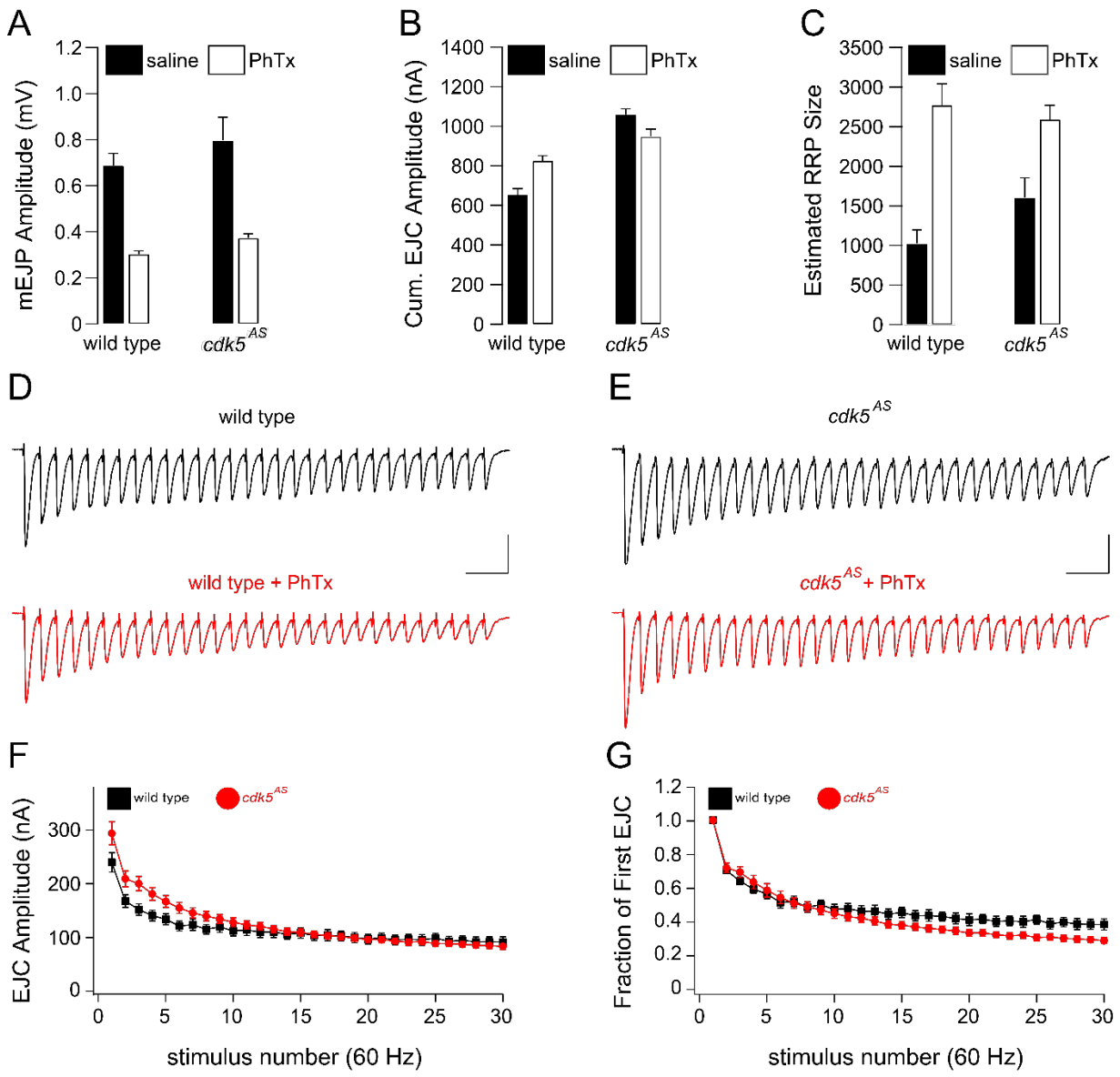
A
mEJP Amplitude (mV)
saline
PhTx
wild type
cdk5AS
B
Cum. EJC Amplitude (nA)
C
Estimated RRP Size
D
wild type
wild type + PhTx
E
cdk5AS
cdk5AS + PhTx
F
EJC Amplitude (nA)
stimulus number (60 Hz)
G
Fraction of First EJC

References

Akbergenova Y, Bykhovskaia M. Synapsin regulates vesicle organization and activity-dependent recycling at Drosophila motor boutons. Neuroscience. 2010 Oct 13;170(2):441-52.

Atwood HL, Govind CK, Wu CF. Differential ultrastructure of synaptic terminals on ventral longitudinal abdominal muscles in Drosophila larvae. J Neurobiol. 1993 Aug;24(8):1008-24.

Banks AS, McAllister FE, Camporez JP, Zushin PJ, Jurczak MJ, Laznik-Bogoslavski D, Shulman GI, Gygi SP, Spiegelman BM. An ERK/Cdk5 axis controls the diabetogenic actions of PPARγ. Nature. 2015 Jan 15;517(7534):391-5.

Bhogal B, Jepson JE, Savva YA, Pepper AS, Reenan RA, Jongens TA. Modulation of dADAR-dependent RNA editing by the Drosophila fragile X mental retardation protein. Nat Neurosci. 2011 Oct 30;14(12):1517-24.

Bianchetta MJ, Lam TT, Jones SN, Morabito MA. Cyclin-dependent kinase 5 regulates PSD-95 ubiquitination in neurons. J Neurosci. 2011 Aug 17;31(33):12029-35.

Bishop AC, Ubersax JA, Petsch DT, Matheos DP, Gray NS, Blethrow J, Shimizu E, Tsien JZ, Schultz PG, Rose MD, Wood JL, Morgan DO, Shokat KM. A chemical switch for inhibitor-sensitive alleles of any protein kinase. Nature. 2000 Sep 21;407(6802):395-401.

Budnik V, Koh YH, Guan B, Hartmann B, Hough C, Woods D, Gorczyca M. Regulation of synapse structure and function by the Drosophila tumor suppressor gene dlg. Neuron. 1996 Oct;17(4):627-40.

Chae T, Kwon YT, Bronson R, Dikkes P, Li E, Tsai LH. Mice lacking p35, a neuronal specific activator of Cdk5, display cortical lamination defects, seizures, and adult lethality. Neuron. 1997 Jan;18(1):29-42.

Chen K, Featherstone DE. Discs-large (DLG) is clustered by presynaptic innervation and regulates postsynaptic glutamate receptor subunit composition in Drosophila. BMC Biol. 2005 Jan 8;3:1.

Cheng L, Locke C, Davis GW. S6 kinase localizes to the presynaptic active zone and functions with PDK1 to control synapse development. J Cell Biol. 2011 Sep 19;194(6):921-35.

Choi DS, Wei W, Deitchman JK, Kharazia VN, Lesscher HM, McMahon T, Wang D, Qi ZH, Sieghart W, Zhang C, Shokat KM, Mody I, Messing RO. Protein kinase Cdelta regulates ethanol intoxication and enhancement of GABA-stimulated tonic current. J Neurosci. 2008 Nov 12;28(46):11890-9.

Choi JH, Banks AS, Estall JL, Kajimura S, Boström P, Laznik D, Ruas JL, Chalmers MJ, Kamenecka TM, Blüher M, Griffin PR, Spiegelman BM. Anti-diabetic drugs inhibit obesity-linked phosphorylation of PPARgamma by Cdk5. Nature. 2010 Jul 22;466(7305):451-6.

Choi JH, Banks AS, Kamenecka TM, Busby SA, Chalmers MJ, Kumar N, Kuruvilla DS, Shin Y, He Y, Bruning JB, Marciano DP, Cameron MD, Laznik D, Jurczak MJ, Schürer SC, Vidović D, Shulman GI, Spiegelman BM, Griffin PR. Antidiabetic actions of a non-agonist PPARγ ligand blocking Cdk5-mediated phosphorylation. Nature. 2011 Sep 4;477(7365):477-81.

Connell-Crowley L, Le Gall M, Vo DJ, Giniger E. The cyclin-dependent kinase Cdk5 controls multiple aspects of axon patterning in vivo. Curr Biol. 2000 May 18;10(10):599-602.

Connell-Crowley L, Vo D, Luke L, Giniger E. Drosophila lacking the Cdk5 activator, p35, display defective axon guidance, age-dependent behavioral deficits and reduced lifespan. Mech Dev. 2007 May;124(5):341-9.

Cull-Candy SG, Miledi R, Trautmann A, Uchitel OD. On the release of transmitter at normal, myasthenia gravis and myasthenic syndrome affected human end-plates. J Physiol. 1980 Feb;299:621-38.

Daniels RW, Collins CA, Chen K, Gelfand MV, Featherstone DE, DiAntonio A. A single vesicular glutamate transporter is sufficient to fill a synaptic vesicle. Neuron. 2006 Jan 5;49(1):11-6.

Davis GW. Homeostatic control of neural activity: from phenomenology to molecular design. Annu Rev Neurosci. 2006;29:307-23.

Davis GW, Goodman CS. Genetic analysis of synaptic development and plasticity: homeostatic regulation of synaptic efficacy. Curr Opin Neurobiol. 1998 Feb;8(1):149-56.

Davis GW, Goodman CS. Synapse-specific control of synaptic efficacy at the terminals of a single neuron. Nature. 1998 Mar 5;392(6671):82-6.

del Castillo J, Katz B. Quantal components of the end-plate potential. J Physiol. 1954 Jun 28;124(3):560-73.

Denker A, Bethani I, Kröhnert K, Körber C, Horstmann H, Wilhelm BG, Barysch SV, Kuner T, Neher E, Rizzoli SO. A small pool of vesicles maintains synaptic activity in vivo. Proc Natl Acad Sci U S A. 2011 Oct 11;108(41):17177-82.

Dickman DK, Davis GW. The schizophrenia susceptibility gene dysbindin controls synaptic homeostasis. Science. 2009 Nov 20;326(5956):1127-30.

Dobrunz LE, Stevens CF. Heterogeneity of release probability, facilitation, and depletion at central synapses. Neuron. 1997 Jun;18(6):995-1008.

Easley-Neal C, Fierro J Jr, Buchanan J, Washbourne P. Late recruitment of synapsin to nascent synapses is regulated by Cdk5. Cell Rep. 2013 Apr 25;3(4):1199-212.

Fletcher AI, Shuang R, Giovannucci DR, Zhang L, Bittner MA, Stuenkel EL. Regulation of exocytosis by cyclin-dependent kinase 5 via phosphorylation of Munc18. J Biol Chem. 1999 Feb 12;274(7):4027-35.

Frank CA, Kennedy MJ, Goold CP, Marek KW, Davis GW. Mechanisms underlying the rapid induction and sustained expression of synaptic homeostasis. Neuron. 2006 Nov 22;52(4):663-77.

Frank CA, Pielage J, Davis GW. A presynaptic homeostatic signaling system composed of the Eph receptor, ephexin, Cdc42, and CaV2.1 calcium channels. Neuron. 2009 Feb 26;61(4):556-69.

Friedel P, Kahle KT, Zhang J, Hertz N, Pisella LI, Buhler E, Schaller F, Duan J, Khanna AR, Bishop PN, Shokat KM, Medina I. WNK1-regulated inhibitory phosphorylation of the KCC2 cotransporter maintains the depolarizing action of GABA in immature neurons. Sci Signal. 2015 Jun 30;8(383):ra65.

Gaviño MA, Ford KJ, Archila S, Davis GW. Homeostatic synaptic depression is achieved through a regulated decrease in presynaptic calcium channel abundance. Elife. 2015 Apr 17;4.

Gitler D, Takagishi Y, Feng J, Ren Y, Rodriguiz RM, Wetsel WC, Greengard P, Augustine GJ. Different presynaptic roles of synapsins at excitatory and inhibitory synapses. J Neurosci. 2004 Dec 15;24(50):11368-80.

Goold CP, Davis GW. The BMP ligand Gbb gates the expression of synaptic homeostasis independent of synaptic growth control. Neuron. 2007 Oct 4;56(1):109-23.

Graf ER, Daniels RW, Burgess RW, Schwarz TL, DiAntonio A. Rab3 dynamically controls protein composition at active zones. Neuron. 2009 Dec 10;64(5):663-77.

Gravells P, Tomita K, Booth A, Poznansky J, Porter AC. Chemical genetic analyses of quantitative changes in Cdk1 activity during the human cell cycle. Hum Mol Genet. 2013 Jul 15;22(14):2842-51.

Hawasli AH, Benavides DR, Nguyen C, Kansy JW, Hayashi K, Chambon P, Greengard P, Powell CM, Cooper DC, Bibb JA. Cyclin-dependent kinase 5 governs learning and synaptic plasticity via control of NMDAR degradation. Nat Neurosci. 2007 Jul;10(7):880-6.

Heckscher ES, Fetter RD, Marek KW, Albin SD, Davis GW. NF-kappaB, IkappaB, and IRAK control glutamate receptor density at the Drosophila NMJ. Neuron. 2007 Sep 20;55(6):859-73.

Horiuchi D, Huskey NE, Kusdra L, Wohlbold L, Merrick KA, Zhang C, Creasman KJ, Shokat KM, Fisher RP, Goga A. Chemical-genetic analysis of cyclin dependent kinase 2 function reveals an important role in cellular transformation by multiple oncogenic pathways. Proc Natl Acad Sci U S A. 2012 Apr 24;109(17):E1019-27.

Houweling AR, Bazhenov M, Timofeev I, Steriade M, Sejnowski TJ. Homeostatic synaptic plasticity can explain post-traumatic epileptogenesis in chronically isolated neocortex. Cereb Cortex. 2005 Jun;15(6):834-45.

Jan LY, Jan YN. Properties of the larval neuromuscular junction in Drosophila melanogaster. J Physiol. 1976 Oct;262(1):189-214.

Juo P, Harbaugh T, Garriga G, Kaplan JM. CDK-5 regulates the abundance of GLR-1 glutamate receptors in the ventral cord of Caenorhabditis elegans. Mol Biol Cell. 2007 Oct;18(10):3883-93.

Kamenetz F, Tomita T, Hsieh H, Seabrook G, Borchelt D, Iwatsubo T, Sisodia S, Malinow R. APP processing and synaptic function. Neuron. 2003 Mar 27;37(6):925-37.

Kuromi H, Kidokoro Y. Two distinct pools of synaptic vesicles in single presynaptic boutons in a temperature-sensitive Drosophila mutant, shibire. Neuron. 1998 May;20(5):917-25.

Kim SH, Ryan TA. Balance of calcineurin Aα and CDK5 activities sets release probability at nerve terminals. J Neurosci. 2013 May 22;33(21):8937-50.

Kim SH, Ryan TA. CDK5 serves as a major control point in neurotransmitter release. Neuron. 2010 Sep 9;67(5):797-809.

Kissler AE, Pettersson N, Frölich A, Sigrist SJ, Suter B. Drosophila cdk5 is needed for locomotive behavior and NMJ elaboration, but seems dispensable for synaptic transmission. Dev Neurobiol. 2009 May;69(6):365-77.

Kittel RJ, Wichmann C, Rasse TM, Fouquet W, Schmidt M, Schmid A, Wagh DA, Pawlu C, Kellner RR, Willig KI, Hell SW, Buchner E, Heckmann M, Sigrist SJ. Bruchpilot promotes active zone assembly, Ca2+ channel clustering, and vesicle release. Science. 2006 May 19;312(5776):1051-4.

Klagges BR, Heimbeck G, Godenschwege TA, Hofbauer A, Pflugfelder GO, Reifegerste R, Reisch D, Schaupp M, Buchner S, Buchner E. Invertebrate synapsins: a single gene codes for several isoforms in Drosophila. J Neurosci. 1996 May 15;16(10):3154-65.

Ko J, Humbert S, Bronson RT, Takahashi S, Kulkarni AB, Li E, Tsai LH. p35 and p39 are essential for cyclin-dependent kinase 5 function during neurodevelopment. J Neurosci. 2001 Sep 1;21(17):6758-71.

Kraybill BC, Elkin LL, Blethrow JD, Morgan DO, Shokat KM. Inhibitor scaffolds as new allele specific kinase substrates. J Am Chem Soc. 2002 Oct 16;124(41):12118-28.

Kwon YT, Tsai LH, Crandall JE. Callosal axon guidance defects in p35(-/-) mice. J Comp Neurol. 1999 Dec 13;415(2):218-29.

Lahey T, Gorczyca M, Jia XX, Budnik V. The Drosophila tumor suppressor gene dlg is required for normal synaptic bouton structure. Neuron. 1994 Oct;13(4):823-35.

Lai KO, Wong AS, Cheung MC, Xu P, Liang Z, Lok KC, Xie H, Palko ME, Yung WH, Tessarollo L, Cheung ZH, Ip NY. TrkB phosphorylation by Cdk5 is required for activity-dependent structural plasticity and spatial memory. Nat Neurosci. 2012 Nov;15(11):1506-15.

Lalioti V, Muruais G, Dinarina A, van Damme J, Vandekerckhove J, Sandoval IV. The atypical kinase Cdk5 is activated by insulin, regulates the association between GLUT4 and E-Syt1, and modulates glucose transport in 3T3-L1 adipocytes. Proc Natl Acad Sci U S A. 2009 Mar 17;106(11):4249-53.

Ledda F, Paratcha G, Ibáñez CF. Target-derived GFRalpha1 as an attractive guidance signal for developing sensory and sympathetic axons via activation of Cdk5. Neuron. 2002 Oct 24;36(3):387-401.

Lew J, Huang QQ, Qi Z, Winkfein RJ, Aebersold R, Hunt T, Wang JH. A brain-specific activator of cyclin-dependent kinase 5. Nature. 1994 Sep 29;371(6496):423-6.

Liang Q, Li L, Zhang J, Lei Y, Wang L, Liu DX, Feng J, Hou P, Yao R, Zhang Y, Huang B, Lu J. CDK5 is essential for TGF-β1-induced epithelial-mesenchymal transition and breast cancer progression. Sci Rep. 2013 Oct 14;3:2932.

Liebl J, Weitensteiner SB, Vereb G, Takács L, Fürst R, Vollmar AM, Zahler S. Cyclin-dependent kinase 5 regulates endothelial cell migration and angiogenesis. J Biol Chem. 2010 Nov 12;285(46):35932-43.

Liebl J, Zhang S, Moser M, Agalarov Y, Demir CS, Hager B, Bibb JA, Adams RH, Kiefer F, Miura N, Petrova TV, Vollmar AM, Zahler S. Cdk5 controls lymphatic vessel development and function by phosphorylation of Foxc2. Nat Commun. 2015 Jun 1;6:7274.

Lilja L, Johansson JU, Gromada J, Mandic SA, Fried G, Berggren PO, Bark C. Cyclin-dependent kinase 5 associated with p39 promotes Munc18-1 phosphorylation and Ca(2+)-dependent exocytosis. J Biol Chem. 2004 Jul 9;279(28):29534-41.

Lilja L, Yang SN, Webb DL, Juntti-Berggren L, Berggren PO, Bark C. Cyclin-dependent kinase 5 promotes insulin exocytosis. J Biol Chem. 2001 Sep 7;276(36):34199-205.

Lin DM, Goodman CS. Ectopic and increased expression of Fasciclin II alters motoneuron growth cone guidance. Neuron. 1994 Sep;13(3):507-23.

Lin H, Lin TY, Juang JL. Abl deregulates Cdk5 kinase activity and subcellular localization in Drosophila neurodegeneration. Cell Death Differ. 2007 Mar;14(3):607-15.

Littleton JT, Bellen HJ, Perin MS. Expression of synaptotagmin in Drosophila reveals transport and localization of synaptic vesicles to the synapse. Development. 1993 Aug;118(4):1077-88.

Liu KS, Siebert M, Mertel S, Knoche E, Wegener S, Wichmann C, Matkovic T, Muhammad K, Depner H, Mettke C, Bückers J, Hell SW, Müller M, Davis GW, Schmitz D, Sigrist SJ. RIM-binding protein, a central part of the active zone, is essential for neurotransmitter release. Science. 2011 Dec 16;334(6062):1565-9.

Locke CJ, Williams SN, Schwarz EM, Caldwell GA, Caldwell KA. Genetic interactions among cortical malformation genes that influence susceptibility to convulsions in C. elegans. Brain Res. 2006 Nov 20;1120(1):23-34.

Madhani HD, Fink GR. The riddle of MAP kinase signaling specificity. Trends Genet. 1998 Apr;14(4):151-5.

Mahr A, Aberle H. The expression pattern of the Drosophila vesicular glutamate transporter: a mWarker protein for motoneurons and glutamatergic centers in the brain. Gene Expr Patterns. 2006 Mar;6(3):299-309.

Marek KW, Davis GW. Transgenically encoded protein photoinactivation (FlAsH-FALI): acute inactivation of synaptotagmin I. Neuron. 2002 Dec 5;36(5):805-13.

Marie B, Pym E, Bergquist S, Davis GW. Synaptic homeostasis is consolidated by the cell fate gene gooseberry, a Drosophila pax3/7 homolog. J Neurosci. 2010 Jun 16;30(24):8071-82.

Marrus SB, Portman SL, Allen MJ, Moffat KG, DiAntonio A. Differential localization of glutamate receptor subunits at the Drosophila neuromuscular junction. J Neurosci. 2004 Feb 11;24(6):1406-15.

Martin AR. A further study of the statistical composition on the end-plate potential. J Physiol. 1955 Oct 28;130(1):114-22.

Matsubara M, Kusubata M, Ishiguro K, Uchida T, Titani K, Taniguchi H. Site-specific phosphorylation of synapsin I by mitogen-activated protein kinase and Cdk5 and its effects on physiological functions. J Biol Chem. 1996 Aug 30;271(35):21108-13.

Merrick KA, Wohlbold L, Zhang C, Allen JJ, Horiuchi D, Huskey NE, Goga A, Shokat KM, Fisher RP. Switching Cdk2 on or off with small molecules to reveal requirements in human cell proliferation. Mol Cell. 2011 Jun 10;42(5):624-36.

Mitra A, Mitra SS, Tsien RW. Heterogeneous reallocation of presynaptic efficacy in recurrent excitatory circuits adapting to inactivity. Nat Neurosci. 2011 Dec 18;15(2):250-7.

Müller M, Davis GW. Transsynaptic control of presynaptic Ca^{2+} influx achieves homeostatic potentiation of neurotransmitter release. Curr Biol. 2012 Jun 19;22(12):1102-8.

Müller M, Genç Ö, Davis GW. RIM-binding protein links synaptic homeostasis to the stabilization and replenishment of high release probability vesicles. Neuron. 2015 Mar 4;85(5):1056-69.

Müller M, Liu KS, Sigrist SJ, Davis GW. RIM controls homeostatic plasticity through modulation of the readily-releasable vesicle pool. J Neurosci. 2012 Nov 21;32(47):16574-85.

Müller M, Pym EC, Tong A, Davis GW. Rab3-GAP controls the progression of synaptic homeostasis at a late stage of vesicle release. Neuron. 2011 Feb 24;69(4):749-62.

Murthy VN, Schikorski T, Stevens CF, Zhu Y. Inactivity produces increases in neurotransmitter release and synapse size. Neuron. 2001 Nov 20;32(4):673-82.

Murthy VN, Stevens CF. Synaptic vesicles retain their identity through the endocytic cycle. Nature. 1998 Apr 2;392(6675):497-501.

Nuwal T, Heo S, Lubec G, Buchner E. Mass spectrometric analysis of synapsins in Drosophila melanogaster and identification of novel phosphorylation sites. J Proteome Res. 2011 Feb 4;10(2):541-50.

Ohshima T, Ward JM, Huh CG, Longenecker G, Veeranna, Pant HC, Brady RO, Martin LJ, Kulkarni AB. Targeted disruption of the cyclin-dependent kinase 5 gene results in abnormal corticogenesis, neuronal pathology and perinatal death. Proc Natl Acad Sci U S A. 1996 Oct 1;93(20):11173-8.

Ou CY, Poon VY, Maeder CI, Watanabe S, Lehrman EK, Fu AK, Park M, Fu WY, Jorgensen EM, Ip NY, Shen K. Two cyclin-dependent kinase pathways are essential for polarized trafficking of presynaptic components. Cell. 2010 May 28;141(5):846-58.

Park M, Watanabe S, Poon VY, Ou CY, Jorgensen EM, Shen K. CYY-1/cyclin Y and CDK-5 differentially regulate synapse elimination and formation for rewiring neural circuits. Neuron. 2011 May 26;70(4):742-57.

Patrick GN, Zukerberg L, Nikolic M, de la Monte S, Dikkes P, Tsai LH. Conversion of p35 to p25 deregulates Cdk5 activity and promotes neurodegeneration. Nature. 1999 Dec 9;402(6762):615-22.

Peled ES, Isacoff EY. Optical quantal analysis of synaptic transmission in wild-type and rab3-mutant Drosophila motor axons. Nat Neurosci. 2011 Apr;14(4):519-26.

Penney J, Tsurudome K, Liao EH, Elazzouzi F, Livingstone M, Gonzalez M, Sonenberg N, Haghighi AP. TOR is required for the retrograde regulation of synaptic homeostasis at the Drosophila neuromuscular junction. Neuron. 2012 Apr 12;74(1):166-78.

Petersen SA, Fetter RD, Noordermeer JN, Goodman CS, DiAntonio A. Genetic analysis of glutamate receptors in Drosophila reveals a retrograde signal regulating presynaptic transmitter release. Neuron. 1997 Dec;19(6):1237-48.

Pilgram GS, Potikanond S, van der Plas MC, Fradkin LG, Noordermeer JN. The RhoGAP crossveinless-c interacts with Dystrophin and is required for synaptic homeostasis at the Drosophila neuromuscular junction. J Neurosci. 2011 Jan 12;31(2):492-500.

Plomp JJ, Van Kempen GT, De Baets MB, Graus YM, Kuks JB, Molenaar PC. Acetylcholine release in myasthenia gravis: regulation at single end-plate level. Ann Neurol. 1995 May;37(5):627-36.

Plomp JJ, van Kempen GT, Molenaar PC. Adaptation of quantal content to decreased postsynaptic sensitivity at single endplates in alpha-bungarotoxin-treated rats. J Physiol. 1992 Dec;458:487-99.

Poore CP, Sundaram JR, Pareek TK, Fu A, Amin N, Mohamed NE, Zheng YL, Goh AX, Lai MK, Ip NY, Pant HC, Kesavapany S. Cdk5-mediated phosphorylation of delta-catenin regulates its localization and GluR2-mediated synaptic activity. J Neurosci. 2010 Jun 23;30(25):8457-67.

Pozo K, Castro-Rivera E, Tan C, Plattner F, Schwach G, Siegl V, Meyer D, Guo A, Gundara J, Mettlach G, Richer E, Guevara JA, Ning L, Gupta A, Hao G, Tsai LH, Sun X, Antich P, Sidhu S, Robinson BG, Chen H, Nwariaku FE, Pfragner R, Richardson JA, Bibb JA. The role of Cdk5 in neuroendocrine thyroid cancer. Cancer Cell. 2013 Oct 14;24(4):499-511.

Prithviraj R, Trunova S, Giniger E. Ex vivo culturing of whole, developing Drosophila brains. J Vis Exp. 2012 Jul 27;(65).

Qin G, Schwarz T, Kittel RJ, Schmid A, Rasse TM, Kappei D, Ponimaskin E, Heckmann M, Sigrist SJ. Four different subunits are essential for expressing the synaptic glutamate receptor at neuromuscular junctions of Drosophila. J Neurosci. 2005 Mar 23;25(12):3209-18.

Robinson SW, Herzyk P, Dow JA, Leader DP. FlyAtlas: database of gene expression in the tissues of Drosophila melanogaster. Nucleic Acids Res. 2013 Jan;41(Database issue):D744-50.

Rosahl TW, Spillane D, Missler M, Herz J, Selig DK, Wolff JR, Hammer RE, Malenka RC, Südhof TC. Essential functions of synapsins I and II in synaptic vesicle regulation. Nature. 1995 Jun 8;375(6531):488-93.

Samuels BA, Hsueh YP, Shu T, Liang H, Tseng HC, Hong CJ, Su SC, Volker J, Neve RL, Yue DT, Tsai LH. Cdk5 promotes synaptogenesis by regulating the subcellular distribution of the MAGUK family member CASK. Neuron. 2007 Dec 6;56(5):823-37.

Sandrock AW Jr, Dryer SE, Rosen KM, Gozani SN, Kramer R, Theill LE, Fischbach GD. Maintenance of acetylcholine receptor number by neuregulins at the neuromuscular junction in vivo. Science. 1997 Apr 25;276(5312):599-603.

Seeburg DP, Feliu-Mojer M, Gaiottino J, Pak DT, Sheng M. Critical role of CDK5 and Polo-like kinase 2 in homeostatic synaptic plasticity during elevated activity. Neuron. 2008 May 22;58(4):571-83.

Shah K, Liu Y, Deirmengian C, Shokat KM. Engineering unnatural nucleotide specificity for Rous sarcoma virus tyrosine kinase to uniquely label its direct substrates. Proc Natl Acad Sci U S A. 1997 Apr 15;94(8):3565-70.

Shuang R, Zhang L, Fletcher A, Groblewski GE, Pevsner J, Stuenkel EL. Regulation of Munc-18/syntaxin 1A interaction by cyclin-dependent kinase 5 in nerve endings. J Biol Chem. 1998 Feb 27;273(9):4957-66.

Sons MS, Busche N, Strenzke N, Moser T, Ernsberger U, Mooren FC, Zhang W, Ahmad M, Steffens H, Schomburg ED, Plomp JJ, Missler M. alpha-Neurexins are required for efficient transmitter release and synaptic homeostasis at the mouse neuromuscular junction. Neuroscience. 2006;138(2):433-46.

Sons MS, Verhage M, Plomp JJ. Role of Munc18-1 in synaptic plasticity at the myasthenic neuromuscular junction. Ann N Y Acad Sci. 2003 Sep;998:404-6.

Su SC, Seo J, Pan JQ, Samuels BA, Rudenko A, Ericsson M, Neve RL, Yue DT, Tsai LH. Regulation of N-type voltage-gated calcium channels and presynaptic function by cyclin-dependent kinase 5. Neuron. 2012 Aug 23;75(4):675-87.

Su SC, Tsai LH. Cyclin-dependent kinases in brain development and disease. Annu Rev Cell Dev Biol. 2011;27:465-91.

Stewart BA, Atwood HL, Renger JJ, Wang J, Wu CF. Improved stability of Drosophila larval neuromuscular preparations in haemolymph-like physiological solutions. J Comp Physiol A. 1994 Aug;175(2):179-91.

Thiagarajan TC, Lindskog M, Tsien RW. Adaptation to synaptic inactivity in hippocampal neurons. Neuron. 2005 Sep 1;47(5):725-37.

Tomizawa K, Ohta J, Matsushita M, Moriwaki A, Li ST, Takei K, Matsui H. Cdk5/p35 regulates neurotransmitter release through phosphorylation and downregulation of P/Q-type voltage-dependent calcium channel activity. J Neurosci. 2002 Apr 1;22(7):2590-7.

Tomizawa K, Sunada S, Lu YF, Oda Y, Kinuta M, Ohshima T, Saito T, Wei FY, Matsushita M, Li ST, Tsutsui K, Hisanaga S, Mikoshiba K, Takei K, Matsui H. Cophosphorylation of amphiphysin I and dynamin I by Cdk5 regulates clathrin-mediated endocytosis of synaptic vesicles. J Cell Biol. 2003 Nov 24;163(4):813-24.

Tripathi BK, Qian X, Mertins P, Wang D, Papageorge AG, Carr SA, Lowy DR. CDK5 is a major regulator of the tumor suppressor DLC1. J Cell Biol. 2014 Dec 8;207(5):627-42.

Trunova S, Baek B, Giniger E. Cdk5 regulates the size of an axon initial segment-like compartment in mushroom body neurons of the Drosophila central brain. J Neurosci. 2011 Jul 20;31(29):10451-62.

Trunova S, Giniger E. Absence of the Cdk5 activator p35 causes adult-onset neurodegeneration in the central brain of Drosophila. Dis Model Mech. 2012 Mar;5(2):210-9.

Tsai LH, Delalle I, Caviness VS Jr, Chae T, Harlow E. p35 is a neural-specific regulatory subunit of cyclin-dependent kinase 5. Nature. 1994 Sep 29;371(6496):419-23.

Turrigiano GG. The self-tuning neuron: synaptic scaling of excitatory synapses. Cell. 2008 Oct 31;135(3):422-35.

Ubersax JA, Woodbury EL, Quang PN, Paraz M, Blethrow JD, Shah K, Shokat KM, Morgan DO. Targets of the cyclin-dependent kinase Cdk1. Nature. 2003 Oct 23;425(6960):859-64.

Ultanir SK, Hertz NT, Li G, Ge WP, Burlingame AL, Pleasure SJ, Shokat KM, Jan LY, Jan YN. Chemical genetic identification of NDR1/2 kinase substrates AAK1 and Rabin8 Uncovers their roles in dendrite arborization and spine development. Neuron. 2012 Mar 22;73(6):1127-42.

Ultanir SK, Yadav S, Hertz NT, Oses-Prieto JA, Claxton S, Burlingame AL, Shokat KM, Jan LY, Jan YN. MST3 kinase phosphorylates TAO1/2 to enable Myosin Va function in promoting spine synapse development. Neuron. 2014 Dec 3;84(5):968-82.

Van Vactor DV, Sink H, Fambrough D, Tsoo R, Goodman CS. Genes that control neuromuscular specificity in Drosophila. Cell. 1993 Jun 18;73(6):1137-53.

Verstegen AM, Tagliatti E, Lignani G, Marte A, Stolero T, Atias M, Corradi A, Valtorta F, Gitler D, Onofri F, Fassio A, Benfenati F. Phosphorylation of synapsin I by cyclin-dependent kinase-5 sets the ratio between the resting and recycling pools of synaptic vesicles at hippocampal synapses. J Neurosci. 2014 May 21;34(21):7266-80.

Verstreken P, Ly CV, Venken KJ, Koh TW, Zhou Y, Bellen HJ. Synaptic mitochondria are critical for mobilization of reserve pool vesicles at Drosophila neuromuscular junctions. Neuron. 2005 Aug 4;47(3):365-78.

Wagh DA, Rasse TM, Asan E, Hofbauer A, Schwenkert I, Dürrbeck H, Buchner S, Dabauvalle MC, Schmidt M, Qin G, Wichmann C, Kittel R, Sigrist SJ, Buchner E. Bruchpilot, a protein with homology to ELKS/CAST, is required for structural integrity and function of synaptic active zones in Drosophila. Neuron. 2006 Mar 16;49(6):833-44.

Wei FY, Nagashima K, Ohshima T, Saheki Y, Lu YF, Matsushita M, Yamada Y, Mikoshiba K, Seino Y, Matsui H, Tomizawa K. Cdk5-dependent regulation of glucose-stimulated insulin secretion. Nat Med. 2005 Oct;11(10):1104-8.

Weyhersmüller A, Hallermann S, Wagner N, Eilers J. Rapid active zone remodeling during synaptic plasticity. J Neurosci. 2011 Apr 20;31(16):6041-52.

Yan Z, Chi P, Bibb JA, Ryan TA, Greengard P. Roscovitine: a novel regulator of P/Q-type calcium channels and transmitter release in central neurons. J Physiol. 2002 May 1;540(Pt 3):761-70.

Yazawa M, Hsueh B, Jia X, Pasca AM, Bernstein JA, Hallmayer J, Dolmetsch RE. Using induced pluripotent stem cells to investigate cardiac phenotypes in Timothy syndrome. Nature. 2011 Mar 10;471(7337):230-4.

Yoshihara M, Littleton JT. Synaptotagmin I functions as a calcium sensor to synchronize neurotransmitter release. Neuron. 2002 Dec 5;36(5):897-908.

Yoshii A, Murata Y, Kim J, Zhang C, Shokat KM, Constantine-Paton M. TrkB and protein kinase Mζ regulate synaptic localization of PSD-95 in developing cortex. J Neurosci. 2011 Aug 17;31(33):11894-904.

Younger MA, Müller M, Tong A, Pym EC, Davis GW. A presynaptic ENaC channel drives homeostatic plasticity. Neuron. 2013 Sep 18;79(6):1183-96.

Yu HP, Xie JM, Li B, Sun YH, Gao QG, Ding ZH, Wu HR, Qin ZH. TIGAR regulates DNA damage and repair through pentosephosphate pathway and Cdk5-ATM pathway. Sci Rep. 2015 Apr 30;5:9853.

Zhang B, Stewart B. Voltage-clamp analysis of synaptic transmission at the Drosophila larval neuromuscular junction. Cold Spring Harb Protoc. 2010 Sep 1;2010(9):pdb.prot5488.

Zheng M, Leung CL, Liem RK. Region-specific expression of cyclin-dependent kinase 5 (cdk5) and its activators, p35 and p39, in the developing and adult rat central nervous system. J Neurobiol. 1998 May;35(2):141-59.

Zinsmaier KE, Eberle KK, Buchner E, Walter N, Benzer S. Paralysis and early death in cysteine string protein mutants of Drosophila. Science. 1994 Feb 18;263(5149):977-80.

Publishing Agreement

It is the policy of the University to encourage the distribution of all theses, dissertations, and manuscripts. Copies of all UCSF theses, dissertations, and manuscripts will be routed to the library via the Graduate Division. The library will make all theses, dissertations, and manuscripts accessible to the public and will preserve these to the best of their abilities, in perpetuity.

Please sign the following statement:

I hereby grant permission to the Graduate Division of the University of California, San Francisco to release copies of my thesis, dissertation, or manuscript to the Campus Library to provide access and preservation, in whole or in part, in perpetuity.

Cody J. Locke
Author Signature

12/17/2015
Date